icmr INDIAN COUNCIL OF MEDICAL RESEARCH | NICED NATIONAL INSTITUTE OF CHOLERA AND ENTERIC DISEASES

आई सी एम आर – राष्ट्रीय हैजा तथा आंत्ररोग संस्थान
स्वास्थ्य अनुसंधान विभाग, स्वास्थ्य और परिवार
कल्याण मंत्रालय, भारत सरकार

ICMR - National Institute of Cholera and Enteric Diseases
Department of Health Research, Ministry of Health and Family Welfare, Government of India

CERTIFICATE FROM THE SUPERVISOR

This is to certify that the thesis entitled **"Therapeutic intervention of *Shigella flexneri* host pathogen interaction."** Submitted by ~~Sri~~/Smt **Priyanka Basak** who got ~~his~~/her name registered on 22/10/2019 for the award of Ph.D. (Science) degree of Jadavpur University, is absolutely based upon her own work under the supervision of **Dr. SUSHMITA BHATTACHARYA** and that neither this thesis nor any part of this has been submitted for either any degree/diploma or any other academic award anywhere before.

14.9.23 Sushmita Bhattacharya

(Signature of the supervisor date with official seal)

Dr. Sushmita Bhattacharya
Scientist - C
Biochemistry Division
ICMR National Institute of Cholera and Enteric Diseases
Beleghata, Kolkata-700010

Therapeutic intervention of *Shigella flexneri* host pathogen interaction

Thesis submitted for the degree of

Doctor of Philosophy (Science)

in

Life Science and Bio-technology

By

PRIYANKA BASAK

(Index No.: 118/19/Life Sc./26)

Department of Life Science and Bio-technology

Jadavpur University

Kolkata, India

2023

To...

Laxmi Basak

Maa

&

SriKrishna Basak

Baba

For being my first teacher and for supporting and encouraging me to believe in myself

ACKNOWLEDGEMENT

In presenting this thesis, it is essential to extend my heartfelt gratitude not only to my own efforts but also to the exceptional individuals who have played an indispensable role in its realization. Their selfless contributions, ceaseless support, encouragement, and astute guidance have been instrumental in shaping the trajectory of this research endeavor. The investment of their time, affection, and commitment has left an indelible mark on the outcome of this work, and for this, I am profoundly thankful.

I could not have completed this work without the unwavering support of my guide, **Dr. Sushmita Bhattacharya.** I have had the opportunity to be under the supervision and be blessed by the guidance of Madam and it has been a journey and association which I will honor and cherish all the days of my life. She has promoted critical thinking and helped me to see the research potential for further discoveries. The journey has been a roller-coaster ride, these last five years and Madam has always in the end stood by me through the numerous problems I have faced both professionally and personally.

I am grateful to **Dr. Shanta Dutta**, the director of ICMR-NICED for providing me the workplace, **Dr. Nabendu Shekhar Chatterjee, Dr. Asish K. Mukhopadhyay, Dr. Hemanta Koley, Dr. Santasabuj Das,** Scientists of ICMR- NICED for helping me with their critical reviews as well providing bacterial strains, cell lines, reagents, and chemicals. I would like to thank **Department of life science and biotechnology, Jadavpur University**. All my **teachers** from my post-graduation days, graduation days as well as school days – thank you, for providing academic co-operation and helping me to grow. To the **non-teaching staffs** and **office staff** who have provided technical help of all sorts, thank you for every help.

For financial assistance I remain ever grateful to **Department of Biotechnology, Government of India** for my fellowship. Here I would also like to thank **Indian Council of Medical Research, Government of India**, for funding the project which forms my thesis.

I want to take this opportunity to express my deep and heartfelt gratitude to my beloved parents, **Srikrishna Basak** and **Laxmi Basak** who allowed me to dream. Their love, guidance, and sacrifices have been invaluable in helping me achieve my goals, and I would not be here today without their constant belief in me. Their sacrifices have enabled me to focus on my studies and pursue my dreams with confidence. I am also indebted to my husband, **Shubham Kundu** who is the constant part of my dream. He has been my rock throughout the ups and downs. His encouragement has pushed me to overcome obstacles and strive for excellence and to believe in myself. His support has not only helped me to achieve my goals, but it has also taught me the value of determination and resilience. They have always been my biggest cheerleaders, providing emotional and financial support whenever I needed it.

I am really very grateful to my lab seniors, **Dr. Rhishita Chourashi, Dr. Suman Das, Dr. Debjyoti Bhakat, Dr. Kalyani Saha, Dr. Deotima Sarkar** for their help in learning the methodologies and techniques. I learnt a lot from my juniors, **Mr. Indranil Mondal, Ms. Uzma Khan, Ms. Priyanka Maitra, Ms. Sushmita Kundu, Mr. Sourin Alu, Mr. Abhishek Singh** and really thankful for their help in execution of my experiments. All the **non-teaching staffs, office staff and trainees** who have provided technical help of all sorts, thank you for every help.

Some family members who have been always been part of my journey- my maternal uncle – **Gobinda Basak** with his wise advice and unwavering belief in me, have always made me confident and excited about the path I am on, and my uncle – **Shyamal Basak**, the most enthusiastic person I have seen has always pushed me to work harder and strive for excellence in everything I do, thank you, for the roles you have played, they have been essential.

To all those of you I could not mention here, thank you too, every big and small role played has helped me to achieve the dream of a PhD degree together.

Date:

(Priyanka Basak)

CONTENTS

SECTION 1

INTRODUCTION

Shigellosis, a severe gastrointestinal infection caused by various species of *Shigella*, remains a public health concern, and contributes to the prevalence of diarrheal diseases worldwide. Antibiotic resistance in *Shigella spp.* is now a global crisis, recognized by the World Health Organization. The emergence of resistance demands the development of new and better antimicrobial drugs to address the problem of treatment. Finding innovative solutions is crucial to combat the escalating problem and preserve the efficacy of treatments for this pathogen. Currently, ongoing research aims to understand the intricate mechanisms employed by pathogens to dampen host innate immune responses. Host Directed Therapy (HDT) is used to target pathogen-exploited pathways. Several host defence mechanisms like autophagy, inflammation play a major role in protection from pathogen invasion and its consequences.

Natural compounds with antibacterial properties have become a subject of growing interest in pharmacological sciences. Several herbal compounds like resveratrol, quercetin, curcumin, ursolic acid, capsaicin etc. are well known antimicrobial agents. Capsaicin and its derivatives are considered highly promising antimicrobial molecules that could potentially serve as complementary or alternative treatments to antibiotics in combating bacterial infections. Capsaicin exhibits significant bactericidal activity against pathogens like *Salmonella tuberculosis, Helicobacter pylori,* and *Vibrio cholerae*. But its effect on host directed therapeutic action is not well studied. The mechanism of Capsaicin mediated autophagy induction and clearance of intracellular *Shigella flexneri* has not been revealed till now. The major focus of our study is to understand the effect of the herbal compound Capsaicin in *S. flexneri* pathogenesis and decipher the underlying mechanism behind intervention of host pathogen interaction. This study also aims to characterize new drug targets to prevent shigellosis.

SECTION 2

REVIEW OF LITERATURE

1. Shigella flexneri

Shigella flexneri, a Gram-negative facultative anaerobic bacterium belongs to the Enterobacteriaceae family **(fig1).** It possesses genetic relatedness with *E. coli* having common characteristic features. There are four species under the genus *Shigella i.e., Shigella flexneri, Shigella boydii, Shigella sonnei and Shigella dysenteriae.* Among them, *S. flexneri* is divided into 13 serotypes based on varying O-antigen along with biochemical differences.

S. flexneri infects primates especially humans via feco-oral route causing bacillary dysentery. Colonic tissue damage, ulceration and inflammation occur due to infection which ultimately leads to abdominal cramp, watery diarrhoea, and bloody stool. Patients may develop septicemia and haemolytic uremic syndrome if kept untreated for a longer time (Bennish, 1991). Among four species *S. flexneri* causes highest mortality rate in developing countries (Bennish and Wojtyniak, 1991). Serotypes 1b, 2a, 3a, 4a and 6 exist predominantly in developing countries. *S. flexneri 2a* can majorly be found in industrialised countries (Pérez et al., 2023). Disease caused by *Shigella spp.* is called shigellosis which is an infectious disease transmitted in unhygienic environment with lack of purified drinking water, poor sanitation and malnutrition. Despite of antibiotics availability for shigellosis treatment, gradual increase in antibiotic resistance in developing countries are now a major concern. Although WHO is prioritizing safe and effective vaccine development, but no licensed vaccine is available in market till now.

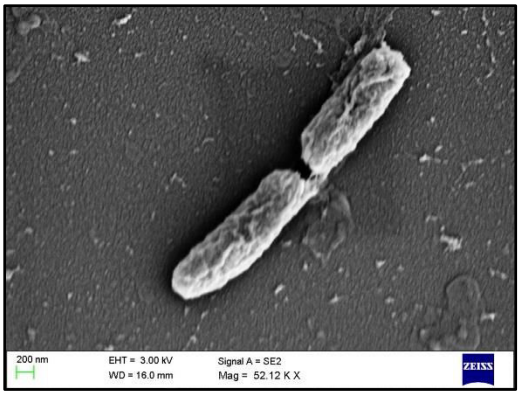

Fig1. Electron Microscopic image of *S. flexneri* (Source: https://www.wikipedia.org/)

S. flexneri chromosome consists of three pathogenicity islands. Several virulence genes are located on a 220kb virulence plasmid **(fig2).** Cell culture studies like invasion assays and *in vivo* models like rabbit ligated–intestinal–loop model helped researchers to understand the role of virulence genes and *Shigella flexneri* pathogenesis (Mallett et al., 1993; Wassef, Keren and Mailloux, 1989).

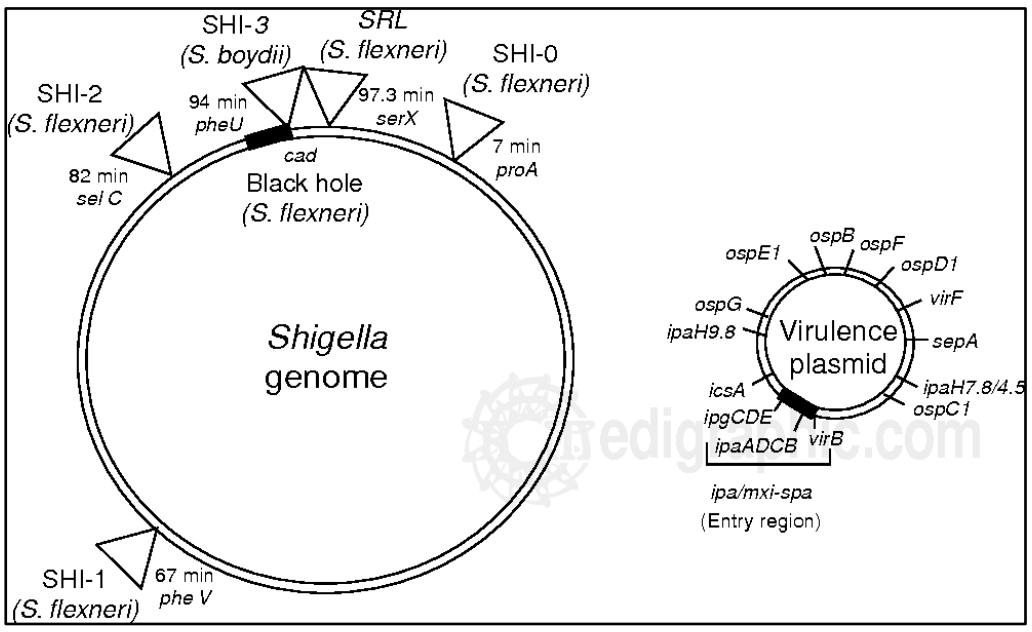

Fig2. Pathogenicity island of *S. flexneri* (Source: https://pubmed.ncbi.nlm.nih.gov/ 17061529/)

2. History

The story of shigellosis, an ancient disease started after identification of *Shigella dysenteriae* by Kiyoshi Shiga **(fig3)** in 1898. In 1899, Simon Flexner identified *Shigella flexneri*. In 1915, Carl Sonne isolated *Shigella sonnei* and Major J.S.K. Boyd discovered another species *Shigella boydii* in 1930. In early 20th century, outbreak of epidemic dysentery caused due to S. *dysenteriae* type 1 in central America (Mata et al., 1970). After 1994 civil war, flow of refugee from middle east to Europe led to continuation of *Shigella flexneri* epidemics into 21st century due to multidrug-resistant *S. flexneri* and *S. sonnei* (Georgakopoulou et al., 2016). In 21st century, dysentery is a significant public health threat as in 2015, diarrhoea caused by *Shigella flexneri* and *Salmonella* was observed as the leading cause of death among all ages.

Fig3. Kiyoshi Shiga (Source: https://www.wikipedia.org/)

3. Shigellosis as a disease

In spite of availability of antibiotics, about 164,000 people die every year due to shigellosis (Taneja et al., 2021). Definition of dysentery is passage of bloody and mucous containing stool along with abdominal cramps **(fig4)**. *Shigella flexneri* co-evolved to find new ways and adapted with continuously changing environment for survival. The primary cause of its adaptation is the intracellular existence of *Shigella flexneri.* It enters human body through feco-oral route and invades colonic epithelia. Once inside the colonic epithelial cells it evades cellular defence mechanism and replicate intracellularly for survival. *Shigella flexneri*, an outstanding model of host pathogen interaction possesses pathogenicity islands, virulence genes leading to hijack of host autophagy machinery and cytoskeletal remodelling.

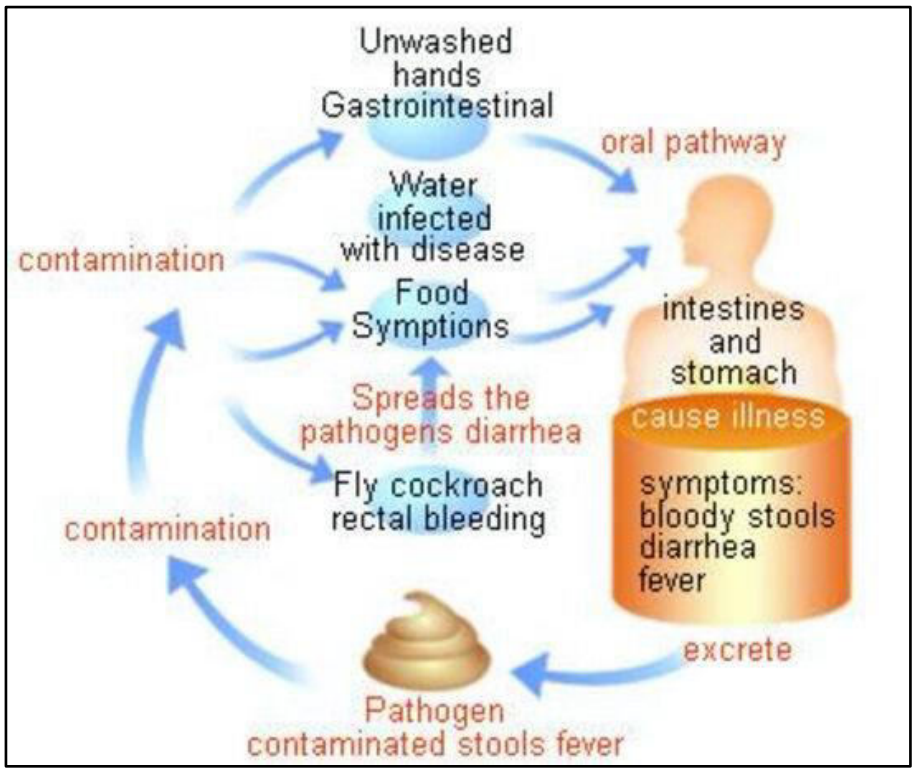

Fig4. Transmission of shigellosis (Source: https://marlerclark.com/)

4. Diagnosis

Stool or a rectal swab containing faeces is used as specimen for identifying shigellosis. Visualization of numerous poly-morphonucleocytes suggest aetiology of *Shigella flexneri* dysentery. *Shigella flexneri* DNA can be identified using PCR from stool culture. Culturing in several selective and differential media confirms presence of *Shigella flexneri* in sample.

5. *Shigella flexneri* culture media

The morphology of *Shigella flexneri* colonies is slightly pink and translucent, with or without rough edges. *Shigella flexneri* can be grown in Luria Agar (LA), Mueller Hinton Agar (MHA), Tryptic Soy Agar (TSA) etc.

There are several selective media for *Shigella flexneri*:

a) **Xylose Lysine Deoxycholate (XLD) Agar** is a selective and differential medium for the isolation of *Shigella spp* from clinical samples showing red colonies **(fig5).** Yeast extract is used as nutrient source, sodium deoxycholate is the selective media which inhibits Gram positive bacteria. Xylose is fermented by all enteric bacteria except *Shigella flexneri* enabling differentiation of *Shigella* species. When xylose is degraded to glucose and lactose, phenol red shows yellow coloration. Decarboxylation of lysine to cadaverine results in red colonies due to pH change on prolonged incubation.

Fig5. *Shigella flexneri* on XLD (Source: https://microbiologyinfo.com)

b) *Salmonella Shigella* (SS) Agar is selective and differential medium for the isolation and differentiation of some strains of *Shigella flexneri*. *Shigella flexneri* is unable to ferment lactose as well as production of hydrogen sulfide gas, thus showing colorless colonies **(fig6).**

Fig6. *Shigella flexneri* on SS agar (Source: https://microbiologyinfo.com)

6. Epidemiology

Shigella flexneri, a Gram negative Enterobacteriaceae, causes bacillary dysentery. It is mostly prevalent in developing countries and causes morbidity and mortality in children primarily below 5 years. Several countries of Asia and Africa where poverty level is noticeable, shigellosis is ubiquitous. Antibiotic-resistant strains of *Shigella flexneri* have emerged worldwide. Resistance to third generation cephalosporins and fluoroquinolones are highly noted. Recent studies have shown resistance to azithromycin also. Among the four serogroups, *S. dysenteriae* usually causes epidemic forms of the disease. India and neighbouring countries show shigellosis caused by *S. boydii* infection. *S. flexneri* was most commonly found species from Asian countries (China, Thailand, Bangladesh, Vietnam, Pakistan, and Indonesia). *S. dysenteriae* can often be seen in southern Asia and sub-Saharan Africa (Lima, Havt and Lima, 2015) **(fig7)**. Data from several parts of India showed *S. flexneri* as the most prevalent serogroup (60%) from 1994-2002, followed by emergence of *S. dysenteriae* type 1. Since 2004, *S. flexneri* again emerged as the predominant serogroup. *S. sonnei* (23.8%), *S. dysenteriae* (9.8%) and *S. boydii* (5.7%) are less prevalent in India (Taneja and Mewara, 2016). Children below 5 years are predominantly infected with *S. flexneri* (74.7%), whereas serotype 2a shows 51%. In Andaman Islands, prevalence of *S. flexneri* (68%) is more than any other serogroups. The heterogenous distribution of *Shigella flexneri* across the country implies requirement of cross protective *Shigella* vaccine. Apart from humans and primates, *Shigella flexneri* can be isolated from rivers and coastal waters. *Shigella flexneri* causes infection at a very low dose (10-100 bacteria) causing large outbreaks (Chang et al., 2012). Lack of hygiene and clean water are the major attributes in developing countries to cause shigellosis. Summer is the peak season of *Shigella flexneri*

infection as virulence genes are activated from 30 to 37°C. Street foods are the major source of pathogenic organisms. During rainy seasons, water samples of the river Narmada in Madhya Pradesh in India as well as surface waters of Bangladesh have been found to harbour *S. flexneri, S. sonnei* and *S. dysenteriae*. A region where human faecal disposal is inadequate, domestic flies' spreads shigellosis through their guts.

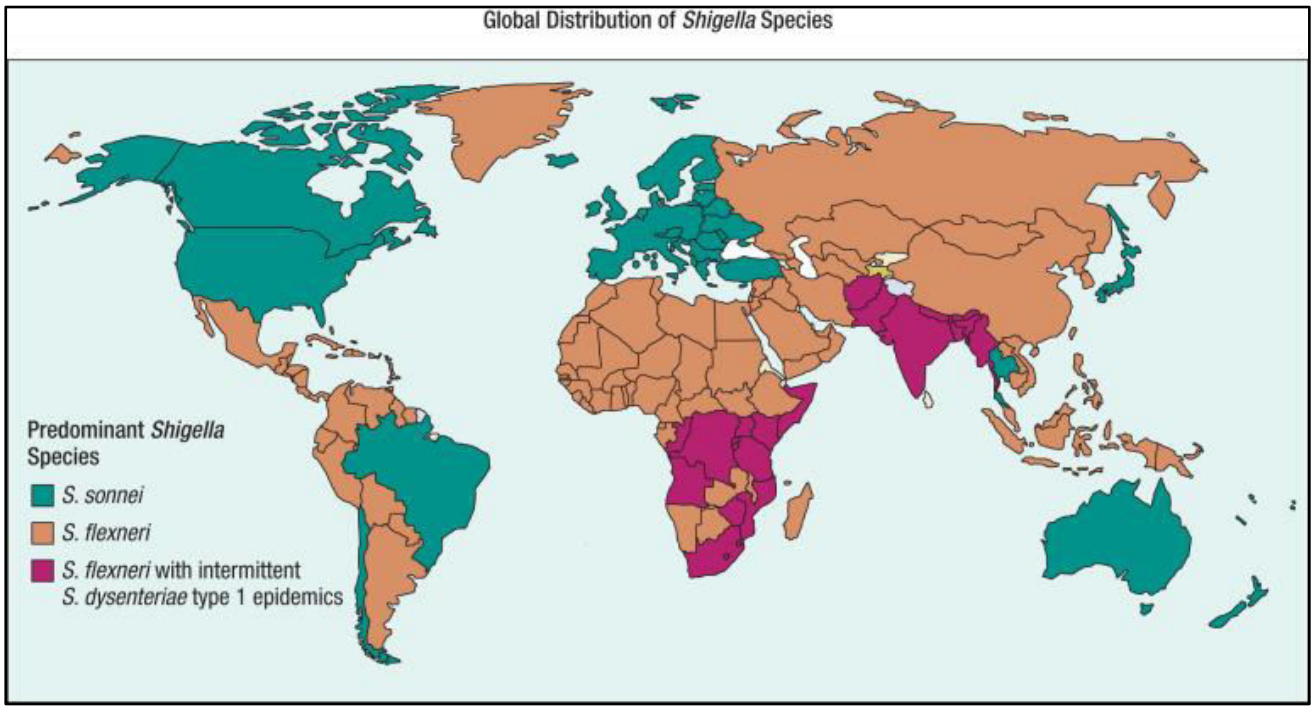

Fig7. Global distribution of *Shigella* (Source: 10.1016/B978-0-323-55512-8.00048-X)

7. Pathogenesis

Characterization of virulence factors and pathogenesis was majorly studied in *S. flexneri* 2a for several decades. For understanding the molecular mechanism of *S. flexneri* pathogenesis $CaCO_2$, an immortalized cell line was used. From human enteroid model basic parameters of infection was established. M cell exploitation enables penetration of epithelial barrier and epithelial cell infection. Intracellular replication, enhanced Muc2 production and IL8 secretion resulting in prolonged infection (Ranganathan et al., 2019) **(fig8)**.

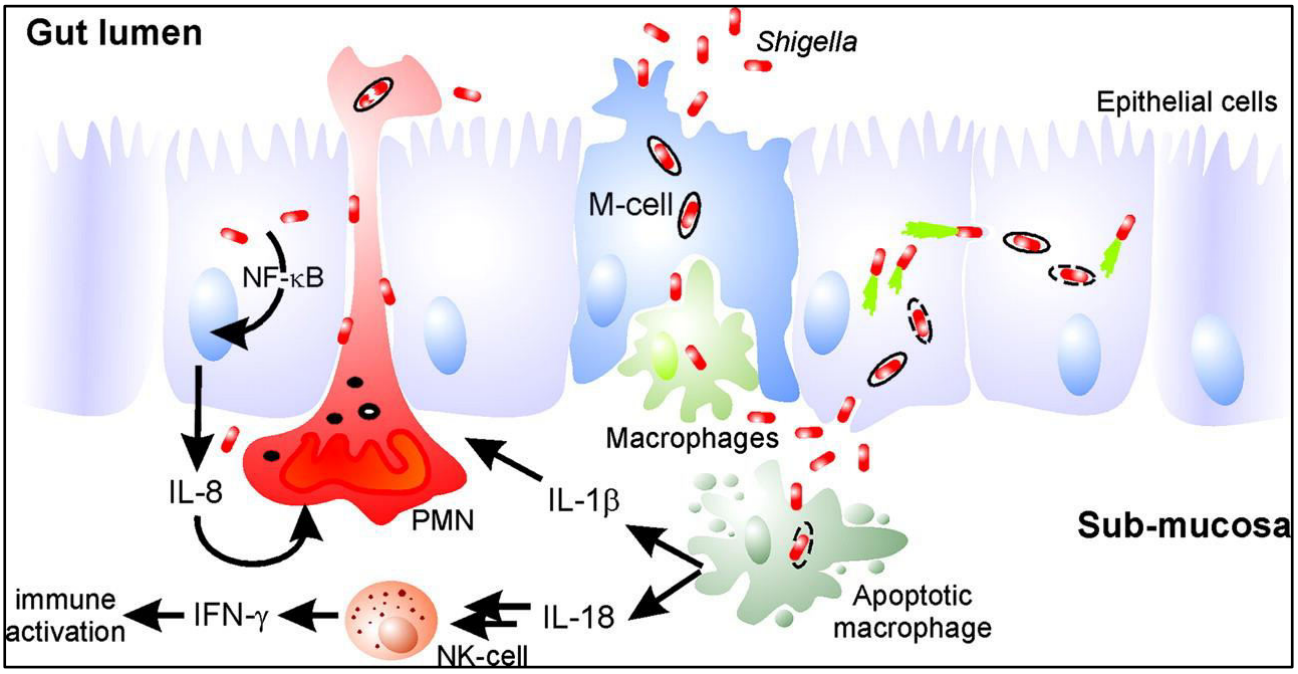

Fig8. Molecular pathogenesis of *Shigella flexneri* (Source: 10.1128/CMR.00032-07)

8. Invasion

Shigella flexneri causes diarrhoea and inflammation in primates via invading the colonic epithelium. Shigellosis causes approximately 300000 deaths in the world. *Shigella flexneri* contains a large 220kb virulence plasmid pWR100 possessing chromosomal pathogenicity island (Parsot and Sansonetti, 1996). Briefly, *S. flexneri* enters via M cells of colonic

epithelium followed by its transition to basolateral face. After transition, the residing macrophages engulf the bacteria. After being phagocytosed, macrophages undergo pyroptosis and death which is followed by infection of epithelial cells. These intracellular spread leads to inflammation and damage. *S. flexneri* infects non phagocytic colonic epithelial cells using its type III secretion system which is a needle like protein complex. Firstly, *S. flexneri* injects T3SS effector proteins into the host cells and causes rearrangement of cytoskeletal system of host leading to ruffled membrane, micropinocytosis and internalisation of bacteria (Schroeder and Hilbi, 2008) **(fig9).** After uptake, effector proteins IpaB, IpaC and IpgD leads to phagocytic vacuole escape and bacteria gets access of cytosol for replication. After entering cytosol, *S. flexneri* hijacks host machinery to survive inside the cell. IcsA, a bacterial effector protein leads to recruitment of N-WASP and the Arp2/3 complex enabling actin polymerization. Pathogen containing membrane protrusions are promoted by actin-based motility and enables engulfment of bacteria by neighbouring cells.

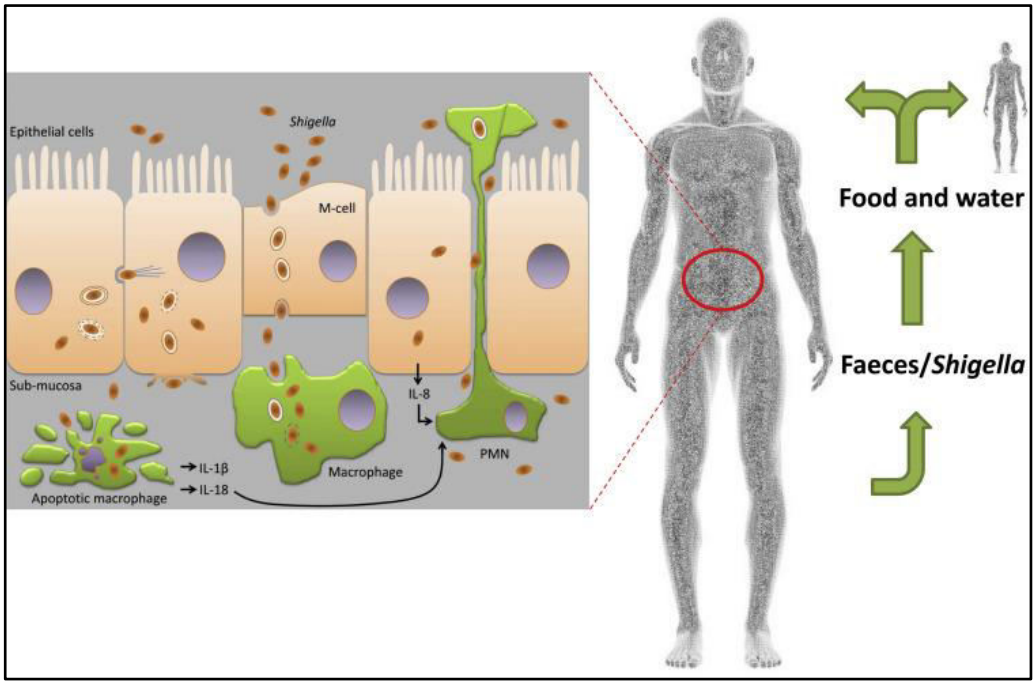

Fig9. Invasion of *S. flexneri* into host system (Source: 10.1016/j.micres. 2015.08.006)

9. Host pathogen interaction

Host immune defenses can be manipulated by *S. flexneri* for successful establishment of infection. A microbe which causes disease in host is termed as a pathogen. Sometimes pathogen resides in host body with/without causing disease. This state is described as host-pathogen interaction. The host–pathogen interaction is sustainability of microbes within host. Microbes divide and cause adverse effects in host on cellular level and disrupt host homeostasis. Host activates several major defense mechanisms against *S. flexneri* infection.

9.1. Autophagy

Autophagy is a self defense mechanism of host by which it can degrade unwanted intracellular materials and pathogens. Canonical autophagy is mainly dependent upon autophagy-related (ATG) proteins. Recruitment of these ATG proteins leads to formation of isolation membrane, phagophore. Elongation of phagophore builds a specialised double-membrane vesicle called the autophagosome. Autophagosomes fuse with lysosome and enhances degradation. Removal of bacteria or other pathogens by xenophagy is dependent upon P62, NDP52 and optineurin receptor as they bind to ubiquitinated pathogens. Bacterial invasion can be reversed by LC3-associated phagocytosis (LAP), a major non canonical autophagy pathway leading to bacterial degradation. Autophagy mechanism can be exploited by several pathogens. LAP can be counteracted by *S. flexneri* using IcsB, an effector virulence protein. After invasion, rupture of phagocytic vacuole by *S. flexneri* triggers autophagy by following mechanisms (Krokowski and Mostowy, 2016) **(fig10)**.

A) Amino acid starvation caused by *S. flexneri* infection downregulates mammalian target of rapamycin complex 1 (mTORC1) leading to autophagy induction.

B) Ubiquitination of vacuole remnants and recognition of p62 as well as NDP52 and recruitment of LC3

C) Exposure of host cell glycans to cytosol due to membrane damage and recognition by gal8

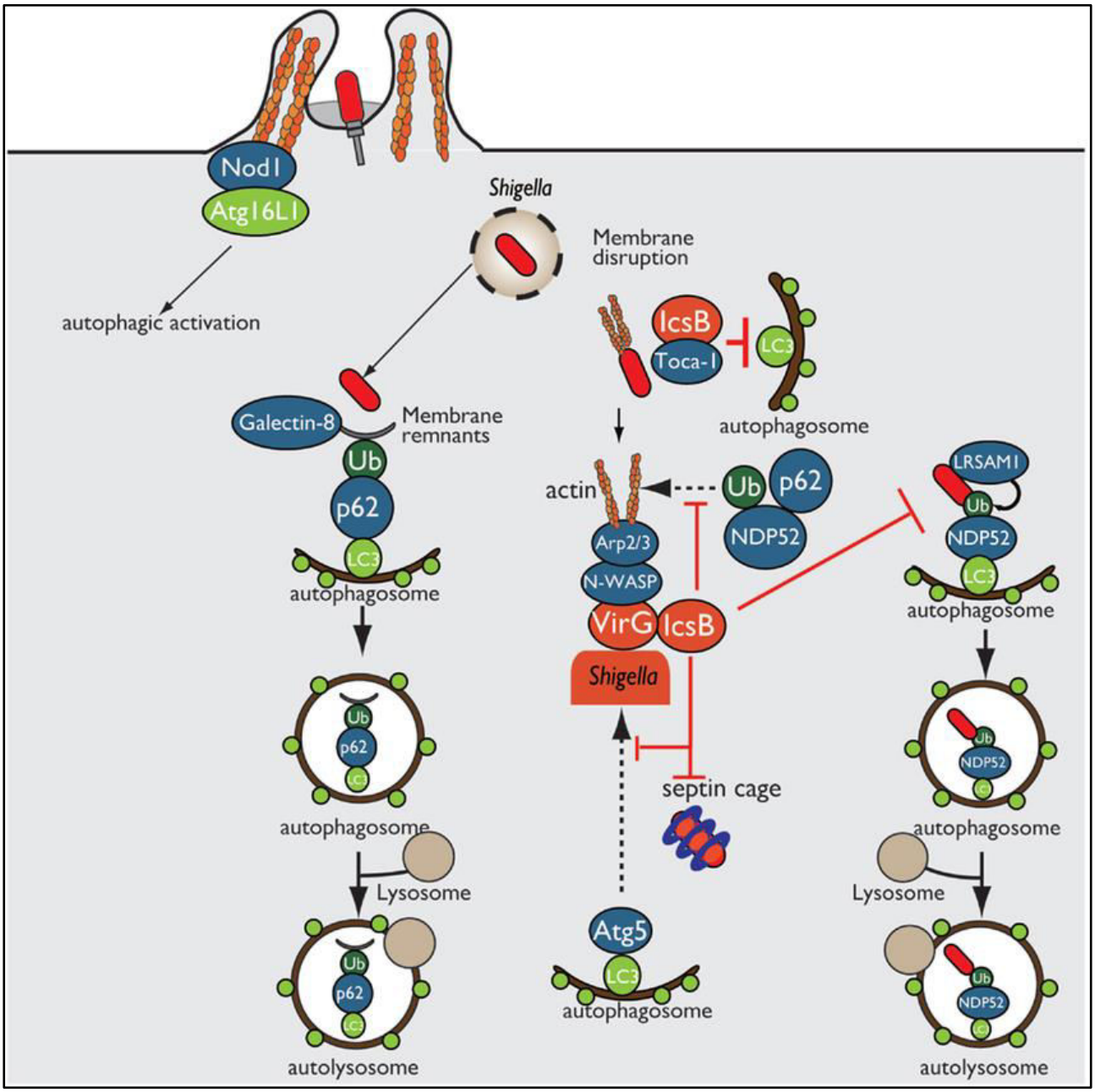

Fig10. *Shigella flexneri* prevents host autophagy (Source: 10.3389/fimmu.2015.00219)

Formation of autophagosome can be initiated after recognition of bacterial virulence protein IcsA by host protein ATG5. Binding of ATG5 to tectonin beta-propeller repeat containing 1 (TECPR1) promotes LC3 recruitment. Several effector proteins inhibit autophagic recognition. As an example, IcsB binds to IcsA and inhibits its binding to ATG5. VirA is another effector protein that intervenes the autophagy machinery. Additionally, *S. flexneri* can directly interfere with the autophagic machinery by producing VirA (Campbell-Valois et al., 2015). VirA disrupts ER-golgi trafficking through inactivation of GTPase Rab1 resulting in reduced autophagosome formation. On the other hand, septin caging leads to p62, NDP52 and LC3 recruitment to surrounding *S. flexneri* present in cytosol. Septin induces formation of cage like structure surrounding *S. flexneri* which gets targeted to autophagy.

Although strong defence mechanisms of host cells to counteract infection exist, *S. flexneri* still evades host autophagy machinery by several strategies. Nucleotide-binding oligomerisation domain (NOD)-like receptor present in cytosol gets activated after sensing bacteria intracellularly. It recognises peptidoglycan and initiates restriction of bacterial survival. It induces transcription of several pro-inflammatory genes. NOD1 and NOD2 links host sensing of bacteria with autophagy. Recruitment of several human GBPs (hGBPs) takes place with bacteria present in cytosol (Wandel et al., 2017). Virulence factor of *S. flexneri*, IpaH9.8 is a E3 ubiquitin ligase which reduces function of GBP and initiates its proteasomal degradation**.** Thus, *S. flexneri* hijacks host cytoskeleton and facilitates its cell to cell spread.

9.2. IpaH9.8, a major virulence factor

Pathogens play antagonistically to major cellular proteins for evading host defense mechanism. GBPs (Guanylate Binding Protein) play important roles in innate immunity, so several strategies were developed by the pathogens against GBP activation. Several proteins of IpaH family could be found in pathogenic bacteria like *S. flexneri* as well as *Salmonella*. Two domains present in IpaH proteins are N-terminal Leucine-rich repeat (LRR) domain and a C-terminal novel E3 ligase (NEL) domain. HECT family of E3 ligases are not related structurally to NEL domain. This domain forms ubiquitin-thioester intermediate thus inducing ubiquitination. Ubiquitination and degradation of GBPs are majorly involved in suppressing host defense machinery leading to induced replication of intracellular *S. flexneri* **(fig11).** The mechanism of GBP degradation by IpaH9.8 is widely studied. From the crystallographic structure analysis of IpaH9.8, specific GBP recognition site was determined. Mutation of that site diminishes the GBP binding ability of IpaH. NF-κB (nuclear factor κB) plays a major role in several cellular processes, including the inflammation and immune responses. IKK (IκB kinase) complex regulates its activation by IκBα degradation. During multiplication of *Shigella flexneri* within epithelial cells peptidoglycans are released. Nod1 recognises the peptidoglycan and stimulates NF-κB pathway, thus activating inflammatory response (Ashida et al., 2010). IpaH9.8 dampens the NF-κB-mediated inflammatory response. IpaH9.8 interacts with NEMO/IKKγ and ABIN-1, a ubiquitin-binding adaptor protein which promotes ABIN-1-dependent polyubiquitylation of NEMO. Polyubiquitylated NEMO undergoes proteasome-dependent degradation, resulting in NF-κB activation. Thus, polyubiquitylation and degradation of NEMO during *S. flexneri* infection is a new bacterial strategy to modulate host inflammatory responses. **(fig12).**

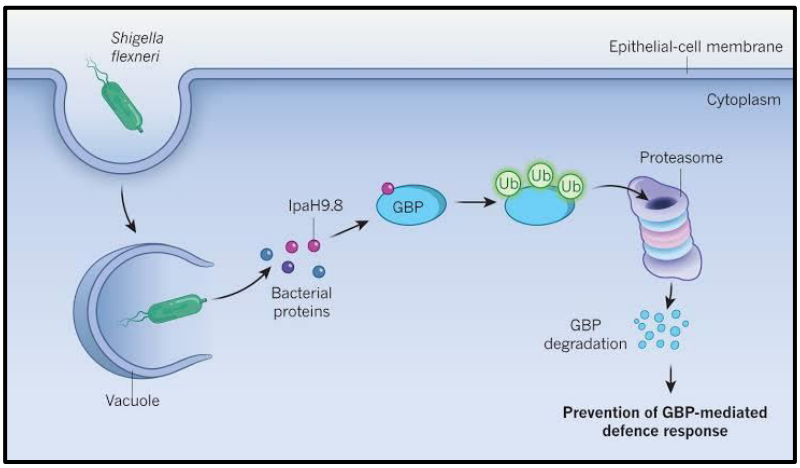

Fig11. Degradation of GBPs by ipah9.8 (Source: 10.1038/nature24157)

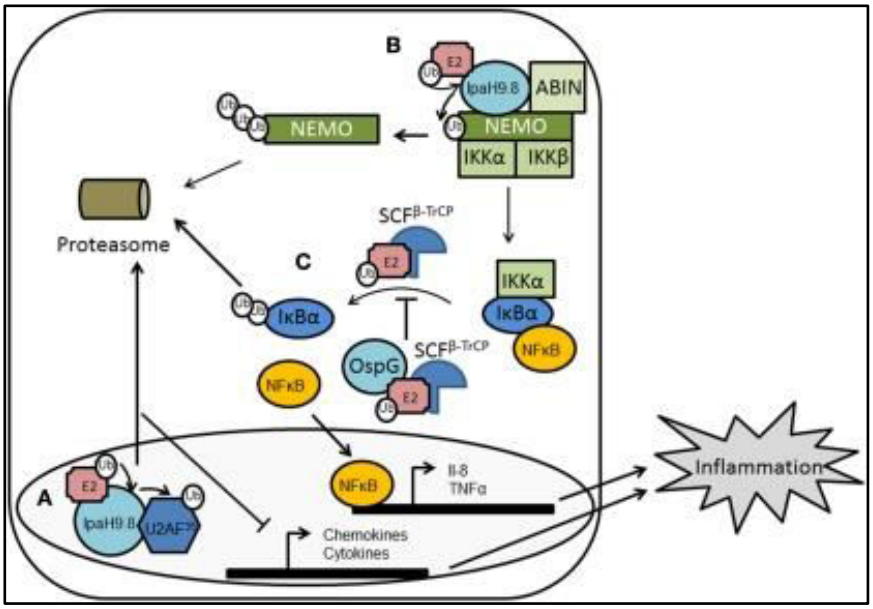

Fig12. Manipulation of host defense pathway by ipah9.8 (Source: 10.3389/ fmicb.2011. 00143)

9.3. Host Proteins involved in *S. flexneri* autophagy

The intracellular process for degradation of cytosolic materials and their delivery to lysosome is known as macroautophagy, which is also popular as autophagy. Autophagy is involved in wide range of microbial infection. Selective delivery of bacteria engulfed cargo is mediated by autophagy receptors **(fig13).** There are several autophagy receptors. p62 is one of the major proteins among them which belongs to SLRs (sequestosome 1/p62-like receptors) group. Removal of intracellular degraded bacteria like *Shigella flexneri, Salmonella, Mycobacterium* is a major example of bacterial autophagy which is also called xenophagy. Among them, some bacteria can avoid degradation mediated via autophagy. On the other hand, some other bacteria exploit the host autophagy mechanism leading to survival of bacteria intracellularly **(fig14).**

S. flexneri can invade intestinal epithelial cells. Cell induced septin cage-like structure formation surrounding *S. flexneri* leads to p62 mediated autophagy. Septin, a GTP binding protein induces filamentation as well as ring formation. This is a component of cytoskeleton helping in scaffolding autophagy machinery surrounding actin-polymerizing bacteria.

A number of infection models in *in vivo* system have been established for exploring immune response of cells against *S. flexneri*. The zebrafish model has evolved as a non-mammalian vertebrate model for studying shigellosis. Translucent zebrafish larva is used for *in vivo* imaging. The lethal dose of *S. flexneri* infection has been determined in zebrafish model, the kinetics of infection has also been studied. This model is also being used to study autophagy during bacterial infection. Depletion of p62 mediated autophagy increases intracellular

bacterial burden. Intracellular burden of *S. flexneri* led to increased mortality in autophagy deficient zebrafish model.

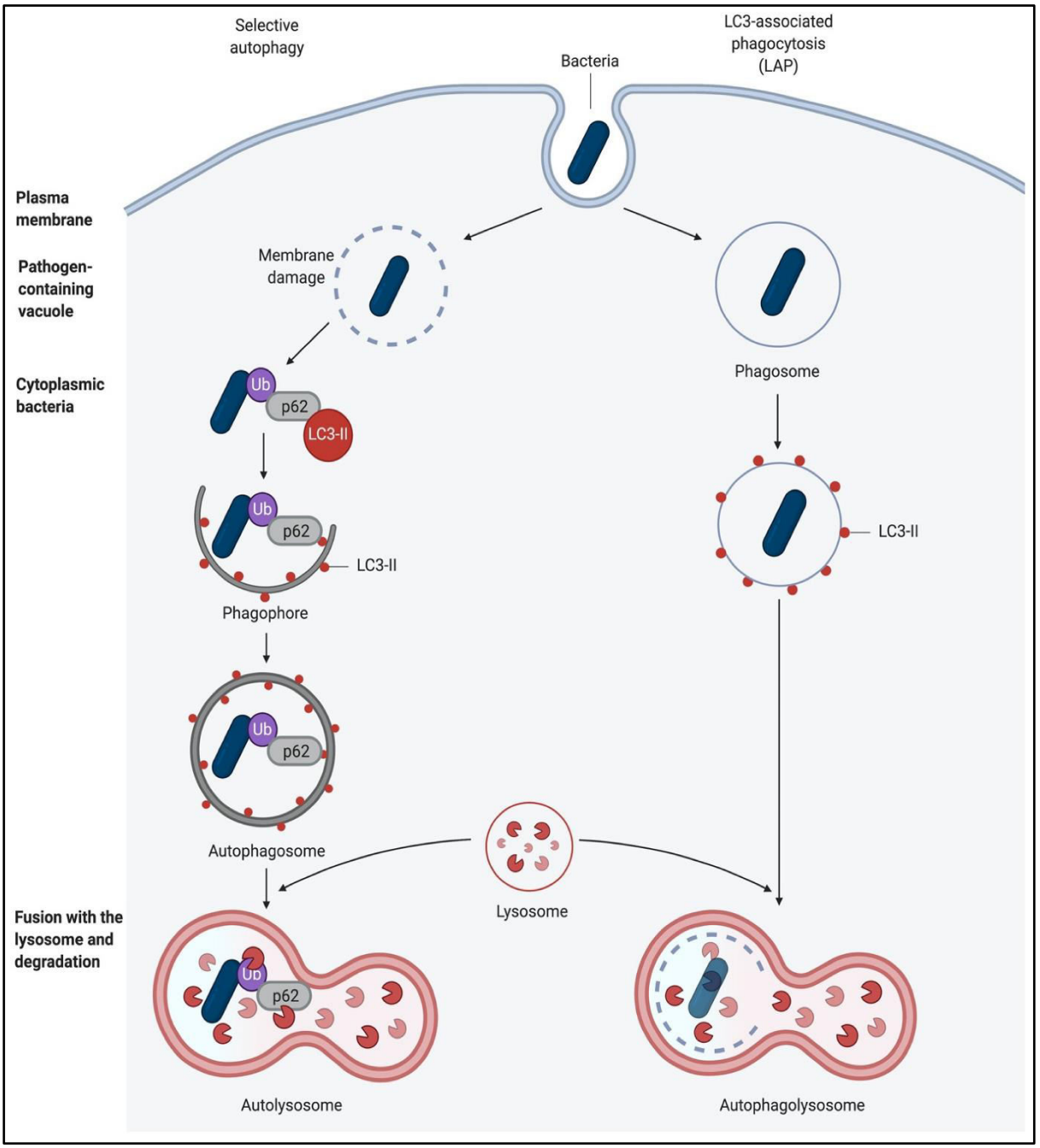

Fig13. Autophagic elimination of invading bacteria (Source: 10.3390/ pathogens10020110)

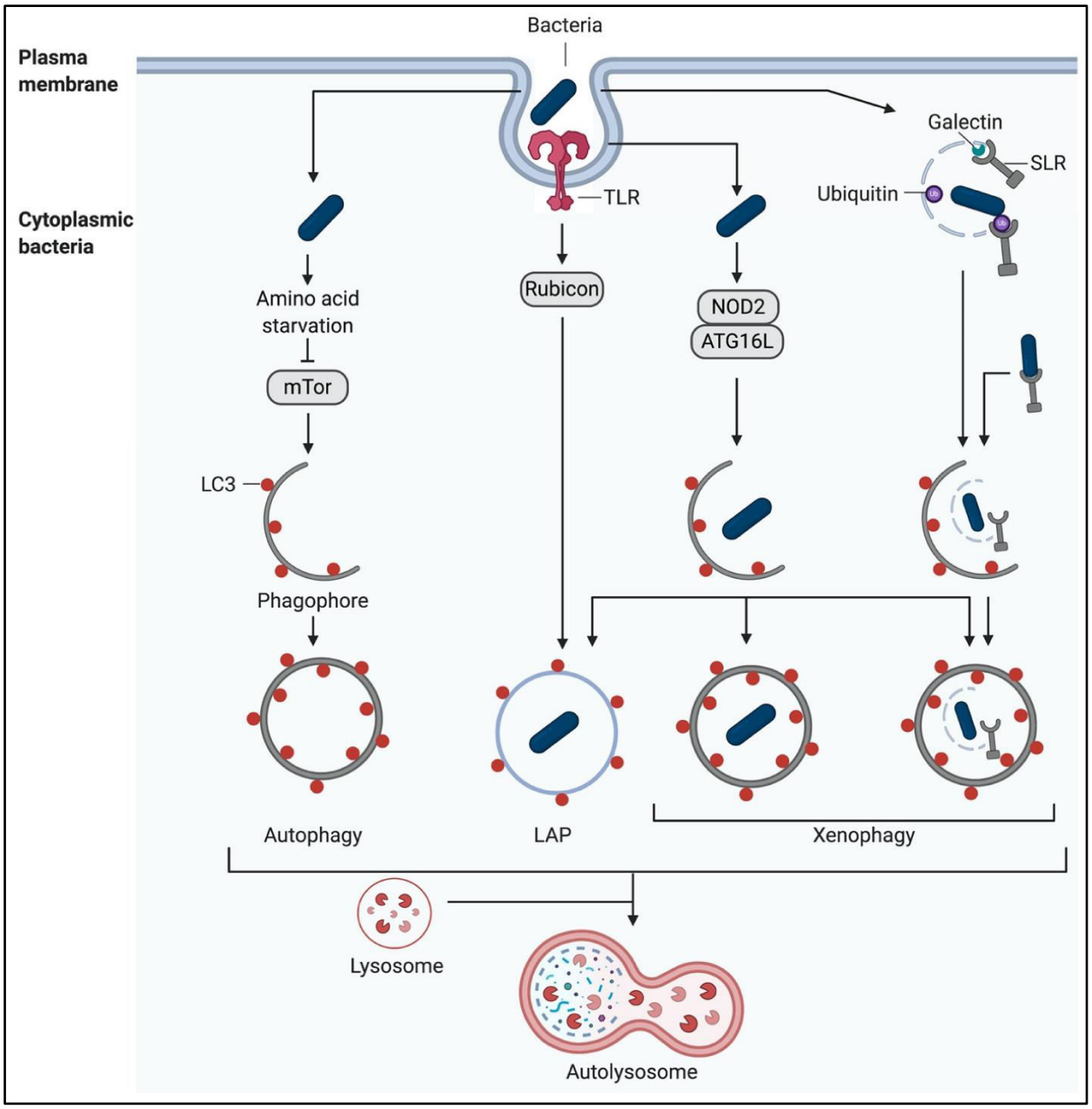

Fig14. Autophagy as an antibacterial defence mechanism (Source: 10.3390/ pathogens10020110)

10. Transcription factors in autophagy

In autoimmune disorders as well as in cancer several stress responsive transcription factors e.g., NFkB, P53 etc. are involved. P53, a multifunctional tumor suppressor protein is involved in autophagic regulation. In cardiomyocytes, FOXO1 and FOXO3 regulate autophagy which may be used as a therapy for several cardiovascular diseases. Starvation of

cardiomyocytes leading to dephosphorylation and nuclear localisation of FOXO induces autophagy (Sengupta, Molkentin and Yutzey, 2009). On the other hand, GATA4 inhibits autophagy in doxorubicin treated cardiomyocytes (Kobayashi et al., 2010). TFE3 (belongs to MIT/TFE family of transcription factors) induces lysosomal biogenesis leading to autophagy. Starvation and several external factors dephosphorylate TFE3 and induce its nuclear localisation resulting in therapeutic effects (Martina et al., 2014). On the contrary, ZKSCAN3 (zinc finger with KRAB and SCAN domains) inhibits lysosomal biogenesis and autophagy (Chauhan et al., 2013).

10.1. TFEB

TFEB is a major transcriptional regulator of autophagy-lysosomal pathway (ALP). Expression of autophagy and lysosomal biogenesis-related genes are regulated as well as autophagosome formation, autophagosome-lysosome fusion is promoted by TFEB. Intracellular substrate clearance through lysosomal exocytosis is promoted by TFEB. Genes of Lysosomal Expression and Regulation (CLEAR) network are transcriptionally upregulated which results in lysosomal biogenesis (Sardiello et al., 2009) **(fig15).** Immunofluorescence studies have shown that overexpression of TFEB increases the number of autophagosomes in HeLa cells. On the other hand, siRNA transfection decreases autophagy by reducing LC3II level both in presence and absence of bafilomycin, an autophagy inhibitor (Settembre et al., 2011). Lysosomal $Ca^{2}+$ signalling is involved in activation of TFEB. Calcineurin gets activated by Lysosomal $Ca^{2}+$ release through mucolipin 1 (MCOLN1) leading to TFEB dephosphorylation and nuclear translocation. Thus, lysosome is identified as a hub for maintenance of cellular homeostasis (Medina et al., 2015). The mammalian target of rapamycin (MTOR), protein kinase complex (MTORC1), transcriptional regulator of

autophagy phosphorylates TFEB at Ser211 and enhances its cytoplasmic retention in association with members of the YWHA (14-3-3) family of proteins. Inhibition of MTORC1 results in dissociation of this complex and TFEB nuclear translocation. Under nutrient enriched condition, active MTORC1 inhibits ATG proteins. In starved condition, MTORC1 dissociates from ULK complex which leads to induction of autophagy. MAP4K3 phosphorylates and inhibits TFEB nuclear translocation (Hsu et al., 2018). TFEB overexpression is a potential therapeutic strategy for treatment of osteoarthritis (Zheng et al., 2018). *S. aureus* infection activates TFEB which in turn induces pro-inflammatory cytokine release (Visvikis et al., 2014). In both *in vitro* and *in vivo* conditions, acacetin activates TFEB and reduces intracellular *S. typhimurium* load (Ammanathan et al., 2020). Peroxisome proliferator–activated receptor α (PPAR-α) activates innate immune response via TFEB activation in host macrophages during mycobacterial infection (Kim et al., 2017). During phagocytosis of Gram-positive or -negative bacteria NOX/PHOX (NADPH oxidase)-dependent oxidative burst plays a major role in TFEB nuclear translocation. In TFEB knockout cells pro-inflammatory cytokine release after bacterial infection was absent. Upon pathogen infection, mTORC1 is inhibited and TFEB is activated by inducing amino acid starvation pathway.

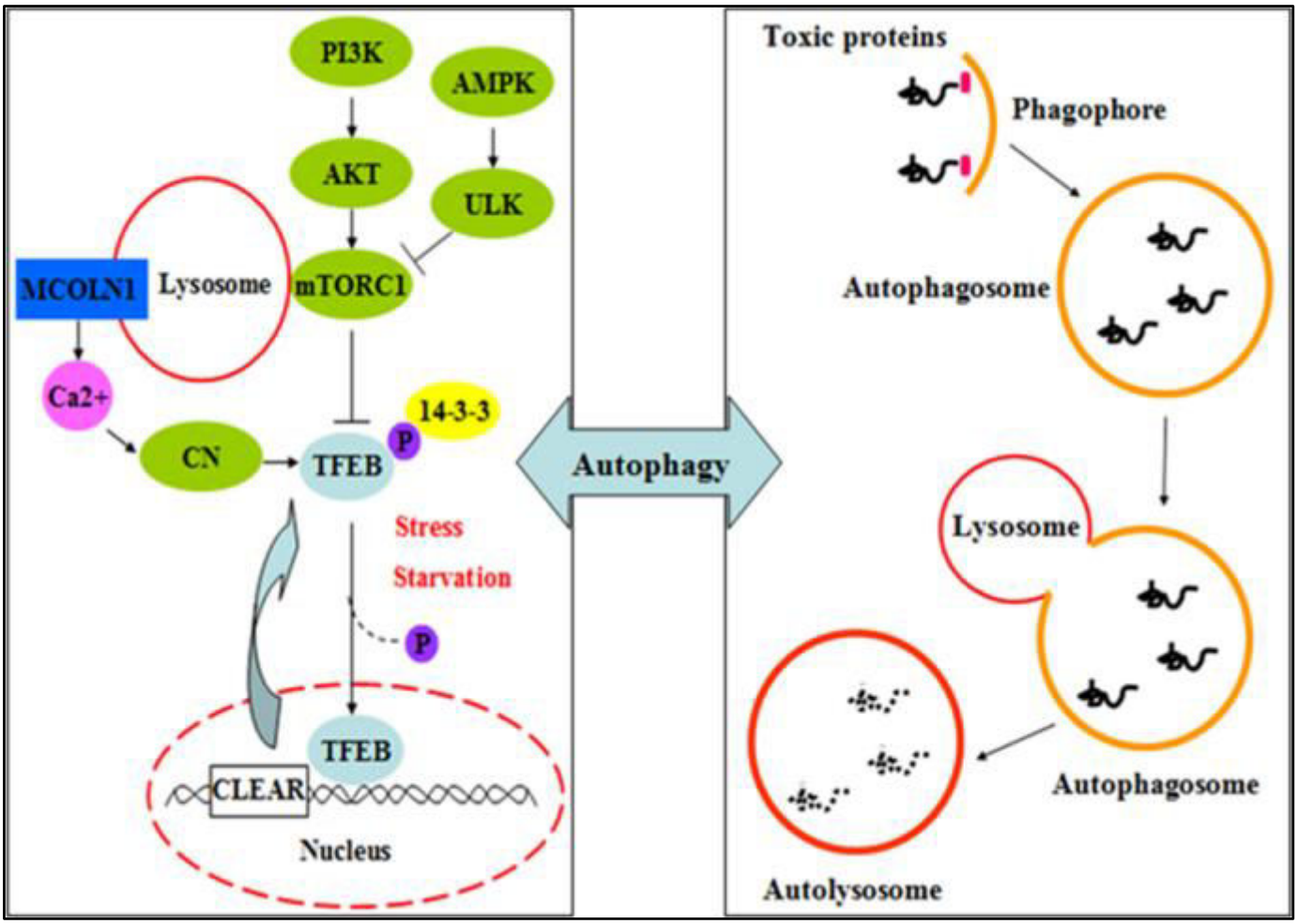

Fig15. Regulation of TFEB (Source: 10.1186/s13020-020-00402-1)

10.2. ZKSCAN3

ZKSCAN3 (ZNF306) is a zinc finger transcription factor with Kruppel-associated box (KRAB) and SCAN domains, known for its role as a transcriptional repressor. It plays a crucial part in cell proliferation, apoptosis, nucleolus maintenance, and neoplastic transformation. Studies have identified ZKSCAN3 as a driver of colon cancer cell proliferation, and silencing leads to increased autophagy and cellular senescence. ZKSCAN3 also regulates the expression of over 60 genes involved in autophagy and lysosomal biogenesis/function. ZKSCAN3 represses transcription of more than 60 genes that are part of

the autophagy pathway, including ULK1, LC3, and DFCP. Protein kinase C (PKC) can inactivate ZKSCAN3 by phosphorylating it and exporting it out of the nucleus. In certain neurodegenerative diseases like Parkinson's disease (PD), the A30P mutant α-synuclein has been shown to suppress autophagy by enhancing ZKSCAN3 activity through the inhibition of JNK signaling in ventral midbrain DA neurons (Yang et al., 2008).

Oxidative stress, caused by excessive reactive oxygen species (ROS) production or reduced antioxidant defenses, damages cellular processes. NAD, including NAD+ and NADH, plays a vital role in mitochondrial function and redox homeostasis. Sirtuin1 (SIRT1), an NAD+-dependent deacetylase enzyme, is known to promote neuronal survival, mitochondrial homeostasis, and redox balance. It also helps in preventing aspects of aging-related mitochondrial dysfunction. SIRT1 plays a role in autophagy regulation by deacetylating key autophagy-related genes (ATGs) such as ATG5, ATG7, LC3, and autophagy-related transcription factors like FOXOs and TFEB. Dysregulation of autophagy and these factors has been implicated in various cellular processes and neurodegenerative diseases, including PD. SIRT1 activation enhances the expression of autophagy-related genes and promotes the translocation of ZKSCAN3 out of the nucleus **(fig16).**

Curcumin, a bioactive compound found in turmeric, has been shown to protect against oxidative stress-induced damage and ischemia-reperfusion injury. It exerts its effects partly through the activation of SIRT1 signaling, which helps in maintaining mitochondrial function and reducing oxidative damage. Post-translational modifications (PTMs) play a crucial role in regulating the nuclear-cytoplasmic shuttling of transcription factors. SIRT1-mediated deacetylation of ZKSCAN3 is an example of such PTMs, leading to its translocation out of the nucleus.

ZKSCAN3 is a key transcription factor involved in regulating autophagy and cellular processes (Wu et al., 2022). Understanding these molecular pathways could potentially pave the way for therapeutic interventions in neurodegenerative and other diseases.

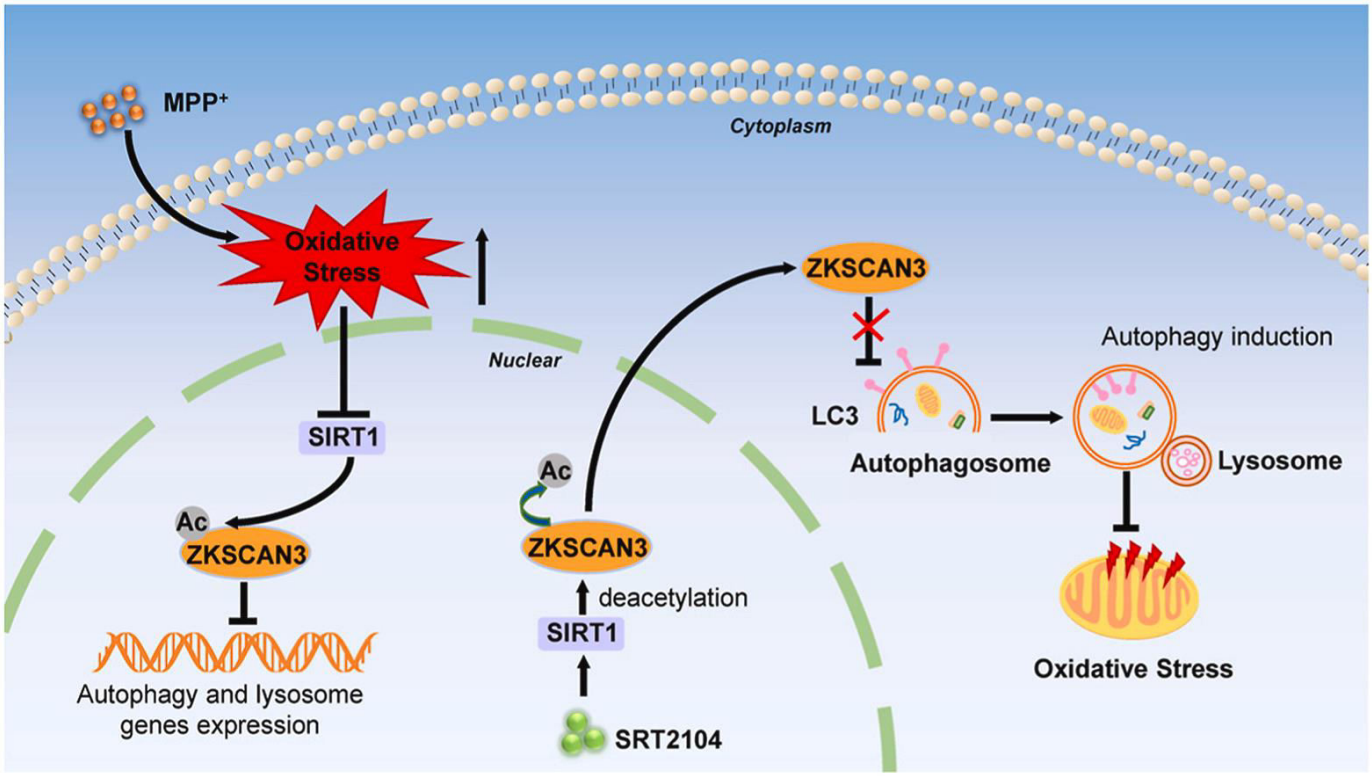

Fig16. Regulation of ZKSCAN3 (Source: 10.1016/j.freeradbiomed.2022.02.001)

11. Autophagy for intracellular pathogen defense

Xenophagy refers to the specific targeting of pathogens through autophagy, a major defense mechanism against various infections (Deretic, Saitoh and Akira, 2013). Noncanonical types of autophagy rely on specific components of the autophagy process, contributing to defense

against intracellular pathogens. One example is LC3-associated phagocytosis (LAP), a subset of ATG proteins that aids in breaking down engulfed pathogens. Numerous ATG proteins play a role in the immune response against pathogens like *Mycobacterium tuberculosis* and *Toxoplasma gondii*, triggered by IFNγ (Bradfute et al., 2013; Sturge and Yarovinsky, 2014).

After entering, the cell engulfment of bacteria by host cell membrane occurs. That results in a single-membrane pathogen-containing vacuole which matures and fuses with the lysosome finally forming a phagolysosome. This process is called phagocytosis. For evading this process and facilitation of their survival and replication intracellularly, several bacteria (e.g., *Salmonella, Mycobacterium etc.*) performs adaptation or modulation of the phagosome, leading to inhibition of autophagosomal and lysosomal fusion (Baxt, Garza-Mayers and Goldberg, 2013). *S. flexneri* escapes the vacuole and hijacks host defense mechanism leading to intracellular spread and survival. mTORC1 negatively regulates the ULK1 complex. During canonical pathway of autophagy, initiation genes like ATG14, ULK1, and ULK2 upregulates the downstream ATG5/ATG12/ATG16L1 complex and leads to LC3-I to LC3-II conversion.

12. Treatment

People infected with *Shigella flexneri* are recommended to drink plenty of water for prevention of dehydration. Anti-diarrheal medication e.g., loperamide (Imodium) is provided to people with bloody diarrhoea. Antibiotics e.g., ciprofloxacin and azithromycin are majorly recommended as oral antibiotics. According to WHO guidelines, ciprofloxacin is used as first line of treatment on the other hand ceftriaxone and azithromycin are used as second line of treatment. **(fig17).**

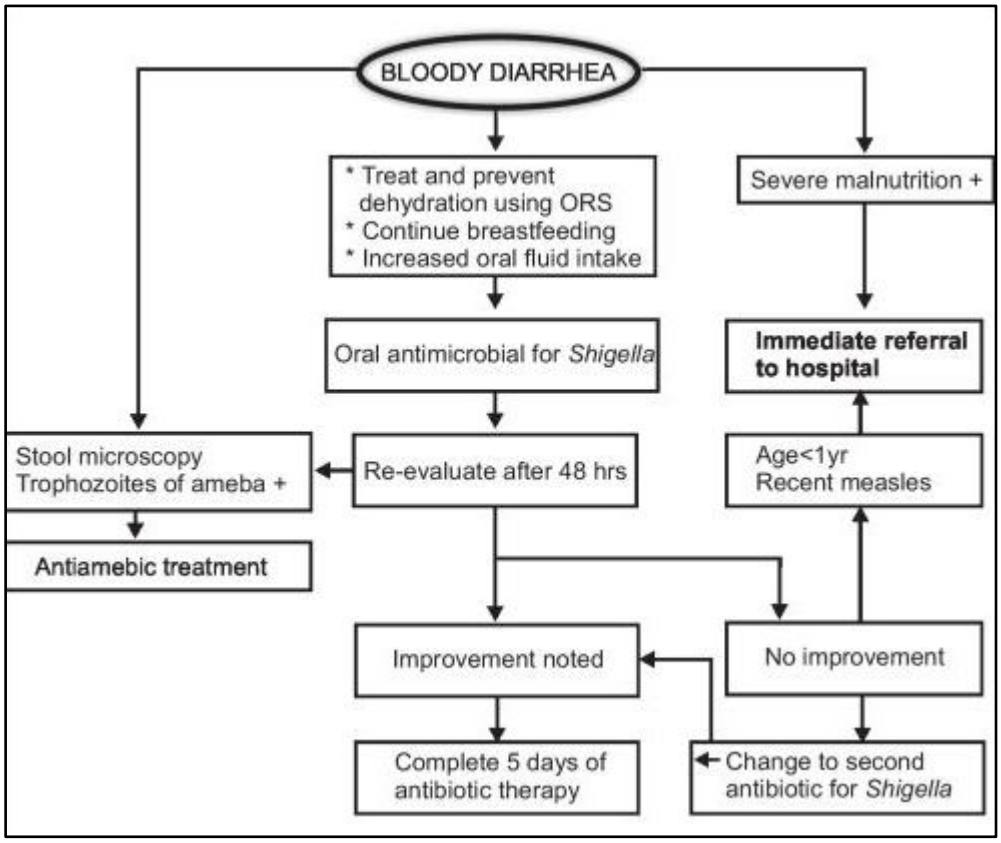

Fig17. Flow chart of treatment of shigellosis (Source: 10.5005/jp/books/10706/2)

13. Antibiotic resistance

Nowadays antibiotic resistance is one of the biggest problems for global health irrespective of age and country. Resistance of bacteria to antibiotics is a natural phenomenon but continuous misuse of antibiotics is leading to acceleration of the same. It may lead to stay in the hospital for long time, enhance medical costs and increase rate of mortality. Prevention and treatment of bacterial infections prevail with antibiotics. Resistance to antibiotics takes place due to excessive use of antibiotics **(fig18).** There are several mechanisms leading to resistance. Cell wall modification, activation of drug-inactivating enzyme, modification of drug target and activation of efflux pump majorly contributes towards antibiotic resistance of bacteria. Resistance profile of *S. flexneri* towards antibiotics is shown in tabular form **(fig19)** (Hossein et al., 2016). Samples isolated from stool were diagnosed and *S. flexneri* was emerged as the most prevalent strain causing shigellosis.

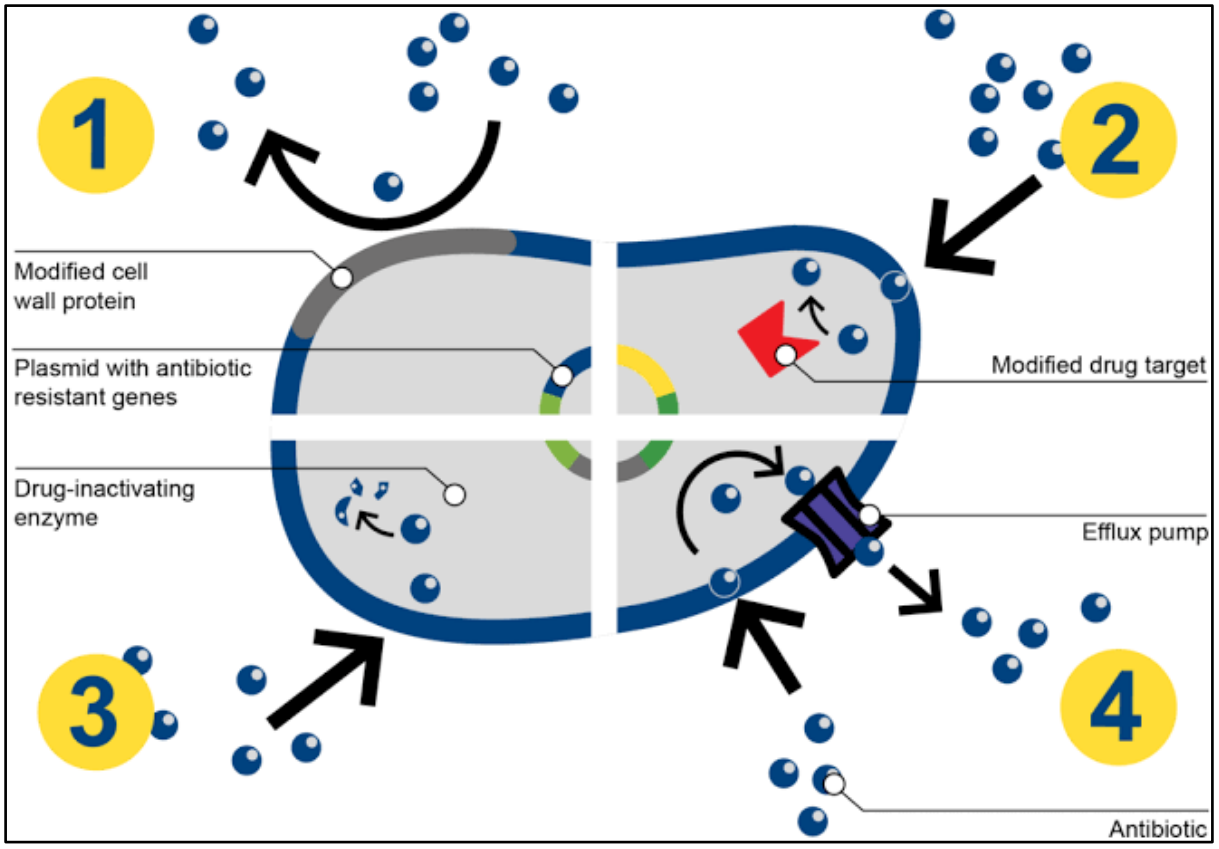

Fig18. Mechanism of antibiotic resistance (Source: The internet)

Antibiotic	*S. flexneri* No. (%)
Trimethoprim-sulphamethoxazole	27(87.1)
Ampicillin	29(93.5)
Tetracycline	22(71)
Chloramphenicol	20(64.5)
Gentamicin	1(3.2)
Ceftriaxone	11(35.5)
Cefotaxime	13(41.9)
Aztreonam	11(35.5)
Nalidixic-acid	8(25.8)
Ofloxacin (5µg)	3(9.7)

Fig19. Antibiotic resistance profile of *S. flexneri* (Source: Gastroenterol Hepatol Bed Bench 2016;9(3):205-210)

14. Host directed therapy

Host directed therapeutic approaches are gradually becoming effective for antimicrobial treatment and this is a potential weapon against drug resistant bacteria. In Host Directed Therapy (HDT) use of several drugs, small molecules, vitamins, cytokines as well as immunomodulators are used to overcome the exploitation of host pathways by pathogen. The principle of HDT is interference with host cell factors required for survival of pathogen **(fig20).**

HDT is effective in several infectious diseases like tuberculosis, sepsis, AIDS, chronic viral hepatitis, fungal infections like aspergillosis etc. (Kaufmann et al., 2018) (Forn-Cuní et al., 2023). In case of multi-drug resistant (MDR) or extremely drug resistant (XDR) *Mycobacterium tuberculosis* (Mtb) affected patients, stimulation of immune response is possible using host directed therapy (Khoza et al., 2022). Mtb inhibits autophago-lysosomal fusion thus enhances its intracellular survival. Expression of LL-37, a host defense peptide is induced by 4-phenylbutyrate (PBA) and/or vitamin D3 (vitD3) is an example of host directed

therapy in tuberculosis (Rekha et al., 2018; Rekha et al., 2015). HDT acts as an adjunctive therapy instead of directly targeting the pathogen. Host-directed therapies can counter antimicrobial resistance through activating autophagy and apoptosis as well as inducing oxidative stress leading to triggered adaptive immune response.

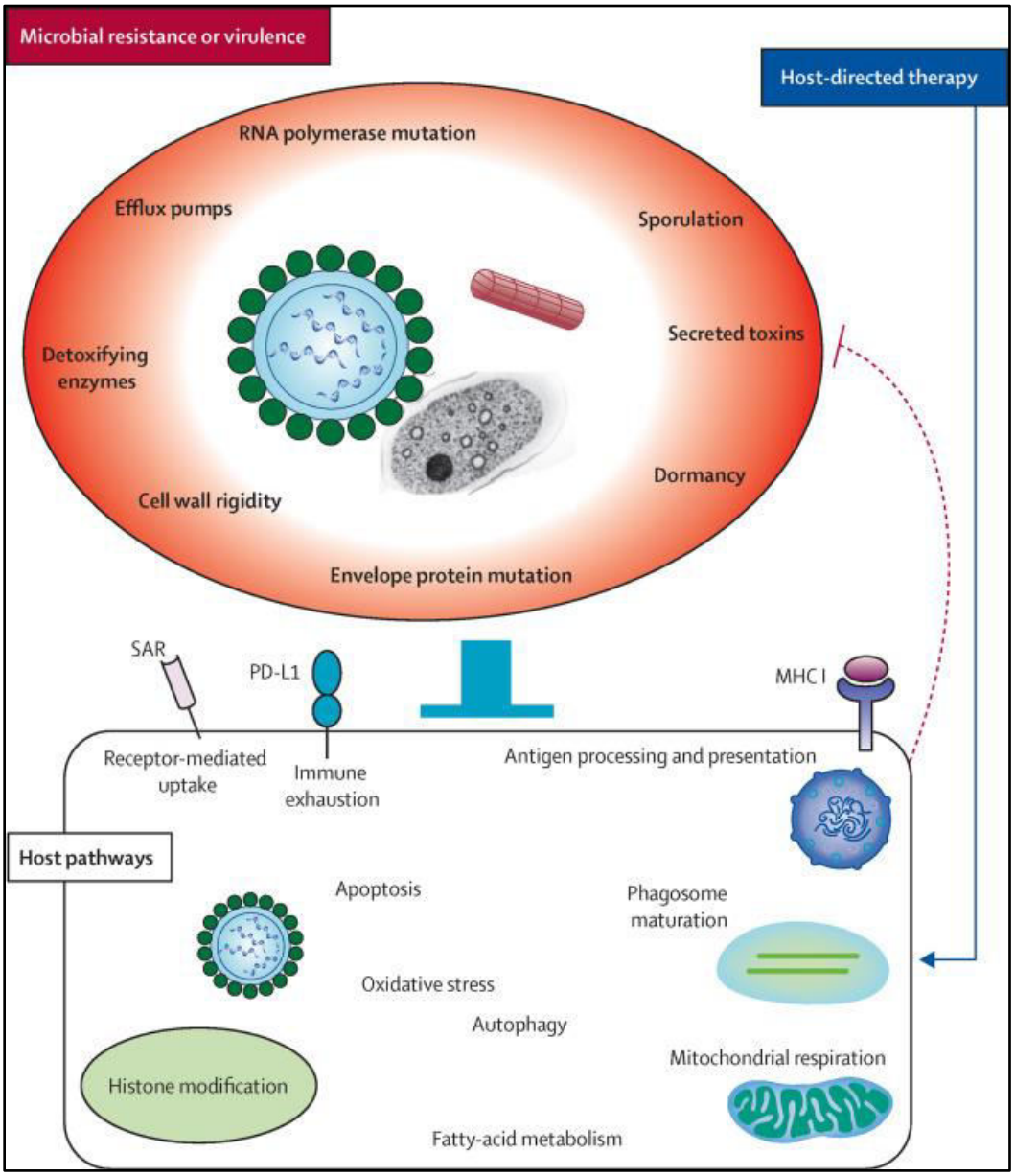

Fig20. Host directed therapeutic approaches (Source:10.1016/S1473-3099(16) 00078-5)

15. Herbal compounds in host directed therapy

There are several immunomodulatory herbal compounds e.g., mangiferin, curcumin, quercetin, glycyrrhizin etc. which are involved in host directed therapy in tuberculosis (Mvubu and Chiliza, 2021). Pasakbumin A, isolated from *Eurycoma longifolia* which is a shrub-tree of southeast Asia induces autophagy by ERK activation (Lee et al., 2019). COVID-19 can be treated post exposure with the help of host directed therapy using anti-inflammatory and immunoregulatory agents (ex: *Tanacetum parthenium*) and anti-complement agents (ex: *Citrus aurantium*). Acacetin works against *Salmonella* by inducing autophagy (Ammanathan et al., 2020). Asiatic acid, a herbal compound of *Centella asiatica* induces antimicrobial peptide gene expression to induce antibacterial activity against *S. flexneri* (Maitra et al., 2023). Prevention of *Helicobacter pylori* is also reported by treating mice with glycyrrhizin, active component of liquorice root (Khan et al., 2023).

16. Capsaicin

Among several herbal compounds involved in host directed therapy Capsaicin is one of them. Capsicum is a popular culinary spice worldwide. Pharmacological study of capsicum started early in 19th century. In 1876 crystallisation of active compound of capsicum was first successfully done by Thresh and named as Capsaicin. In 1919, Nelson determined the chemical structure which is 8-methyl-N-vanillyl-trans-6-nonenamide **(fig21).** It is the primary compound responsible for pungency of red pepper. In 1878 Endre Ho″gyes published pharmacological effects of Capsaicin which included induction of gastrointestinal mobility, reduction of body temperature etc (Gavva, 2008).

Fig21. Source and molecular structure of Capsaicin (Source: The internet)

Pungency of chilli peppers is measured in Scoville heat units (SHU) depending upon the concentration of Capsaicinoids among which Capsaicin is the major component. This scale is known as Scoville scale. According to the Scoville heat scale pure Capsaicin has a value of 15,000,000 Scoville Heat Units (SHU) **(fig22).**

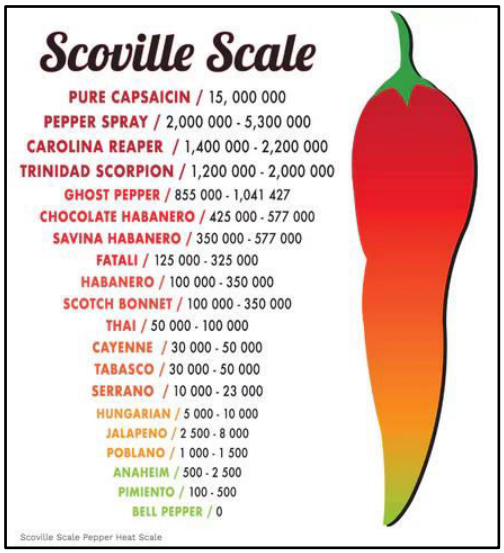

Fig22. Scoville scale of pungency (Source: The internet)

16.1. Bioavailability and metabolism of Capsaicin

Capsaicin is primarily (85-95% of orally administered Capsaicin) absorbed in gastrointestinal lumen. Capsaicin is majorly metabolised in the liver. From HPLC data it has been observed that at 1 hour after administration, blood and intestine display maximum amount of Capsaicin (Banerjee et al., 2021). At 3hour and 6hour, liver and kidney show peak concentrations respectively **(fig23).** About 24.4% of Capsaicin localizes in tissues after 1 hour of oral administration. The amount drops down to 1.24% in 24 hours and 0.057% in 48 hours. Within 4 days Capsaicin is completely metabolised in those tissues. The half-life of Capsaicin in the blood is 25 minutes. The highest concentration of Capsaicin in plasma was noted to be 2.5 ng/mL(~8.2 nM) at 45 minutes. After 105 minutes, no Capsaicin was detected in the blood. Oral bioavailability of Capsaicin loaded microemulsions was 2.64 times faster compared to free Capsaicin.

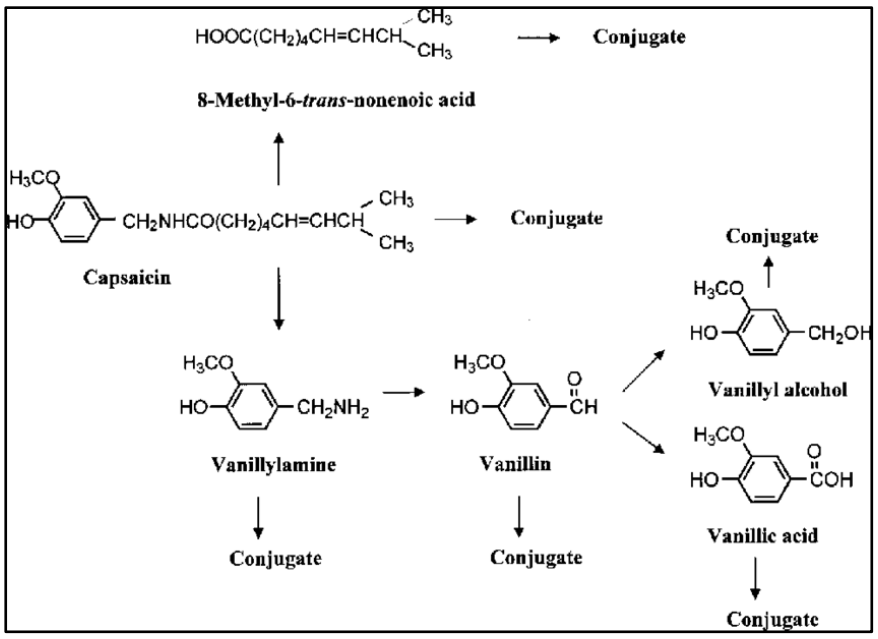

Fig23. Metabolism of Capsaicin (Source : 10.1248/jhs.52.660)

16.2. Pharmacology of Capsaicin receptor

The Capsaicin receptor is known as the transient receptor potential vanilloid type 1 ion channel (TRPV1). This receptor is linked to sensations of pain and the inflammatory response. Capsaicin produces its biological effects through activating TRPV1 receptor. Intake of Capsaicin via oral route produces burning sensation and increased bowel movements. There are several other TRPV1 activating plant derived compounds e.g., Allyl isothiocyanate from genus *Brassica* and camphor from *Cinnamomum camphora*. It is also activated by acidic pH and several external stimuli like heat and pressure. There are several competitive and non-competitive inhibitors of TRPV1 binding site of Capsaicin. Capsazepine which is a synthetic antagonist of Capsaicin (Bevan, 1999) inhibits TRPV1 currents induced by Capsaicin in sensory neurons (Szallasi and Blumberg, 1989) **(fig24).** Capsazepine at 500nM concentration (Bevan et al., 1992) reduced Ca^{2+} uptake by binding with transmembrane domain of TRPV1 receptor in a competitive manner (Hellmich and Gaudet, 2014).

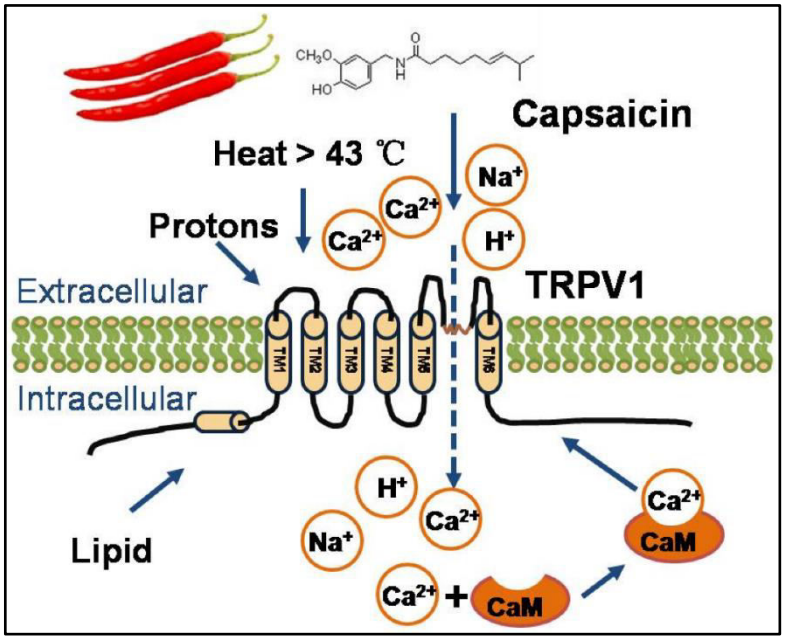

Fig24. Pharmacology of TRPV1 receptor (Source: doi.org/10.3390/nu8050174)

16.3. Capsaicin therapeutic effects:

Capsaicin plays major role in thermoregulation, antinociception, gastroprotection, cancer, obesity, and osteoarthritis pain management **(fig25).** Capsaicin is involved in thermoregulation by activating cutaneous warm receptors. Hypothermic effect of Capsaicin was abolished in TRPV1$^{-/-}$ mice (Szolcsányi, 2015). Polymodal nociceptors are activated by Capsaicin by depolarization of neuronal membrane. Blockage of C-fibre conduction as well as release of neuropeptides by topically applied Capsaicin represents anti-nociceptive role of Capsaicin (Dray, 1992). Capsaicin acts as a gastroprotective agent in non-steroidal anti-inflammatory drugs (NSAID) or *H. pylori* induced gastric ulcer (Mózsik, 2014). It induces indomethacin induced mucosal bleeding. Capsaicin alone or in combination with some drugs is effective in reducing several gastrointestinal disorders. Studies in genetically obese mice undergone high fat diet have shown that Capsaicin is responsible for attenuating metabolic dysregulation. Dietary Capsaicin induces expression of adiponectin and its receptor, AdipoR2, increases hepatic AMPK, reduce fasting glucose and triglycerides hence, validating its anti-obesity effect (Kang et al., 2011). Capsaicin is therapeutically potent for pain management (Anand and Bley, 2011). Generation of reactive oxygen species, mitochondrial membrane potential disruption, NFkB activation, induced intracellular calcium release results in apoptosis in cancer cells. Role of autophagy has also been elucidated in anti-carcinogenic role of Capsaicin. In nasopharyngeal cancer cells autophagy and apoptosis is induced by Capsaicin activated PI3K/AKT/mTOR pathway (Lin et al., 2017).

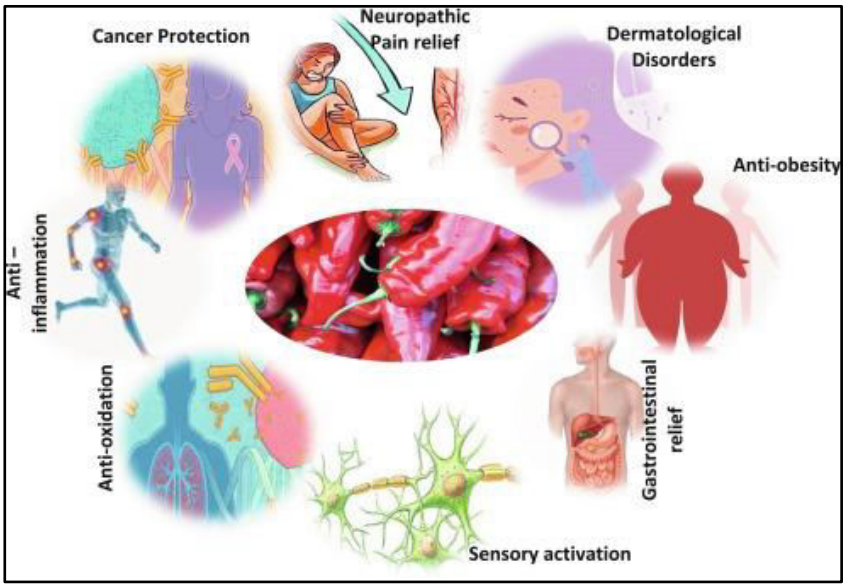

Fig25. Therapeutic effects of Capsaicin (Source:10.1016/B978-0-12-822923-1.00 025 -X)

17. Capsaicin in autophagy

Autophagy is induced by PI3K/AKT/mTOR pathway downregulation in human nasopharyngeal carcinoma cells during capsaicin treatment (Lin et al., 2017) **(fig26).** It induces LC3-II and Atg5 level and decreases expression of p62 and Fap-1. Translation of cyclin D1 was promoted by Akt. In MCF-7 breast cancer cells Capsaicin induces autophagy by inducing ER stress. Activation of p38 and deactivation of ERK led to LC3II induction by Capsaicin. Treatment of 3MA, an autophagy inhibitor is able to reverse these autophagic effects (Oh, Choi and Jung, 2010). Pharmacological or genetic downregulation of STAT3 inhibited Capsaicin induced autophagy in HepG2 cancer cells (Chen et al., 2016). In cholangiocarcinoma, Capsaicin induces autophagy as an adjuct therapeutic approach with common chemotherapeutic drugs via PI3K/AKT/mTOR pathway inhibition (Hong et al., 2015). Capsaicinoids are known as dietary chemopreventive agent. DihydroCapsaicin (DHC), an analog of Capsaicin induces

autophagy in a p53 independent manner (Oh et al., 2008) in human colon cancer cell line (HCT116).

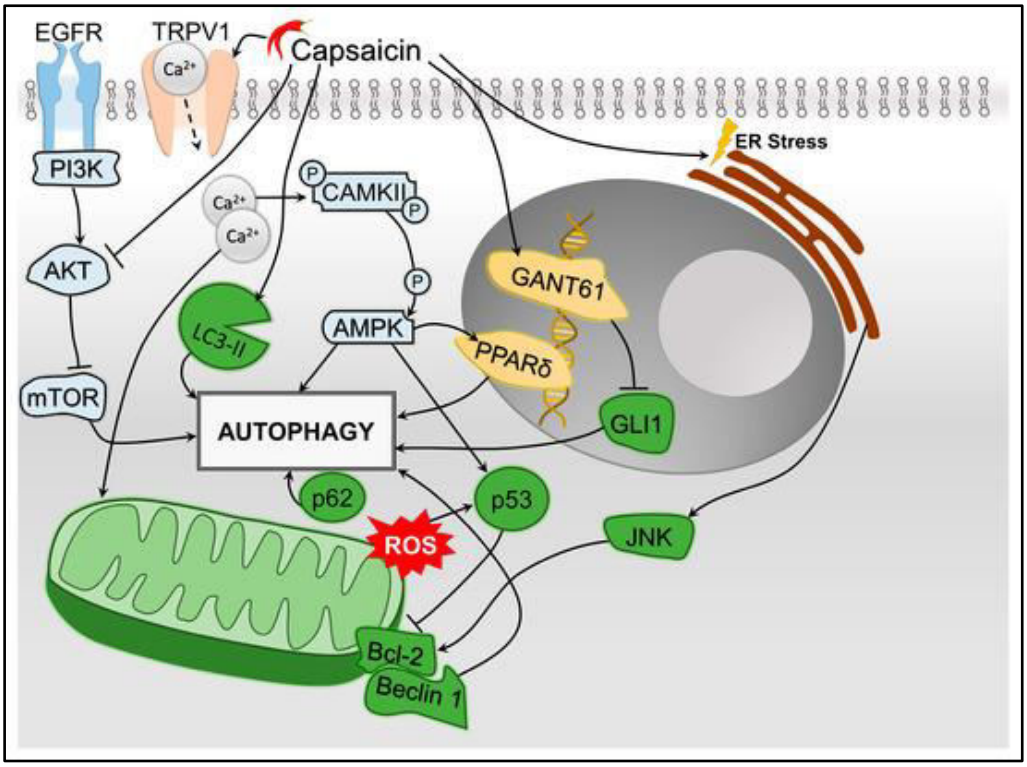

Fig26. Capsaicin in autophagy (Source: 10.3390/molecules24132350)

18. Synergistic effects of Capsaicin with antibiotics

Combination of phytochemicals with antimicrobial drugs is emerging as a potential therapeutic approach for increasing multidrug resistant strains of bacteria. In fluoroquinolone resistant *S. aureus,* Capsaicin in combination reduces MIC of ciprofloxacin almost 2-4 times. In Colistin-Resistant *Acinetobacter baumannii* infection Capsaicin in combination with antibiotics inhibited biofilm formation (Kalia et al., 2012). Capsaicin inhibits *H. pylori*

infection synergistically with metronidazole by reducing urease enzyme activity (Tayseer et al., 2020). In tetracycline resistant *Escherichia coli* Capsaicin induces the efficacy of tetracyclin and inhibits the activity of efflux pump AcrAB-Tol C of *E.coli*. In multidrug-resistant *Mycobacterium tuberculosis* infection combination of metformin, an existing frontline antibiotics and Capsaicin is a potential therapeutic approach (Vashisht and Brahmachari, 2015). Thus, combination therapy of Capsaicin with several antibiotics/drugs is gradually getting light as novel and affordable way to tackle multidrug-resistant bacteria.

SECTION 3

MATERIALS AND METHODS

Materials

Capsaicin and all antibiotics were purchased from Sigma-Aldrich Chemical company. Cell lines were purchased from ATCC. BCA (Bicinchoninic assay) kit and 4′,6-diamidino-2-phenylindole (DAPI) were purchased from Thermo Fisher Scientific, USA. ELISA kits were bought from Krishgen. Plasmid isolation kit, RNA isolation kit, Autophagy PCR array kit were purchased from Qiagen. TFEB transcription factor assay kit and ChIP kit were purchased from Ray Biotech and Millipore respectively. cDNA synthesis kit, CE-NE isolation kit, protease inhibitor and phosphatase inhibitor cocktail were purchased from ThermoFisher Scientific. Antibodies were purchased from Abcam (Cambridge, UK), Cell Signaling (Cell Signaling Technology Inc., Danvers, MA), U.S.A., Santacruz Biotechnology Inc. and BioBharti Life Sciences Private Limited, India. Prestained protein ladder, DNA ladder was obtained from BR Biochem LifeScience Pvt. Ltd., India. Ethanol, Methanol, Chloroform and dimethyl sulphoxide (DMSO) were bought from Merck. The DMEM, MEM, RPMI-1640, McCoys's 5A, antibiotics, non-essential amino acids, cell freezing media, Fetal bovine serum (FBS), trypsin-EDTA were purchased from GIBCO. LB, MHB and agar media were purchased from Himedia. All other chemicals, glass wares and plastic wares used in the study were of the highest experimental grade available and purchased from Sisco Research Laboratory.

Methods

1. Bacterial Strains

Shigella flexneri (sf2457T) serotype 2a, plasmid cured *Shigella flexneri* (sf2457T)2a and *Shigella flexneri* resistant strain (NA/CIP/NOR/OFX/TET/S/C/AM/E/ST) (BCH12702, BCH12654) were obtained from (Dr Asish Mukherjee and Dr. Hemanta Koley) NICED, Kolkata, India.

2. Culture conditions

Bacteria were routinely cultured in Mueller Hinton Broth (MHB) (Himedia) at 37°C incubator with shaker. Storage of all bacterial strains is in media containing 15 % (v/v) glycerol at -80°C. Bacteria were grown in MHB and for plates, 1.8% bacto agar was used. For selective plates, 0.01% (w/v) Congo red dye was added in MHB.

3. Broth Dilution assay

Broth dilution assay was performed in presence of DMSO as control, 16µM and 32µM Capsaicin in 3 separate flasks containing MHB. 10^9 *S. flexneri* from overnight culture was added into the flasks. $O.D._{600nm}$ was measured at regular interval and graphically represented.

4. Cell culture conditions

HT-29 (ATCC HTB-38) and murine macrophage cell RAW264.7 (ATCC TIB-71) were used during this study. HT-29 cells were cultured with McCoy's 5A Medium (Sigma-Aldrich) containing 10% heat inactivated FBS (Sigma, USA),1% non-essential amino acids and 1% penicillin-streptomycin (Himedia, India). Experiments were conducted with maximum 5-10

passage number. RAW264.7 cells were grown in RPMI1640 with 10% FBS and 1% penstrep. Experiments were conducted with maximum 3-5 passage number. Cells were maintained in a 37°C humidified incubator with 5% CO_2.

5. Invasion assay

Intestinal and macrophage cells were cultivated in 6-well plates and subjected to 24-hour incubation at 37°C with 5% CO_2 before infection. Following this, cells were cultured overnight without antibiotics. Virulent *S. flexneri* 2457t colonies (red) were selected from Congo red plates, indicating the presence of virulence plasmid. *S. flexneri* was cultivated in MHB at 37°C with agitation, sub-cultured to OD600 of 0.5-0.6, and bacterial pellets were collected through centrifugation. After washing with PBS, the pellets were suspended in incomplete tissue culture media.

For pre-treatment, intestinal cells were exposed to varying concentrations of Capsaicin (1.6µM to 32µM) or vehicle control (DMSO) for different durations (2h to 24h) in incomplete media. Subsequently, infection with *S. flexneri* was carried out at an MOI of 200:1. To synchronize, infected plates were centrifuged, followed by a 2-hour incubation to facilitate bacterial entry. Gentamicin treatment for 2 hours eradicated extracellular bacteria, and after PBS washing, cell lysis was achieved using 0.1% Triton X100. The obtained cell lysates were plated on MHA at 37°C for 18 hours to determine CFU/ml.

For post-treatment analysis, cells were infected with *S. flexneri*, then treated with Capsaicin and eventually gentamicin treatment and cell lysis was done. The same methodology was applied to *S. flexneri* highly resistant cells (BCH12702) with or without Capsaicin treatment, 12 hours post-infection, for invasion. The CFU/ml count was showed graphically.

siATG5, siTFEB transfected cells were treated with Capsaicin and infected for gentamicin survival assay to count CFU/ml compared to scrambled siRNA. TFEB overexpression was also performed by lipofectamine 2000 using pEGFP-N1-TFEB plasmid and empty vector (pcDNA3-EGFP) respectively.

6. Geimsa staining

RAW264.7 cells were seeded on 15 mm^2 cover slip into 6 well Costar tissue culture plates at a density of $1X10^5$ cells/ml per well with RPMI-10% FBS. The cells were allowed to adhere at 37°C in a 5% humidified CO_2 atmosphere. Infection of *S. flexneri* was performed as described previously. After 2h of infection, the media was replaced by 50 µg/ml gentamicin containing incomplete RPMI and kept for 3h at 37°C incubator. The wells were washed thoroughly with PBS and fixed with methanol for 5 mins. Then those were stained using 0.05% giemsa stain for 1h. After proper washing with deionized water, the cover slips were placed upon slides and observed under 100X bright field microscope.

7. RNA isolation

TRIzol method:

Samples collected were lysed in RNAiso Plus (TaKaRa). Volumes of TRIzol are modified according to requirement.

a) For adherent cells: Media is aspirated and cells are washed with 1X PBS. 1-2ml TRIzol was added and kept at room temperature for 10-15 mins.
b) For tissues: Tissues are evenly homogenized using tissue homogeniser with 1ml Trizol for 100mg tissue.

Lysed cells/tissues were centrifuged at 12000g for 15 mins. Supernatant was collected after discarding pellet. 200µl of chloroform was added in 1ml lysate and centrifuged at 12000g for 15 mins at 4^0C. Among the three layers formed, top liquid layer contains RNA. It was transferred into another tube and 500µl of isopropanol was added and kept at room temperature for 10 mins. The mixture was centrifuged at 12000g for 15 mins at 4^0C. After removal of supernatant, 500µl of 75% ethanol was added and centrifuged at 7500g for 5 mins at 4^0C. Supernatant was discarded and RNA pellet was kept for drying. RNA was dissolved in appropriate volume (30-50µl) of DNAse RNAse free water.

Isolation method using kit:

RNA isolation was also performed using RNeasy Mini kit (Qiagen) according to the following protocol.

a) Cells were trypsinized and washed using 1X PBS. Cells were disrupted using buffer RLT (600 µl for $5X10^6$ cells).
b) Equal volume of 70% ethanol was mixed well with the homogenized lysate.
c) Transfer 700 µl of sample to a RNeasy spin column and centrifuged at 10000rpm for 30s and flow-through was discarded.
d) 700 µl of buffer RW1 was added to spin column and centrifuged at 10000rpm for 30s and flow-through was discarded.
e) 500 µl of buffer RPE was added to spin column and centrifuged at 10000rpm for 30s and flow-through was discarded.
f) Free centrifugation was done for 1 min at 10000rpm to remove any residual volume of buffer.

g) Spin column was placed into a 1.5 ml microcentrifuge tube and 50 µl of RNAse-free water was added for elution of RNA.

h) Concentration of eluted RNA was calculated.

8. Calculation of DNA and RNA concentration:

Concentration of DNA and RNA was measured using spectrophotometer. Absorbance at 260nm was measured and concentration was calculated according to the following formulae:

Concentration of RNA (µg/mL) = A_{260} measurement x 40µg/mL x dilution factor

Concentration of DNA (µg/mL) = A_{260} measurement x 50µg/mL x dilution factor

As, 1 OD_{260} of RNA= 40µg/mL; 1 OD_{260} of DNA= 50µg/mL

Purity of both DNA and RNA was measured using ratio of OD_{260}/ $OD_{280.}$ For pure DNA OD_{260}/ OD_{280} is 1.8 and for pure DNA OD_{260}/ OD_{280} is 2.0. Purity of RNA was also observed in 1.2% agarose gel run at 90V for 15 mins. Intensity of 28s rRNA and 18s rRNA should be 2:1 for pure RNA in agarose gel.

9. cDNA synthesis

1µg of cDNA was prepared from RNA according to manufacturer's protocol (Verso cDNA synthesis kit; Thermo Scientific). Firstly, RNA was denatured at 70^0C for 10 mins and immediately placed on ice for 3mins. RT-PCR master mix was prepared using components listed below. The master mix was added in the RNA and PCR cycle was run. Firstly, cDNA synthesis step was performed at 42^0C for 30 mins followed by inactivation step at 95^0C for 2 mins. After completion, RT-PCR products were kept in 4^0C for 5mins and stored at -20^0C.

Components	Volume (µl)
5X cDNA synthesis buffer	4
dNTP mix	2
RNA primer	1
RT enhancer	1
Verso enzyme mix	1
Template (RNA)	1-5
Nuclease free water	To 20
Total volume	20

Components	Volume (µl)	Final concentration
2X SYBR green	10	1X
Forward primer	1	100nM
Reverse primer	1	100nM

Template	variable	1µg
Water	To make 20	
Total	20	

10. Real time PCR

Real-Time Quantitative Reverse Transcription PCR was performed to understand the expressions of several genes for varying conditions. cDNA was amplified using the following components and protocol. Primers were designed from IDT (Integrated DNA Technologies, Inc.) using PrimerQuest™ Tool according to genes to be amplified. SYBR green was used as the fluorescent dye and C_t values were obtained from ABI 7500 Real time PCR systems. 1µg of cDNA was used for 20µl assay mixture. The expression patterns were analysed using $^{\Delta\Delta}$Ct method and normalized using the internal control GAPDH. $^{\Delta\Delta}$Ct were calculated by the following formula: ΔΔCt= test - internal control-test control

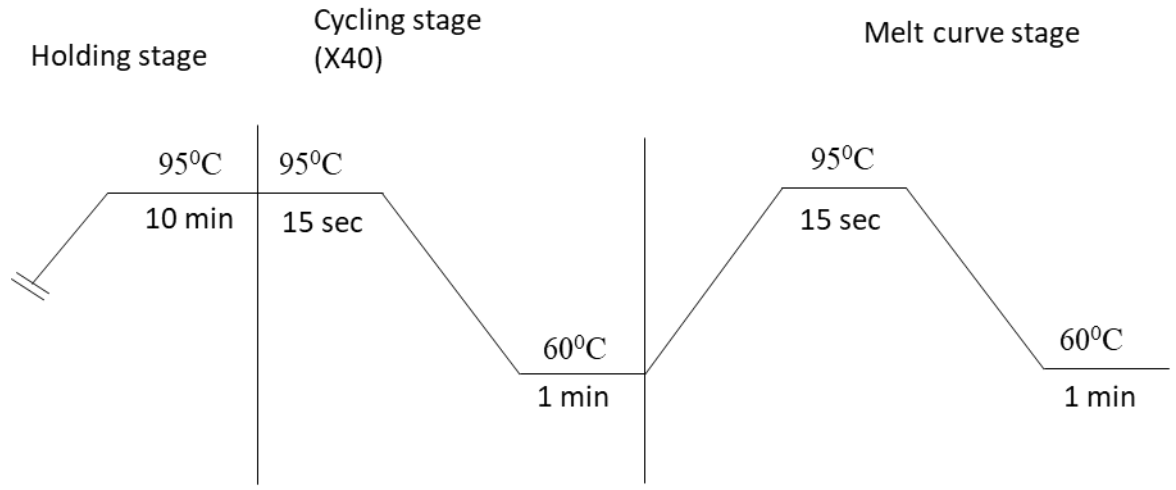

Primer sequences are listed below:

Name	Primer sequence (5'-3') FP	Primer Sequence (5'-3') RP	Specificity
GAPDH	GTGACCAATTCTGTATC	AGACCATAGTTGATTC	Human
MAP1LC3B	CCTGCTGGGTGATTTCTT	CCTTGATTCTCTGGACAATTCT	Human
ATG5	ATGTATGCCACCATCTAT	CCAGTAGTCACACTTCTT	Human
WIPI1	TGATCCACAAGGCATTAGAG	TGAACATACTGACGGACATC	Human
UVRAG	GTATCCTCTGGTTCTTCAT	GGCATCTTGGTATCTCTT	Human
TFEB	CGTCCTGGACAAGACCAAGT	ATTGCTGTCCCGAATGTCTC	Human
FOXO1	AACGTCAATGAGCAAAGGTATTAA	TACGGGAGGCAGCAGTGG	Human
BECN1	GGCCAATAAGATGGGTCTGA	CACTGCCTCCAGTGTCTTCA	Human
MAP1LC3B	GTCCTGGACAAGACCAAGTTCC	CCATTCACCAGGAGGAAGAAGG	Mouse

GAPDH	GATCTTCGACAAGGGAG CTAAA	TCGCATTCTTCTACACGA TAACA	Mouse

11. PCR array

Analysis of differential gene expression within the autophagy pathway was conducted using the Human Autophagy PCR array. This array consisted of 84 genes arranged in a 96-well plate format. To observe variations among uninfected, infected, and Caps-infected samples, fold changes were represented in a column graph. The RT² Profiler™ PCR Array Human Autophagy (#PAHS-084Z) was used, following Qiagen's instructions, to comprehensively understand the autophagy profile in both control and treated samples. Subsequently, cDNA was synthesized using specific reagents and combined with the provided SYBR Green Mastermix. The Quantitative Real-Time PCR was carried out utilizing the Applied Biosystems StepOnePlus system. The acquired melt curves and $^{\Delta\Delta}$Ct values underwent analysis using the web-based RT² Profiler™ PCR Array data analysis software.

12. ELISA

ELISA was used to quantitate the concentration of released cytokines in cell media and serum of mice according to manufacturer's protocol (KRISHGEN Biosystems). Samples and standards were diluted in assay diluent and wells of 96 well plate was coated and incubated at 37^0C for 90 minutes. After washing 3 times with wash buffer, 100 µl of detection antibody was added in each well and incubated for 1hr. Addition of 100 µl HRP-conjugate was

followed by TMB substrate and incubated until colour develops. The reaction was stopped using stop solution and OD was measured at 450nm using spectrophotometer.

Standard curves were prepared with standard dilution using the following table. From the generated curve equation was calculated.

Concentration of proteins were determined using the equation and putting the OD values as "x"

Standard no.	**Conc.Of Standard (ng/ml)**	**Reaction**
7	100	10µl stock (10µg/ml) + 990µl assay diluent
6	50	500µl standard 7 + 500µl assay diluent
5	25	500µl standard 6 + 500µl assay diluent
4	12.5	500µl standard 5 + 500µl assay diluent
3	6.25	500µl standard 4 + 500µl assay diluent
2	3.13	500µl standard 3 + 500µl assay diluent
1	0.5	500µl standard 2 + 500µl assay diluent

13. Cell cytotoxicity (LDH) Assay

Cells were seeded in 96 well plates ($1X10^4$ cells/ml). Capsaicin (Caps) was purchased from Sigma chemicals (CAS Number:404-86-4). At this seeding density, cells were treated with varying concentrations of Caps (16µM, 32µM) for 24h keeping an uninfected DMSO control and a positive control 0.1% triton X_{100}. The plates were incubated for indicated time periods at 37°C incubator. LDH assay of the collected supernatant was performed using LDH Cytotoxicity detection Kit (Takara)(#MK401) and % cytotoxicity was calculated as = (ER – TS – ES)/ (MR – ES) *100, where, ER represents release from cells incubated with Caps, TS represents release from target cells, ES represents release from only Caps. MR represents maximum release from the cells lysed with Triton X_{100}). % Cytotoxicity was graphically represented.

14. Plasmids

The eGFP-LC3 plasmid was a gift from Prof. Parimal Karmakar (Department of Biotechnology, Jadavpur University, India). pEGFP-N1-TFEB plasmid was a gift from Dr. Ravi Manjithaya, Autophagy lab, JNCASR, Bangalore. Control EGFP plasmid was a kind gift from Dr Santa Sabuj Das, ICMR, NICED, Kolkata. The plasmids were transformed in DH5α and purified by mini-prep plasmid isolation kit (Promega). The plasmid DNA was suspended in nuclease free water and stored in -20^{o}C.

15. Preparation of competent cells

1:100 of inoculum was added in fresh LB from overnight culture of *E. coli* and kept at 37 °C until OD 0.5. After keeping the culture on ice for 10 mins, it was centrifuged for 15 mins at 8000g. The supernatant was discarded and pellet was resuspended in 0.1M ice-cold $CaCl_2$. Incubation was performed in ice for 20 mins and centrifuged at 8000g for 20 mins. The pellet was dissolved in 1ml 0.1M $CaCl_2$ + 15% glycerol and distributed in aliquots 50µl each. The prepared competent cell stocks were stored at -80°C.

15. Transformation of plasmid DNA

E. coli DH5α cells were cultured overnight. The culture was then centrifuged for 10 mins at 3000 rpm, 4℃. After discarding the supernatant, 20ml ice cold 0.1M $CaCl_2$ was added to the pellet and kept in ice for about 30 mins. Competent cells were obtained followed by centrifugation and discarding the supernatant. These cells were stored at -80℃. The competent DH5α cells were thawed on ice before transformation. The cells were mixed gently with the pipette tip and aliquot of 50µl of cells were mixed gently with 5 µl of DNA followed by 30 mins incubation on ice. Heat shock was done at 42℃ for 30 seconds followed by keeping in ice for 2 mins. Tubes were kept @ 37℃ shaker incubator for 1hr. About 250 µl of pre-warmed LB was added and kept on shaker at 37℃ for 1 hour. Lastly, 20 µl of transformed DH5α was plated in presence of appropriate antibiotic and kept @ 37℃ overnight.

16. Plasmid DNA Isolation

Transformed DH5α was cultured overnight in LB media at 37°C and 10 ml culture was used for isolation of plasmid DNA using QIAamp® DNA Mini Kit according to manufacturer's protocol (Qiagen). Culture was centrifuged at 6000g for 15 mins at 37°C. Supernatant was

discarded and pellet was resuspended in 300 µl of buffer P1 (with RNase A). After vigorous shaking 300 µl of buffer P2 (lysis buffer) was added and inverted for 4-6 times and kept at room temperature for 5 mins. 300 µl of buffer P3 (neutralisation buffer) was added, mixed, and incubated on ice for 5 mins. Genomic DNA was coagulated and after centrifugation at 13000rpm for 5 mins, clear supernatant containing plasmid DNA was promptly collected in fresh tube. QIAGEN-tip 20 column was equilibriated with buffer QBT and collected supernatant containing plasmid DNA was passed. Column was then washed thrice with buffer QC and DNA was eluted using buffer QF. Alcohol precipitation was performed using isopropanol and plasmid DNA was obtained as pellet. DNA pellet was air dried and dissolved in TE buffer (pH 8).

17. Plasmid DNA transfection

The following plasmids were transfected in HT29 cells using lipofectamine 2000 reagent: GFP-LC3B, GFP-TFEB and pcDNA3-eGFP. 1µg plasmid was incubated using 3µl of lipofectamine. Both HT29 and RAW 264.7cells were seeded and transfected in incomplete media at 70-80% confluency. Media was replaced with complete media after 6 hrs and transfected cells were kept for 48 hrs and further experiments were performed.

18. Infection assay in transfected cells

After transfection for 48 hours, the cells were treated with Capsaicin at a concentration of 16µM. This was followed by infection with *S. flexneri*. The objective was to perform immunofluorescence assays targeting *S. flexneri* and concurrently detecting autophagy. For this purpose, cells transfected with GFP-LC3B were subjected to infection by *S. flexneri*. Specifically, 400µl of *S. flexneri* from an overnight culture with an optical density (O.D)

ranging from 0.5 to 0.6 was used for infection in intestinal cells and macrophages. Subsequent to the infection, the cells underwent immunofluorescence staining. Cells were fixed in pre-chilled 100%methanol for 5 mins at room temperature. In brief, the fixed cells were exposed to an anti-*Shigella* antibody (ab65282) at a dilution ratio of 1:250. Following this, a TRITC-conjugated anti-rabbit secondary antibody (Cat# AP132R) at a dilution ratio of 1:2000 was used. Finally, the prepared coverslips were mounted using the ProLong™ Gold Antifade reagent containing DAPI from ThermoFisher. The observation process was conducted using an inverted confocal microscope by Carl Zeiss (model LSM 710). GFP-positive cells were specifically chosen for observation in each sample.

19. siRNA transfection

The following siRNAs were purchased from IDT and used for knockdown of those genes: ATG5 siRNA (Design ID hs.Ri. ATG5.13.1) and TFEB siRNA (Design ID hs.Ri. TFEB.13.1). Scrambled siRNA was used as a universal negative control. HT 29 cells at 60-70% confluency were transfected with 12 picomoles of siRNA/ Scrambled siRNA and 2µl of lipofectamine was added per well in a 6 well plate. Media was changed with fresh complete media after 6hrs. 48 hours after transfection, infection assay was performed in cells infected with *S. flexneri* with and without Capsaicin pre-treatment. Cells were lysed for CFU/ml counting or processed for RNA/protein extraction.

20. Immunofluorescence microscopy

Cells were cultured on coverslips for fluorescence microscopy and Capsaicin treatment was done before subjecting the cells to *S. flexneri* infection. After infection, the cells were fixed using 4% formaldehyde. Subsequently, these fixed cells were subjected to a blocking process

in a solution containing 3% BSA and 0.01% Triton X100 dissolved in PBS. This blocking step occurred for a duration of 1 hour at room temperature. Following blocking, an overnight incubation was conducted using an anti-TFEB antibody at a dilution ratio of 1:250. Following the incubation, the fixed cells were immersed in a blocking buffer that contained a TRITC-conjugated anti-rabbit secondary antibody (Cat# AP132R) at a dilution ratio of 1:2000. Finally, the prepared coverslips were mounted onto glass slides by adding a droplet of ProLong™ Gold Antifade reagent from ThermoFisher that contained DAPI. The resulting images were captured using a Zeiss LSM 710 confocal system by Carl Zeiss.

21. Protein isolation (whole cell lysate/tissue homogenate) for western blot analysis

After treatment and infection, cultured cells were washed thrice with PBS and harvested with trypsin-EDTA for 5 mins and centrifuged for 10 mins at 5000g. Cell pellets were lysed in RIPA lysis buffer using sonication on ice with 5 seconds pulse for 30 mins. For *in vivo* samples, tissues were lysed in RIPA buffer using tissue homogeniser. Then it was centrifuged at 8000g for 15 mins. Collected supernatant was used as sample for immunoblotting.

22. Nuclear and cytoplasmic protein extraction

Nuclear and cytosolic extracts were prepared by using NE-PER™ Nuclear and Cytoplasmic Extraction Reagents of Thermo-Scientific (Cat#78833) following manufacturer's protocol. Cell pellets were resuspended in 200µl CER I for 10^6 cells by vigorous vortexing. 11 µl of CER II was added and kept on ice for 5 mins followed by centrifugation at 13000rpm for 10 mins. The supernatant was collected and stored as cytoplasmic extract. Pellets obtained were

lysed with NER keeping on ice for 45 mins and frequently vortexed. Centrifugation at 16000g was performed and supernatant was collected as nuclear extract.

23. Estimation of protein concentration

Concentration of protein was estimated using reagents following Lowry method.

Reagent A: 2% Na_2CO_3 in 0.1 M NaOH+1% Na-K tartarate in H_2O and 0.1%SDS

Reagent B: 0.5% $CuSO_4.5H_2O$ in H_2O

Reagent C was prepared by mixing 1 ml of reagent A and 10 µl of reagent B. 600 µl reagent C was added in 200 µl diluted proteins and kept at room temperature for 15 mins. 1N Folin–Ciocalteu reagent was added and kept in dark for 30 mins. OD was measured at 660nm and concentration of protein was calculated using following equation obtained from BSA standard curve: Concentration of protein (µg/ml) = OD_{660} /0.0026*dilution factor

24. Western blotting

After protein estimation, lysates were boiled in SDS-PAGE sample buffer and run on 10% or 12.5% SDS- PAGE gel at 80V in stacking and 120V in resolving gels. Composition of gels is listed below.

Resolving Gel (Composition)	**Volume (ml) for 1 gel**
30% acrylamide & bis-acrylamide (Solution A)	1.67

1.5M Tris-HCl (pH 8.8) (Solution B)	0.625
Water	2.5
10% SDS	0.15
10% APS	0.05
TEMED	0.005

Stacking Gel (Composition)	**Volume (ml) for 1 gel**
30% acrylamide & bis-acrylamide (Solution A)	0.66
0.5M Tris-HCl (pH 6.8) (Solution C)	1.26
Water	3.0
10% SDS	0.05
10% APS	0.025
TEMED	0.005

Gels were transferred to methanol activated PVDF membrane using transfer buffer in BioRad semi dry transfer apparatus. After 30 mins of transfer, membranes were blocked in 5%

skimmed milk dissolved in TBST buffer for 1h at room temperature, washed in TBST and incubated overnight with primary antibodies at 4°C. Primary antibodies were listed in table2.

Name	Specificity	Cat no.#	Dilution
Anti-GAPDH	Rabbit monoclonal	D16H11	1:3000
Anti-SQSTM1/P62	Rabbit polyclonal	ab91526	1:3000
Anti- ATG5	Rabbit monoclonal	ab228668	1:1000
Anti-beclin 1	Rabbit monoclonal	Ab207612	1:1000
anti-LC3B	Rabbit polyclonal	Ab51520	1:3000
anti-TFEB	Rabbit monoclonal	D2070	1:1000
anti-ZKSCAN3	Mouse monoclonal	sc-551285	1:1000
anti-LAMP1	Rabbit monoclonal	9091	1:3000
Anti-Histone	Rabbit monoclonal	9715	1:1000
Anti-mTOR	Rabbit monoclonal	2972	1:1000
Anti-p-mTOR	Rabbit polyclonal	2971	1:1000
Anti-Akt	Rabbit polyclonal	ab8805	1:1000
Anti-p-Akt (S473)	Rabbit polyclonal	ab81283	1:1000
Anti-p-Akt (T308)	Rabbit polyclonal	Ab38449	1:1000

After the initial treatment with the primary antibody, the membranes were placed on a shaker at room temperature for duration of 2 hours. During this time, they were exposed to either horseradish peroxidase (HRP) conjugated goat anti-rabbit secondary antibody (dilution 1:10000) or goat anti-mouse secondary antibody (dilution 1:10000). Following this incubation, the membranes underwent a final wash using TBST for a period of 30 minutes. The resulting protein bands were visualized using the ChemiDoc MP Imaging System from Biorad. This visualization process was achieved by using Millipore immobilon western chemiluminescent HRP substrate, which consists of luminol and hydrogen peroxide, serving as the substrate for the chemiluminescent reaction.

25. Electron microscopy

Cells, both uninfected and infected (HT29 and RAW264.7), were subjected to various treatments, including with or without Capsaicin. These cells were then fixed using a solution of 3% glutaraldehyde in 0.1 M sodium cacodylate buffer. The fixation process was followed by an additional fixation step involving 1% osmium tetroxide. Subsequently, a process of dehydration was carried out using increasing concentrations of acetone. The cells were eventually embedded in Agar 100 resin and polymerized at a temperature of 60 °C. Ultrathin sections with a thickness of approximately 40 to 50 nm were created utilizing a Leica Ultracut UCT ultramicrotome from Leica Microsystems in Germany. These sections were then placed onto nickel grids and subjected to a dual staining process involving 2% aqueous uranyl acetate and 0.2% lead citrate. These sections were examined under a FEI Tecnai 12 Biotwin transmission electron microscope from FEI in Hillsboro, OR, USA. The microscope operated at an accelerating voltage of 100 kV. The quantification of autophagosome formation was accomplished by calculating the percentage: (Number of cells containing

autophagosomes / Total number of cells) multiplied by 100. Autophagic bodies were outlined using Adobe Photoshop software for further analysis.

26. Chromatin immunoprecipitation assay (ChIP assay)

HT-29 cells were pre-treated with Capsaicin and infected according to infection protocol described previously. After incubation, Chromatin immunoprecipitation protocol was performed according to the protocol of CHIP assay kit (#7-295; Merck Millipore).

a) Cross-linking of histones to DNA was performed by addition of 1% formaldehyde in infected plates and kept for 10 mins.
b) Formaldehyde was inactivated by adding glycine.
c) Media was discarded and plates were washed with PBS containing PMSF and protease inhibitor.
d) Cells were scraped and centrifuged at 2000rpm for 5mins.
e) SDS lysis buffer was added to resuspend the pellet.
f) Cells were sonicated to shear the DNA. Shearing was checked in agarose gel electrophoresis.
g) Samples were centrifuged at 13000rpm for 15 mins and supernatant was collected.
h) Supernatant was diluted using ChIP dilution buffer and pre-cleared with addition of protein A agarose.
i) TFEB antibody (5µg/sample) was added to the supernatant and kept at 4^0C overnight with rotation.
j) Pellets were washed with low salt, high salt, LiCl wash buffer once each and TE buffer twice respectively.

k) Histone complex was eluted from the antibody using elution buffer.

l) Crosslinking of DNA and histone was reversed using 20µl 5M NaCl and heating at 65^0C for 4hrs.

m) 10 µL of 0.5 M EDTA, 20 µL 1 M Tris-HCl, pH 6.5 and 2 µL of 10mg/mL Proteinase K were added and incubated for one hour at 45°C.

n) DNA was recovered using phenol-chloroform extraction method and DNA pellets were dried and resuspended in DNase RNase free water.

o) Real time PCR was performed using appropriate primers and fold change was calculated.

The chromatin fraction, which lacks primary antibody, was taken as 'input'. Real-time PCR was performed using the following ChIP primer assemblies. Primers were designed for amplifying CLEAR elements in the promoter region of TFEB using Primer: MAP1LC3B-forward; 5'-GAAGGCTCGGGACAAAAGCAG-3', reverse; 5'-GTGGGTGGCTTCCGGGGAG-3'. The PCR cycle was conducted in accordance with the manufacturer's instructions. The data was represented graphically as % of input.

27. Transcription factor assay

The assessment of TFEB transcription factor activity was carried out through the utilization of the RayBio® Human TFEB TF-Activity Assay Kit Protocol. Nuclear extracts from cells treated with Capsaicin as well as control cells were used as the samples. These samples were introduced into wells coated with oligonucleotides that contained the CLEAR sequence. After the introduction of the primary antibody, a secondary antibody conjugated with HRP was used. After this step, the TMB substrate reagent was added, initiating a reaction that was

subsequently halted by the addition of the stop solution. The optical density (O.D.) was measured at 450 nm using a spectrophotometer. The calculated fold change was then presented graphically for analysis and interpretation.

28. Co-immunoprecipitation (co-IP)

The following steps were performed for co-immunoprecipitation of ZKSCAN3 with the help of IpaH9.8 antibody.

a) Cell lysis

The cell lysis buffer used was different from RIPA. Non detergent, low salt lysis buffers with protease and phosphatase inhibitors were used. Depending upon the abundance of protein, 400ug of lysate were used for pulldown after lysis.

b) Addition of antibody and agarose beads

Specific antibody (IpaH9.8) was added and incubated for 2 hrs for antigen antibody binding. Next protein A agarose beads were added to the Ag-Ab complex and rotated overnight at 4° C avoiding agitation.

c) Collection and washing of beads

Beads bound to Ag-Ab complex was pulled down using centrifugation followed by washing with ice cold lysis buffer, PBS, water.

d) Detection of target protein

Isolated complex was boiled in sample buffer, run in SDS-PAGE and developed using target protein (ZKSCAN3) antibody.

29. Calcium influx assay

Cells were seeded in 96 well plates ($1X10^4$ cells/ml). At this seeding density, cells were pre-treated with Bapta-AM for 2hrs at 5µM and 10 µM concentration and infected with *Shigella flexneri* at MOI200. Intracellular calcium mobilization was detected using Fluo-8 Calcium Flux assay Kit (ab112129). Fluorescence was measured at Ex/Em 490/525 nm and graphically represented as fold change compared to DMSO control.

30. Animal Experiment

30.1. Ethics statement

The animal study was reviewed and approved by IAEC (Institutional Animal Ethical Committee), NICED, Kolkata (PRO/157/-July 2022). Experiments were conducted according to the operational procedure by CPCSEA (Committee for the Purpose of Supervision and Control Experiments on Animals).

30.2. Infection assay in mice

Mice undergone fasting for 6 hours followed by pathogenic *Shigella flexneri* (sf2457T) injection intraperitoneally (Yang et al., 2014). In the experimental design, 4 groups (n=4) were created accordingly Group 1. Control: Received only DMSO as the vehicle. Group 2. Infected: Received *S. flexneri* suspension ($0.5X10^9$ CFU/ml) in PBS. Group 3. Infected +Caps: Received *S. flexneri* suspension followed by Caps (20 mg kg−1 body weight)

treatment for 2h. Group 4. Caps: Received Caps (20 mg kg−1 body weight). Each group was kept in an individual cage. Experiments were repeated at least thrice.

30.3. Animals

20-22g male BALB/c (8 weeks) mice were utilized for *S. flexneri* infection. Animals were adjusted under standard laboratory conditions. Mice were provided with a standard diet and water ad libitum. IAEC (Institutional Animal Ethical Committee), NICED, Kolkata (PRO/157/-July 2022) guidelines were followed during all the experiments. Animals were maintained at the animal house with 75% humidity and specific pathogen free healthy individuals were selected.

30.4. Collection of colons

Post 2 hours of *S. flexneri* sf2457T infection, Capsaicin treatment was performed. After 2 hours of Capsaicin treatment, all the animals were sacrificed. Colon from drug treated, untreated, infected and control mice were aseptically removed. Crushed colon was plated for bacterial colony count. The tissues were kept at −80 °C until further experiments were performed.

30.5. Preparation of colon tissue homogenate

Preparation of colon tissue homogenate involved the collection of colon samples post-dissection, followed by rinsing in PBS buffer. Subsequently, the samples were homogenized while kept at a low temperature using ice-cold RIPA lysis buffer for western blot analysis, and using TRIzol reagent (RNAiso Plus, TaKaRa) for RNA isolation. After homogenization, the resulting mixtures were subjected to centrifugation at 12,000 rpm and 4 °C for 10

minutes. The supernatants obtained from this process were then used for subsequent experimental procedures. For RNA isolation, the RNA was extracted from the samples, and the conversion from RNA to cDNA was carried out using the Verso cDNA Synthesis Kit from Thermo Scientific. This was followed by quantitative real-time PCR (qRT-PCR) to analyze the synthesized cDNA.

31. Checkerboard Assays

Checkboard assays were carried out to test the MIC of the combination of antibiotics (Ampicillin, tetracycline, streptomycin, ciprofloxacin, ceftriaxone, nalidixic acid, Azithromycin) and Capsaicin. Briefly, increasing concentrations of Capsaicin (0–10 mg/mL) in each column and increasing concentrations of antibiotics (0–5 mg/mL) in each row were set up in 96-well microtiter plates. Each well was inoculated with 100 µL of 10^5 CFU/mL *S. flexneri* culture, and then the required concentration of antibiotics/Capsaicin was added to a final volume of 200 µL. The plates were incubated at 37°C for 24 h. Experiments were repeated thrice.

32. Synergistic assay

The microtitre plates were used for determining MIC of Capsaicin and antibiotics alone as well as in combination. FICI was calculated for each well with the equation $FICI = FIC_A + FIC_B = (C_A/MIC_A) + (C_B/MIC_B)$, where MIC_A and MIC_B are the MICs of drugs A and B alone, respectively, and C_A and C_B are the concentrations of the drugs in combination.

The values of FICI were interpreted as follows: (1) FICI ≤ 0.5 means a synergistic effect; (2) when FICI >0.5 and <1 means an additive or indifferent effect and (3) FICI >1 means an antagonistic effect.

33. Combination effect *in vitro*

HT29 cells were infected for 2hrs with resistant *S. flexneri* (BCH12702, BCH12654) followed by antibiotics/ Capsaicin post treatment for 24hours and gentamicin protection assay was performed. Concentration of Capsaicin was 10, 20, 50ug/ml and antibiotics (streptomycin/ nalidixic acid/Azithromycin) concentration were 0.5ug/ml. After 24 hrs, cells were lysed and plated for CFU/ml count which were graphically represented.

34. Combination effect *in vivo*

Mice undergone fasting for 6 hours followed by resistant *Shigella flexneri* (BCH12702, BCH12654) injection intraperitoneally. In the experimental design, 4 groups (n=4) were created accordingly Group 1. Control: Received only DMSO as the vehicle. Group 2. Infected: Received *S. flexneri* suspension ($0.5X10^9$ CFU/ml) in PBS. Group 3. Infected +Caps: Received *S. flexneri* suspension followed by Caps (50 mg kg−1 body weight) treatment. Group 4. Infected + Caps + Antibiotics (Nal/ strep/ azi): Received Caps (50 mg kg−1 body weight) + Ab (10 mg kg−1 body weight). 5. Infected + Antibiotics (Nal/ strep/azi): Received Ab (10 mg kg−1 body weight). Each group was kept in an individual cage for 24h. Experiments were repeated at least thrice. After 24h, mice were sacrificed and colon were crushed for CFU/ml count which were graphically represented.

35. Statistical analysis

Test information was presented as mean ± S.E.M. Statistical analyses were performed and bar graphs were processed in GraphPad Prism 5 after the data processing in Microsoft Excel. For comparison between two groups, Unpaired t-test is done and for multiple comparison, one-way ANOVA or Kruskal-Walis test with Dunn's post hoc test is performed. For multiple variants in gentamicin survival assay two-way ANOVA is performed. Significance level has been marked as, * for $p < 0.05$ which implies significant, ** for $p < 0.01$ which implies very significant, *** for $p < 0.001$ which implies highly significant.

SECTION 4

AIMS AND OBJECTIVES

Antibiotic treatment plays an essential role in prevention of *Shigella flexneri* infection. However, antibiotic resistance is rising globally and creating a major challenge in treating bacterial infection. In this context, newer approaches are urgently needed to reduce *S. flexneri* burden. Several herbal compounds are emerging as alternative therapeutic approaches to fight against multidrug-resistant bacteria.

In this perspective, the objectives of the proposed study are as follows:

Objective1: Investigating the effect of a herbal compound Capsaicin on *Shigella flexneri* host pathogen interaction

Objective2: Dissecting the role of autophagic clearance by Capsaicin on *Shigella flexneri*

Objective3: Deciphering and characterizing new drug targets to fend of infection during *S. flexneri* pathogenesis

SECTION 5

RESULTS

OBJECTIVE I

Chapter 1

Screening and identification of a herbal compound for potential antibacterial activity against Shigella flexneri

Background

Shigella flexneri, a common gastrointestinal pathogen causes bacillary dysentery affecting millions every year worldwide (Nandy et al., 2011; Rogawski McQuade et al., 2020; Taneja and Mewara, 2016; Williams and Berkley, 2018). According to available information, *S. flexneri* infection is highly predominant in developing nations and responsible for severe morbidity and mortality in children below five years. The pathogen invades the intestinal epithelial and immune cells causing ulcerative lesions in the gut under severe conditions (Puzari, Sharma and Chetia, 2018). So far, the only treatment option is antibiotics as no licensed vaccine has been developed (Hajialibeigi, Amani and Gargari, 2021). Recently, the reverse vaccinology approach has been considered to improve vaccine research against *Shigella flexneri* (Rubinsztein, Codogno and Levine, 2012). As *Shigella flexneri* is gradually becoming resistant against a large number of antibiotics, alternative therapeutic approaches are gradually becoming a requirement for treating shigellosis (Kaufmann et al., 2018). In fact, some recent evidences of resistance to well-known drugs against *Shigella flexneri* have increased serious complications regarding control of this invasive pathogen (Young, Walzl and Du Plessis, 2020). Hence, in the current scenario, there is an imperative need to search for alternative approaches in treating *S. flexneri* infection.

The clinical manifestations of shigellosis start after the entry of bacterium into the epithelium, followed by multiplying and spreading to adjacent cells leading to cell death (Ashida, Mimuro and Sasakawa, 2015). A large virulence plasmid of *Shigella flexneri*

encodes T3SS system which injects bacterial virulence factors into the host cell (Puhar and Sansonetti, 2014).

Manipulation of immune defences by *Shigella flexneri* successfully establishes infection. Host–pathogen interaction leads to survival of the pathogen within the host. Host cells possess several major defence mechanisms i.e., innate immune defence machinery and autophagy to fight against *S. flexneri* infection (Torraca et al., 2023).

The urgency of addressing the issue related to understanding of this disorder and identifying drug molecules in the context of this understanding requires a focused approach on a priority basis. Modulation of host defence machinery by *Shigella flexneri* effector proteins is the major thrust area of research in the current scenario. New approaches to combat *Shigella flexneri* infection are required like controlling host-pathogen interaction (Munguia and Nizet, 2017).

Current status of antibiotic resistance in *Shigella flexneri* leads to development of alternative sources like plant products for therapeutic use. In this context, new drug candidates should be identified against *Shigella flexneri* and novel drug targets are required for development of therapeutics rather than direct killing of bacteria *in vitro*. This aspect will provide us with developing innovative approaches in treating shigellosis. Treating shigellosis by plant derived molecules would lead to an alternative approach where a cost-effective therapy will be provided. As vaccine development against *Shigella flexneri* is still in trial we can initiate an alternative cost-effective drug which can reach to people easily. It would be worthwhile to mention that medicine from natural resource especially from plants traditionally used is better option for future drug development.

After screening of few herbal compounds, we worked with a herbal compound from chilli plant. Capsaicin, a dietary compound from chilli plants, is reported to have anticancer properties (Lin et al., 2018). Emerging evidences have pointed out that Capsaicin also possess antimicrobial activities against gastrointestinal pathogens.

Materials and Methods

Broth dilution assay and microdilution assay were performed to determine concentration of Capsaicin for *S. flexneri* inhibition. Gentamicin protection assay was performed to determine effect of Capsaicin during invasion of *S. flexneri*. Methods are already described in the materials and methods section.

Results

1.1. Virulence property of *Shigella flexneri 2457T*

1.1.1. Presence of virulence plasmid

Shigella flexneri was grown in Congo red agar plate (0.1%) which showed reddish pink colonies. Congo red plates were used as a selective media for *S. flexneri* which correlates with the presence of virulence plasmid (presence of T3SS) of *S. flexneri*. The result was compared with virulent *Vibrio cholerae* strain where T3SS is absent, thus showed no colony. Congo red positive colony (virulent *S. flexneri*) was taken for further culture and infection experiments. **(Fig1.1)**

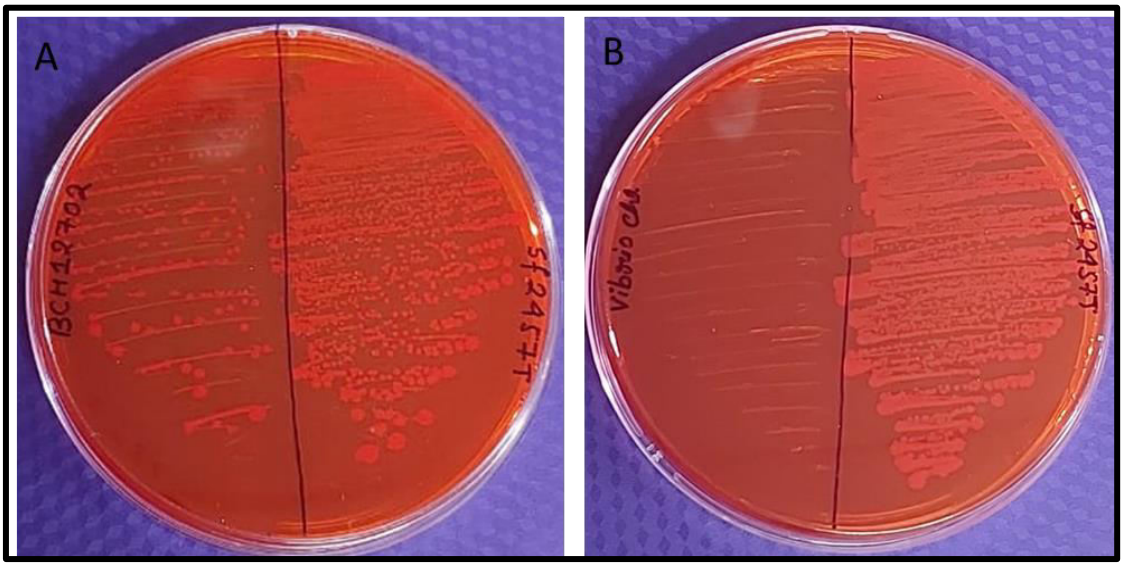

Fig1.1. Congo-red binding assay. (A) *Shigella flexneri* grown in Congo-red agar plate showed Orange-pink colour colonies which indicate the highly virulent nature of *S. flexneri* (sf2457T) and multi-drug resistant clinical isolate (BCH12702) **(B)** Culture of *Vibrio cholerae* showed no colony due to absence of T3SS.

1.1.2. Infection model of *S. flexneri*

Cellular infection was visualized under compound microscope (100X) after Giemsa staining (2.5%). Intracellular presence of *Shigella flexneri* was observed in RAW267.4 (macrophage cell line). **(Fig1.2).**

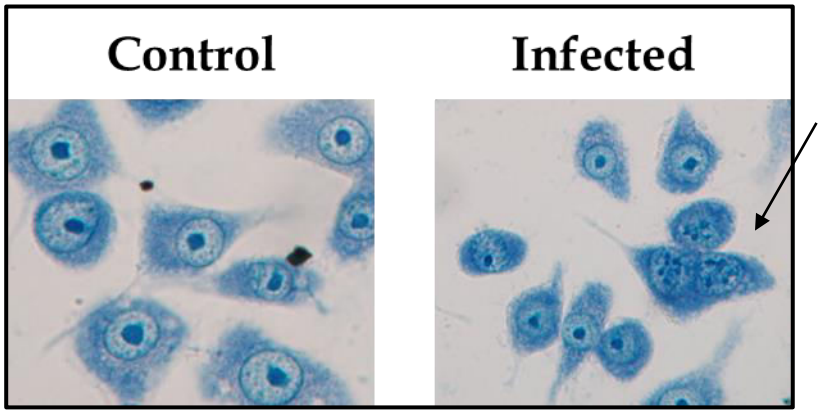

Fig1.2. Visualization of intracellular *S. flexneri* using Geimsa stain. Cells were grown on slides and infected with *S. flexneri.* Cells were stained using Geimsa stain (2.5%) and after 60 minutes of incubation visualized under microscope. Intracellular presence of bacteria was observed.

1.2. Antibacterial effect of Capsaicin

1.2.2 Capsaicin inhibits *S. flexneri* growth in broth culture

To investigate the antibacterial property of Capsaicin, MIC of Capsaicin (Caps) was determined using broth dilution methods. From the growth curve, it has been observed that, OD @600nm is almost similar at different doses of Capsaicin with increasing time of culture up to 64 µM. From 80 µM concentration Capsaicin showed noticeable decrease in OD but the result is far different from the data observed with Nalidixic acid (NA), an antibiotic treatment (positive control) **(Fig1.3.A).** Capsaicin at different concentrations reduces colony count (CFU/ml) of *Shigella flexneri2457T* culture. Capsaicin decreased the number of colony forming unit (CFU/ml) in MHA plate dose dependently (0, 80, 160 µM). At different time points (0.5, 1, 2, 3, 4h), growth of *Shigella flexneri* is inhibited in presence of Capsaicin as compared to control (DMSO). At 160 µM dose of Capsaicin, the inhibition is significant. There was apparently no change in bacterial growth for cultures treated with Capsaicin below that concentration **(Fig1.3.B).**

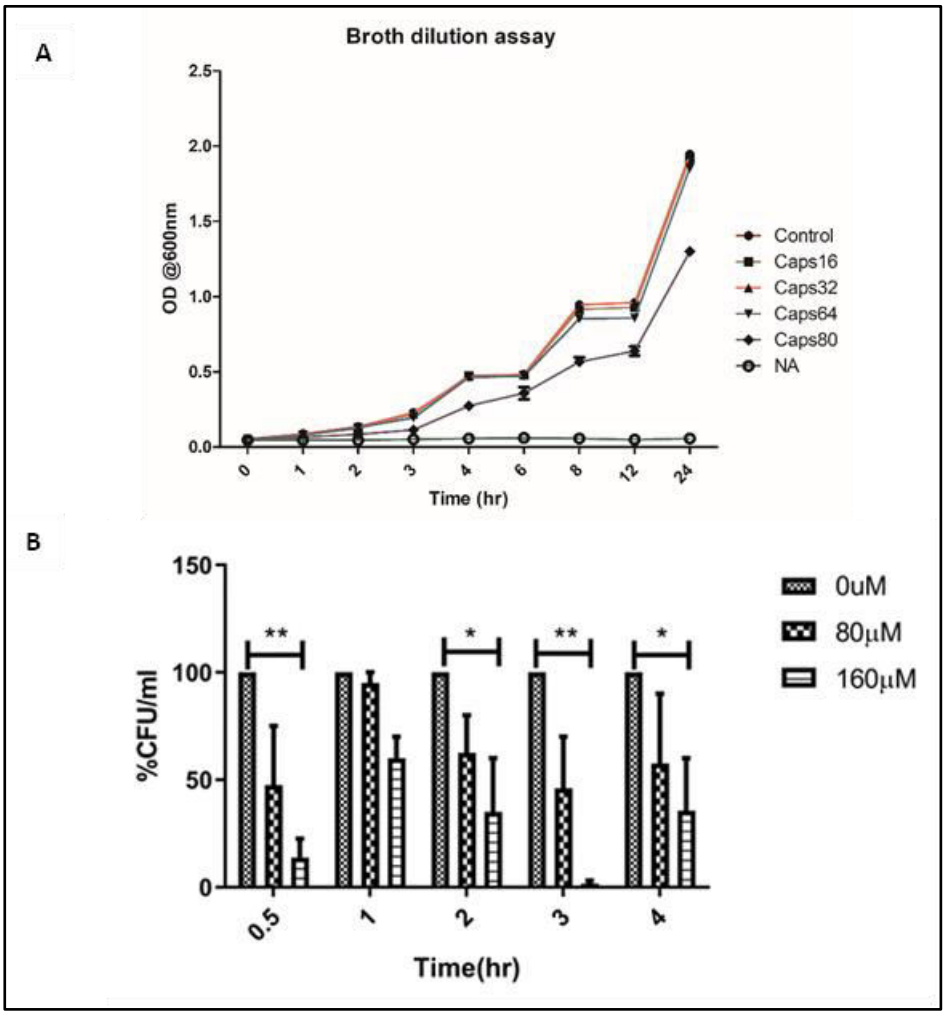

Fig1.3. Broth dilution assay indicating antibacterial effect of Capsaicin at higher doses in broth culture

(A) Broth dilution assay was performed with DMSO, 16, 32, 64, 80µM capsaicin and nalidixic acid followed by addition of 10^9 *S. flexneri* overnight culture. O.D.600nm was measured with regular interval and graphically represented (N=3). **(B)** CFU/ml was calculated from the culture treated with DMSO, 80 and 160µM Caps. %CFU/ml was calculated and graphically represented (N=3). Two-way ANOVA was done * $p < 0.05$, ** $p < 0.01$, *** $p < 0.001$.

1.2.3. Determination of MIC of Capsaicin using 96 well plate assay

Minimum inhibitory concentrations (MICs) are the lowest concentration of compounds which inhibit the visible growth of microbes following overnight incubation. MICs are calculated mainly using microdilution method to check bacterial resistance against drugs.

MIC of Capsaicin was determined using 96 well plate microdilution method. Standard strain of *S. flexneri* (sf2457t) and 4 highly antibiotic resistant strains were assessed for determining MIC and represented in tabular form. It was observed that MIC of Capsaicin varies between concentration range of 5-10 mg/ml against different multidrug resistant strains of *S. flexneri* **(Fig1.4).** Following is the chart showing resistant profile of antibiotic resistant strains:

Strain name	**MIC of Capsaicin (mg/ml)**
Sf2457T	5
BCH12702	8
BCH12654	8
BCH12904	10
BCH12689	8

Fig1.4. Determination of MIC of Capsaicin. Microdilution assay was performed in 96 well plate using Capsaicin at different concentrations against a number of multidrug resistant *S. flexneri*. MICs were observed and represented.

1.3. Antibacterial effect of Capsaicin *in vitro*

1.3.1. Capsaicin inhibits invasion of *S. flexneri* in intestinal cells

It has been reported earlier that Capsaicin has antibacterial potential against *Vibrio cholerae, H. pylori* and other bacteria. (Füchtbauer et al., 2021). But there is no such report against *Shigella flexneri.* We checked the effect of Capsaicin at lower doses on intracellular clearance of *Shigella* as *S. flexneri* is an intracellular bacterium. An intracellular invasion assay was performed to identify the inhibitory effect of Capsaicin on *S. flexneri* infection model. We took HT-29 cells as *S. flexneri* invades the intestinal epithelial cells.

HT29 cells were pre-treated with different doses (16 μM and 32 μM) of Capsaicin for 2h followed by *S. flexneri* infection at MOI200. At this condition, Caps treatment reduced multiplication of *S. flexneri* significantly (**Fig1.5.A**). HT29 cells when pre-treated with Capsaicin at 16 μM dose for different time points (2, 4, 6, 12, and 24 h) reduced intracellular *S. flexneri* growth **(Fig1.5.B).** Capsaicin is also effective to induce bacterial clearance when treated post infection. *S. flexneri* growth was reduced significantly at 12 h by post treatment of Capsaicin but in 24 h, infected cells died hence no significant reduction in growth due to drug treatment **(Fig1.5.C).** Results were validated also in CaCO2 cells where intracellular *S. flexneri* load was reduced in Capsaicin pre-treated condition **(Fig1.5.D)**.

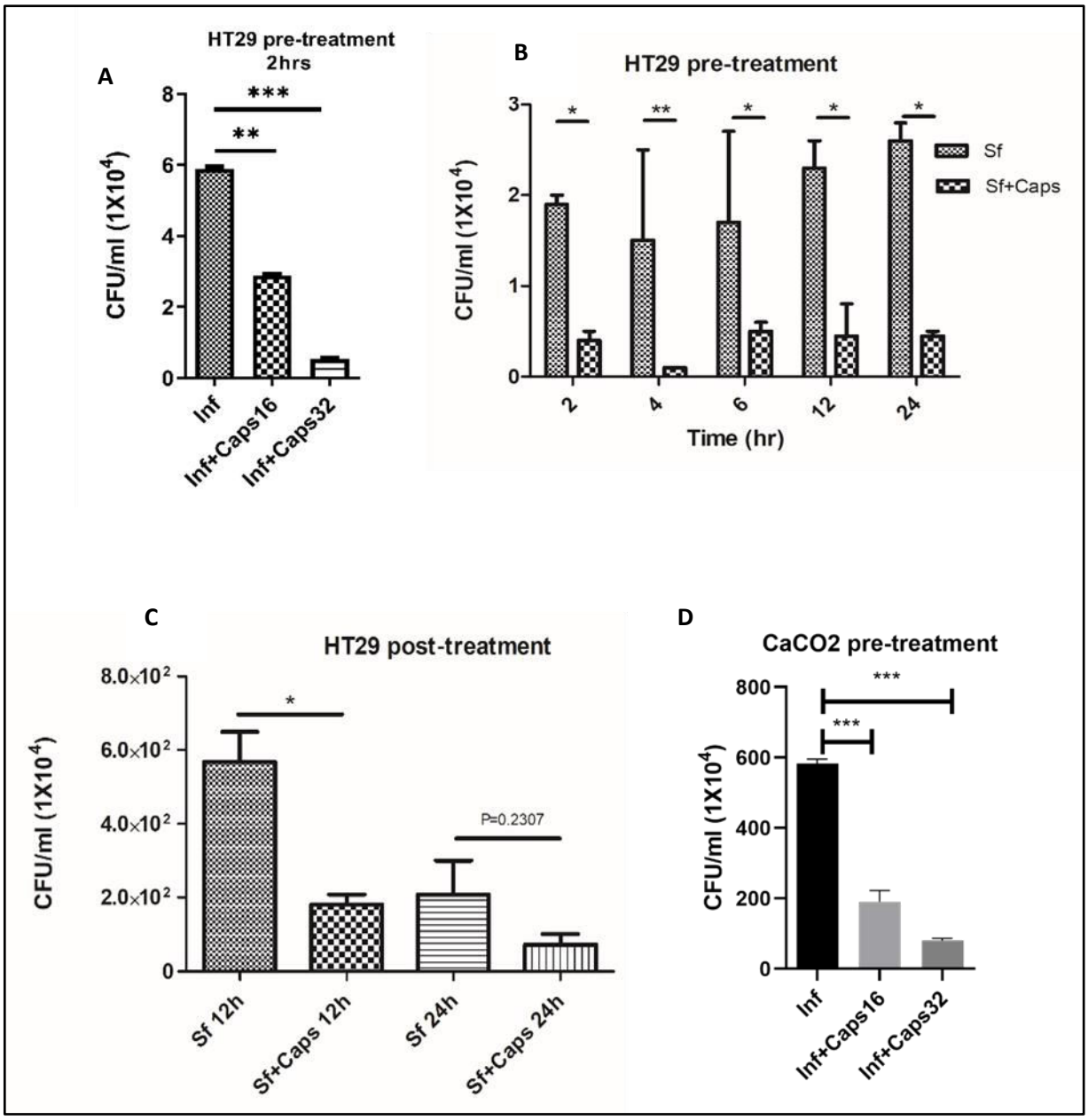

Fig1.5. Capsaicin (Caps) inhibits *S. flexneri* invasion in intestinal cells. **(A)** Gentamicin protection assay (GPA) was performed for comparison of colony forming unit (CFU/ml) in HT29 cells at different doses (16µM and 32µM) of Caps. **(B)** GPA in HT29 cells at different time point of Caps pre-treatment **(C)** GPA in HT29 cells at 12hrs and 24hrs of Caps post-treatment after 2h infection. **(D)** GPA was performed for comparison of colony forming unit (CFU/ml) in CaCO2 cells at various doses (16µM and 32µM) of Caps and graphically represented. One-way/ Two-way ANOVA was done * $p < 0.05$, ** $p < 0.01$, *** $p < 0.001$.

1.3.2. Capsaicin inhibits intracellular invasion of *S. flexneri* in macrophage cells

Inhibitory effect of Capsaicin (Caps) was also checked in *S. flexneri* infected macrophages. Macrophages are the immune cells and site of infection for *S. flexneri* during pathogenesis. Caps post-treatment for 4h significantly reduced intracellular bacterial load in RAW264.7 cells **(Fig1.6.A)**. Infected RAW cells at MOI200 were post-treated with Capsaicin for different time periods (4, 6, 8, 12h) **(Fig1.6.B)**. Capsaicin showed significant reduction in bacteria only after 4h treatment. Macrophage cells were infected with different MOI (20, 50,100) and post-treated with Capsaicin where it was observed that Capsaicin is significantly effective in bacterial clearance infected with *S. flexneri* 2457T at MOI100 **(Fig1.6.C)**.

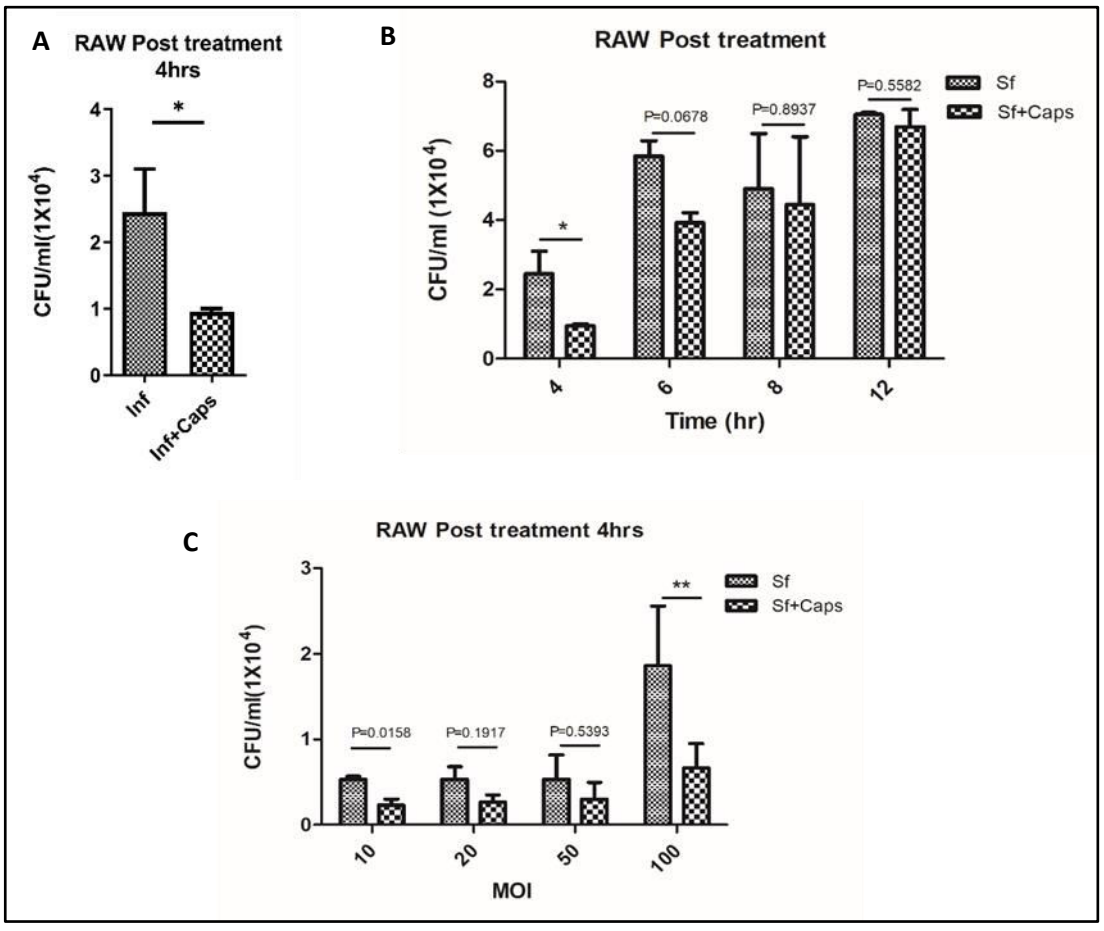

Fig1.6. Capsaicin (Caps) inhibits *S. flexneri* invasion in macrophage cells. **(A)** Gentamicin Protection Assay in RAW macrophage cells after Caps post treatment; Unpaired t-test was done; **(B)** RAW cells were infected for 30 mins followed by caps post-treatment at different time points. **(C)** GPA in RAW cells at 4 hrs of Caps post-treatment after 30 mins infection at different MOI; Cells were lysed and plated overnight for counting the number of colonies (n=3); Two-way ANOVA was done * $p < 0.05$, ** $p < 0.01$, *** $p < 0.001$.

1.4. Capsaicin at lower doses is less/non-toxic for host cells

As intracellular invasion of *S. flexneri* was inhibited by Capsaicin in intestinal and macrophage cells we checked the toxicity of Capsaicin. Bacterial growth might be reduced due to cellular toxicity**.** LDH assay data showed that Capsaicin treatment is almost nontoxic or less toxic for *S. flexneri* treated as well as untreated HT29 and RAW cells compared to Triton-X which is a positive control for cell lysis. Capsaicin toxicity is not significant in HT29 cells when treated for 24hrs **(Fig1.7.A)** as well as 48hrs **(Fig1.7.B)**. Capsaicin is also insignificantly toxic in RAW cells treated for 24hrs and 48 hrs **(Fig1.7.C)**. Capsaicin pre-treatment in *S. flexneri* infected intestinal cells also showed insignificant toxicity **(Fig1.7.D).** %cytotoxicity was calculated using the formula: $(OD_{(Cell+drug)}-OD_{drug})/(OD_{(Cell+TritonX)}-OD_{TritonX})*100\%$

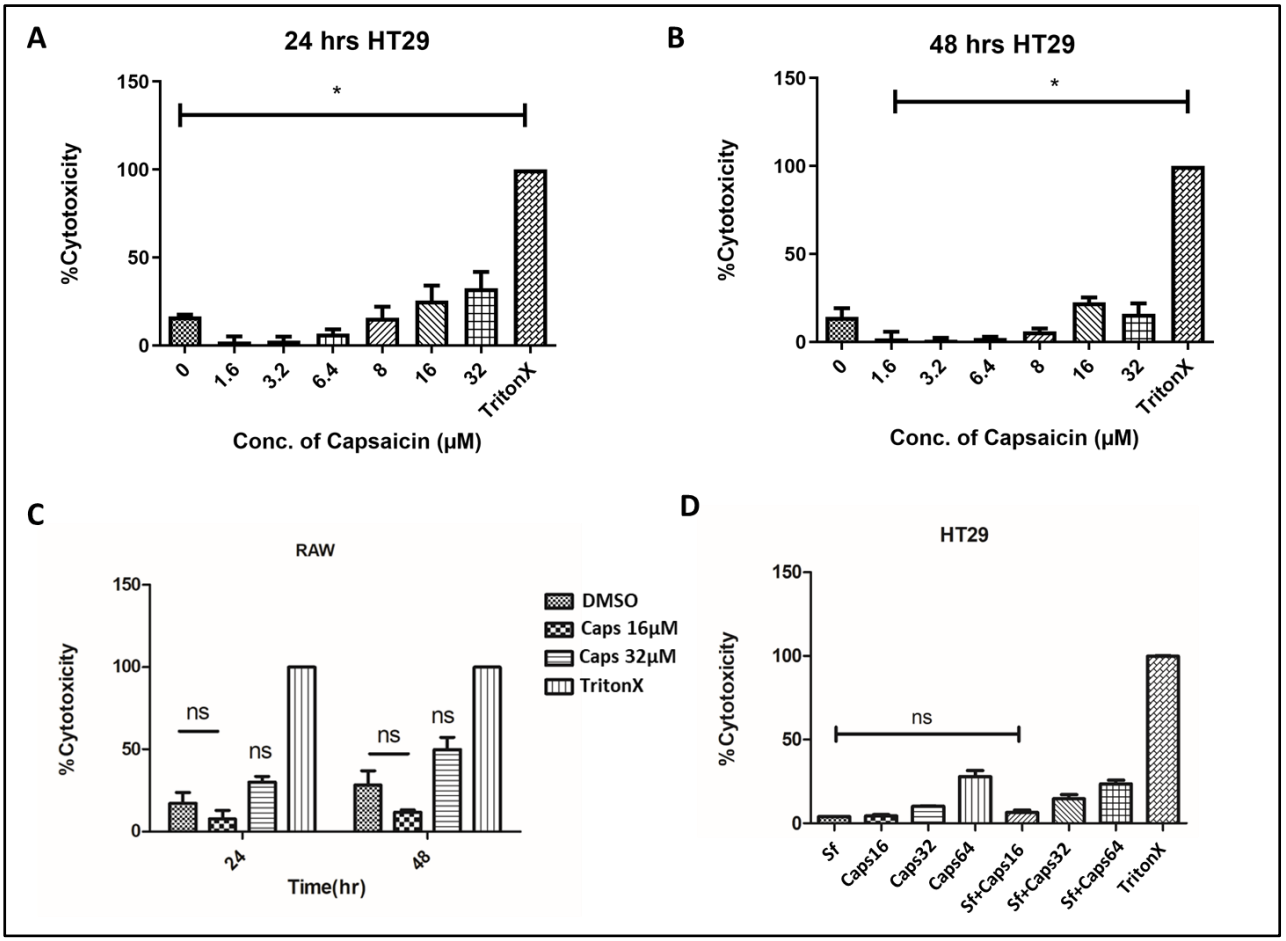

Fig1.7. Cytotoxicity study in HT29 and RAW cells. **(A-C)** HT29 and RAW cells were treated with different concentration of Capsaicin (0.5-10µg/ml) or DMSO for 24 hrs and 48 hrs. **(D)** HT29 cells were pre-treated with Caps for 24hrs followed by *S. flexneri* infection for 2 hrs. LDH assay was performed to measure % cytotoxicity level. %Cytotoxicity was graphically represented. (n=3) and One-way ANOVA was performed. * $p < 0.05$, ** $p < 0.01$, *** $p < 0.001$.

Chapter 2

Capsaicin induces autophagy in intestinal cells

Background

Macroautophagy, also known as autophagy, is a process by which long-lived or misfolded proteins as well as damaged cytoplasmic organelles and invading pathogens in eukaryotic cells are degraded. Autophagy is a dynamic process which is comprised of three steps: autophagosome formation, autophagosomal lysosomal fusion and degradation. The mechanism of autophagy plays a definitive role in different disease models like aggregation prone disorders, cancer and infectious diseases. "Autophagic flux" is used to represent the dynamics of autophagy. Autophagic flux encompasses the complete autophagy events, involving the development of autophagosomes, fusion between autophagosomes and lysosomes, macromolecule breakdown, and subsequent release into the cytosol. Autophagosomal accumulation indicates either activation of autophagy or a downstream blockage of autophagy, like inefficient fusion or reduced lysosomal degradation.

In the multi-step process of autophagy, several proteins are involved. Microtubule-associated proteins 1A/1B light chain 3B (MAP1LC3B) is a protein encoded by *MAP1LC3B* gene. LC3, most widely used autophagosomal marker plays an important role in the autophagy pathway. Autophagy related 5 (ATG5), an autophagy protein, is encoded by the *ATG5* gene. ATG5 is the central protein involved in phagophoric membrane extension in autophagic vesicles. The ATG12-ATG5:ATG16L complex elongates the phagophore. ATG7 activates ATG12, and ATG10 conjugates ATG5 to the complex which forms a complex with ATG16L.ATG12-ATG5:ATG16L complex conjugates phosphatidylethanolamine (PE) to LC3-I in the phagophore membrane, and converts into LC3-II. Accumulation of LC3II appears as puncta.

The complex dissociates followed by formation of the autophagosome. WD repeat domain phosphoinositide-interacting protein 1 (WIPI1), encoded by the *WIPI1* gene accumulates at ER-produced PtdIns3*P* upon initiation of autophagy. Different pools of WIPI proteins are recruited to different sites of PtdIns3*P* production. Another important lysosomal membrane protein is LAMP1 (Lysosome associated membrane protein-1) which is involved in lysosomal biogenesis (Eskelinen et al., 2004).

Autophagy is a host defence mechanism induced to fight infection during pathogen invasion. There are several autophagy enhancers reported to inhibit infection caused by both bacterial and viral pathogens (Floto et al., 2007). Autophagy plays a beneficial role in microbial diseases as it degrades the pathogen on one hand and also activates the host immune system against pathogens. *Shigella flexneri* releases effector proteins which evade the autophagy mechanism to establish itself and intracellularly replicates in the epithelial cells and macrophages.

On this context, we examined the effect of Capsaicin on autophagy in intestinal cells and macrophages as these are the sites of infection for *S. flexneri*. Capsaicin induced autophagy is not reported in intestinal cells previously. We examined the effect of Capsaicin on autophagy and evaluated the possibility for the anti-*Shigella* effect in intestinal cells and macrophages.

Methods

Autophagy protein expression levels were checked using western blot and gene levels were checked using qRT-PCR. Autophagosome formation was observed using confocal microscopy and TEM. All methods are previously described in materials and methods section.

Results

2.1. Capsaicin induces autophagy in a dose dependent manner

2.1.1. Activation of autophagy genes

As Capsaicin is a known autophagy modulator, we checked the effect of Capsaicin on upregulation of autophagy in HT29 cells. For this, we have treated cells with Capsaicin dose-dependently and observed that it induced expression of genes involved in autophagy. Expression of several major autophagy genes (MAP1LC3B, ATG5 and WIPI1) was significantly upregulated in 16µM and 32µM Capsaicin treated cells (**Fig2.1.A-C**).

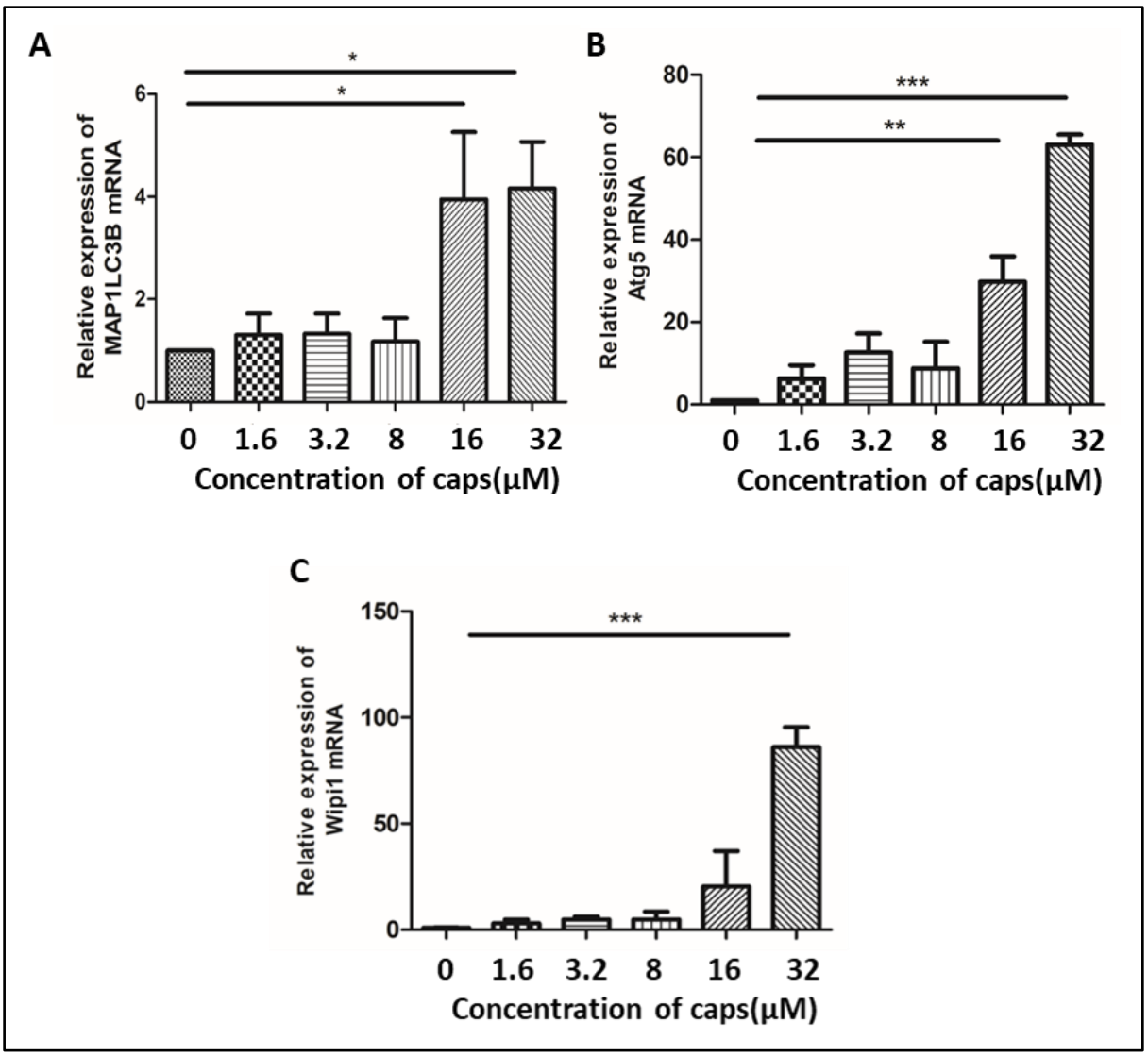

Fig2.1. Capsaicin induced autophagy genes in intestinal cells. (A-C) HT29 cells were treated with either Capsaicin (at concentrations of 16µM and 32µM) or DMSO for 2 hours. Following this, qRT-PCR was conducted to assess the expression levels of autophagy-associated marker genes (MAP1LC3B, ATG5, WIPI1), with GAPDH as the reference gene. The resulting relative fold change was computed and visually presented through a graph (n=3). Subsequently, a one-way ANOVA statistical analysis was carried out, revealing significance levels denoted as * for $p < 0.05$, ** for $p < 0.01$, and *** for $p < 0.001$.

2.1.2. Induction of autophagic protein expression

Moreover, we checked the expression of autophagy markers at the protein level. Capsaicin induced expression of proteins involved in autophagy. From the western blot data, it has been observed that level of P62 was degraded dose dependently in HT29 cells. As degradation of P62 is a marker of autophagy upregulation, we checked for expression of major autophagy proteins, Atg5 and Beclin1. Expression of Atg5 and Beclin1 proteins were significantly upregulated dose dependently **(Fig2.2A-D)**. The effect is mostly observed at 16µM and 32µM doses of Capsaicin treatment in intestinal cells.

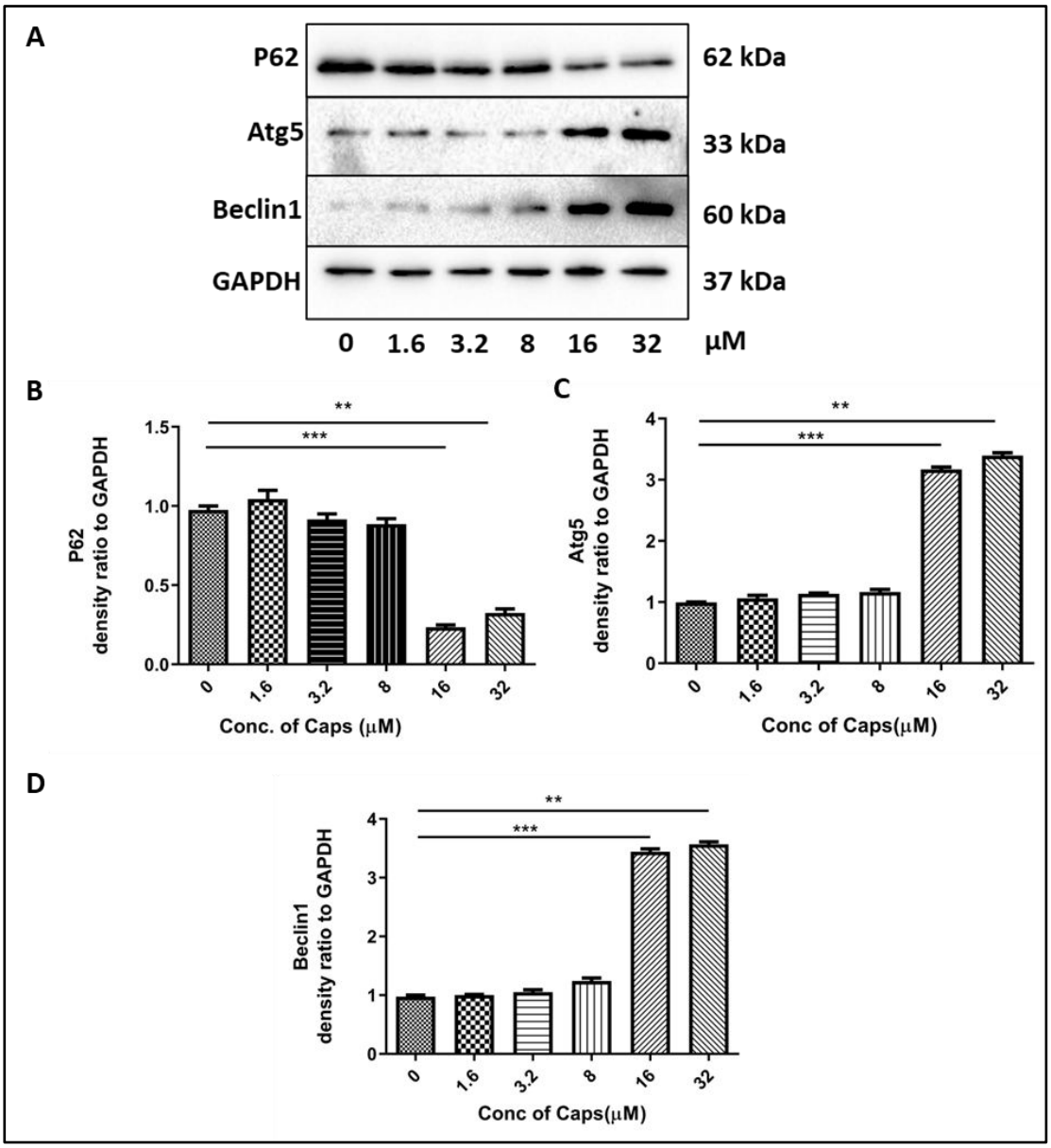

Fig2.2. Capsaicin induced autophagic protein expression in intestinal cells. (A) HT29 cells underwent treatment with varying concentrations of Capsaicin (ranging from 1.6μM to 32μM) or DMSO over a span of 2 hours. Immunoblotting was used to observe the expression of key autophagy-associated marker proteins, namely P62, Atg5, and Beclin1. Gapdh was used as loading control. **(B-D)** Densitometric analyses of these observations were graphed for clarity (n=3), and subsequently, a one-way ANOVA analysis was performed to determine significance levels, depicted as * for $p < 0.05$, ** for $p < 0.01$, and *** for $p < 0.001$.

2.2. Capsaicin enhances autophagosome formation

2.2.1. Visualization of autophagosome using TEM

Autophagosome formation is an indication of functional autophagy and autophagosome maturation helps in lysosomal fusion and degradation. Subsequently, we confirmed autophagosome formation by microscopic methods. Transmission electron microscopic (TEM) images showed enhanced autophagosome formation in Capsaicin treated intestinal cells **(Fig2.3)**. Graphical representation shows significant increase of %autophagosome formation in Capsaicin treatment as compared to control.

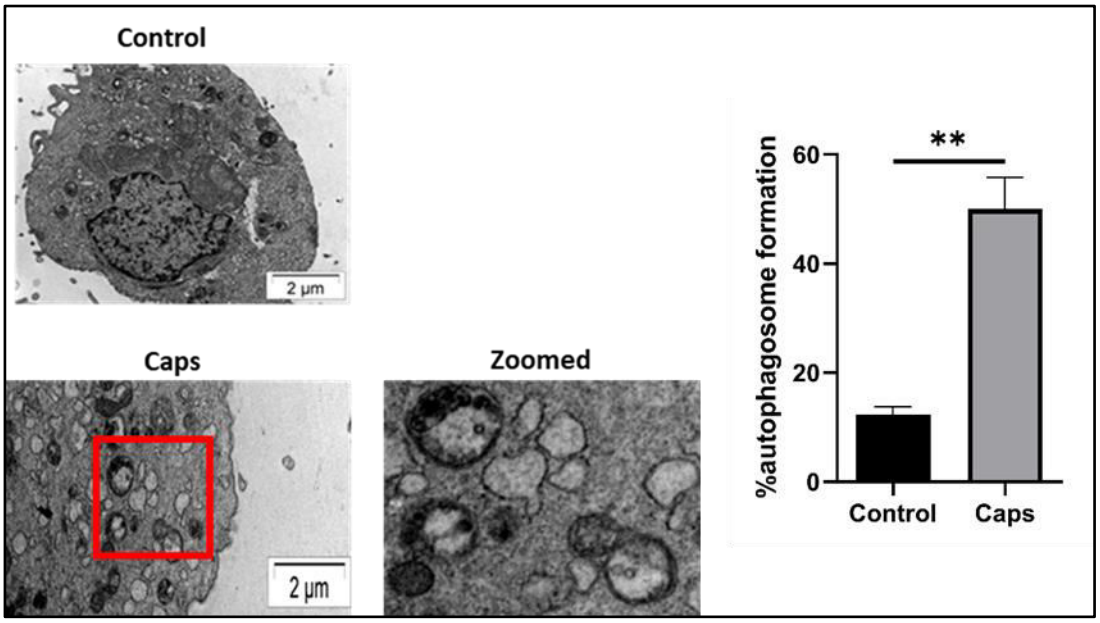

Fig2.3. Treatment with Capsaicin enhanced autophagosome formation. Transmission electron microscopy (TEM) images revealed the presence of autophagosome formation in HT-29 cells with Capsaicin treatment over a 4-hour period. Zoomed-in images focused on specific areas, with a scale bar of 2µm. The percentage of autophagosome formation observed in TEM images was graphically presented. Statistical analysis involved an unpaired t-test, and significance levels were denoted as * $p < 0.05$, ** $p < 0.01$, *** $p < 0.001$.

2.2.2. Visualization of autophagosome formation using confocal microscopy

LC3B puncta is associated with matured autophagosome formation. Hence, we checked LC3B puncta formation. Confocal microscopic images showed that Capsaicin enhances LC3B puncta formation in GFP-LC3B transfected HT29 cells **(Fig2.4.A)**. Graphical representation shows significant increase of %LC3B puncta formation in Capsaicin treatment as compared to control. Puncta formation is associated with conversion of LC3I to LC3II after addition of phosphatidylethanolamine (PE). Similarly, we also treated the macrophage cells with Capsaicin after transfection with GFP-LC3B. We observed increase in LC3B puncta significantly in drug treated cells as compared to control cells(e-GFP) **(Fig2.4.B).**

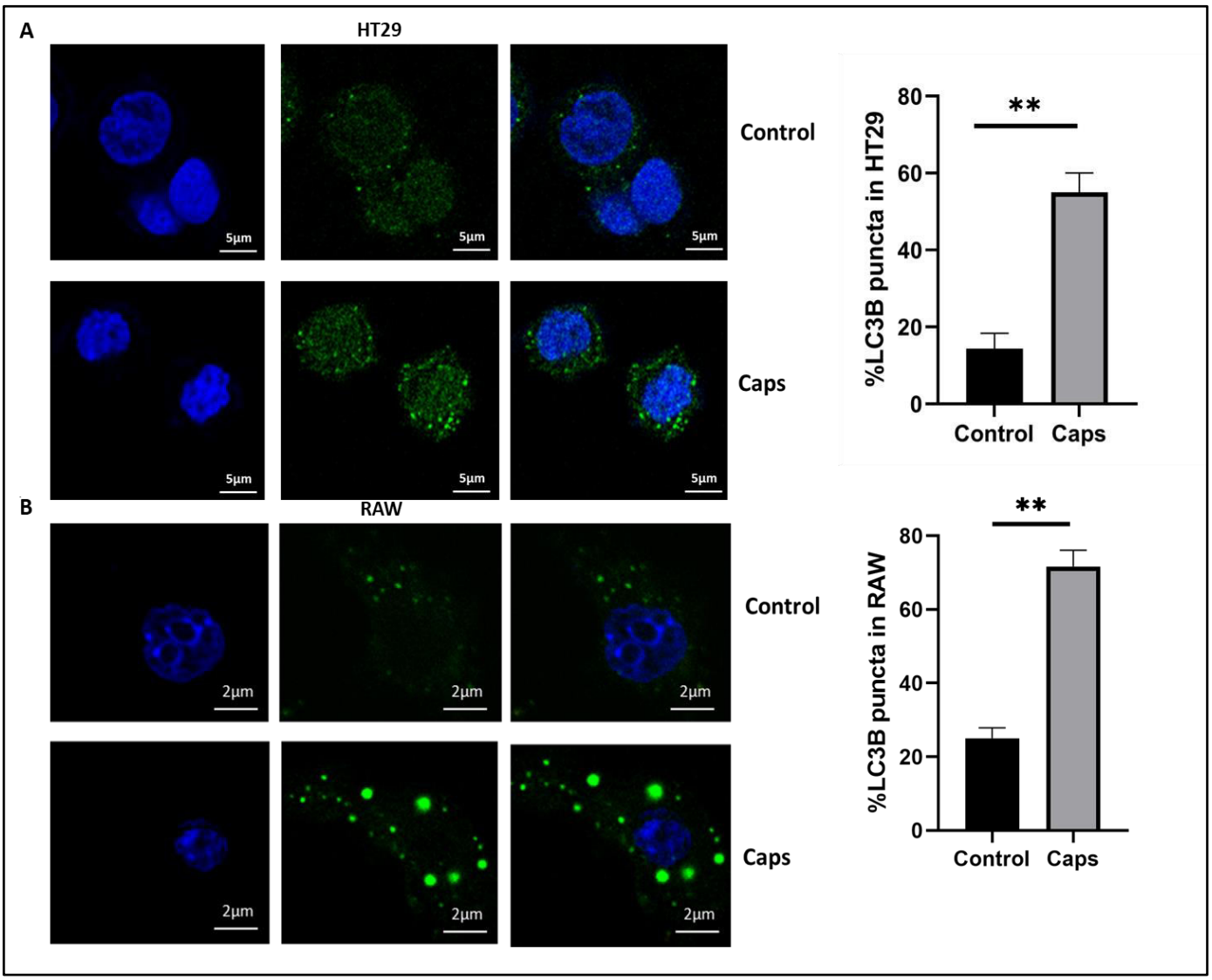

Fig2.4. Capsaicin treatment showed autophagosome formation in confocal microscopy. (A-B) Confocal microscopy images displayed the development of LC3B puncta (green spots) in intestinal cells (HT-29) and macrophage cells (RAW267.4) after transfection with GFP-LC3B plasmid. Following this, cells were exposed to Capsaicin for a 4-hour period and observed under a confocal microscope. The percentage of LC3B puncta formation was represented. Statistical analysis included an unpaired t-test (n=3); significance levels were indicated as * for $p < 0.05$, ** for $p < 0.01$, and *** for $p < 0.001$.

OBJECTIVE II

Chapter 3

Upregulation of autophagy in S. flexneri infected cells by Capsaicin

Background

S. flexneri possess a virulence plasmid encoding a type III secretion system (T3SS) which is a needle-like apparatus for injecting bacterial effector proteins into the host cell (Ogawa et al., 2008; Pinaud, Sansonetti and Phalipon, 2018). During the invasion process in host cells, lysis of phagocytic vacuole takes place gaining access to the host cytosol which is the site for its replication. For counteracting replication of *S. flexneri* in the cytosol, a variety of antimicrobial responses are employed which are primarily antibacterial autophagy and septin caging (Mostowy and Cossart, 2012). For evading cytosolic immune responses, cytosolic *Shigella flexneri* modifies host actin cytoskeleton for cell-to-cell spreading and thereby evades host immune defense system (Welch and Way, 2013).

Shigella flexneri infection leads to activation of autophagy primarily in three steps, i.e., invasion, rupturing phagocytic vacuole and replicating in the cytosol (Krokowski and Mostowy, 2016).

Firstly, autophagy is induced during *S. flexneri* infection in the host cells. In non-phagocytic epithelial cells, the invasion of *S. flexneri* relies on the release of T3SS effector proteins. These proteins prompt a reorganization of the host cytoskeleton system, causing membrane ruffling and facilitating bacterial uptake (Cossart and Sansonetti, 2004). Once inside, NOD proteins interact with ATG16L1, which then recruits autophagy-related machinery to the site where the bacteria entered through the cell's plasma membrane. This connection between NOD proteins and bacterial detection leads to the formation of autophagosomes. Interestingly, ATG16L1 also plays a role beyond autophagy, influencing the regulation of NOD-triggered inflammatory responses in epithelial cells (Philpott et al., 2014). Here,

ATG16L1, in an autophagy independent manner inhibits NOD1- and NOD2-driven cytokine responses. LC3B, the autophagy marker recognizes *S. flexneri* during entrapped condition of bacteria in a double-membrane vacuole (Campbell-Valois et al., 2015). Bacterial effector proteins IcsB and VirA help to avoid autophagic degradation which also leads to escape of bacteria from LC3-positive vacuoles.

Secondly, bacteria rupture autophagic vesicles and gains access to the cytosol. Ruptured membrane remnants get ubiquitinated which are being recognized by p62 and NDP52 and that further results in LC3B positive membrane recruitment for autophagosome biogenesis. p62, present on membrane remnants leads to activation of nuclear factor kappa B (NF-κB) signaling.

Thirdly, *S. flexneri* expresses IcsA and recruits N-WASP and the actin related protein 2/3 (ARP2/3) complex that leads to subvertion of the host actin cytoskeleton resulting in actin-based motility for spreading from cell-to-cell. IcsA is recognized by ATG5, another host autophagic protein for degradation. Finally, ATG5 binds to the adaptor protein tectonin beta-propeller repeat containing 1 (TECPR1 independent of ubiquitin. TECPR1 interacts with WIPI-2 and PI(3)P and recruits LC3B for autophagic degradation. Cytosolic *S. flexneri* secretes IcsB which inhibits the interaction between IcsA and ATG5 thus protecting itself from autophagic recognition.

Therefore, host autophagic response is responsible for controlling *Shigella flexneri* infection. *S. flexneri* has evolved with a well-defined T3SS system which secretes virulent factors that helps in evading autophagy to survive within the host.

Materials and Methods

PCR array was performed to assess the effect of Capsaicin (Caps) on autophagic gene expression. Western blots were performed to evaluate autophagic protein expression levels. Autophagosome formation was observed using confocal microscopy and TEM. Lipofectamine mediated transfection was done to knock down intestinal cells for Atg5.qRT-PCR was used to assess expression level of autophagy genes. Detailed methods are already described in the materials and methods section.

Results

3.1. Capsaicin induces overexpression of autophagy genes in *S. flexneri* infected intestinal cells

To assess the effect of Capsaicin on autophagic gene expression, a PCR array was performed. Differential gene expression was observed due to Caps treatment in intestinal cells for 4h. More than 78% of the genes are augmented by Caps alone at a dose of 16µM. In *S flexneri* infected cells, drug treatment also increased the expression of autophagy genes. **(Fig3.1.A)**

Further, we confirmed the induction of autophagy flux by Capsaicin in infected cells. Intestinal cells were treated with Capsaicin for various doses and subjected to lysis. Autophagic flux was measured. Induction of autophagy was shown in Capsaicin pre-treated cells. Capsaicin at 16µM and 32µM doses induced autophagic flux significantly. Rapamycin was used as a positive autophagy inducer. Capsaicin also induced autophagic flux in *S. flexneri* infected cells at different doses **(Fig3.1.B)**.

A

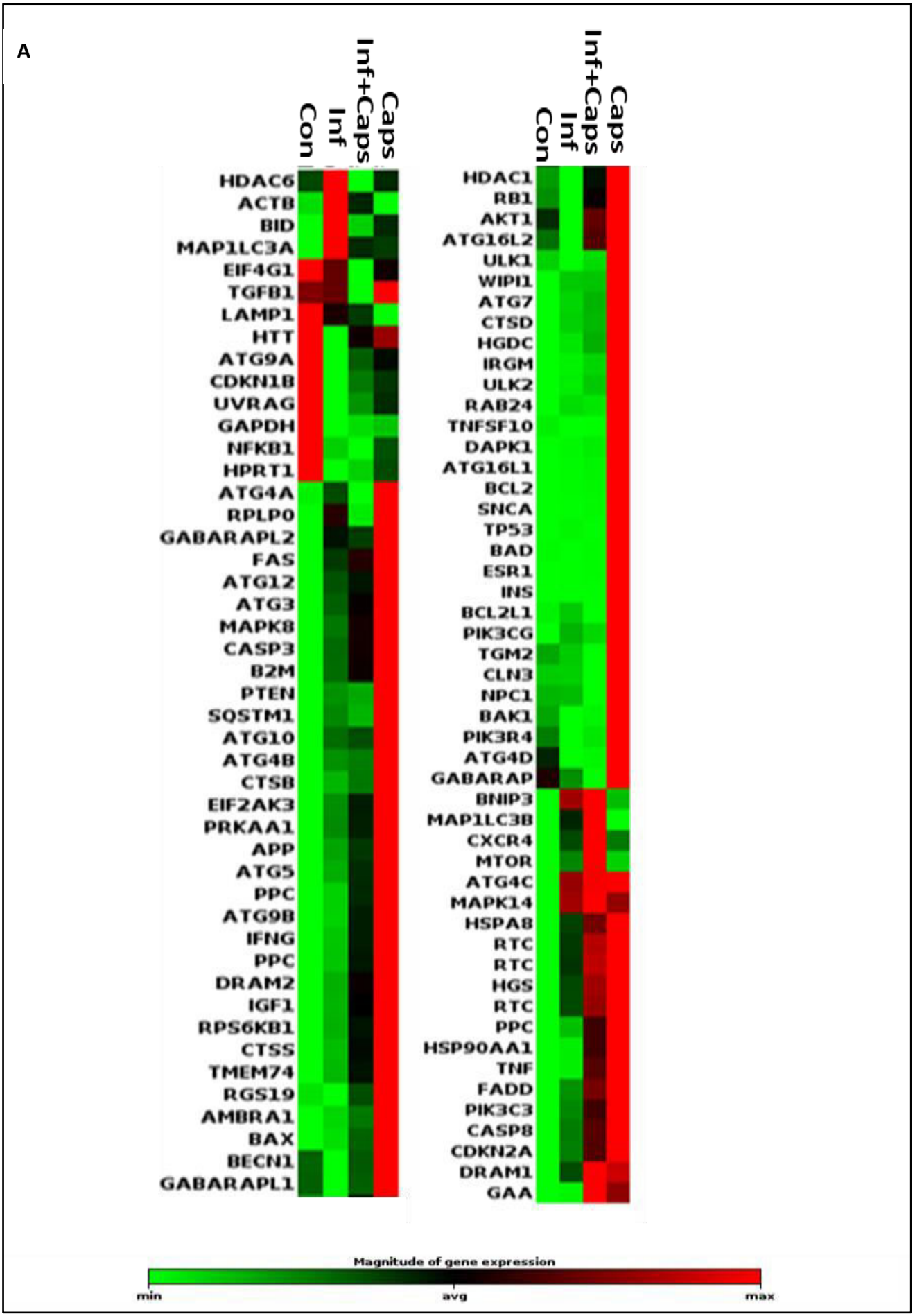
Con
Inf
Inf+Caps
Caps
HDAC6
ACTB
BID
MAP1LC3A
EIF4G1
TGFB1
LAMP1
HTT
ATG9A
CDKN1B
UVRAG
GAPDH
NFKB1
HPRT1
ATG4A
RPLP0
GABARAPL2
FAS
ATG12
ATG3
MAPK8
CASP3
B2M
PTEN
SQSTM1
ATG10
ATG4B
CTSB
EIF2AK3
PRKAA1
APP
ATG5
PPC
ATG9B
IFNG
PPC
DRAM2
IGF1
RPS6KB1
CTSS
TMEM74
RGS19
AMBRA1
BAX
BECN1
GABARAPL1
HDAC1
RB1
AKT1
ATG16L2
ULK1
WIPI1
ATG7
CTSD
HGDC
IRGM
ULK2
RAB24
TNFSF10
DAPK1
ATG16L1
BCL2
SNCA
TP53
BAD
ESR1
INS
BCL2L1
PIK3CG
TGM2
CLN3
NPC1
BAK1
PIK3R4
ATG4D
GABARAP
BNIP3
MAP1LC3B
CXCR4
MTOR
ATG4C
MAPK14
HSPA8
RTC
RTC
HGS
RTC
PPC
HSP90AA1
TNF
FADD
PIK3C3
CASP8
CDKN2A
DRAM1
GAA
Magnitude of gene expression
min
avg
max

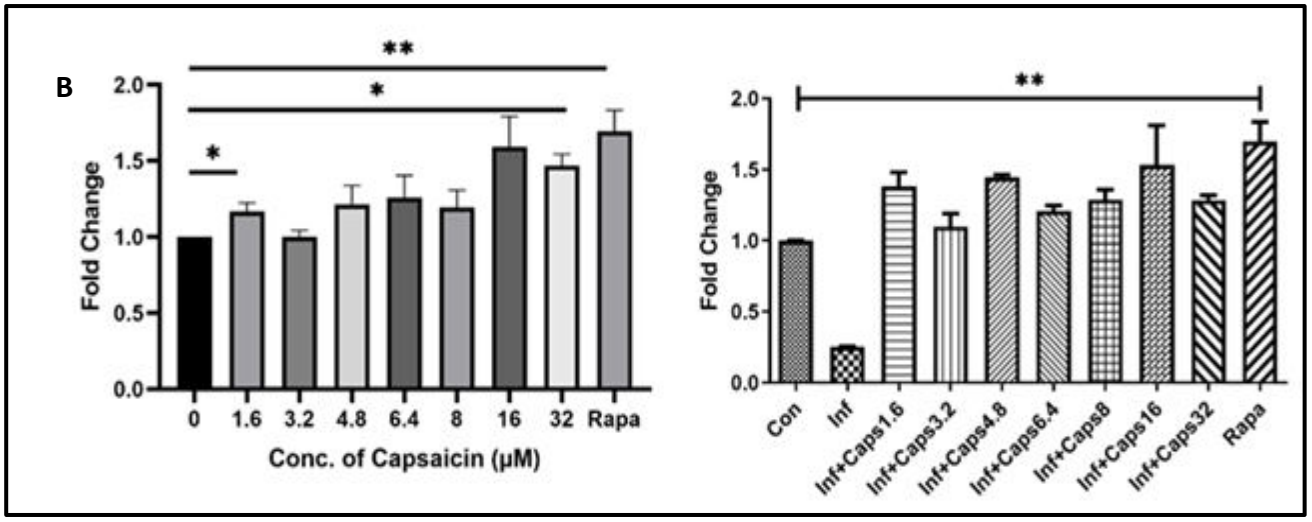

Fig3.1. Autophagy is upregulated in Capsaicin treated infected cells. **(A)** PCR array was performed with control, infected, Capsaicin treated, infected and only Capsaicin treated samples. [Con = DMSO treated cells, Inf = *Shigella flexneri* sf2457T infected cell, Inf+Capsaicin = Capsaicin pre-treatment at a dose of 16μM followed by sf2457T infection, Capsaicin = Capsaicin treatment at a dose of 16μM]. Heat map generated represents differential gene expression. **(B)** Capsaicin induced autophagy flux dose dependently in intestinal cells. HT29 cells were treated with Capsaicin (0, 1.6, 3.2, 4.8, 8, 16, 32 μM). Capsaicin pre-treated cells were further infected with *S. flexneri* (MOI 200) and lysed cells were examined. Rapamycin (500nM) was used as a positive control. Autophagic flux was measured at 480/530 nm using a fluorescent microplate reader (n=3); * $p < 0.05$, ** $p < 0.01$, *** $p < 0.001$.

3.2. Upregulation of autophagy genes by Capsaicin in infected cells.

In addition, we validated the expression of important autophagic genes by quantitative PCR in intestinal cells. Capsaicin induced expression of genes involved in autophagy in infected HT29 cells. Expression of MAP1LC3B, ATG5 and WIPI1 genes were evaluated in Capsaicin treated infected cells and compared with control cells.**(Fig3.2A,B,C)**.Rapamycin was used as positive control. Capsaicin augmented the expression of MAP1LC3B and Atg5 significantly.

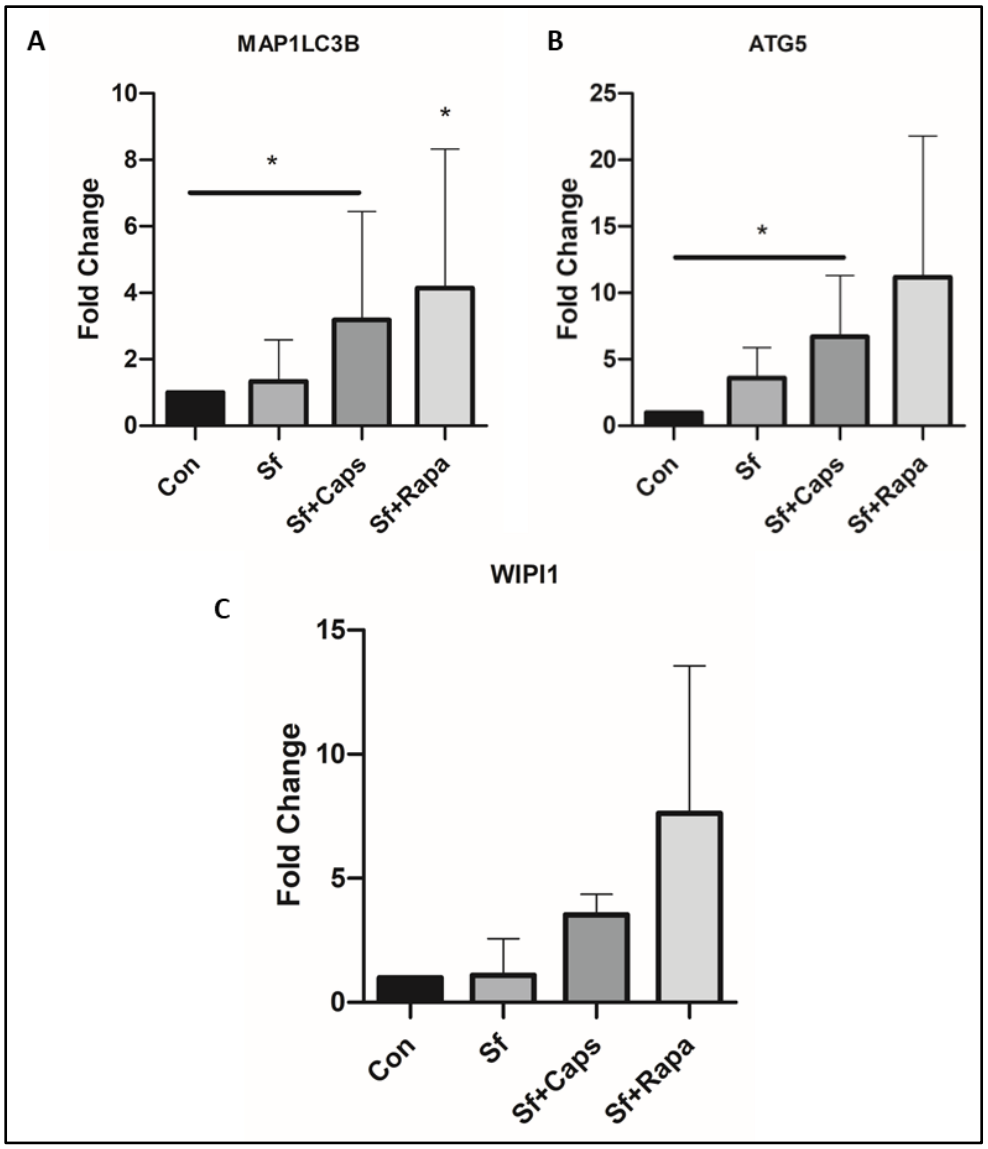

Fig3.2. Autophagy genes upregulated in Capsaicin treated infected cells. **(A-C)** HT29 cells were pre-treated with Capsaicin(16μM) for 2h followed by infection. After infection cells were lysed. Quantitative PCR was performed to evaluate the expression level of autophagy associated marker genes (MAP1LC3B, WIPI1, ATG5) in infected HT29 cells pre-treated with Capsaicin (n=3). Fold changes were graphically represented. One-way ANOVA was performed (n=3); * $p < 0.05$, ** $p < 0.01$, *** $p < 0.001$.

3.3. Autophagy marker proteins are activated due to Capsaicin treatment

We further confirmed activation of autophagy triggered by Capsaicin using western blot analysis in both infected and uninfected cells. In drug-treated cells, both LC3B and LAMP1

proteins, which are end stage markers of autophagy, were upregulated. **(Fig3.3.A)**. Density ratios were calculated and graphically represented **(Fig3.3.B).**

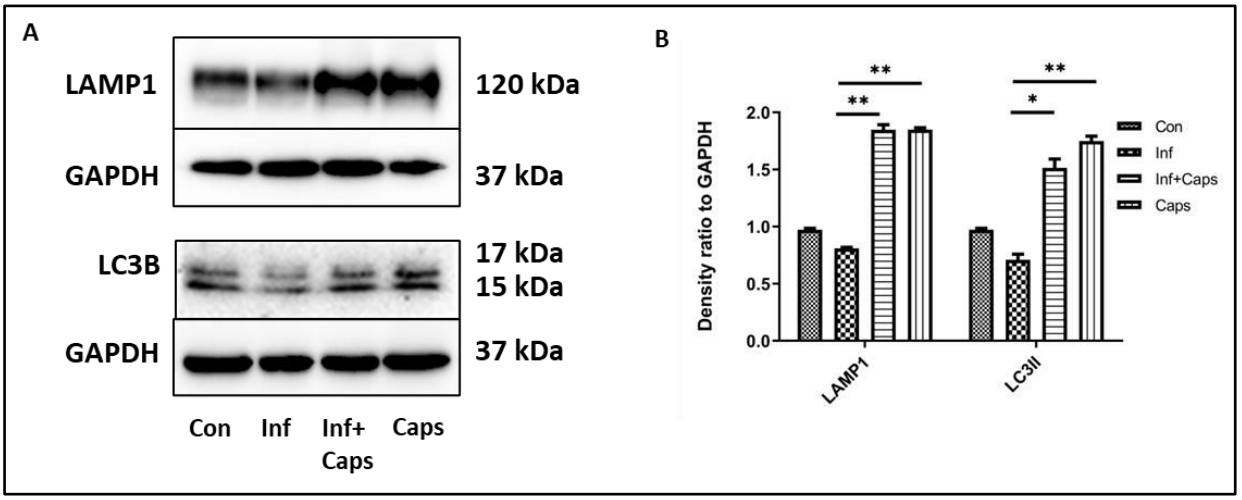

Fig3.3. Autophagy proteins upregulated in Capsaicin treated infected cells. **(A, B)** HT29 cells were pre-treated with Capsaicin for 2h followed by infection. After infection cells were lysed. Cell lysates were subjected to immunoblotting. Increase in LC3B and LAMP1 expression was shown by western blotting and densitometric analyses were graphically represented. One-way ANOVA was performed (n=3); * $p < 0.05$, ** $p < 0.01$, *** $p < 0.001$.

3.4. Capsaicin induces autophagosome formation in infected cells

3.4.1. Visualisation using Transmission electron microscopy

Finally, we confirmed autophagosome formation in drug treated infected cells by microscopic methods. Transmission electron microscopy (TEM) images showed enhanced double membraned bound autophagosome formation in Capsaicin treated infected intestinal cells **(Fig3.4.A)**. Graphical representation shows significant increase of %autophagosome formation in Capsaicin treated infected cells as compared to only infected cells. We also confirmed the capture of bacteria by autophagosomes in macrophages **(Fig3.4.B)**. TEM

images showed engulfment of *S. flexneri* by autophagosome. Capsaicin treatment increased % autophagosome formation significantly as compared to only infected cells.

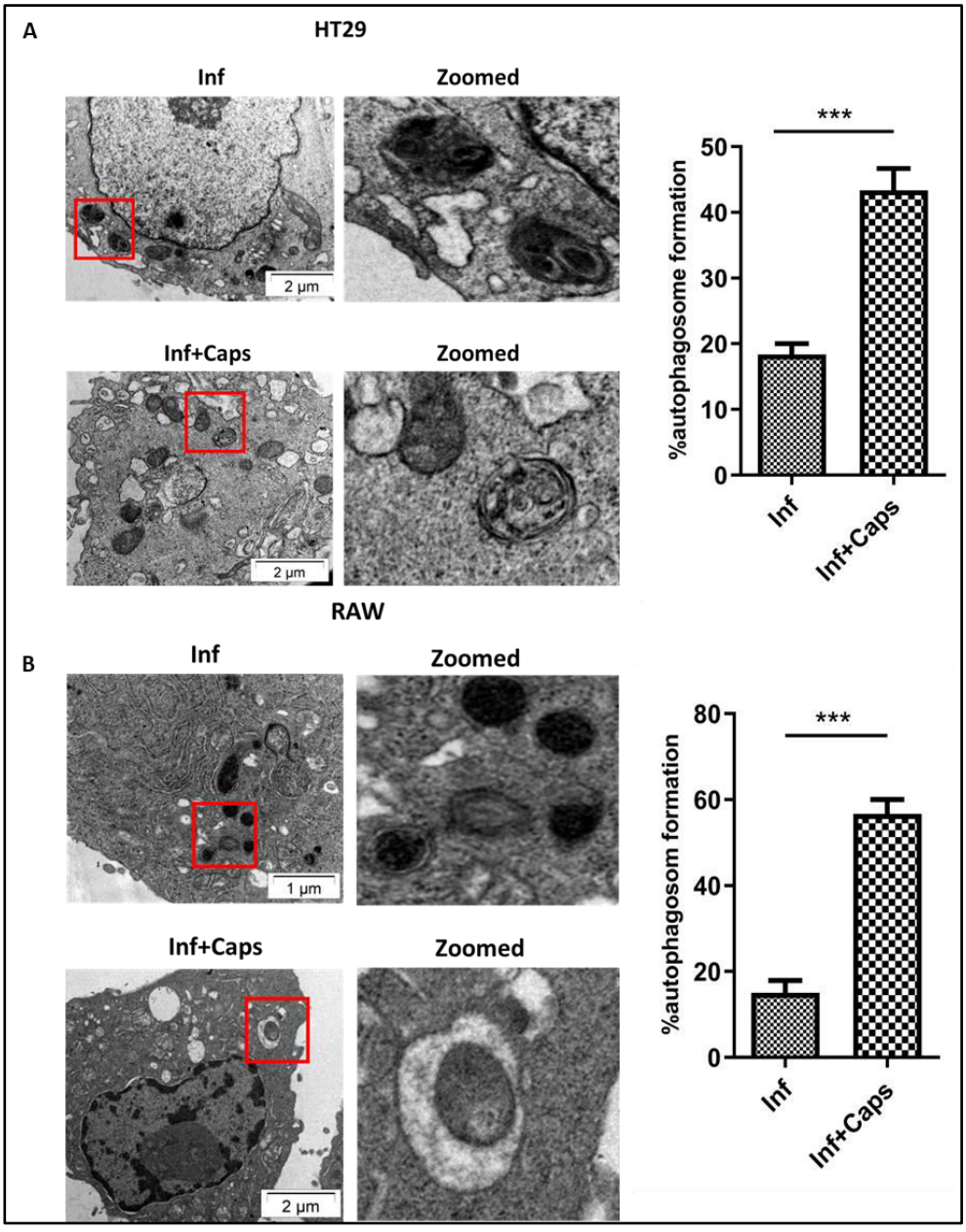

Fig3.4. Capsaicin treatment resulted in engulfment of bacteria by autophagosome. **(A)** Transmission Electron Microscopy (TEM) images showed the existence of autophagosome formation in infected intestinal cells due to Capsaicin exposure. **(B)** TEM images of autophagosome formation in infected and infected+Caps RAW267.4 cells. Capture of bacteria by autophagosome is shown. Graphical representation of % autophagosome formation as observed in TEM. Zoomed images of the highlighted region are also provided. The scale bar was set at 2µm. An unpaired t-test was conducted (n=3) to analyse the data, with significance levels denoted as * for $p < 0.05$, ** for $p < 0.01$, and *** for $p < 0.001$.

3.4.2. Visualization using confocal microscopy

Similarly, immunofluorescence studies showed increased LC3B puncta formation in Capsaicin treated infected intestinal cells. Graphical representation shows significant increase of LC3B recruitment to bacteria in Capsaicin treated infected cells compared to only infected cells **(Fig3.5.A)**. Macrophage cells also showed recruitment of bacteria to autophagosome due to LC3B puncta formation **(Fig3.5.B)**. LC3B is associated to mature autophagosome formation.

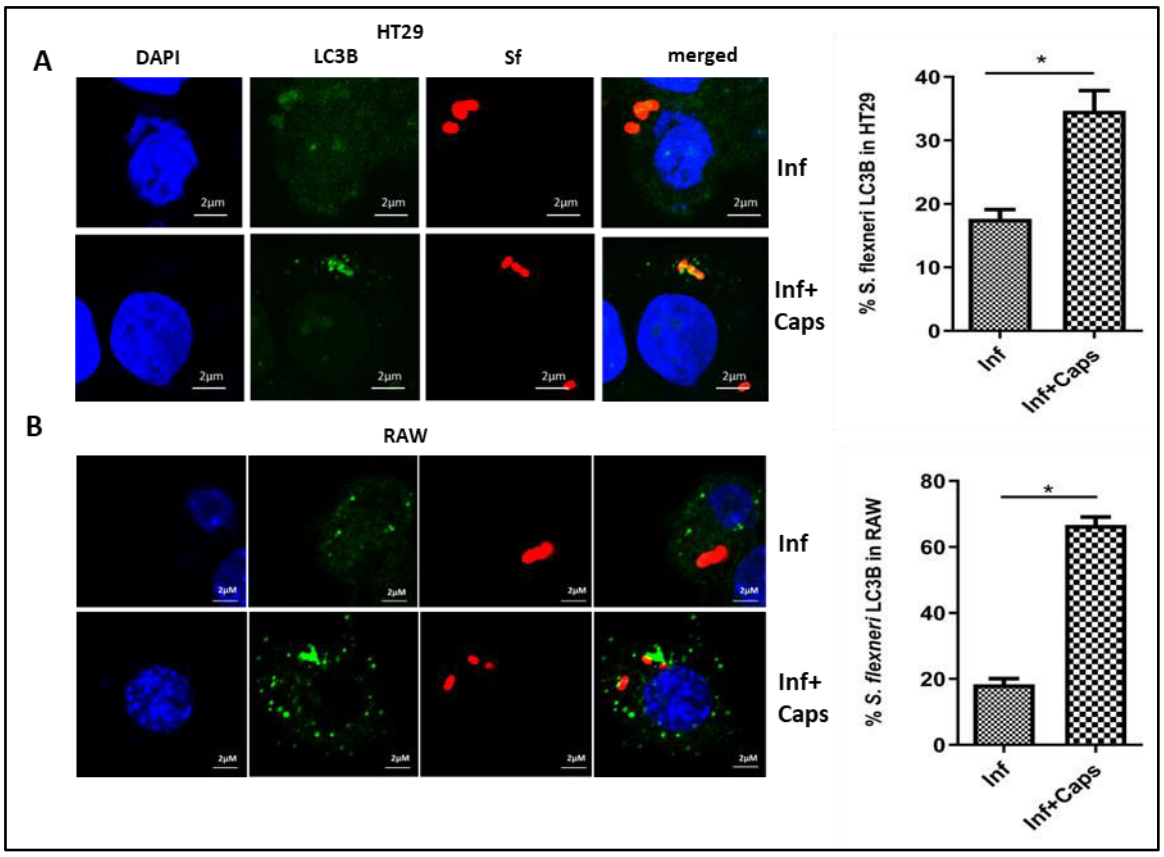

Fig3.5. LC3B recruitment to bacteria by Capsaicin treatment in confocal microscopy. (A) Confocal images of GFP-LC3B transfected intestinal cells (HT-29) depicted the recruitment of *S. flexneri* (red) to LC3B (green). Briefly, cells were first transfected with GFP-LC3B plasmid, then subjected to a 2-hour Capsaicin treatment, followed by a 2-hour infection with *S. flexneri*. **(B)** In panel B, microscopy images represented GFP-LC3B transfected macrophages (RAW 267.4) infected with bacteria and treated with or without Capsaicin. The graph represented the number of bacteria colocalising with LC3B. The scale bar was set at

2μM. A statistical analysis using an unpaired t-test (n=3) was conducted, with significance levels indicated as * for $p < 0.05$, ** for $p < 0.01$, and *** for $p < 0.001$.

3.4.3. Capsaicin induces autophagosomal engulfment of virulent *Shigella flexneri*

In order to confirm intracellular capture of *Shigella flexneri* by Capsaicin induced autophagy, we have taken a T3SS (Type III secretion system) null strain (plasmid cured). On Congo red plates, *S. flexneri* colonies appeared white instead of the typical red, indicating the absence of virulence factors (T3SS) **(Fig3.6.A)**. Confocal microscopy findings demonstrated lack of bacterial recruitment to LC3B in cells treated with Capsaicin, with a majority of bacteria located outside the cells. T3SS factors play a key role in the intracellular colonization of *S. flexneri* **(Fig3.6.B)**.

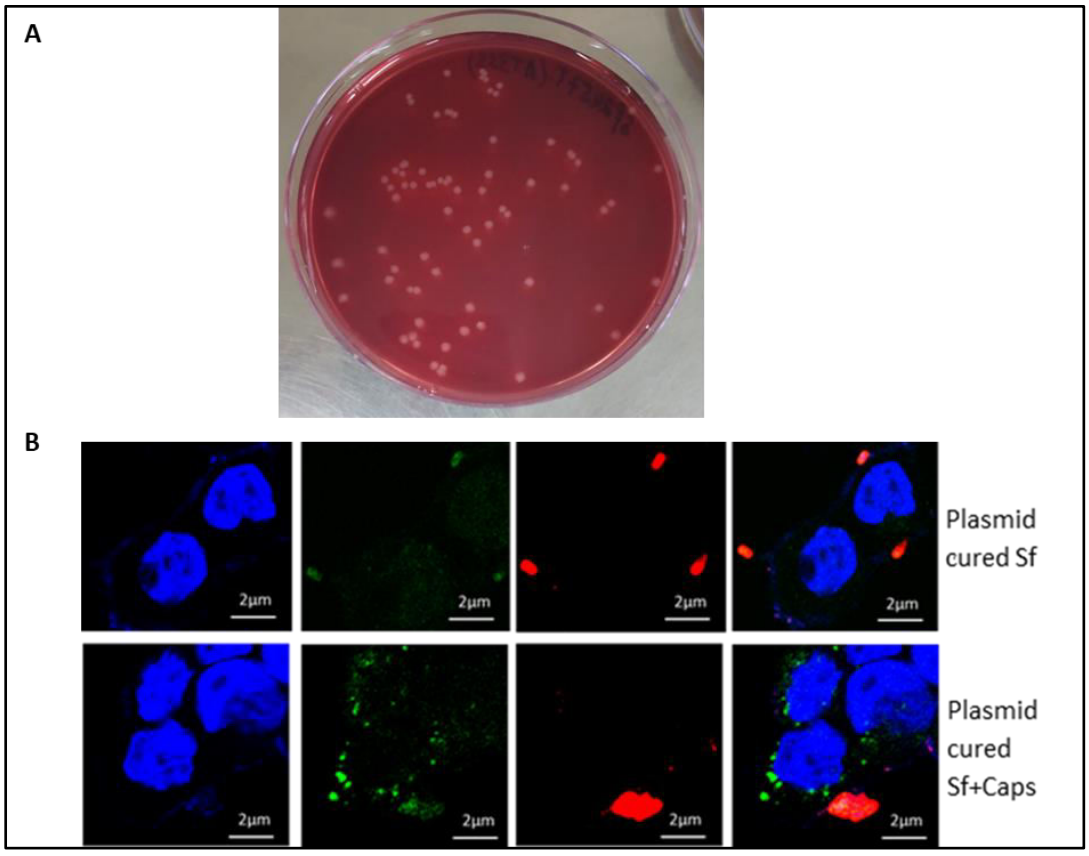

Fig3.6. LC3B recruitment is absent in Capsaicin treated plasmid cured *S. flexneri* infected cells. **(A)** T3SS negative *S. flexneri* generated white colonies in Congo red plate. **(B)** Confocal microscopy of HT-29 cells infected with plasmid cured *S. flexneri* (Red) and treated with Capsaicin. LC3B (Green) puncta formation in GFP-LC3B overexpressed HT29 cells. Scale bar: 2μM.

3.5. Effect of autophagy inhibition in Capsaicin treated intestinal cells

Following our investigations, we aimed to assess the impact of autophagy on *S. flexneri* growth. We used autophagy inhibitors such as 3 methyl-adenine (3MA). As anticipated, the use of 3MA led to increase in intracellular *S. flexneri*, and the combination of Capsaicin with 3MA failed to hinder the growth of intracellular *S. flexneri.* **(Fig3.7).** Thus, the killing of bacteria is dependent on autophagic activation. Consistent with the results of autophagy inhibition, we specifically inhibited a major autophagy player Atg5. Knockdown of Atg5 by siRNA transfection method inhibits autophagy mechanism during *S. flexneri* infection in HT29 cells. We transfected HT29 cells with scrambled and Atg5 siRNA. Upon Capsaicin treatment, LC3B puncta formation takes place in both infected and uninfected cells as observed previously. But, in Atg5 knockdown cells, LC3B puncta formation decreased. **(Fig3.8).**

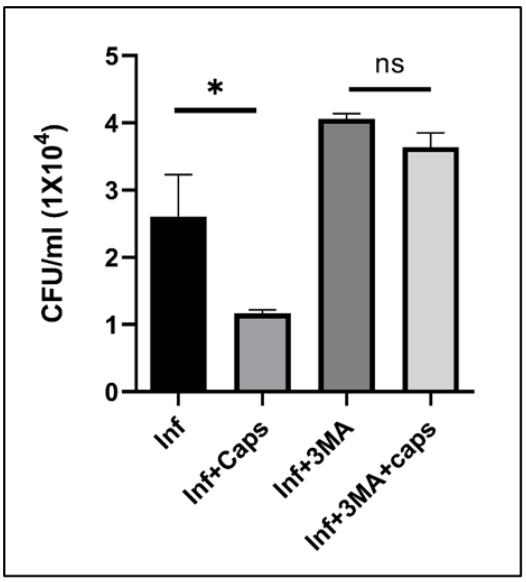

Fig3.7. Autophagy inhibitor (3MA) altered Capsaicin induced autophagy. Intestinal cells treated with 3MA (5 mM) and Capsaicin (16μM) for duration of 2 hours. Subsequently, they were infected with *S. flexneri*

for 2 hours and then exposed to gentamicin. An infection assay was conducted, and the graph shows the colony count of intracellular bacteria. Statistical analysis was performed using a one-way ANOVA. The data were presented in graphs using GraphPad Prism 5, showing the mean ± SEM (n = 3). Significance levels were determined through two-way ANOVA; denoted as * for $p < 0.05$, ** for $p < 0.01$, and *** for $p < 0.001$.

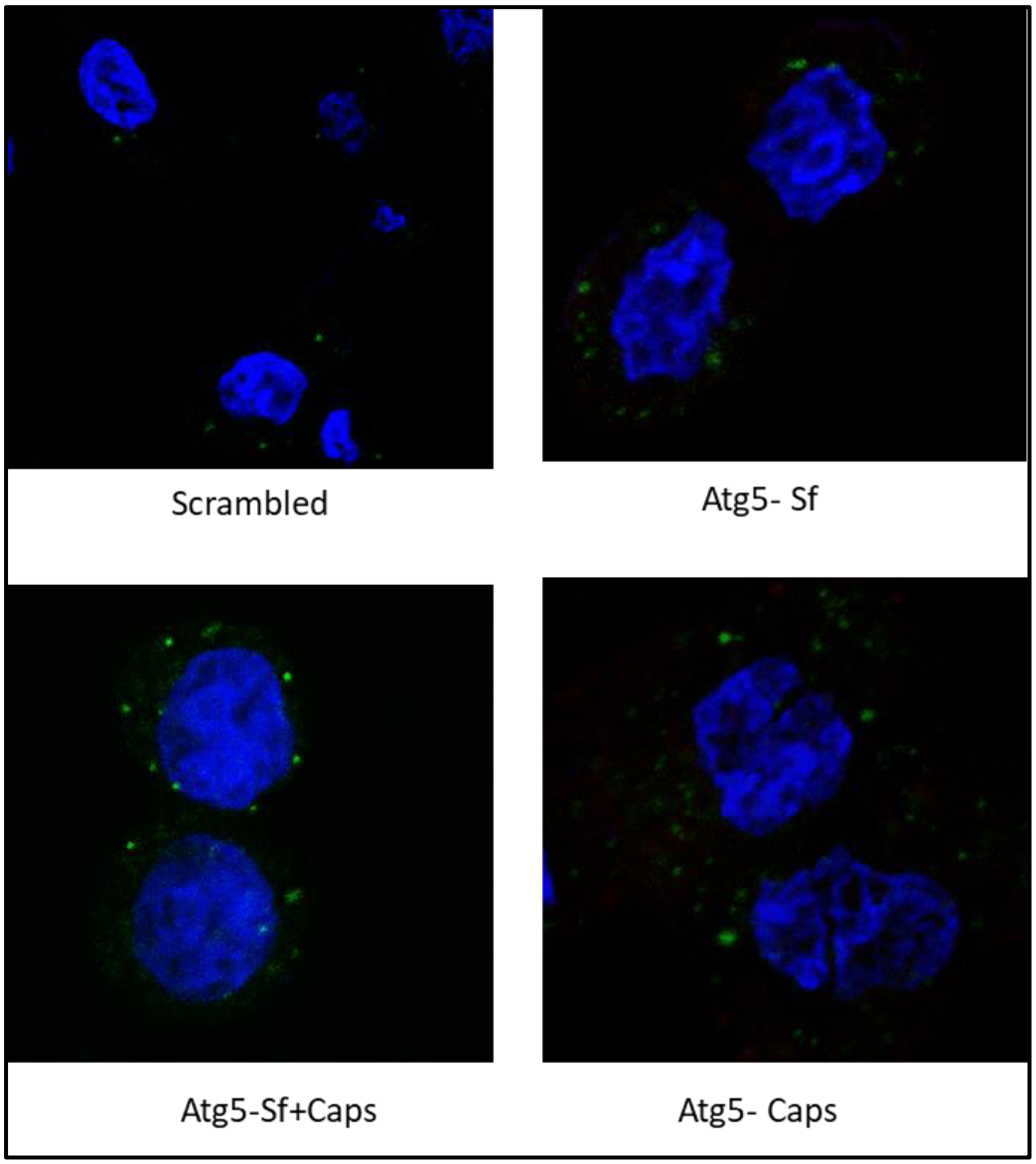

Fig3.8. Autophagy is inhibited by specific knockdown of Atg5 gene. Confocal microscopy studies showed LC3B puncta formation in control, scrambled siRNA and knock down ($Atg5^{-}$) cells. The cells were transfected with scrambled or Atg5 siRNA, and GFP-LC3 plasmid. After transfection, cells were treated with Caps, followed by bacterial infection and gentamicin addition. The cells were fixed with 4% formaldehyde and permeabilized using 0.1% Triton X-100.The nucleus was subsequently stained with DAPI. Scale bar corresponds to 5µm.

Successful Atg5 knockdown has been shown in western blot (**Fig3.9.A)**. Gentamicin protection assay performed in transfected cells showed insignificant changes in intracellular *S. flexneri* growth as well as Capsaicin treated infected conditions **(Fig3.9.B)**. Further transfection of Atg5 at time points (2,4,6h) showed no visible alteration in *S. flexneri* growth **(Fig3.9.C).** These results showed that intracellular reduction in bacterial load is due to Capsaicin induced autophagy.

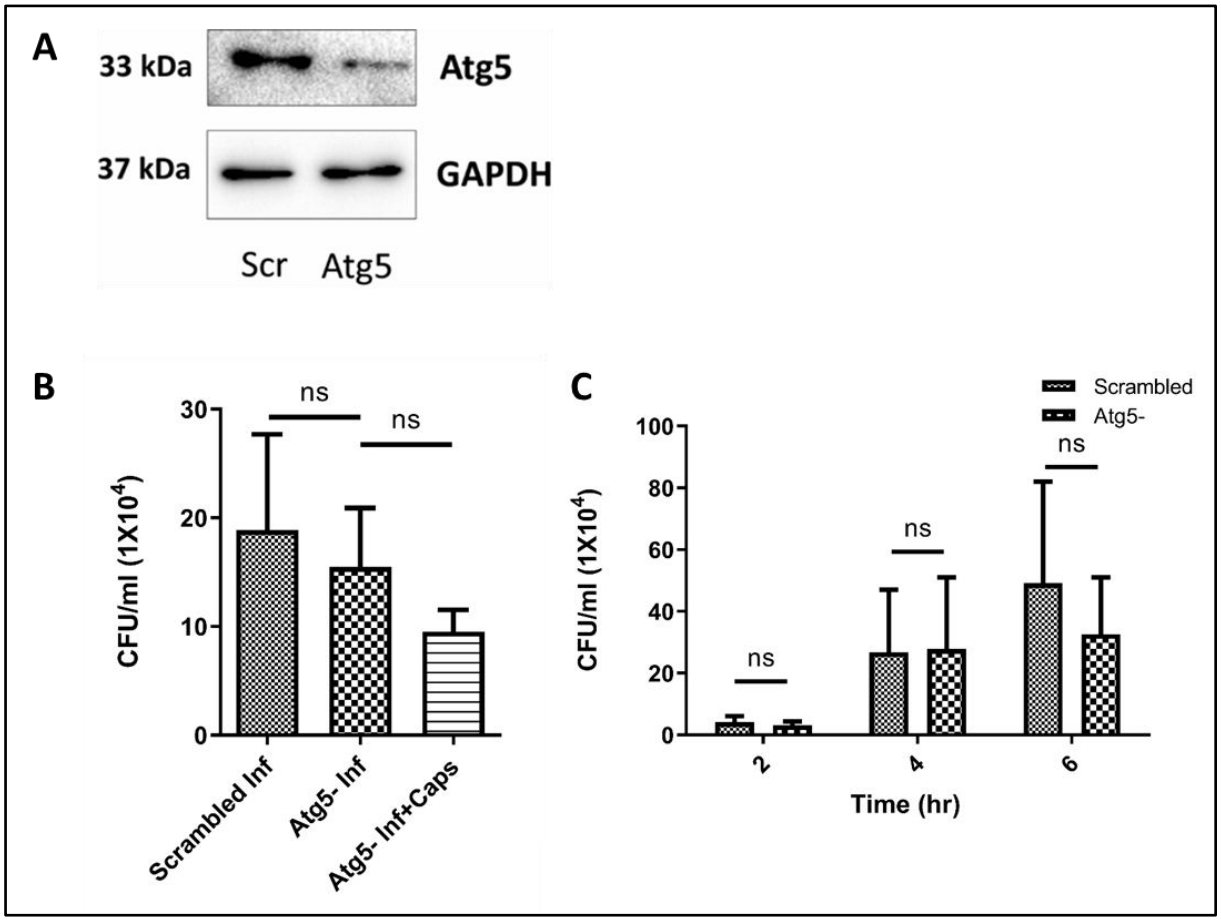

Fig3.9. Inhibition of autophagy altered the effect of Capsaicin. **(A)** Cells were subjected to transfection with both scrambled and Atg5 siRNA. Western blot was conducted to analyse Atg5 expression in both scrambled and knockdown cells, with GAPDH as a control. **(B)** An infection assay was carried out in cells treated with Caps for 2 hours after being transfected with scrambled and Atg5 knockdown siRNA. The CFU/ml are presented graphically. Statistical analysis was performed using one-way ANOVA. **(C)** An infection assay was conducted in cells transfected with scrambled and Atg5 knockdown siRNA for different

time periods (2, 4, 6 hours). Following transfection, cells were infected for 4h and CFU counts were determined after cell lysis and plating. Graphs were generated using GraphPad Prism 5, representing the mean ± SEM (n = 3); statistical significance was determined using two-way ANOVA; *p < 0.05, **p < 0.01, ***p < 0.001.

Chapter 4

Amelioration of Shigella flexneri infection by Capsaicin in mice model

Background

Shigella flexneri causes bacillary dysentery by invading the colonic epithelium and it causes inflammatory destruction of the colonic mucosa. Validating the *in vitro* data in *in vivo* mice model is pre-requisite for therapeutic formulation. *In vivo* mice model of *Shigella flexneri* was not much reported earlier. But in recent studies *in vivo* mice models are accepted by various researchers. Here, we used an intraperitoneal infection model of *S. flexneri* (Yang et al., 2013). Virulent *S. flexneri* 2a (YSH6000) results in diarrhea in adult mice model by intraperitoneal infection. Epithelial shedding, barrier integrity, goblet cell hyperplasia and expression of proinflammatory cytokines were found in the colon and severe diarrhoea was observed at 2h. We confirmed the anti-*Shigella* activity of Capsaicin in *in vivo* mice model and further evaluated the efficacy of Capsaicin as an alternative therapeutic for *S. flexneri* infection in near future.

Materials and Methods

Congo red plating was performed from crushed colons of infected and treated mice to assess the presence of virulent *S. flexneri* in the mice colon. Western blots were performed to observe change in the expression levels of marker autophagic proteins. qRT-PCR was used to assess the expression level of autophagy genes. Methods are already described in the materials and methods section.

Results

4.1. Capsaicin induces bacterial clearance in mice colonic tissues

We have infected BALB/c mice by intraperitoneal challenge with *S. flexneri 2457T* strain for 2h. Mice were further treated with Capsaicin (20 mg/kg) orally for 2hrs and then sacrificed for further studies **(Fig4.1.A)**. The dose of Capsaicin was selected in the infection model based on available data of Capsaicin (Sarpras et al., 2018). Capsaicin reduced bacterial load from intestine of *S. flexneri* infected BALB/c mice **(Fig4.1.B)**. Congo red plating of crushed colon represented significant reduction in bacterial load in Capsaicin treated infected mice as compared to only infected mice.

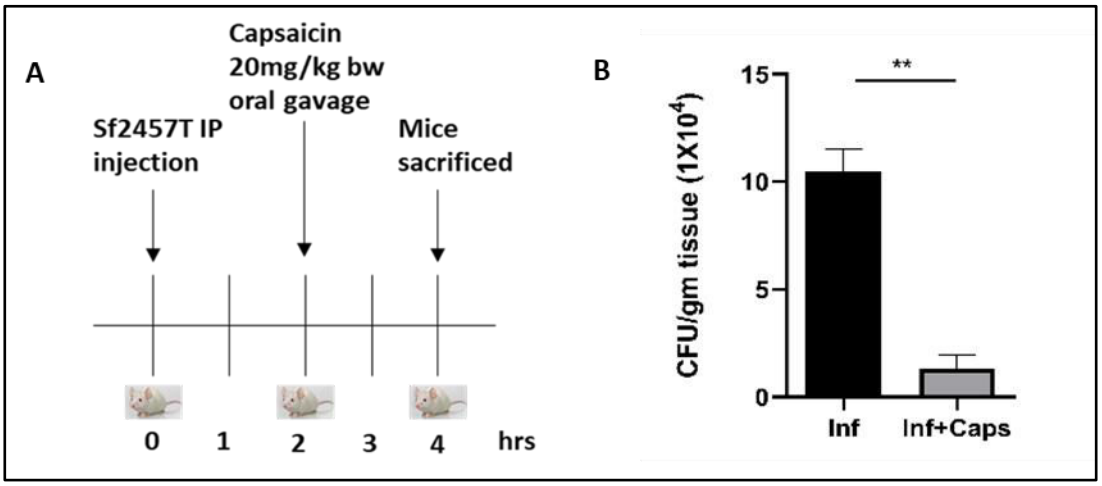

Fig4.1. Capsaicin reduced bacterial growth *in vivo* conditions. **(A)** Capsaicin was administered to BALB/c mice infected with *Shigella flexneri 2457T*. In brief, mice were infected for 2 hours, followed by a 2-hour treatment with Capsaicin (20 mg/kg body weight). Four groups (n=4) were established as follows: Group 1 - Control: Only DMSO was utilized as the vehicle. Group 2 - Infected: Received *S. flexneri* suspension (0.5×10^9 CFU/ml) in PBS. Group 3 - Infected + Capsaicin: Received *S. flexneri* suspension and then Capsaicin treatment for 2 hours. Group 4 - Capsaicin: Received Capsaicin (20 mg/kg body weight). Each group was housed separately. **(B)** Following infection and treatment, mice colons were aseptically collected, crushed, and plated on Congo red plates. The colony-forming units per gram of tissue (CFU/gm) were calculated and depicted graphically. An unpaired t-test was conducted (n=3); * $p < 0.05$, ** $p < 0.01$, *** $p < 0.001$.

4.2. Capsaicin induces autophagic gene expression *in vivo*

Subsequently, we analysed the induction of autophagy in mice model by Capsaicin. Colonic tissues of mice from control, infected, infected +Caps treated and only Caps treated samples were analysed for gene expression. Capsaicin induced expression of genes involved in autophagy in *in vivo* condition. Expression of MAP1LC3B gene was significantly upregulated both in only Capsaicin treated as well as Capsaicin treated infected mice **(Fig4.2)**.

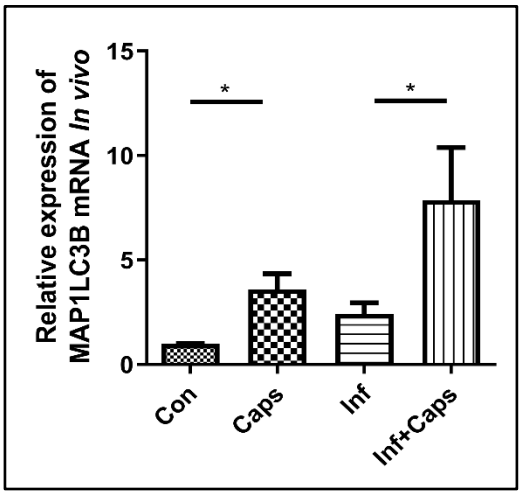

Fig4.2. Capsaicin induced autophagy gene expression in *in vivo* conditions. Quantitative real-time PCR (qRT-PCR) was conducted to assess the expression of the autophagy-related marker gene MAP1LC3B in various mouse tissue samples: control, infected, infected with Capsaicin treatment, and only Capsaicin treated. The reference housekeeping gene Gapdh was used for normalization. Statistical analysis was carried out using one-way ANOVA (n=3); * $p < 0.05$, ** $p < 0.01$, *** $p < 0.001$.

4.3. Treatment with Capsaicin enhances the expression level of autophagy proteins.

Mice colonic tissues were further processed for immunoblot analysis. Capsaicin induced expression of proteins involved in autophagy in *in vivo* condition. Expression of beclin1 and Atg5 was significantly upregulated and P62 degradation was enhanced both in only Capsaicin treated as well as Capsaicin treated infected mice **(Fig4.3A,B)**. LC3IIB degradation was observed in mice tissues treated with Capsaicin.

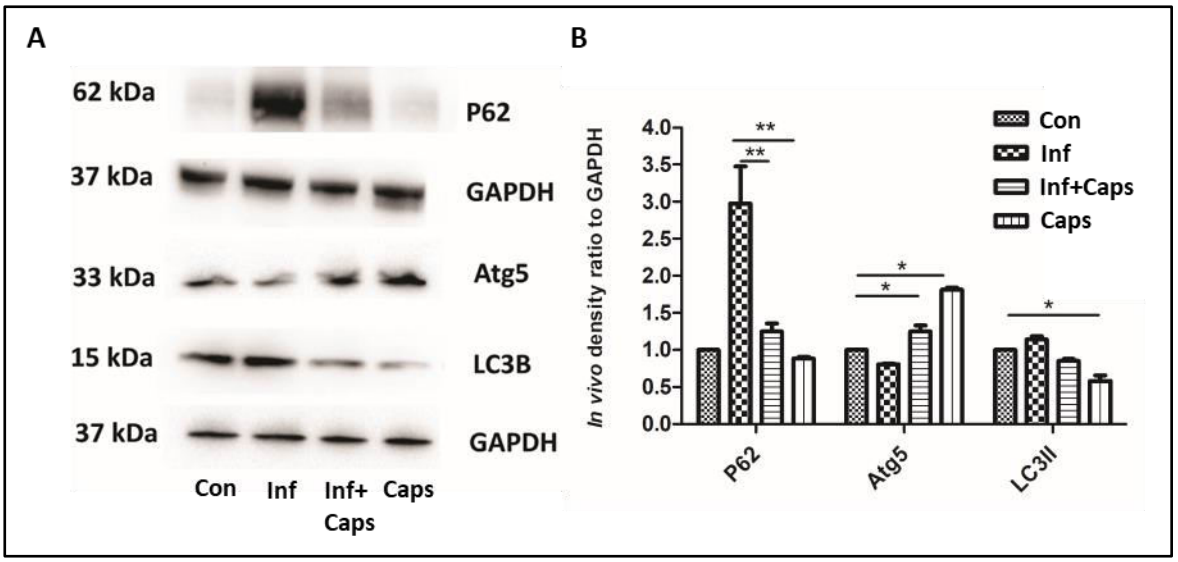

Fig4.3. Capsaicin induced autophagic protein expression in *in vivo* conditions. **(A)** Expression of major autophagy associated marker protein p62 degradation , Atg5 and LC3IIB degradation were observed in western blot. Gapdh was used as loading control. **(B)** Densitometric analyses were graphically represented (n=3); Significance was calculated * $p < 0.05$, ** $p < 0.01$, *** $p < 0.001$

OBJECTIVE III

Chapter 5

Role of TFEB, a transcription factor in Capsaicin induced autophagy during Shigella flexneri infection

Background

A molecule or a protein which is associated with disease pathology and targeted by a drug for therapy is known as a drug target. It is a target involved in cell signaling or metabolism and specific for disease pathology. Pathogen infection and following responses is a complex process which initiate transcriptional changes rapidly resulting in change in cellular homeostasis by modifying the signalling pathways. Intestinal epithelial cells act as first line of defence against pathogen invasion. *Shigella flexneri*, one of the most common human bacterial pathogens target intestinal epithelium. In intestinal epithelial cells, autophagy pathway is circumvented due to *Shigella flexneri* infection.

There are transcription factors involved in autophagy induction. One of the key transcription factors is TFEB. TFEB, belongs to MIT family of transcription factors and known as master regulator of autophagosomal and lysosomal biogenesis. Activation of TFEB takes place during nutrient starved condition as well as in stressed condition. It is already reported that, in *Salmonella* infected mammalian macrophage cells, TFEB gets activated (Ammanathan et al., 2020). During basal state, TFEB resides in the cytosol in phosphorylated condition induced by mTORC1. Dephosphorylation of TFEB and its nuclear import occurs during ER as well as genotoxic stress condition. Nuclear translocation of TFEB induces transcription of several autophagolysosomal as well as antimicrobial genes (Visvikis et al., 2014). Activated TFEB plays a major role in bacterial killing and clearance.

TFEB can be a potential drug target. TFEB enhancers are nowadays reported for the development of therapeutics against intracellular pathogens (Kim et al., 2019). Hence it is a targeted transcription factor.

Materials and Methods

Confocal microscopic analysis was performed to visualize subcellular localization of TFEB both in Capsaicin treated and untreated condition. Western blots were performed to observe nuclear and cytosolic TFEB level in infected and uninfected condition. Transcriptional activity was estimated by TFEB-TF assay and Chromatin immunoprecipitation (ChIP). Calcium influx assay was performed to check calcium influx in presence of Capsaicin both in infected and uninfected cells. Cells were transfected with siRNA and eGFP-TFEB plasmid to understand the effect of Capsaicin in TFEB knocked down and overexpressed condition. Gentamicin Protection assay (GPA) was performed to check intracellular survival of *S. flexneri* after treatment with drug, inhibitors, and transfection. Detailed methods are already described in the materials and methods section.

Results

5.1. Effect of TRPV1 inhibitor (Capsazepine) in Capsaicin treated cells

It is well known that Capsaicin binds to TRPV1 receptor in epithelial cells (Reilly et al., 2005). Capsazepine, a TRPV1 inhibitor, works as an antagonist of Capsaicin. It blocks binding of Capsaicin with TRPV1 receptor. Capsazepine treatment at 10µM along with Capsaicin showed little or no effect of Capsaicin in intracellular bacterial growth. Blockage

of Capsaicin binding by capsazepine increased intracellular bacterial load both in only infected and Caps treated infected HT29 cells **(Fig5.1).** CFU/ml represented increase in *S. flexneri* infection in capsazepine treated cells as compared to untreated cells. Capsazepine treatment inhibits the effect of Capsaicin and hence intracellular bacterial growth is increased.

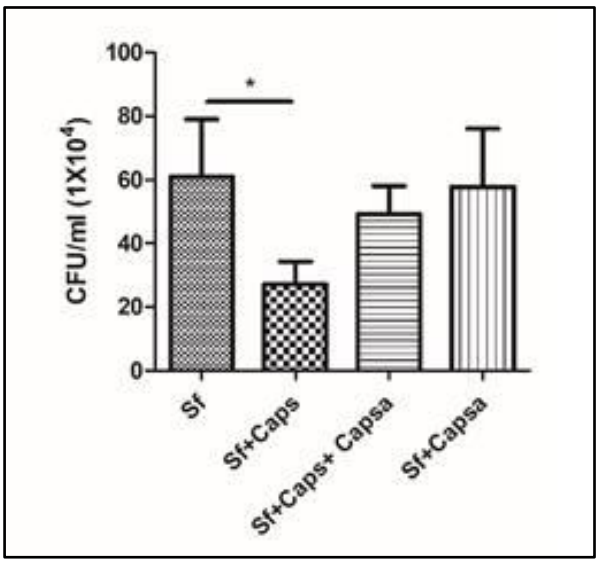

Fig5.1. Capsazepine inhibited the effect of Capsaicin. CFU/ml was graphically represented in cells exposed to Capsaicin and Capsazepine (10μM) or both treated for 2hr, followed by bacterial infection and gentamicin addition. Graphs were represented using GraphPad Prism 5 as mean ± SEM (n = 3); significance was calculated by two-way ANOVA; *p < 0.05, **p < 0.01, ***p < 0.001.

5.2. Capsaicin induces transcription factor activity of TFEB

As autophagy genes are upregulated by Capsaicin, we further investigated in depth the mechanism behind this upregulation. There are transcription factors involved in autophagosomal activity. TFEB, a transcription factor for autophagosomal and lysosomal biogenesis, binds to its promoter region following nuclear translocation. Moreover, binding of Capsaicin to TRPV1 receptor further intrigued us to examine TFEB activation as calcium

influx is induced due to Caps-TRPV1 binding. Transcription factor activity assay has shown that Capsaicin treatment induced binding of TFEB to CLEAR sequence/promoter sequence of autophagy genes. 4hour Capsaicin treatment induced transcription factor activity of TFEB almost 3 times as compared to control **(Fig5.2)**.

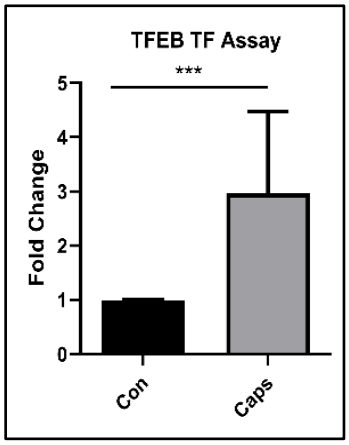

Fig5.2. Capsaicin treatment induced transcription factor activity of TFEB. Cells with Capsaicin treatment for 2h and control were analyzed using a TFEB transcription assay kit. This assay demonstrated the activation of the TFEB binding to the CLEAR sequence by Caps. An unpaired t-test was conducted to assess the statistical significance. The results were visualized in graphs using GraphPad Prism 5, with the data presented as mean ± SEM (n = 3). Significance levels were determined as follows: *p < 0.05, **p < 0.01, ***p < 0.001.

5.3. Capsaicin induces DNA binding affinity of TFEB

To further confirm Capsaicin induced TFEB activation, we performed ChIP assay. Chromatin immunoprecipitation (ChIP) study represents DNA binding ability of protein. qRT-PCR was performed in immunoprecipitated DNA with TFEB using specific primer(MAP1LC3B). This showed induced expression of MAP1LC3B gene. Graphical representation revealed that there is a significant transcription factor binding as compared to control in immunoprecipitated DNA of Capsaicin treated cells **(Fig5.3)**.

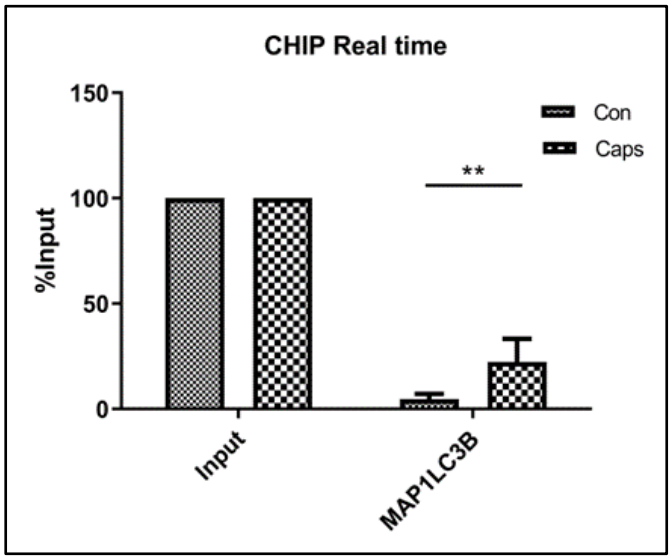

Fig5.3. Capsaicin (Caps) treatment induced DNA binding affinity of TFEB. ChIP assay was conducted using either an anti-TFEB antibody or an input control. Real-time PCR was performed to examine the expression of MAP1LC3B in both untreated and Caps-treated intestinal cells, comparing the results to the input. The obtained data were visually presented in graphs using GraphPad Prism 5, indicating mean ± SEM (n = 3). Significance levels were determined as follows: *p < 0.05, **p < 0.01, ***p < 0.001, after performing a two-way ANOVA analysis.

5.4. Capsaicin induces nuclear localization of TFEB

As transcription factor activity is enhanced, we examined the effect of Capsaicin on TFEB nuclear translocation. Cytoplasmic to nuclear localization of TFEB was induced in presence of Capsaicin. From immunofluorescence studies, it has been shown that Capsaicin treatment induced translocation of TFEB (red) into nucleus (blue), which resulted in reduced red intensity in the cytosol and induced red intensity in nucleus in 4h Caps treated HT29 cells as compared to control **(Fig5.4.A)**. %nuclear localization was calculated and graphically represented **(Fig5.4.B).**

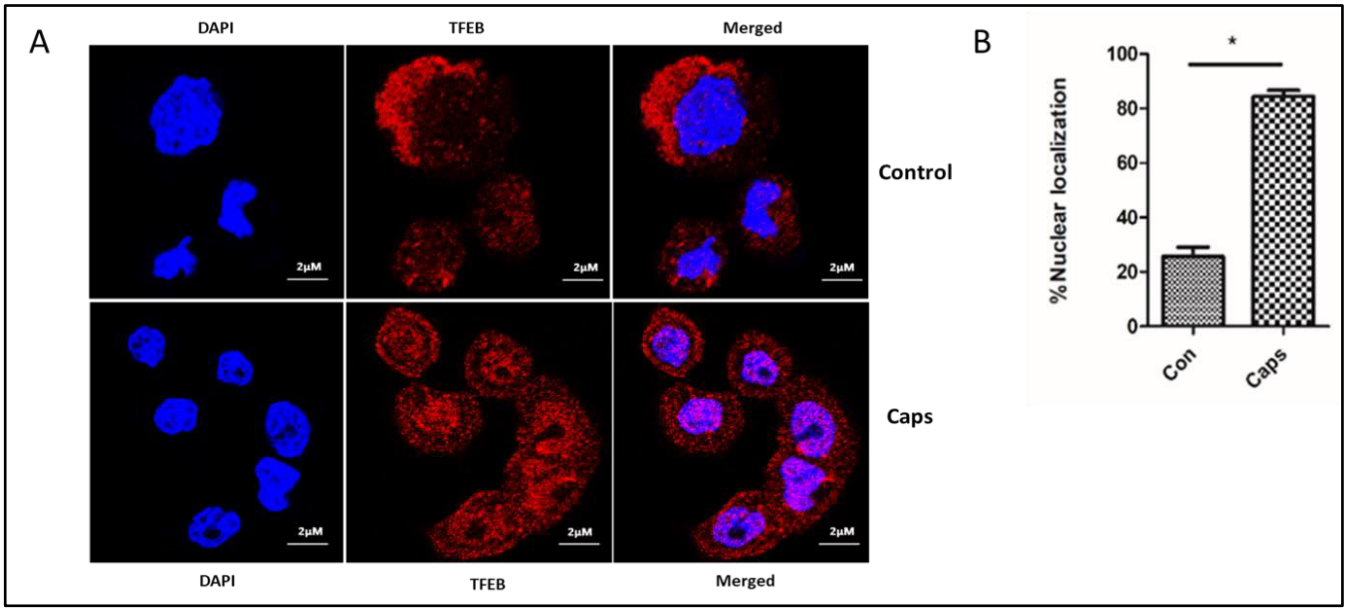

Fig5.4. Capsaicin (Caps) treatment induced TFEB nuclear translocation. **(A)** Confocal microscopy data illustrates the localisation of TFEB to the nucleus after a 2-hour treatment with Caps (16μM) in HT29 cells. Immunofluorescence microscopy was done, and a scale bar of 2μm is included. **(B)** The percentage of TFEB nuclear localization was graphically showed for both Caps-treated and untreated conditions. To assess significance, an unpaired t-test was conducted. Graphs presenting the data, using GraphPad Prism 5, displayed the mean ± SEM (n = 3), and statistical significance was determined as follows: *p < 0.05, **p < 0.01, ***p < 0.001.

5.5. Effect of Capsaicin in TFEB knocked down cells

We checked the role of TFEB in intracellular *S. flexneri* growth. Expression of TFEB was inhibited using TFEB siRNA. Successful knock down of TFEB was confirmed by immunoblot after transfection of siTFEB and a negative control (scrambled) siRNA in HT29 cells **(Fig5.5.A)**. Gentamicin protection assay performed in transfected cells showed insignificant changes in case of *S. flexneri* infected as well as Capsaicin treated conditions although there was a slight increase in bacterial growth in knockdown cells **(Fig5.5.B)**.

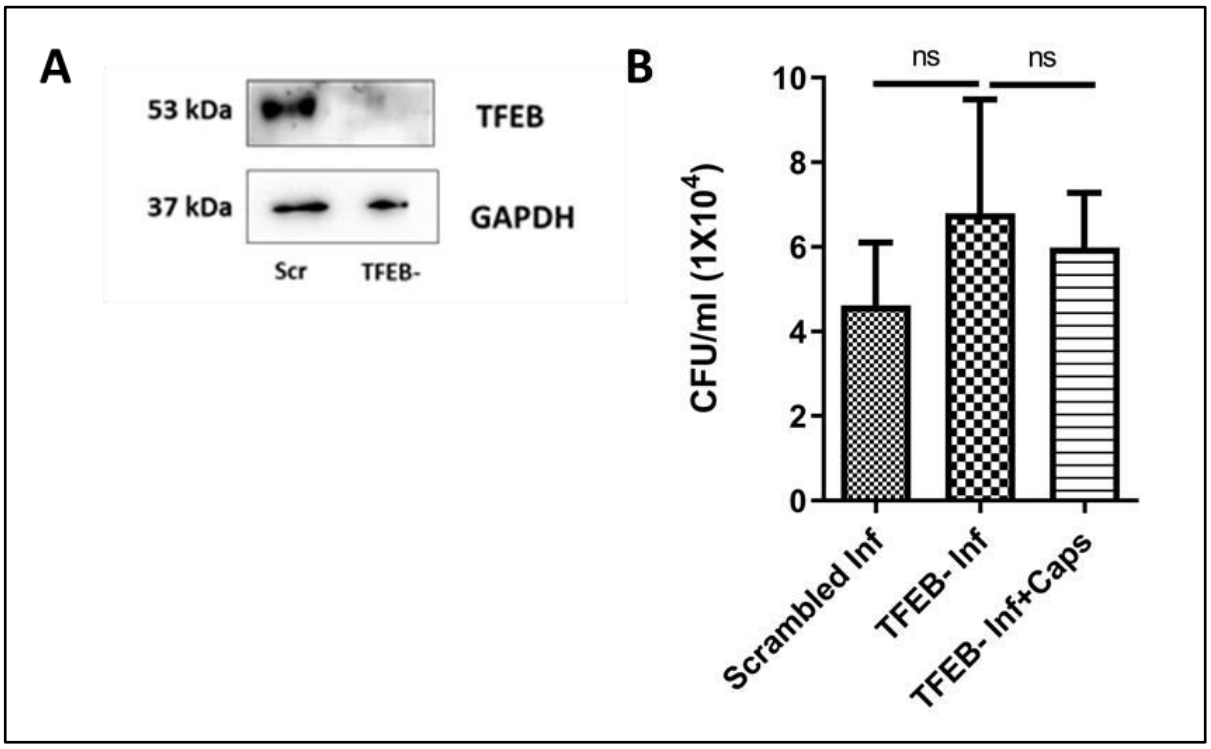

Fig5.5. Downregulation of TFEB altered the effect of Capsaicin in intracellular bacterial growth. (A) Transfection was performed on cells using scrambled and TFEB siRNA. The Western blot analysis showed the expression of TFEB in both scrambled and knockdown cells, with GAPDH as a housekeeping control. **(B)** Cell transfection involved the use of scrambled siRNA or TFEB siRNA. Following transfection for 48h, a 2-hour Caps treatment was performed, followed by a 2-hour *S. flexneri* infection and subsequent gentamicin treatment. Cells were then lysed and plated, and a one-way ANOVA analysis was conducted. The data were graphed with GraphPad Prism 5, showing mean ± SEM (n = 3), and statistical significance was determined with *p < 0.05, **p < 0.01, ***p < 0.001.

5.6. Effect of Capsaicin in TFEB overexpressed cells

Expression of TFEB was induced using TFEB overexpression plasmid. Successful overexpression of TFEB was confirmed by immunoblot after transfection of GFP-TFEB and a control (e-GFP) in HT29 cells **(Fig5.6.A)**. Gentamicin protection assay performed in transfected cells showed that overexpression of TFEB reduced intracellular *S. flexneri* growth significantly **(Fig5.6.B)**.

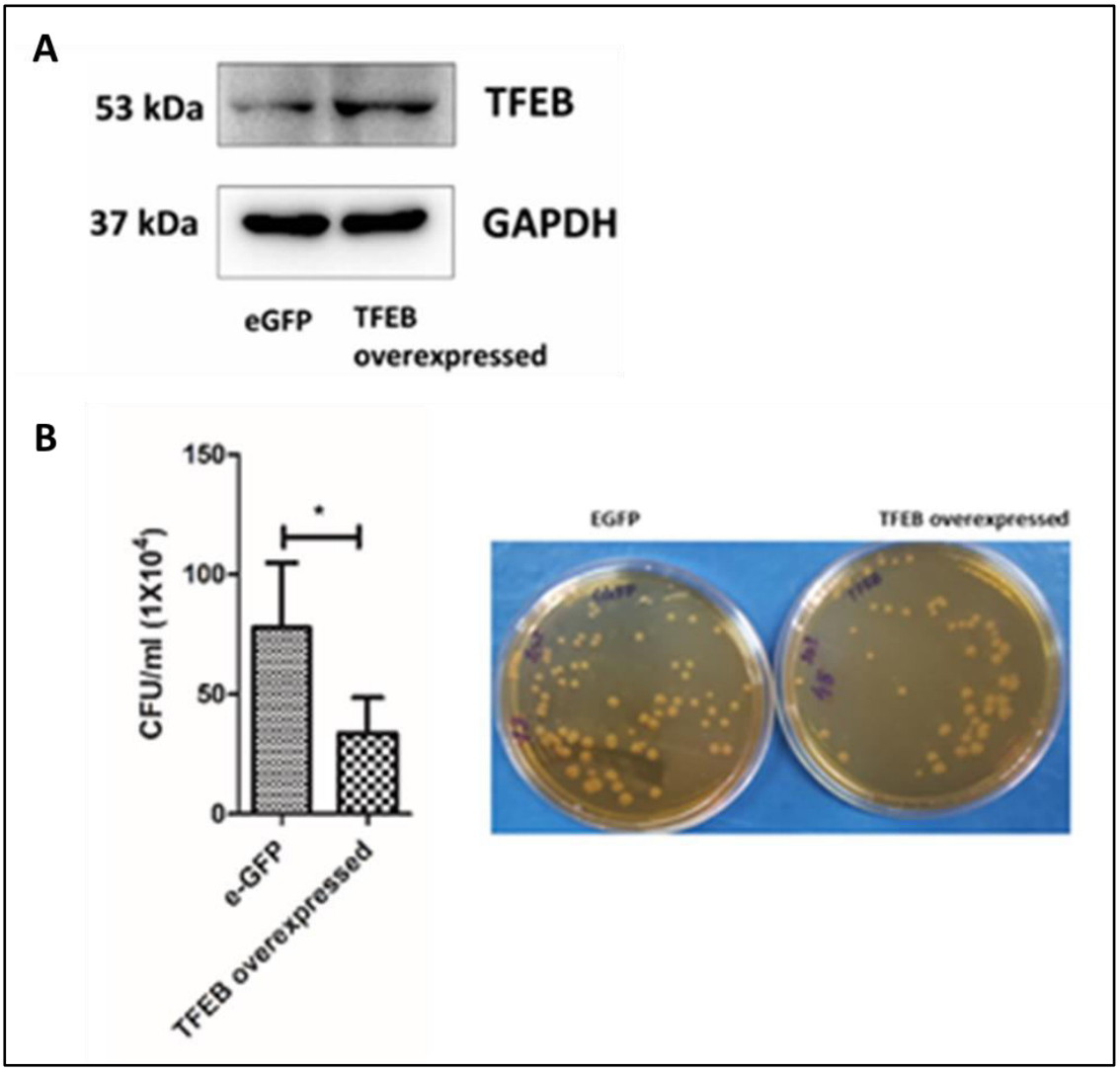

Fig5.6. Overexpression of TFEB reduced intracellular survival of *Shigella flexneri*. **(A)** Cells were transfected with eGFP and eGFP-TFEB plasmid. Western blot showed TFEB expression in overexpressed cells. GAPDH was kept as a housekeeping control. (**B**) Cells were transfected with an empty vector eGFP or

eGFP-TFEB plasmid followed by *S. flexneri* infection. Cells were lysed and plated for CFU. Unpaired t-test was performed. Graphs were represented using GraphPad Prism 5 as mean ± SEM (n = 3); Significance was calculated; *p < 0.05, **p < 0.01, ***p < 0.001.

5.7. Effect of calcium influx on nuclear localisation of TFEB

A key challenge is to understand the sequential events leading to TFEB nuclear translocation induced by Capsaicin. As Caps has the potential to trigger calcium influx via TRPV1 receptor, we further investigated the effect of calcium influx on nuclear localisation of TFEB and its effect on *S. flexneri* growth. We tested the influence of calcium influx by using an intracellular calcium chelator BAPTA-AM. Firstly, we examined the effect of BAPTA-AM on *S. flexneri* intracellular survivability (5,10 µM). BAPTA-AM has no effect on *S. flexneri* growth in combination with Caps **(Fig5.7.A).** Secondly, we checked nuclear translocation of TFEB. There was no effect on TFEB due to treatment with BAPTA-AM (5µM). Immunoblots indicated increased nuclear expression of TFEB in Caps treated cells along with BAPTA-AM **(Fig5.7.B)**. Finally, we examined the effect of BAPTA-AM on calcium influx. Calcium influx assay showed insignificant effect of Caps and BAPTA-AM in calcium influx in intestinal cells. Therefore, these results indicate that Caps stimulated TFEB regulation is independent of calcium influx **(Fig5.7.C)**.

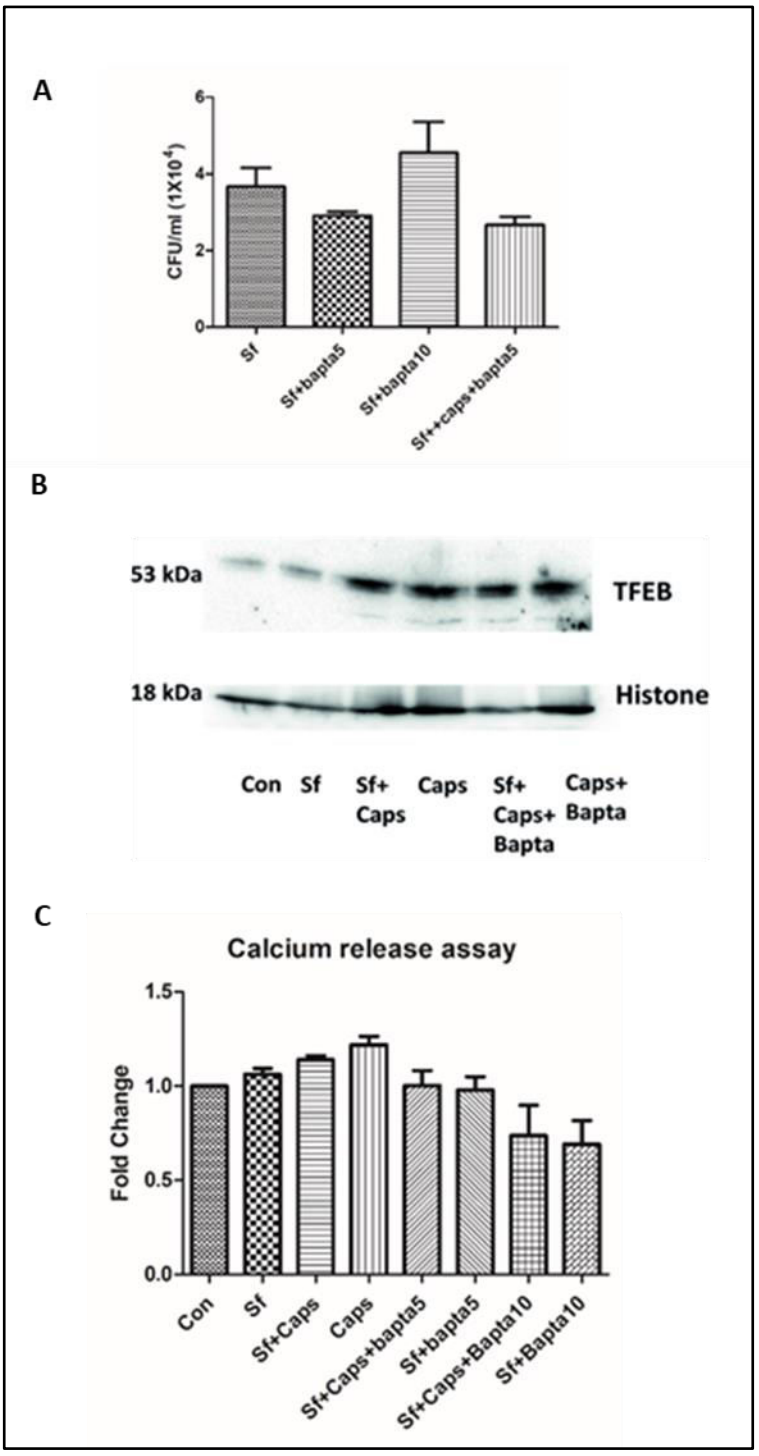

Fig5.7. Regulation of TFEB by calcium influx. **(A)** Cells were pre-treated with Bapta-AM at 5μM and 10 μM concentration for 2hrs followed by infection and gentamicin treatment. Cells were lysed and CFU/ml was

counted and plotted (n=3). **(B)** Western blot analysis was performed showing effect of BAPTA-AM in nuclear localization of TFEB. Histone was used as loading control. **(C)** Calcium release assay in infected cells both in presence and absence of a calcium channel inhibitor (BAPTA-AM) and capsaicin. (n=3), ANOVA was done.

5.8. Regulation of TFEB activation by Caps.

TFEB dephosphorylation is known to be stimulated by different pathways (AMPK, JNK, pAkt, mTOR and others). As, TFEB activation by Caps is independent of calcium influx we investigated other pathways. We examined the role of Caps in TFEB regulation. Caps augmented AMPK phosphorylation in infected cells. AMPK has the potential to dephosphorylate TFEB and induce nuclear localisation. Further we studied the role of Akt in *S. flexneri* infected cells. As expected, Akt phosphorylation is also inhibited by Caps at T308 and S473 which is known to be stimulated due to *S. flexneri* infection. Downstream of Akt is mTOR, an important regulator of autophagy. mTOR dephosphorylates TFEB in multiple sites to induce nuclear localisation. Here, we observed downregulation of mTOR phosphorylation by Caps in both infected and uninfected cells **(Fig5.8.A)**. TFEB activation by capsaicin is represented schematically **(Fig5.8.B)**.

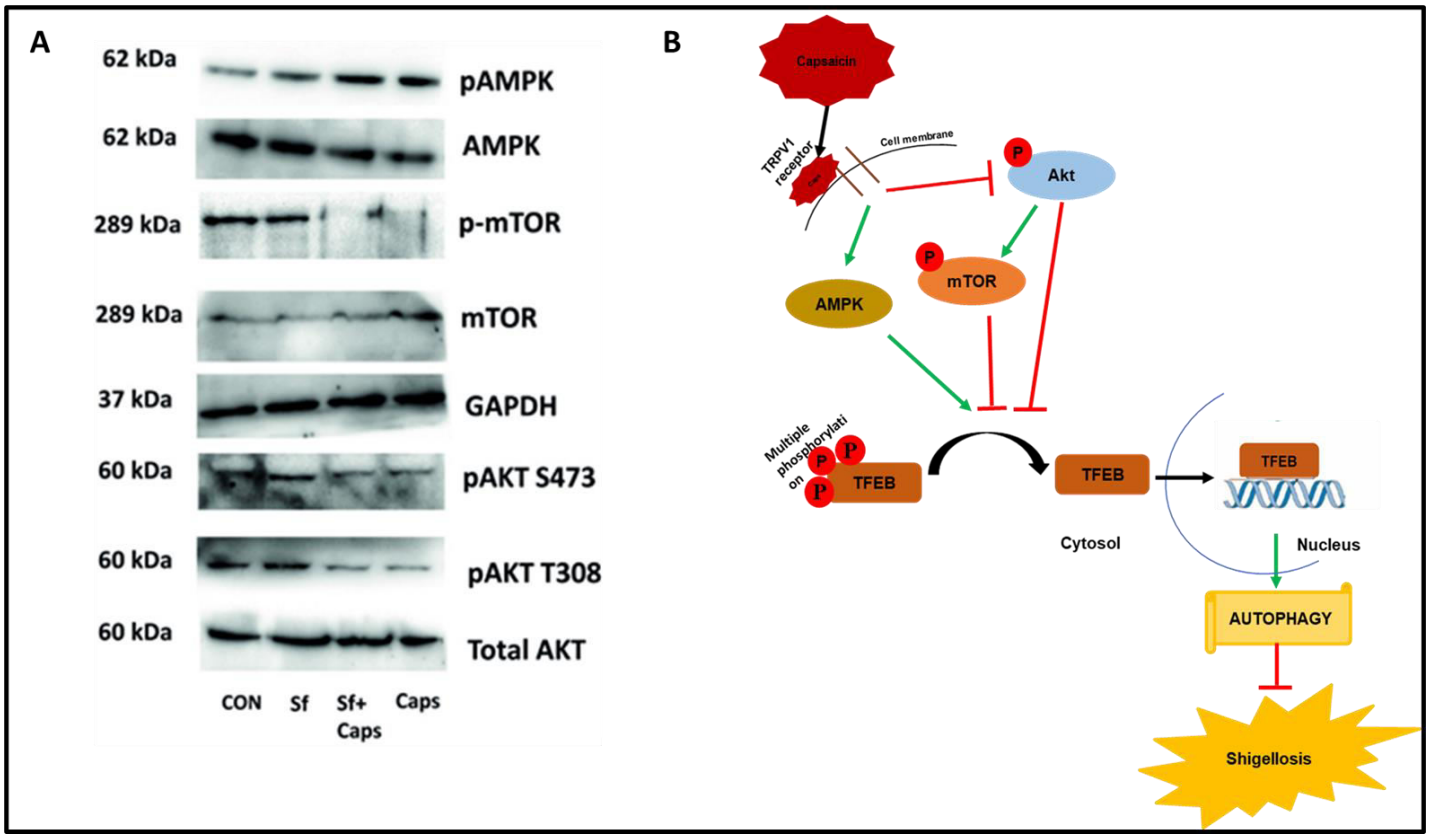

Fig5.8. Capsaicin mediated TFEB nuclear localisation is regulated by different signalling molecules. (A) Immunoblotting analysis was done for AMPK, phospho-AMPK, phospho-mTOR and mTOR, total AKT, p-AKT at ser473 and thr308, in control, infected and Caps treated cells. Gapdh was used as protein loading control. **(B)** Schematic representation of TFEB regulation by Capsaicin has been shown.

Chapter 6

Deciphering and characterizing new drug targets to fend of infection during S. flexneri pathogenesis.

Background

TFEB is a major target in the field of autophagosomal lysosomal disorders. It induces host response by targeting autophagy, antimicrobial response and immune response genes that are essential for host tolerance. Capsaicin is able to target TFEB to fend of intracellular *S. flexneri* infection. TFEB (Transcription factor EB) is a transcription factor that binds to CLEAR box and upregulates several autophagolysomal genes (Zhang et al., 2020). On the other hand, ZKSCAN3 (Zinc-finger protein with KRAB and SCAN domains 3) is a transcriptional repressor acting as a TFEB counterpart.ZKSCAN3 downregulates the expression of WIPI2 (Chauhan et al., 2013). ZKSCAN3 is also known to be upregulated in different infectious diseases (Nabar et al., 2017). Hence, TFEB/ZKSCAN3 can be a major target to control *S. flexneri* infection and pathogenesis. On the other hand, it has been reported recently that *S. flexneri* infection modulates TFEB nuclear localisation (Cabral-Fernandes et a., 2022). There are also other transcription factors involved in autophagy. Forkhead box proteins (FOXO) is a transcription factor which is a regulator of autophagy (Eijkelenboom and Burgering, 2013). FOXO1 gets phosphorylated at multiple sites by AKT and is sequestered in the cytosol resulting in its ubiquitination and degradation (Huang and Tindall, 2007). On other aspect, a recent article (Liu et al., 2016) reported that Foxo1 controls the transcription of TFEB transcription factor.

Autophagy is a dynamic process and it is modulated by host pathogen interaction at various stages and time intervals. At lower MOI, cells are more active to eliminate invaded bacteria but at higher MOI (>50), *S. flexneri* hijacks host machinery which favours intracellular

survival (Tanner, 2016). This mechanism is controlled by several effector proteins secreted by *S. flexneri* to modulate the host autophagic response.

Materials and methods

Western blots were performed to observe TFEB and ZKSCAN3 expression levels. qRT-PCR was used to assess expression level of autophagy genes. Pull down assay was performed to check if IpaH9.8 interacts with ZKSCAN3 and ubiquitination assay to identify ubiquitination status. Detailed methods are already described in the materials and methods section.

Results

6.1. Subcellular localization of TFEB and ZKSCAN3 at different MOI of *S. flexneri* infection

In order to examine the effect of different MOI on autophagic response, we tested the effect of *S. flexneri* infection at varying MOI on the subcellular localization of TFEB and ZKSCAN3 in HT29 cells. Immunoblot analysis showed a reduction in the expression of ZKSCAN3 in cytosolic extract than nuclear extract in infected cells with MOI200 compared to control cells **(Fig6.1)**. On the other hand, TFEB expression in both CE and NE are almost similar. In cells infected with both MOI 50 and MOI 100 showed upregulated TFEB/ZKSCAN3 nuclear translocation and at MOI 200 ZKSCAN3 nuclear localization is similar to MOI 100 whereas TFEB nuclear localization is slightly less as compared to MOI 100.

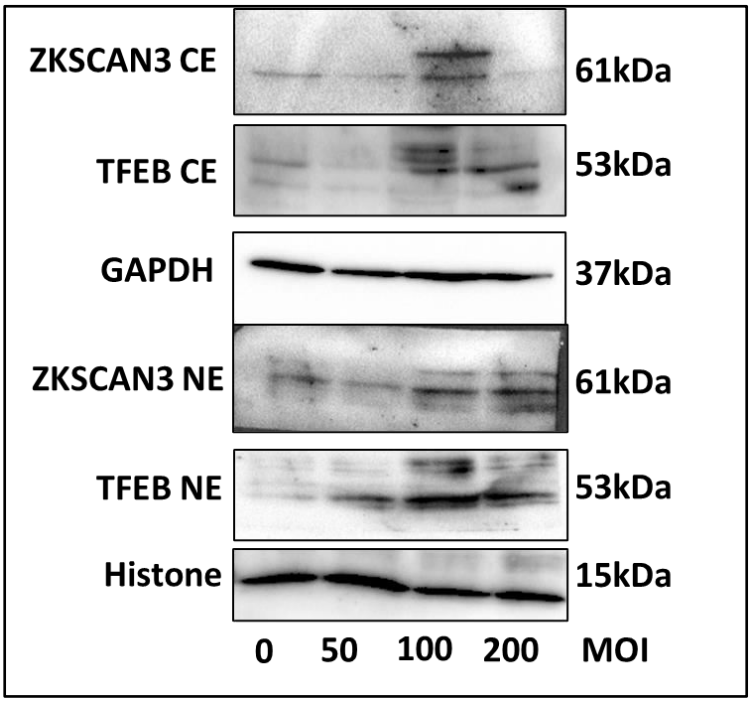

Fig6.1. *S. flexneri* infection modified cytosolic and nuclear localization of TFEB and ZKSCAN3. *S. flexneri* infection at varying MOI (0, 50, 100, 200) for 4h resulted in altered nuclear and cytosolic localization of TFEB and ZKSCAN3. Western blot analysis was performed for determining the protein level of TFEB and ZKSCAN3 in both cytosolic (CE) and nuclear extracts (NE). GAPDH was kept as a housekeeping control for cytoplasmic cell extracts. Histone was used as a control for nuclear extracts.

6.2. Autophagic gene expression at different MOI of *S. flexneri* infection

Subsequently, we checked the effect of infection at different MOI on autophagic gene regulation **(Fig6.2A-E)**. *S. flexneri* infection at different MOI for 4h induced expression of genes involved in autophagy in HT29 cells. After 4h of infection, expression of ATG5 was upregulated in MOI 100, WIPI2 and FOXO1 genes were significantly upregulated in MOI 50 and TFEB gene expression was upregulated both in MOI 50 and MOI 100 infected cells. But, at MOI 200 all the genes related to autophagy have reduced expression.

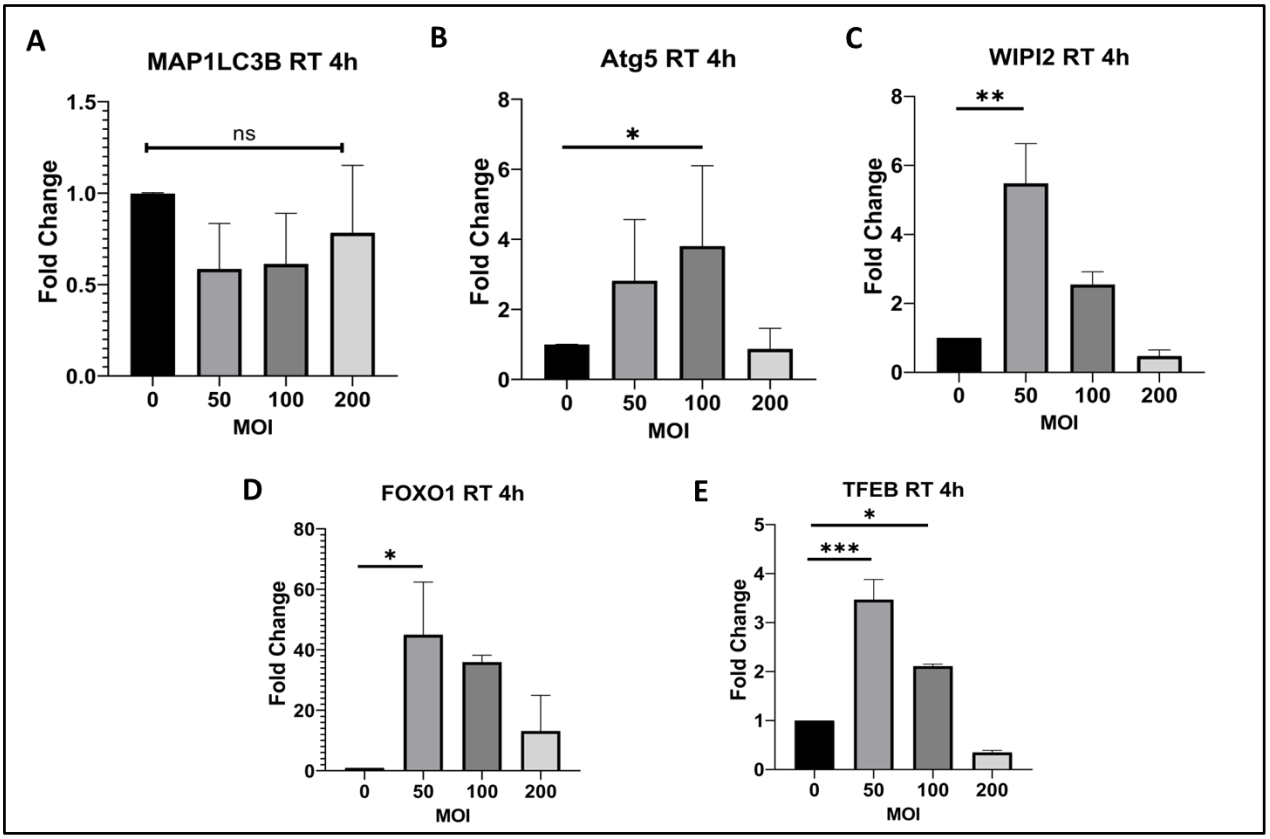

Fig6.2. *S. flexneri* infection for 4h altered autophagy gene expression. (A-E) HT29 cells were infected at different MOI (0, 50, 100, 200) for 4h. After infection cells were lysed. Quantitative PCR was performed to evaluate the expression level of autophagy associated marker genes (MAP1LC3B, ATG5, WIPI2, FOXO1, TFEB) in infected HT29 cells(n=3). Fold changes were graphically represented. Gapdh was used as internal control. One-way ANOVA was performed (n=3); * $p < 0.05$, ** $p < 0.01$, *** $p < 0.001$.

6.3. Autophagic gene expression at different MOI of *S. flexneri* for longer duration (24h infection)

As autophagy is a dynamic process and it varies for different time points, we further investigated the effect for longer duration of infection. *Shigella flexneri* infection at different MOI for 24h induced expression of autophagy genes in HT29 cells (**Fig6.3A-E**). Expression of MAP1LC3B, ATG5 and TFEB genes were significantly downregulated in infected cells with MOI 200.

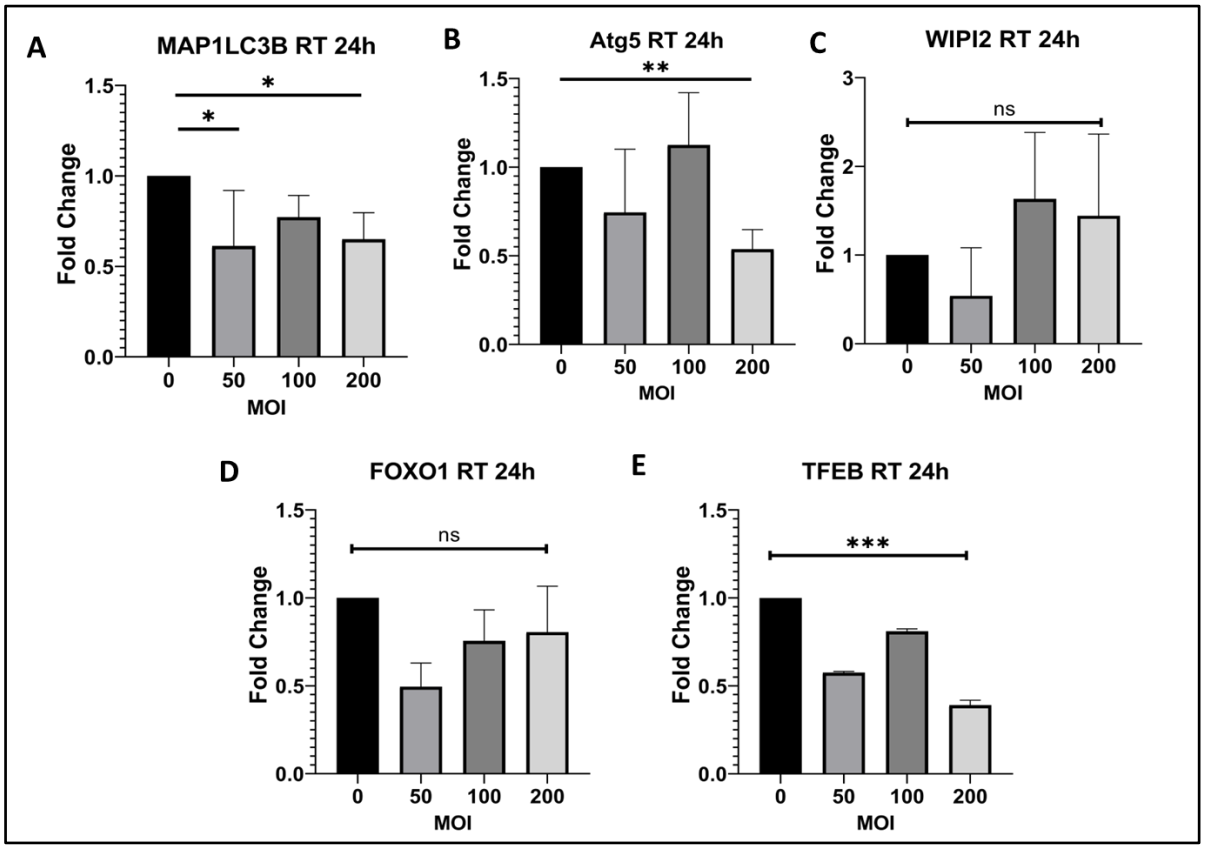

Fig6.3. *S. flexneri* infection for 24h altered autophagy gene expression. (A-E) HT29 cells were infected at different MOI (0, 50, 100, 200) for 24h. After infection cells were lysed. Quantitative PCR was performed to evaluate the expression level of autophagy associated marker genes (MAP1LC3B, ATG5, WIPI2, FOXO1, TFEB) in infected HT29 cells (n=3). Fold changes were graphically represented. Gapdh was used as internal control. One-way ANOVA was performed (n=3); * $p < 0.05$, ** $p < 0.01$, *** $p < 0.001$.

6.4. IpaH9.8 interaction with ZKSCAN3 at different multiplicity of infection of *Shigella flexneri*

TFEB/ZKSCAN3 probably plays a major role in host autophagic response during infection. Now, we searched for putative bacterial factors which might be interacting with the transcription factors to modulate host response. By bioinformatics approach, we found that host protein ZKSCAN3 interacts with IpaH9.8, a T3SS effector protein of *S. flexneri* **(Fig6.4.A)**. To validate IpaH9.8 interaction with transcription factor ZKSCAN3, *in vitro*, co-immunoprecipitation experiments were performed using lysates of HT29 cells infected with *S. flexneri* at different MOI (50, 100, 200) **(Fig6.4.B)**. Complexes containing ZKSCAN3 were precipitated using IpaH9.8-specific monoclonal antibody and examined by Western blotting using a ZKSCAN3 monoclonal antibody. This data indicated that as the MOI is increased interaction of Ipah9.8 with ZKSCAN3 is simultaneously induced.

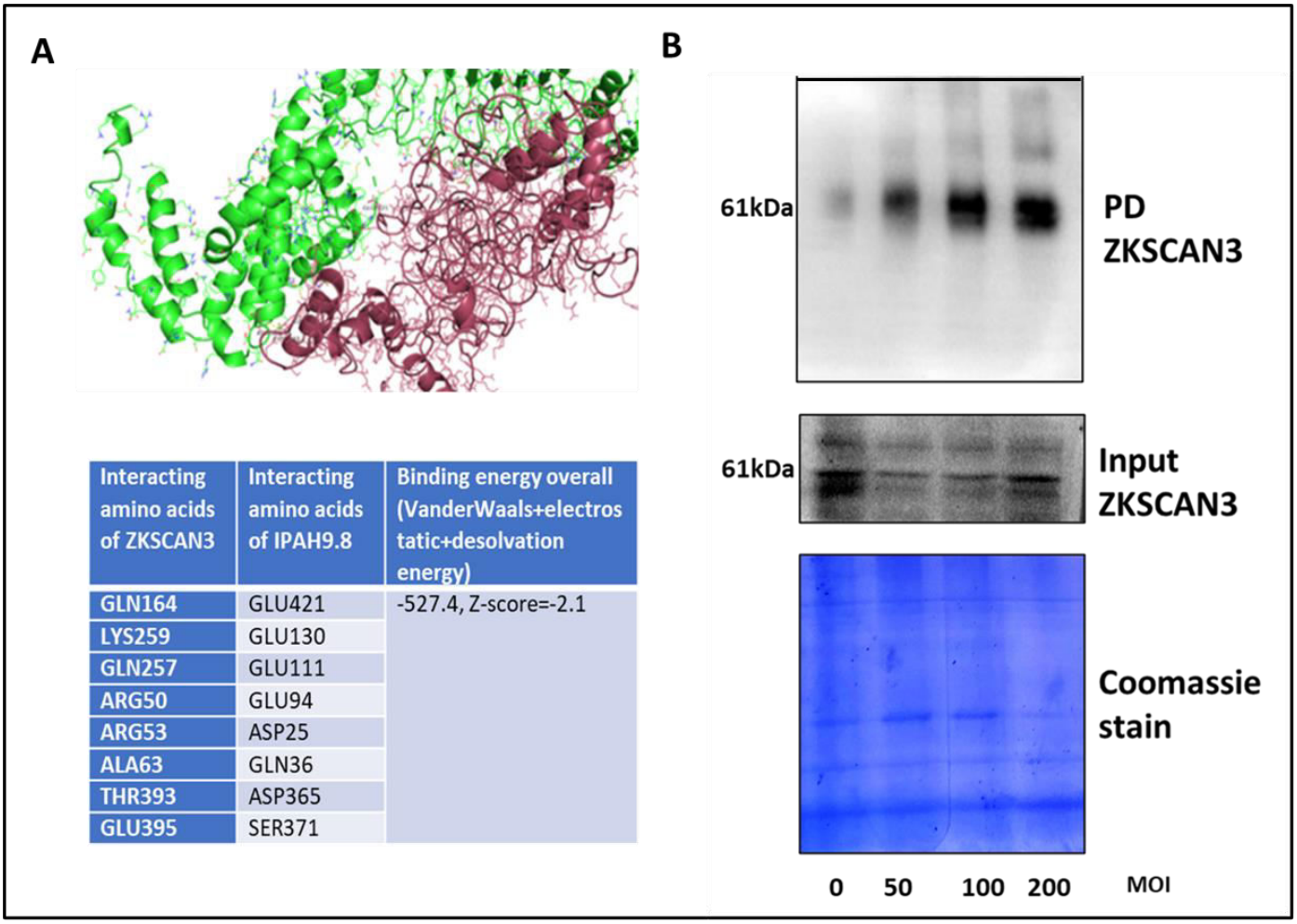

Interacting amino acids of ZKSCAN3	Interacting amino acids of IPAH9.8	Binding energy overall (VanderWaals+electrostatic+desolvation energy)
GLN164	GLU421	-527.4, Z-score=-2.1
LYS259	GLU130	
GLN257	GLU111	
ARG50	GLU94	
ARG53	ASP25	
ALA63	GLN36	
THR393	ASP365	
GLU395	SER371	

Fig6.4. Pull down of ZKSCAN3 using IpaH9.8 antibody from *S. flexneri* infected HT29 cells. **(A)** Bioinformatics approach showed that IpaH9.8 interacted with host autophagic protein ZKSCAN3. Interacting amino acids are shown in the table. **(B)** Cell extracts were prepared 24 h after infection at different MOI (0, 50, 100, 200) and complexes containing ZKSCAN3 were immunoprecipitated with an IpaH9.8-specific monoclonal antibody. Immunoprecipitates were analysed for ZKSCAN3 by SDS-PAGE and Western blotting using IpaH9.8-specific monoclonal antibody. For input, cell lysates were blotted with anti-ZKSCAN3 antibody. To check for protein expression, aliquots of the cell lysates were analysed directly by Western blotting and Coomassie stain.

6.5. IpaH9.8 induces ubiquitination at different MOI of *Shigella flexneri*

Moreover we further confirmed that IpaH9.8, a E3 ubiquitin ligase induces ubiqitination activity in *S. flexneri* infected cells by ubiquitination assay. HT29 cells were infected with varying MOI (50,100,200) **(Fig6.5)**. The effect of IpaH9.8 on ubiquitination was detected by immunoprecipitation with an anti-Ub antibody. The results showed that IpaH9.8 led to a sharp increase in the level of ubiquitination in case of MOI 50 and a gradual decrease in MOI 100 and MOI 200. The co-immunoprecipitation assay results showed that the ubiquitination of cellular proteins was catalyzed by IpaH9.8 and varies for different MOI of *S. flexneri* infection.Probably, ZKSCAN3 is ubiquitinated by IpaH9.8.

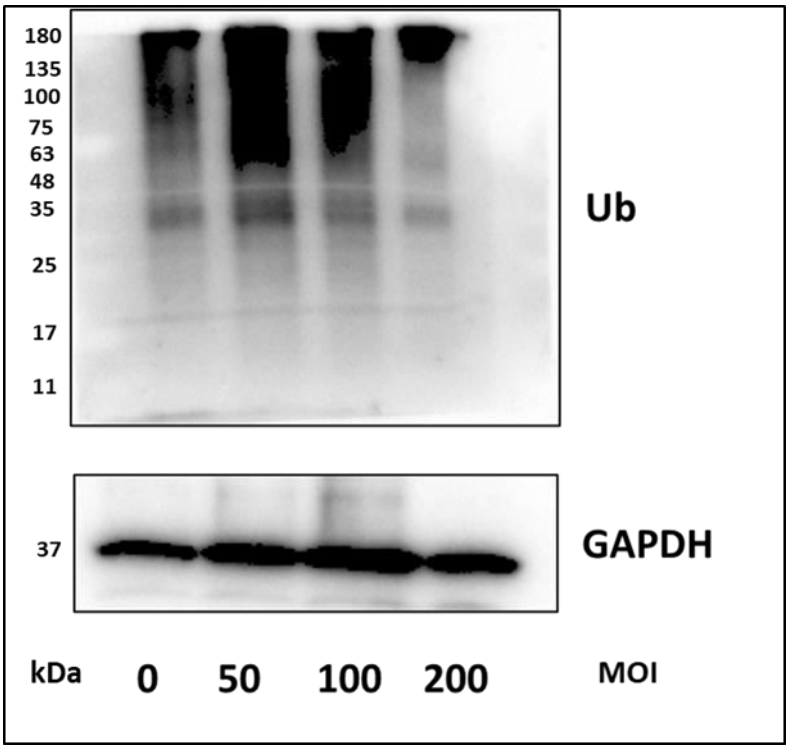

Fig6.5. IpaH9.8 stimulates ubiquitination during infection. Cells were infected with *S. flexneri* at different MOI (0, 50, 100, 200). Cell lysates were immunoprecipitated with an anti-IpaH9.8 antibody followed by western blot with an anti-Ubiquitination antibody. GAPDH was used as loading control.

6.6. Induction of TFEB nuclear translocation in presence of Capsaicin

As we have found that Capsaicin is an inducer of TFEB nuclear translocation, we observed the effect of Capsaicin treatment on TFEB nuclear localisation at MOI 200. Immunoblots have shown altered subcellular localisation of TFEB in presence of Capsaicin and infection. In infected cells, cytosolic fraction of TFEB was increased leading to downregulation of TFEB nuclear translocation and autophagy **(Fig6.6).** On the other hand, Capsaicin treatment upregulated nuclear fraction of TFEB and reduction in its cytosolic fraction both in Capsaicin treated *S. flexneri* infected and only Capsaicin treated cells.

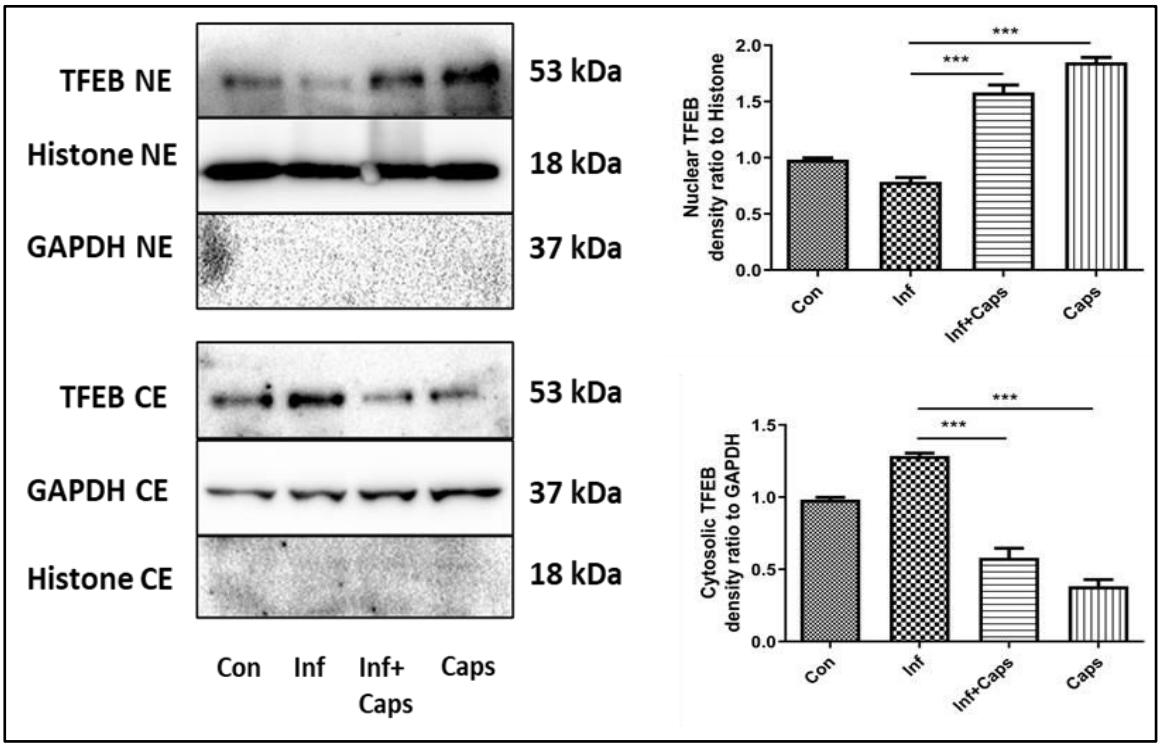

Fig6.6. Caps treatment augmented cytosolic and nuclear localization of TFEB. To assess the impact of Caps treatment, Western blot analysis was conducted on protein extracts from both cytosolic (CE) and nuclear (NE) fractions in both *S. flexneri* infected and uninfected cells. For cytoplasmic extracts, GAPDH served as a housekeeping control, while histone was used as a control for nuclear extracts. Densitometric analyses were performed and visually depicted in graphs. Statistical analysis involved a one-way ANOVA test. The data were graphically presented using GraphPad Prism 5, indicating mean ± SEM (n = 3), and significance levels were denoted as *p < 0.05, **p < 0.01, ***p < 0.001.

6.7. Capsaicin induces promoter binding activity of TFEB

Transcription factor activity assay has shown that Capsaicin treatment induced binding of TFEB to CLEAR sequence/promoter sequence of autophagy genes in infected cells. 4h Capsaicin treatment in infected cells induced transcription factor activity of TFEB as compared to only infected cells(**Fig6.7.A**). Chromatin immunoprecipitation (ChIP) study represents DNA binding ability of protein. qRT-PCR performed in immunoprecipitated DNA with TFEB using specific primer resulted in induced expression of MAP1LC3B **(Fig6.7.B)**. Graphical representation showed immunoprecipitated DNA of Capsaicin treatment in infected cells induced significant fold change of TFEB binding to promoter sequence.

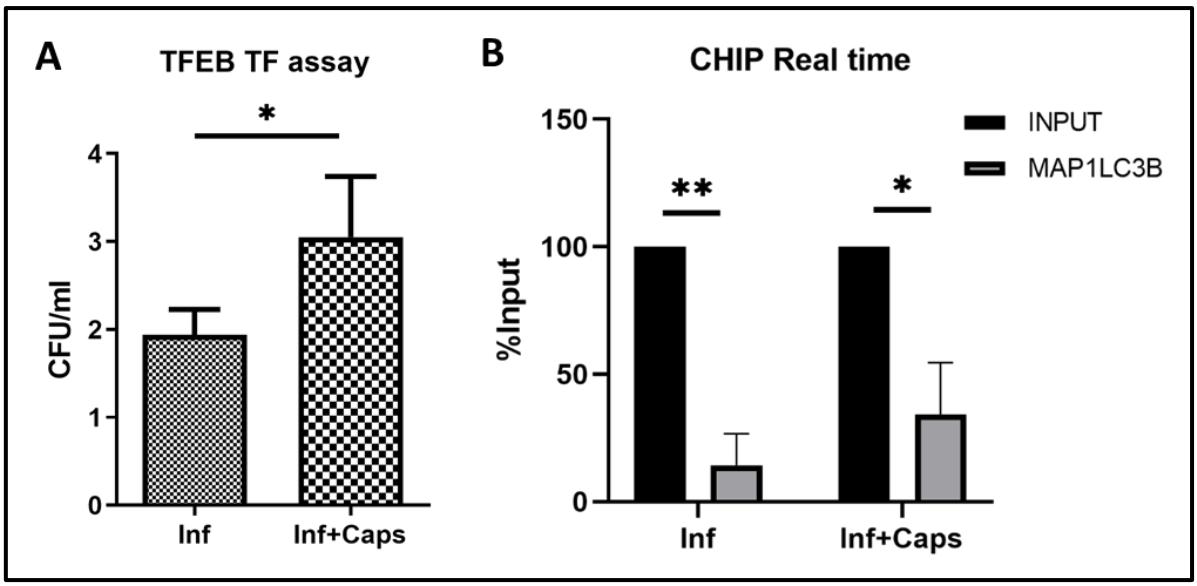

Fig6.7. Capsaicin treatment induced promoter binding activity of TFEB. **(A)** Cells pre-treated with Caps and subsequently infected were used for TFEB promoter activity assay. This assay showed the activation of TFEB binding to the CLEAR sequence due to Caps treatment. Statistical significance was assessed through an unpaired t-test. **(B)** For infected cells and Caps-treated infected cells, a CHIP assay was conducted using anti-TFEB antibody (input was included). The expression of MAP1LC3B was assessed and compared to the input through a real-time PCR assay. A two-way ANOVA analysis was performed. Graphs presenting the data, using GraphPad Prism 5, displayed the mean ± SEM (n = 3), and statistical significance was indicated as *$p < 0.05$, **$p < 0.01$, ***$p < 0.001$.

Chapter 7

Synergistic effects of Capsaicin with antibiotics against resistant S. flexneri strains

Background

Antimicrobial resistance (AMR) is a major crisis globally for human health. Emergence of multidrug resistant bacteria is becoming a major hindrance in treating several common bacterial pathogens (Theuretzbacher, 2017). There are wide range of pathogens which cause diarrhoeal syndrome and *Shigella spp*. is among the potential microbe causing bacillary dysentery. Its prevalence is mostly among the children below 5 years in developing countries although immunocompromised individuals are also affected. *Shigella spp.* cause approximately 150 million cases of disease as well as 300,000 deaths per annum (Khalil et al., 2018). Due to absence of any licensed vaccine against *Shigella spp.*, antimicrobials are the major reliable therapy to limit severity and complications of this disease (Christopher et al., 2010). Earlier *Shigella spp.*, were susceptible to ampicillin, chloramphenicol, co-trimoxazole and nalidixic acid but now resistance against fluoroquinolones, cephalosporins and azithromycin has resulted in outbreaks of shigellosis (Puzari, Sharma and Chetia, 2008). According to WHO, ciprofloxacin, azithromycin, pivmecillinam and ceftriaxone are ultimate drugs recommended. WHO has considered *Shigella spp*. as moderate pathogen (2017). As *Shigella spp.*, is acquiring multidrug resistance rapidly, new therapeutic interventions are required to combat this problem. Efficacy of existing antibiotics can be enhanced by combination therapy. Several biologically active compounds from natural sources are getting attention as they possess antiviral or antibacterial properties and act as antibiotic potentiators. Capsaicin (8-methyl-N-vanillyl-6-nonenamide), a phenolic compound produced by chilli plants is known to inhibit growth of several pathogenic bacteria like *Vibrio cholerae* (Chatterjee et al., 2010) and *Salmonella Typhimurium* (Ha and Kang, 2013). There are several reports that Capsaicin

drastically potentiates effects of several chemotherapeutic drugs. Capsaicin and sorafenib synergistically reduce hepatocellular carcinoma (Dai et al., 2018). Not only that, Capsaicin enhances combination therapy in breast cancer with paclitaxel (Lan et al., 2019) and genistein (Hwang et al., 2009). Moreover, Capsaicin along with ciprofloxacin and colistin reduces intracellular invasion of *Staphylococcus aureus* (Kalia et al., 2012) and *Acinetobacter baumanii* (Guo et al., 2021) respectively. This compound which is acting as an autophagy inducer may be effective against multidrug resistant *S. flexneri* in combination with known antibiotics.

Materials and methods

Gentamicin protection assay was performed to determine the combining effect of Capsaicin and antibiotics in multidrug resistant *S. flexneri*. Treatment was performed in *S. flexneri* infected mice model. Mice undergone fasting for 6 hours followed by multidrug resistant pathogenic *Shigella flexneri* (BCH12702/BCH12654) injection intraperitoneally (Yang et al., 2014). In the experimental design, 4 groups (n=4) were created accordingly Group 1. Only PBS Group 2. Infected: Received *S. flexneri* (BCH12702) suspension (0.5×10^9 CFU/ml) in PBS. Group 3. Infected+Azi10: Received *S. flexneri* suspension followed by azithromycin (10 mg/kg b.w.) treatment for 24 h. Group 4. Infected +Azi10/Strep+Caps50: Received *S. flexneri* suspension followed by azithromycin (10 mg/kg b.w.)/streptomycin and Capsaicin (50 mg/kg b.w.) treatment for 24 h. Each group was kept in an individual cage. Mice were sacrificed and collected colons were crushed and plated in a Congo red plate for CFU/ml count. Experiments were repeated at least thrice. Methods are already described in detail in the materials and methods section.

Results

7.1. Minimum Inhibitory Concentrations (MIC) of different antibiotics for *S flexneri resistant strains*

MIC was calculated from 96 well plate for antibiotic susceptibility of *S. flexneri* strains (BCH12702 & BCH12654) and compared with the existing CLSI guidelines (**Table 7.1, 7.2**). These strains were gift from Dr. Asish Mukhopadhyay's Microbiology laboratory, ICMR NICED. These are clinical isolates form West Bengal.

Name of Antibiotics	**MIC (µg/ ml)**	**MIC breakpoint of Resistance (CLSI guideline) µg/ml**	**Sensitive/ Resistant**
Nalidixic Acid (NA)	1250	≥8	Highly Resistant
Ciprofloxacin (CIP)	1250	≥1	Highly Resistant
Norfloxacin (NOR)	625	≥16	Resistant
Ofloxacin (OFX)	2500	≥8	Highly Resistant
Tetracyclin (TET)	312	≥16	Resistant
Streptomycin (S)	1250	≥32	Resistant
Chloramphenicol (C)	1250	≥32	Highly Resistant
Ampicillin (AM)	312	≥32	Resistant
Erythromycin (E)	1250	≥16	Highly Resistant

Trimethoprim/ sulfamethoxazole (ST)	1000	≥4	Highly Resistant
Gentamicin	1	≥4	Sensitive

Table7.1: MIC of different antibiotics of BCH12702 strain. *Shigella flexneri* (BCH12702) was treated with antibiotics (NA/CIP/NOR/OFX/TET/S/C/AM/E/ST). Tabular representation shows the MIC (µg/ml) values and cut off for resistance according to CLSI guidelines.

Name of Antibiotics	**MIC (µg/ ml)**	**MIC breakpoint of Resistance (CLSI guideline) µg/ml**	**Sensitive/ Resistant**
Nalidixic Acid (NA)	1000	≥8	Highly Resistant
Ciprofloxacin (CIP)	625	≥1	Highly Resistant
Norfloxacin (NOR)	1250	≥16	Resistant
Ofloxacin (OFX)	2500	≥8	Highly Resistant
Tetracyclin (TET)	312	≥16	Resistant
Streptomycin (S)	1250	≥32	Resistant
Chloramphenicol (C)	625	≥32	Highly Resistant
Ampicillin (AM)	625	≥32	Resistant
Erythromycin (E)	1250	≥16	Highly Resistant
Trimethoprim/ sulfamethoxazole (ST)	1250	≥4	Highly Resistant
Gentamicin	1	≥4	Sensitive

Table7.2: MIC of different antibiotics of BCH12654 strain. *Shigella flexneri* (BCH12654) was treated with antibiotics (NA/CIP/NOR/OFX/TET/S/C/AM/E/ST) at different concentration in 96 well plate for 24hours

and MIC was determined. Tabular representation shows the MIC (µg/ml) values and cut off for resistance according to CLSI guidelines.

7.2. Effects of Capsaicin and antibiotics combination against *S. flexneri* in 96 well plate

The fractional inhibitory concentration index (FICI) was calculated using the following formula: FICI = ($MIC_A^{combi}/MIC_A^{alone}$) + ($MIC_B^{combi}/MIC_B^{alone}$). A FICI of ≤0.5 was defined as synergy, a FICI of >0.5 but ≤4.0 was defined as no interaction, and a FICI of >4.0 was defined as antagonism **(Table 7.3)**.

***S. flexneri* strains**	**MIC values in µg/ml**				
	Capsaicin (MIC_A)	**Streptomycin (MIC_B)**	**Capsaicin +Streptomycin (MIC_{A+B})**	**FICI**	**Effect**
BCH12702	500±0.8	625±1.5	125±0.6	0.45	**Synergistic**
BCH12654	375±0.6	625±1.2	100±1.2	0.42	**Synergistic**
	Capsaicin (MIC_A)	**Nalidixic acid (MIC_B)**	**Capsaicin +Nalidixic acid (MIC_{A+B})**	**FICI**	**Effect**
BCH12702	500±0.8	750±0.5	250±0.3	0.8	**No interaction**
BCH12654	375±0.6	625±0.8	200±0.8	0.85	**No interaction**
	Capsaicin (MIC_A)	**Azithromycin (MIC_B)**	**Capsaicin +Azithromycin (MIC_{A+B})**	**FICI**	**Effect**
BCH12702	500±0.8	250±1.3	75±0.4	0.45	**Synergistic**
BCH12654	375±0.6	250±0.6	75±0.5	0.5	**Synergistic**
	Capsaicin (MIC_A)	**Tetracyclin (MIC_B)**	**Capsaicin + Tetracyclin (MIC_{A+B})**	**FICI**	**Effect**
BCH12702	500±0.8	500±1.3	125±0.4	0.5	**Synergistic**
BCH12654	375±0.6	500±0.6	100±0.5	0.47	**Synergistic**

Table7.3: Capsaicin along with antibiotics showed synergistic effects. Synergism was calculated using checkerboard assay treating *S. flexneri* strains with antibiotics and Capsaicin combination. FICI was calculated using MIC values (mean±sem) (n=3).

7.3. Capsaicin and antibiotics synergistically inhibit intracellular *S. flexneri* growth

An intracellular invasion assay was performed to identify the synergistic inhibitory effect of Capsaicin with antibiotics in an *in vitro S. flexneri* infection model. *S. flexneri* (BCH12702, BCH12654 strains) infected HT29 cells were post-treated with different doses of (10µg/ml, 20µg/ml and 50µg/ml) of Capsaicin along with 0.2 µg/ml of antibiotics (Azithromycin/ Streptomycin) or only antibiotics for 24h. In antibiotics treated condition, multiplication of *S. flexneri* reduced significantly while treatment with combination of Azithromycin and Capsaicin for cells infected with BCH12702 as well as BCH12654 strains reduced intracellular bacterial growth more effectively as compared to antibiotics treatment alone.(**Fig7.1.A-C**).

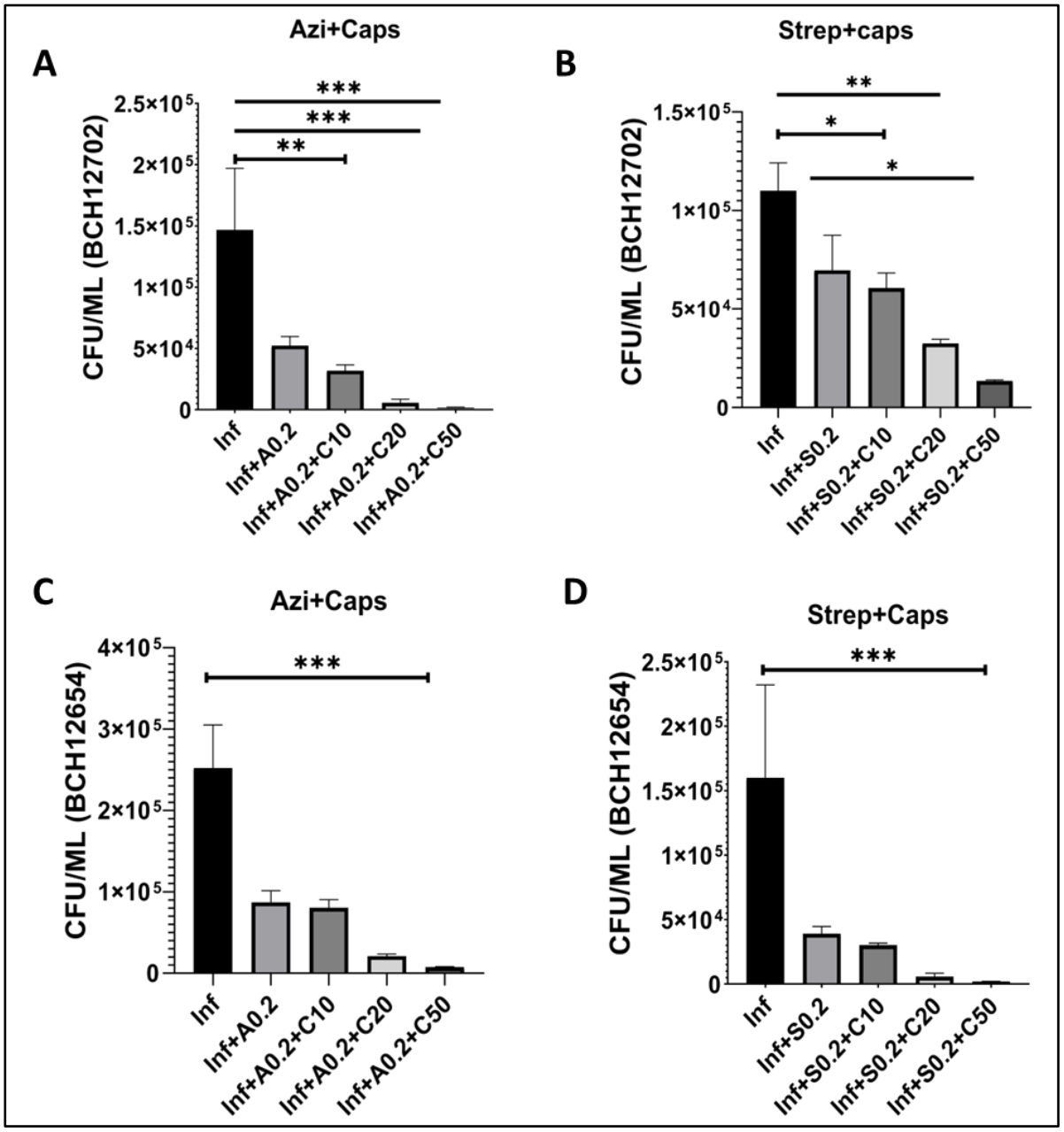

Fig7.1: Capsaicin along with antibiotics showed synergistic effects in intracellular invasion assay. (A) Gentamicin protection assay (GPA) was performed for comparison of colony forming unit (CFU/ml) in HT29 cells at various doses (10µg/ml, 20µg/ml and 50µg/ml) of Caps and azithromycin treatment for 24h post treatment against multi-drug resistant *S. flexneri* (BCH12702) infection at MOI100. **(B)** GPA in HT29 cells with Caps and streptomycin treatment for 24h post *S. flexneri* (BCH12702) infection. **(C)** GPA in HT29 cells with Caps and azithromycin treatment for 24h post *S. flexneri* (BCH12654) infection. **(D)** GPA in HT29 cells with Capsaicin and streptomycin treatment for 24h post *S. flexneri* (BCH12654) infection. CFU/ml was calculated and graphically represented (n=3). One-way ANOVA was done * $p < 0.05$, ** $p < 0.01$, *** $p < 0.001$.

7.4. Capsaicin and antibiotics synergistically inhibit *S. flexneri* infection in *in vivo* conditions

Mice were treated orally either with azithromycin (10 mg/kg b.w.) or streptomycin (10 mg/kg b.w.) along with or without oral Capsaicin (50 mg/kg b.w.) administration after intraperitoneal infection of *S. flexneri* (BCH12702) for 24hrs. Capsaicin reduced bacterial load from intestine of *S. flexneri* infected BALB/c mice when co-treated with azithromycin more than only azithromycin treatment **(fig7.1.A)** Congo red plating of crushed colon represented significant reduction in bacterial load in Capsaicin +Azithromycin treated infected mice as compared to only infected mice. Streptomycin in combination with capsaicin didn't show decrease in bacterial load significantly **(fig7.2.B)**.

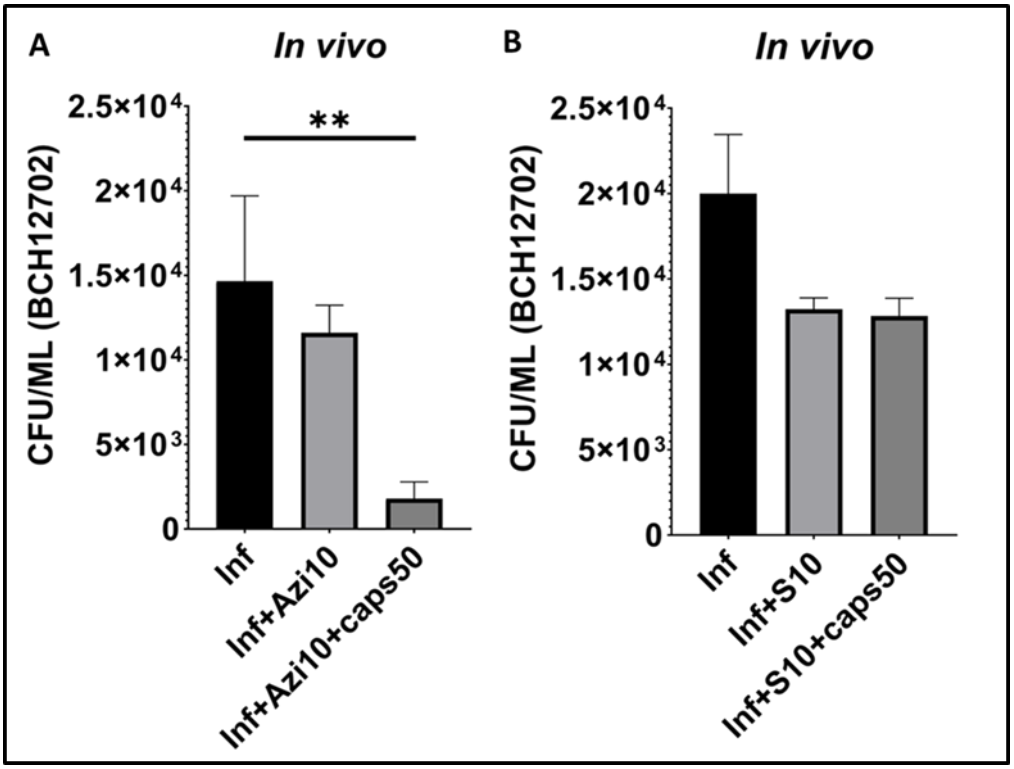

Fig7.2: Capsaicin combined to antibiotics showed synergistic effects *in vivo*. (A) Capsaicin and azithromycin treatment in *Shigella flexneri* (BCH12702)-infected BALB/c mice. Briefly, mice were infected for 2 h followed by azithromycin (10 mg/kg b.w.) treatment with or without Caps (50 mg/kg b.w.) treatment for 24 h. 3 groups (n=4) were created accordingly Group 1. Infected: Received *S. flexneri* (BCH12702)

suspension (0.5×10^9 CFU/ml) in PBS. Group 2. Infected+Azi10: Received *S. flexneri* suspension followed by azithromycin (10 mg/kg b.w.) treatment for 24 h. Group 3. Infected +Azi10+Caps50: Received *S. flexneri* suspension followed by azithromycin (10 mg/kg b.w.) and Capsaicin (50 mg/kg b.w.) treatment for 24 h. Each group was kept in an individual cage. **(B)** Capsaicin and streptomycin combination treatment was done in infected mice and compared to only streptomycin. The 3 groups were Inf: Infected, Inf+S10: Infected + streptomycin (10 mg/kg b.w.), Inf+S10+caps50: Infected + streptomycin (10 mg/kg b.w.), + Capsaicin (50 mg/kg b.w.). Mice were sacrificed and collected colons were crushed and plated in a Congo red plate for CFU/ml count and the values were graphically represented. One-way ANOVA was performed (n=3); * $p < 0.05$, ** $p < 0.01$, *** $p < 0.001$

SECTION 6

DISCUSSION

Antimicrobial resistance (AMR) is a global concern and - scarcity of novel antimicrobials in pipeline is another major issue for infectious diseases (Prestinaci et al., 2015). Alternative complementary medicines have become an interesting topic of study for the researchers (Thombre et al., 2019). Misuse of antibiotics and their easy accessibility without prescription lead to resistance. Further these results in recurring infection by more virulent and resistant strains of the microbes. As a solution, vaccines can primarily be used to prevent infectious diseases (Zhang et al., 2019). Although vaccines are strong preventive measure, vaccination may fail in the case of genetic drift, escape mutants and serotype or strain replacement diseases. Exploration of alternative therapies is gradually becoming the future focus. With this kind of approach, microbial growth can be inhibited as well as virulence can be controlled. Bacteriophage therapy (Nakai et al., 2002) and quorum sensing (Naga et al., 2023) inhibitors are gradually emerging to treat infectious diseases. Novel anti-microbial compounds from medicinal plants have a broad spectrum of activity against both Gram-negative and Gram-positive bacteria with less side effects. Among many herbal compounds our study focussed on Capsaicin (8-methyl-N-vanillyl-6-nonenamide), an active component of chili pepper plants having medicinal values for many years. We observed in *in vitro* intracellular invasion assay that Capsaicin at 16µM concentration reduces intracellular survival of *S. flexneri* both in intestinal and macrophage cell lines.

Research on host-pathogen interaction in the field of *Shigella flexneri* has predominantly focused on understanding the molecular mechanisms that shows how the bacteria invade and survive within host cells. *S. flexneri* is an intracellular pathogen that causes diarrhoea and dysentery in humans by infecting and replicating within the epithelial cells of the large intestine. The type III secretion system of the bacteria injects effector proteins into host cells

to manipulate the cytoskeleton and facilitate bacterial uptake, while outer membrane proteins and lipopolysaccharides mediate adhesion to host cells. However, recent studies have broadened the scope of research, revealing that *S. flexneri* can elicit a range of host responses including inflammation, cell death, and autophagy. Additionally, *S. flexneri* has been shown to interact with various host cells and tissues such as macrophages, dendritic cells, and the liver, suggesting that the infection may have systemic effects. Thus, while the molecular mechanisms of invasion and intracellular survival remain an essential focus, there is increasing recognition of the wider host-pathogen interactions in the *S. flexneri* field. Here, we showed for the first time that Capsaicin activates a host defence mechanism named autophagy to induce bacterial clearance.

Autophagy is a crucial defence mechanism that helps in maintaining cellular homeostasis in response to stress. In the context of host-pathogen interactions, autophagy plays a critical role in regulating the fate of intracellular pathogens. Many intracellular bacteria, such as *Mycobacterium* and *Salmonella*, have evolved mechanisms to avoid or subvert autophagy and establish a successful infection (Ammanathan et al., 2020; Kim et al., 2012; Noad et al., 2017). For example, *Salmonella* can prevent autophagy by inhibiting the formation of autophagosomes or by interfering with autophagy-related signaling pathways. On the other hand, boosting autophagy can enhance the host's defense against intracellular pathogens. Studies have shown that small molecule enhancers of autophagy, such as rapamycin, can promote the clearance of intracellular bacteria and reduce infection. These small molecules work by activating the autophagy pathway and enhancing the delivery of the cargo to the lysosome for degradation. In summary, autophagy is a critical process in regulating host-pathogen interactions. Intracellular pathogens have evolved mechanisms to avoid or subvert

autophagy, while enhancing autophagy using small molecule enhancers can help control bacterial infections. Understanding the interplay between autophagy and intracellular pathogens may lead to the development of novel therapeutics for infectious diseases (Floto et al., 2007; Lin et al., 2017). Targeting host factors of autophagy, offers a promising strategy to overcome the problem of antimicrobial resistance.

Several studies have shown that targeting autophagy using small molecule enhancers can enhance bacterial clearance and reduce the burden of antibiotic-resistant pathogens. For example, the small molecule rapamycin has been shown to enhance autophagy and promote bacterial clearance in various infection models, including drug-resistant *Mycobacterium tuberculosis*. Moreover, recent studies have identified novel small molecules that target autophagy and enhance bacterial clearance. For example, a small molecule called AB1 has been shown to induce autophagy and promote bacterial clearance in models of methicillin-resistant *Staphylococcus aureus* (MRSA) infection.

So, targeting host factors like autophagy offers a promising strategy to combat antimicrobial resistance. The development of small molecule enhancers of autophagy and other host factors holds promise for the development of novel therapeutics for infectious diseases, particularly for antibiotic-resistant pathogens.

This study provides the first evidence that Capsaicin (Caps) induces autophagy for the intracellular killing of *S. flexneri*. It has been demonstrated that Capsaicin, a herbal compound with known anticancer properties, exerts a novel approach for inhibiting *S. flexneri* infection. Previous studies have shown that Capsaicin induces autophagy in tumor cells by overexpressing autophagy proteins such as beclin1, Atg5, and LC3B (Jin et al., 2014). It has been seen that Capsaicin also induces autophagy in intestinal epithelial cells and

macrophages at a lower dose (16μM), which is non-toxic to cells. The induction of autophagy by Capsaicin inhibited the intracellular infiltration of *S. flexneri*, thereby reducing bacterial burden. Hence, Capsaicin-induced autophagy can be used as a potential strategy to enhance host defence against bacterial infections, including those caused by antibiotic-resistant strains. The study also highlights the potential of natural compounds as a source of novel antimicrobial agents. The study provides further evidence of the safety of Capsaicin as a potential therapeutic agent by demonstrating its insignificant toxicity in HT29 cells and macrophages. This is a crucial finding, as toxicity is a major concern in the development of new antimicrobial agents. Moreover, the study shows that Capsaicin treatment results in the overexpression of autophagy genes in intestinal cells. This is an important observation, as it sheds new light on the mechanism by which Capsaicin induces autophagy. While previous studies have shown that Capsaicin can overexpress autophagy proteins such as beclin1, Atg5, and LC3B, the transcriptional upregulation of autophagy by Capsaicin has not been reported before. Further downstream events showed that Capsaicin induced autophagosome formation in intestinal and macrophage cells. This is a significant finding, as autophagy plays a crucial role in the clearance of intracellular pathogens. The transcriptional activation of autophagy by Capsaicin, which results in autophagosome formation, represents a potential mechanism by which Capsaicin can enhance host defense against *S. flexneri* infection.

The study reveals that Capsaicin not only induces autophagy but also contributes to the killing of *S. flexneri* in intestinal epithelial cells and macrophages. This is also a significant finding, as it suggests that Capsaicin has host directed therapeutic effects. This could potentially be harnessed to combat bacterial infections. Furthermore, the study shows that Capsaicin treatment results in autophagosome formation in infected cells. This observation is

supported by electron and confocal microscopic studies, which reveal that bacteria are associated with autophagosomes in drug-treated cells. The association of bacteria with autophagosomes in drug-treated cells provides further evidence of the potential of Capsaicin as a therapeutic agent for the treatment of bacterial infections. The study provides compelling evidence that Capsaicin enhances autophagy by increasing LC3B puncta formation and targeting bacteria to autophagosomes. Moreover, it has been examined that Capsaicin is unable to target bacteria in a plasmid-cured avirulent strain of *S. flexneri* (lacking T3SS). This suggests Capsaicin's ability to target only intracellular *S. flexneri* which has functional T3SS.

The requirement of T3SS for the intracellular infiltration of *S. flexneri* is well established in the literature, with studies demonstrating the importance of IcsB, VirA, and other T3SS proteins for bacterial invasion and survival within host cells. Overall, the study provides valuable insights into the mechanisms underlying Capsaicin's ability to target only intracellular bacteria and highlights the potential of Capsaicin as a novel therapeutic agent for the treatment of intracellular bacterial infections. Based on the information provided, it appears that Capsaicin, might act as specific drug against intracellular bacteria, and it does not have a direct effect on *S. flexneri*. However, it has been found that the anti*Shigella* effect of Capsaicin is autophagy-dependent.

Autophagy is a natural process by which cells can break down and recycle their own components, including damaged or invading microbes, to maintain cellular homeostasis. In the case of bacterial infections, autophagy can act as an important defense mechanism by selectively capturing and degrading intracellular pathogens. The finding that Capsaicin's anti-*Shigella* effect is autophagy-dependent suggests that Capsaicin likely works by enhancing or

activating the autophagy pathway, leading to the capture and degradation of *S. flexneri* within host cells. This is in line with previous studies that have demonstrated the importance of autophagy in controlling intracellular bacterial infections. Furthermore, the lack of a direct effect of Capsaicin on *S. flexneri* suggests that Capsaicin may not directly target the bacteria itself, but instead affects host cell processes that are necessary for bacterial clearance. This could potentially limit the development of antibiotic resistance, as the target of Capsaicin is not a bacterial component that can easily mutate to evade the drug. Overall, these findings provide insight into the mechanism of action of Capsaicin and highlight the importance of autophagy in the host response to bacterial infections.

Previous reports have shown that the protein Atg5 is essential for LC3 recruitment to the bacteria, indicating its involvement in the autophagy process. However, the current study suggests that Atg5 does not affect the intracellular growth of *S. flexneri* in intestinal cells. The study also found that treatment with Capsaicin in Atg5 knockdown cells resulted in the loss of pathogen restriction, indicating the critical role of autophagy in inhibiting bacterial growth. This suggests that while Atg5 may not directly affect the intracellular growth of *S. flexneri*, it plays an essential role in autophagy, which is necessary for restricting bacterial growth. Overall, the study provides new insights into the mechanisms underlying the interaction between *S. flexneri* and host cells. It highlights the complexity of the autophagy process and emphasizes the need to understand the role of Atg5 and other autophagy-related proteins in bacterial infections.

It was further investigated to highlight the mechanism underlying Capsaicin-mediated clearance of *S. flexneri* by autophagy induction. The study found that Capsaicin enhances the nuclear translocation of TFEB, which leads to the transcription of autophagic genes. This

mechanism could explain the crucial role of autophagy in the inhibition of bacterial growth and the loss of pathogen restriction observed in Atg5 knockdown cells treated with Capsaicin. The findings also suggest that Capsaicin treatment can induce autophagy in both infected and uninfected cells. Additionally, the study highlights the importance of TFEB in the regulation of autophagy. The findings have important implications for the development of new treatments and therapies for bacterial infections and suggest that Capsaicin may have broader applications in the regulation of autophagy.

TFEB (Transcription Factor EB) is a well-known transcriptional regulator plays a crucial role in the biogenesis of autophagosomes and lysosomes (Fan et al., 2018). It is responsible for inducing the transcription of several genes involved in autophagy and lysosomal function. The TFEB enhancers are being studied for developing therapeutics against intracellular pathogens. In this context, Caps (Capsaicin) has been found to induce TFEB binding to promoter elements, thereby augmenting the transcription of autophagic genes.

The induction of TFEB binding to promoter elements by Capsaicin is a novel finding that could have significant implications in the field of autophagy and lysosomal function. Capsaicin is well-known to have a wide range of biological activities, including anti-inflammatory and analgesic effects. The present study has uncovered a new mechanism by which Capsaicin induces the transcription of autophagic genes. The results of this study further suggest that Capsaicin may have therapeutic potential in the treatment of diseases associated with impaired TFEB activation that results in autophagy and lysosomal dyfunction.

Further studies revealed the role of TFEB (transcription factor EB) and Capsaicin (Caps) in controlling the growth of *S. flexneri* (*Shigella flexneri*), a bacterial pathogen that causes

intestinal infections. This study inferred that TFEB plays a critical role in regulating autophagy during infection, and Capsaicin induced TFEB-mediated autophagy limits intracellular bacterial growth.

TFEB knockdown in intestinal cells led to an increase in *S. flexneri* growth, indicating that TFEB is essential for controlling bacterial infection. Capsaicin treatment was also ineffective in restricting bacterial growth in TFEB knockdown cells, indicating that Capsaicin-mediated autophagy requires TFEB. In contrast, overexpression of TFEB reduced bacterial growth, suggesting that TFEB can enhance autophagy-mediated intracellular killing of *S. flexneri*. Capsaicin is known to bind to the TRPV1 receptor, which induces calcium influx and is expressed in intestinal cells (Chen et al., 2015). This study suggests that Caps-induced autophagy is due to TRPV1 activation, which triggers TFEB-mediated transcription of autophagy genes. Calcium influx is not involved in this pathway.Overall, this study highlights the importance of TFEB-mediated autophagy in controlling bacterial infections and suggests that Capsaicin enhanced TFEB-mediated autophagy to limit bacterial growth. This finding has important implications for the development of novel therapies for bacterial infections that target TFEB-mediated autophagy.

We further investigated in detail the mechanism that leads to TFEB nuclear translocation. In our study, TRPV1 antagonist Capsazepine has an insignificant effect on *S. flexneri* growth in Caps treated cells. This explains Capsaicin's role in the activation pathway by TRPV1. It is known that TFEB is regulated by several signaling pathways and Capsaicin at the same time has the ability to trigger different pathways (Chang and Zou, 2020). We found that Capsaicin augmented AMPK phosphorylation in *S. flexneri* infected cells. Simultaneously, dephosphorylation of pAkt was observed. This is an additional host protective function to

regulate autophagy as *S. flexneri* infection induces Akt phosphorylation (Ganesan et al., 2017). Both AMPK and Akt have roles in the phosphorylation status of TFEB. AMPK is known to dephosphorylate TFEB and in contrast, Akt induces TFEB phosphorylation. Simultaneously, a downstream target of Akt is mTOR. Finally, we found that mTOR is dephosphorylated due to Capsaicin. Small molecule compounds as inhibitors of mTOR are known to boost autophagy and help in the amelioration of infectious diseases (Halma, Marik and Saleeby, 2023; Kocak et al., 2022). mTOR can phosphorylate TFEB at multiple sites (Kocak et al., 2022). Hence, mTOR dephosphorylation by Capsaicin is an important finding which correlates with autophagy stimulation. These findings suggest that Capsaicin induced a coordinated activation of TFEB by diverse pathways. Finally, TFEB activation leads to the amelioration of shigellosis.

Further it has been observed that Capsaicin inhibited the intracellular growth of *Shigella flexneri* resistant strain at a higher dose, indicating that Capsaicin has the potential to address the problem of antimicrobial resistance in near future.

To further investigate the efficacy of Capsaicin, the researchers conducted an *in vivo* mouse model study. Capsaicin increased the clearance of *S. flexneri* in the intestinal tissues of infected mice. Additionally, Capsaicin treatment induced autophagy in the mice. The *in vivo* mouse model study provides evidence that Capsaicin is effective in inducing autophagy and reducing *S. flexneri* burden, which is promising for future clinical studies.

It is important to note that while this study provides evidence for the potential of Capsaicin as an antimicrobial agent, further research is necessary to fully understand its mechanism of action and potential side effects. Additionally, the study was conducted in a preclinical

model, and further studies in humans are needed to determine the safety and efficacy of Capsaicin in clinical settings.

Characterization of new drug targets in *Shigella flexneri* pathogenesis is a critical step in developing effective treatments for *S. flexneri* infection. The complex interplay between *S. flexneri* and the host cells during infection involves numerous virulence factors and host signaling targets. Identifying key targets within cellular pathways that are specific to *S. flexneri* and essential for its survival could lead to the development of novel therapeutics. Recent advances in genomics and proteomics have allowed for a more comprehensive understanding of the pathogenesis, providing opportunities to discover new drug targets. Additionally, the use of high-throughput screening techniques, such as phenotypic screening and chemical genetic approaches, may enable the identification of compounds that target specific *S. flexneri* virulence factors. Overall, the characterization of new drug targets in *S. flexneri* pathogenesis holds great promise for the development of more effective treatments.

Transcription factors have been identified as potential drug targets in *Shigella flexneri* infections. We have already identified TFEB to be a host transcriptional target for *S. flexneri*. Next, we observed changes in TFEB nuclear localisation for varying MOIs. As we gradually increase the MOI TFEB nuclear localisation is first induced and then decreased . These findings suggest that probably TFEB is induced during *S. flexneri* infection to activate the host defence mechanism. Therin, we observed that a repressor of TFEB, another transcription factor ZKSCAN3 is also induced during infection. ZKSCAN3 belongs to SCAN and KREB family of transcription factors. It inhibits autophagic gene transcription. Nuclear localisation of ZKSCAN3 is induced at higher MOI. Therefore all these findings suggest that the autophagic transcriptional targets TFEB and ZKSCAN3 are induced due to infection. But the

underlying molecular mechanism is still not clear. Hence, we further performed bioinformatic analysis to find whether any virulence factors of the bacteria are interacting with the host transcriptional targets. Surprisingly, the effector protein IpaH9.8 which is a ubiquitin ligase is binding with ZKSCAN3. In line, ubiquitin assay was performed to verify the activity of IpaH9.8. Cellular proteins are ubiquitinated and IpaH 9.8 binding was observed as we increased the MOI of *S. flexneri*. Thus these results indicated host pathogen interaction due to *S. flexneri* infection and the interaction further effects the host defence machinery. Autophagic gene transcription is reduced at higher MOI. Still, further understanding of the exact mechanism needs elucidation. We need to explore the TFEB/ZKSCAN3 interplay during *S flexneri* infection.Overall, targeting transcription factors in *S. flexneri* pathogenesis offers a promising strategy for developing new drugs.

Emerging evidence suggests that targeting the transcription factor EB (TFEB) could be a promising approach for developing novel drugs to combat *Shigella flexneri* infection. TFEB is a key regulator of lysosomal biogenesis and autophagy, which are cellular processes that play important roles in host defense against intracellular pathogens, including *S. flexneri*. Our studies have shown that activation of TFEB can enhance the antibacterial response of host cells against *Shigella flexneri* by reducing their intracellular survival. Moreover, TFEB induction during *S. flexneri* infecition at higher MOI shows that this transcription factor is required to activate host defence mechanims like autophagy.It has been identified that Capsaicin can activate TFEB and it has shown promising results in *in vitro* conditions for treating infections caused by *Shigella flexneri*. Therefore, targeting TFEB in *S. flexneri* pathogenesis offers a potential new avenue for developing effective treatments for bacterial infections.

Traditional medicines and plant products are emerging as a blessing in medical sciences due to their easy availability and insignificant side effects. More attention to herbal formulation is being paid in last decade. The study showed that Capsaicin, a natural compound found in chili peppers, can enhance the efficacy of antibiotics against drug-resistant *S. flexneri* bacteria. The combination of Capsaicin with azithromycin demonstrated a synergistic effect in both *in vitro* and *in vivo* experiments, meaning that the combination was more effective than the sum of the individual components. In a murine model of shigellosis, which is a type of bacterial infection caused by *S. flexneri*, the Capsaicin /azithromycin combination therapy significantly reduced the bacterial load in the target tissues compared to the untreated control and the streptomycin/azithromycin groups. This suggests that Capsaicin could be a promising adjunctive therapy for the treatment of drug-resistant *S. flexneri* infections. It is important to note that while Capsaicin has shown potential as a synergistic agent for antibiotics, further research is needed to determine its safety and efficacy in humans.

SECTION 7

CONCLUSION

This thesis aimed to understand the therapeutic intervention of *Shigella flexneri* host pathogen interaction by a herbal compound named Capsaicin. Conclusions of this study are:

- Capsaicin at 16μM is effective to reduce burden of intracellular *Shigella flexneri* both in pre- and post-treated condition in intestinal epithelial and macrophage cells
- Capsaicin is less/non-toxic for cells(intestinal and macrophage) at 16μM concentration.
- Capsaicin is able to inhibit *Shigella flexneri* infection by inducing host directed defence mechanism such as autophagy.
- It upregulates several autophagy genes and proteins both in *in vitro* and *in vivo* condition
- It induces double membrane bound autophagosome formation.
- Capsaicin upregulates host autophagy mechanism by enhancing autophagosomal engulfment of invaded *Shigella flexneri*
- It enhances nuclear translocation of transcription factor EB (TFEB) leading to transcription of autophagosomal genes.
- Capsaicin enhances transcriptional activity and promoter binding ability of TFEB
- Capsaicin activates TFEB by targeting AMPK, mTOR and Akt.
- Host cell promotes autophagy during the early stage of infection but with increased infection load, effector proteins released by *S. flexneri* hijacks cell autophagy machinery and escapes autophagosomal engulfment leading to its intracellular survival and progression of disease.
- Transcription factors TFEB and ZKSCAN3 are involved in regulation of autophagy and play a major role during *S flexneri* infection.

- Bacterial virulent factor IpaH9.8 interacts with ZKSCAN3 during *S flexneri* infection.
- Combination of Capsaicin with antibiotic (azithromycin) shows synergistic effect against drug resistant *S. flexneri* strains.

Future Prospects:

Our research will help in filling up important knowledge gaps in our understanding of *Shigella flexneri* pathogenesis in *in vitro* and *in vivo* conditions. This knowledge of Capsaicin mediated autophagy induction and prevention of shigellosis by host directed therapeutic approach will also help to fight against multidrug-resistant strains of *S. flexneri*. In the future, more research work will be conducted to translate this basic knowledge for rational designing of safe and effective drugs against *S. flexneri* infection. Additionally, this concept may be applicable to autophagy mediated bacterial clearance. Further in-depth studies on the regulation of TFEB and its modulation will help in interventing host pathogen interaction. In addition, more studies on Capsaicin will establish it as a potent drug candidate along with other drugs /antibiotics.

SECTION 8

REFERENCES

Agaisse H (2016) Molecular and cellular mechanisms of *Shigella flexneri* dissemination. *Frontiers in cellular and infection microbiology* **6**:29.

Ammanathan V, Mishra P, Chavalmane AK, Muthusamy S, Jadhav V, Siddamadappa C and Manjithaya R (2020) Restriction of intracellular *Salmonella* replication by restoring TFEB-mediated xenophagy. *Autophagy* **16**:1584-1597.

Anand P and Bley K (2011) Topical Capsaicin for pain management: therapeutic potential and mechanisms of action of the new high-concentration Capsaicin 8% patch. *British journal of anaesthesia* **107**:490-502.

Ashida H, Kim M, Schmidt-Supprian M, Ma A, Ogawa M, Sasakawa C (2010) A bacterial E3 ubiquitin ligase IpaH9.8 targets NEMO/IKKγ to dampen the host NF-κB-mediated inflammatory response. Nature cell biology 1:66-73.

Ashida H, Mimuro H and Sasakawa C (2015) Shigella flexneri manipulates host immune responses by delivering effector proteins with specific roles. *Frontiers in Immunology* **6**:219.

Banerjee S, Katiyar P, Kumar L, Kumar V, Saini SS, Krishnan V, Sircar D and Roy P (2021) Black pepper prevents anemia of inflammation by inhibiting hepcidin over-expression through BMP6-SMAD1/IL6-STAT3 signaling pathway. *Free Radical Biology and Medicine* **168**:189-202.

Basak P, Maitra P, Khan U, Saha K, Bhattacharya SS, Dutta M and Bhattacharya S (2022) Capsaicin inhibits *Shigella flexneri* intracellular growth by inducing autophagy. *Frontiers in Pharmacology* **13**:903438.

Baxt LA, Garza-Mayers AC and Goldberg MB (2013) Bacterial subversion of host innate immune pathways. *Science* **340**:697-701.

Bennish ML (1991) Potentially lethal complications of shigellosis. *Reviews of infectious diseases* **13**:S319-S324.

Bennish ML and Wojtyniak BJ (1991) Mortality due to shigellosis: community and hospital data. *Reviews of infectious diseases* **13**:S245-251.

Bevan S (1999) Capsaicin and pain mechanisms, in *Pain and neurogenic inflammation* pp 61-80, Springer.

Bevan S, Hothi S, Hughes G, James I, Rang H, Shah K, Walpole C and Yeats J (1992) Capsazepine: a competitive antagonist of the sensory neurone excitant Capsaicin. *British journal of pharmacology* **107**:544-552.

Bradfute SB, Castillo EF, Arko-Mensah J, Chauhan S, Jiang S, Mandell M and Deretic V (2013) Autophagy as an immune effector against tuberculosis. *Current opinion in microbiology* **16**:355-365.

Cabral-Fernandes L, Goyal S, Farahvash A, Tsalikis J, Philpott DJ, Girardin SE (2022) Invading Bacterial Pathogens Activate Transcription Factor EB in Epithelial Cells through the Amino Acid Starvation Pathway of mTORC1 Inhibition. Molecular and Cellular Biology **42**(9):e00241-22.

Campbell-Valois F-X, Sachse M, Sansonetti PJ and Parsot C (2015) Escape of actively secreting *Shigella flexneri* from ATG8/LC3-positive vacuoles formed during cell-to-cell spread is facilitated by IcsB and VirA. *MBio* **6**:10.1128/mbio. 02567-02514.

Chang H and Zou Z (2020) Targeting autophagy to overcome drug resistance: further developments. *Journal of hematology & oncology* **13**:1-18.

Chang Z, Lu S, Chen L, Jin Q and Yang J (2012) Causative species and serotypes of shigellosis in mainland China: systematic review and meta-analysis. *PLoS One* **7**:e52515.

Chatterjee S, Asakura M, Chowdhury N, Neogi SB, Sugimoto N, Haldar S, Awasthi SP, Hinenoya A, Aoki S and Yamasaki S (2010) Capsaicin, a potential inhibitor of cholera toxin production in Vibrio cholerae. *FEMS microbiology letters* **306**:54-60.

Chauhan S, Goodwin JG, Chauhan S, Manyam G, Wang J, Kamat AM and Boyd DD (2013) ZKSCAN3 is a master transcriptional repressor of autophagy. *Molecular cell* **50**:16-28.

Chen J, Li L, Li Y, Liang X, Sun Q, Yu H, Zhong J, Ni Y, Chen J and Zhao Z (2015) Activation of TRPV1 channel by dietary Capsaicin improves visceral fat remodeling through connexin43-mediated Ca2+ influx. *Cardiovascular diabetology* **14**:1-14.

Chen X, Tan M, Xie Z, Feng B, Zhao Z, Yang K, Hu C, Liao N, Wang T and Chen D (2016) Inhibiting ROS-STAT3-dependent autophagy enhanced Capsaicin–induced apoptosis in human hepatocellular carcinoma cells. *Free Radical Research* **50**:744-755.

Christopher PR, David KV, John SM and Sankarapandian V (2010) Antibiotic therapy for *Shigella flexneri dysentery*. *Cochrane Database of Systematic Reviews*.

Cossart P and Sansonetti PJ (2004) Bacterial invasion: the paradigms of enteroinvasive pathogens. *Science* **304**:242-248.

Dai N, Ye R, He Q, Guo P, Chen H and Zhang Q (2018) Capsaicin and sorafenib combination treatment exerts synergistic anti-hepatocellular carcinoma activity by suppressing EGFR and PI3K/Akt/mTOR signaling. *Oncology Reports* **40**:3235-3248.

Deretic V (2021) Autophagy in inflammation, infection, and immunometabolism. *Immunity* **54**:437-453.

Deretic V, Saitoh T and Akira S (2013) Autophagy in infection, inflammation and immunity. *Nature Reviews Immunology* **13**:722-737.

Dray A (1992) Neuropharmacological mechanisms of Capsaicin and related substances. *Biochemical pharmacology* **44**:611-615.

Dupont N, Lacas-Gervais S, Bertout J, Paz I, Freche B, Van Nhieu GT, van Der Goot FG, Sansonetti PJ and Lafont F (2009) Shigella flexneri phagocytic vacuolar membrane remnants participate in the cellular response to pathogen invasion and are regulated by autophagy. *Cell host & microbe* **6**:137-149.

Eijkelenboom A and Burgering BM (2013) FOXOs: signalling integrators for homeostasis maintenance. *Nature reviews Molecular cell biology* **14**:83-97.

Eskelinen E-L, Schmidt CK, Neu S, Willenborg M, Fuertes G, Salvador N, Tanaka Y, Lullmann-Rauch R, Hartmann D and Heeren J (2004) Disturbed cholesterol traffic but normal proteolytic function in LAMP-1/LAMP-2 double-deficient fibroblasts. *Molecular biology of the cell* **15**:3132-3145.

Fan Y, Lu H, Liang W, Garcia-Barrio MT, Guo Y, Zhang J, Zhu T, Hao Y, Zhang J and Chen YE (2018) Endothelial TFEB (Transcription Factor EB) positively regulates postischemic angiogenesis. *Circulation research* **122**:945-957.

Floto RA, Sarkar S, Perlstein EO, Kampmann B, Schreiber SL and Rubinsztein DC (2007) Small molecule enhancers of rapamycin-induced TOR inhibition promote autophagy, reduce toxicity in Huntington's disease models and enhance killing of mycobacteria by macrophages. *Autophagy* **3**:620-622.

Forn-Cuní G, Welvaarts L, Stel F, van den Hondel C, Arentshorst M, Ram A and Meijer A (2023) Stimulating the autophagic-lysosomal axis enhances host defense against fungal infection in a zebrafish model of invasive Aspergillosis. *Autophagy* **19**:324-337.

Ganesan R, Hos NJ, Gutierrez S, Fischer J, Stepek JM, Daglidu E, Krönke M and Robinson N (2017) Salmonella Typhimurium disrupts Sirt1/AMPK checkpoint control of mTOR to impair autophagy. *PLoS pathogens* **13**:e1006227.

Gavva NR (2008) Body-temperature maintenance as the predominant function of the vanilloid receptor TRPV1. *Trends in pharmacological sciences* **29**:550-557.

Georgakopoulou T, Mandilara G, Mellou K, Tryfinopoulou K, Chrisostomou A, Lillakou H, Hadjichristodoulou C and Vatopoulos A (2016) Resistant Shigella flexneri strains in refugees, August–October 2015, Greece. *Epidemiology & Infection* **144**:2415-2419.

Guo T, Li M, Sun X, Wang Y, Yang L, Jiao H and Li G (2021) Synergistic activity of Capsaicin and colistin against colistin-resistant Acinetobacter baumannii: *In vitro/vivo* efficacy and mode of action. *Frontiers in Pharmacology* **12**:744494.

Ha J-W and Kang D-H (2013) Simultaneous near-infrared radiant heating and UV radiation for inactivating Escherichia coli O157: H7 and Salmonella enterica serovar Typhimurium in powdered red pepper (Capsicum annuum L.). *Applied and environmental microbiology* **79**:6568-6575.

Hajialibeigi A, Amani J and Gargari SLM (2021) Identification and evaluation of novel vaccine candidates against *Shigella flexneri* through reverse vaccinology approach. *Applied Microbiology and Biotechnology* **105**:1159-1173.

Halma M, Marik P and Saleeby Y (2023) Exploring Therapeutic Applications of Autophagy in Spike Protein-Related Pathology.

Hellmich UA and Gaudet R (2014) Structural biology of TRP channels. *Mammalian Transient Receptor Potential (TRP) Cation Channels: Volume II*:963-990.

Hong Z-F, Zhao W-X, Yin Z-Y, Xie C-R, Xu Y-P, Chi X-Q, Zhang S and Wang X-M (2015) Capsaicin enhances the drug sensitivity of cholangiocarcinoma through the inhibition of chemotherapeutic-induced autophagy. *PloS one* **10**:e0121538.

Hsu CL, Lee EX, Gordon KL, Paz EA, Shen W-C, Ohnishi K, Meisenhelder J, Hunter T and La Spada AR (2018) MAP4K3 mediates amino acid-dependent regulation of autophagy via phosphorylation of TFEB. *Nature Communications* **9**:942.

Huang H and Tindall DJ (2007) Dynamic FoxO transcription factors. *Journal of cell science* **120**:2479-2487.

Hwang JT, Lee YK, Shin JI and Park OJ (2009) Anti-inflammatory and Anticarcinogenic effect of genistein alone or in combination with Capsaicin in TPA-treated rat mammary glands or mammary cancer cell line. *Annals of the New York Academy of Sciences* **1171**:415-420.

Jensen T and Edwards JG (2012) Calcineurin is required for TRPV1-induced long-term depression of hippocampal interneurons. *Neuroscience letters* **510**:82-87.

Jin J, Lin G, Huang H, Xu D, Yu H, Ma X, Zhu L, Ma D and Jiang H (2014) Capsaicin mediates cell cycle arrest and apoptosis in human colon cancer cells via stabilizing and activating p53. *International journal of biological sciences* **10**:285.

Kalia NP, Mahajan P, Mehra R, Nargotra A, Sharma JP, Koul S and Khan IA (2012) Capsaicin, a novel inhibitor of the NorA efflux pump, reduces the intracellular invasion of Staphylococcus aureus. *Journal of antimicrobial chemotherapy* **67**:2401-2408.

Kang J-H, Tsuyoshi G, Le Ngoc H, Kim H-M, Tu TH, Noh H-J, Kim C-S, Choe S-Y, Kawada T and Yoo H (2011) Dietary Capsaicin attenuates metabolic dysregulation in genetically obese diabetic mice. *Journal of medicinal food* **14**:310-315.

Kaufmann SH, Dorhoi A, Hotchkiss RS and Bartenschlager R (2018) Host-directed therapies for bacterial and viral infections. *Nature reviews Drug discovery* **17**:35-56.

Khalil IA, Troeger C, Blacker BF, Rao PC, Brown A, Atherly DE, Brewer TG, Engmann CM, Houpt ER and Kang G (2018) Morbidity and mortality due to Shigella flexneri and enterotoxigenic Escherichia coli diarrhoea: the Global Burden of Disease Study 1990–2016. *The Lancet infectious diseases* **18**:1229-1240.

Khan U, Karmakar BC, Basak P, Paul S, Gope A, Sarkar D, Mukhopadhyay AK, Dutta S and Bhattacharya S (2023) Glycyrrhizin, an inhibitor of HMGB1 induces autolysosomal degradation function and inhibits Helicobacter pylori infection. *Molecular Medicine* **29**:1-15.

Khoza LJ, Kumar P, Dube A, Demana PH and Choonara YE (2022) Insights into innovative therapeutics for drug-resistant tuberculosis: Host-directed therapy and autophagy inducing modified nanoparticles. *International Journal of Pharmaceutics* **622**:121893.

Kim J-J, Lee H-M, Shin D-M, Kim W, Yuk J-M, Jin HS, Lee S-H, Cha G-H, Kim J-M and Lee Z-W (2012) Host cell autophagy activated by antibiotics is required for their effective antimycobacterial drug action. *Cell host & microbe* **11**:457-468.

Kim YS, Lee H-M, Kim JK, Yang C-S, Kim TS, Jung M, Jin HS, Kim S, Jang J and Oh GT (2017) PPAR-α activation mediates innate host defense through induction of TFEB and lipid catabolism. *The Journal of Immunology* **198**:3283-3295.

Kim YS, Silwal P, Kim SY, Yoshimori T and Jo E-K (2019) Autophagy-activating strategies to promote innate defense against mycobacteria. *Experimental & Molecular Medicine* **51**:1-10.

Kobayashi S, Volden P, Timm D, Mao K, Xu X and Liang Q (2010) Transcription factor GATA4 inhibits doxorubicin-induced autophagy and cardiomyocyte death. *Journal of Biological Chemistry* **285**:793-804.

Kocak M, Ezazi Erdi S, Jorba G, Maestro I, Farrés J, Kirkin V, Martinez A and Pless O (2022) Targeting autophagy in disease: established and new strategies. *Autophagy* **18**:473-495.

Krokowski S and Mostowy S (2016) Interactions between *Shigella flexneri* and the autophagy machinery. *Frontiers in cellular and infection microbiology* **6**:17.

Lan Y, Sun Y, Yang T, Ma X, Cao M, Liu L, Yu S, Cao A and Liu Y (2019) Co-delivery of paclitaxel by a Capsaicin prodrug micelle facilitating for combination therapy on breast cancer. *Molecular pharmaceutics* **16**:3430-3440.

Lee H-J, Ko H-J, Kim SH and Jung Y-J (2019) Pasakbumin A controls the growth of Mycobacterium tuberculosis by enhancing the autophagy and production of antibacterial mediators in mouse macrophages. *PLoS One* **14**:e0199799.

Lima IF, Havt A and Lima AA (2015) Update on molecular epidemiology of Shigella flexneri infection. *Current opinion in gastroenterology* **31**:30-37.

Lin R-J, Wu I-J, Hong J-Y, Liu B-H, Liang R-Y, Yuan T-M and Chuang S-M (2018) Capsaicin-induced TRIB3 upregulation promotes apoptosis in cancer cells. *Cancer management and research* 4237-4248.

Lin Y-T, Wang H-C, Hsu Y-C, Cho C-L, Yang M-Y and Chien C-Y (2017) Capsaicin induces autophagy and apoptosis in human nasopharyngeal carcinoma cells by downregulating the PI3K/AKT/mTOR pathway. *International Journal of Molecular Sciences* **18**:1343.

Liu L, Tao Z, Zheng LD, Brooke JP, Smith CM, Liu D, Long YC, Cheng Z (2016) FoxO1 interacts with transcription factor EB and differentially regulates mitochondrial uncoupling proteins via autophagy in adipocytes. Cell death discovery **2**(1):1-8.

Maitra P, Basak P, Okamoto K, Miyoshi S-i, Dutta S and Bhattacharya S (2023) Asiatic acid inhibits intracellular *Shigella flexneri* growth by inducing antimicrobial peptide gene expression. *Journal of Applied Microbiology* **134**:lxac076.

Mallett C, VanDeVerg L, Collins H and Hale T (1993) Evaluation of Shigella flexneri vaccine safety and efficacy in an intranasally challenged mouse model. *Vaccine* **11**:190-196.

Martina JA, Diab HI, Lishu L, Jeong-A L, Patange S, Raben N and Puertollano R (2014) The nutrient-responsive transcription factor TFE3 promotes autophagy, lysosomal biogenesis, and clearance of cellular debris. *Science signaling* **7**:ra9-ra9.

Mata LJ, Gangarosa EJ, Cáceres A, Perera DR and Mejicanos ML (1970) Epidemic shiga bacillus dysentery in Central America. I. Etiologic investigations in Guatemala, 1969. *The Journal of Infectious Diseases*:170-180.

Medina DL, Di Paola S, Peluso I, Armani A, De Stefani D, Venditti R, Montefusco S, Scotto-Rosato A, Prezioso C and Forrester A (2015) Lysosomal calcium signalling regulates autophagy through calcineurin and TFEB. *Nature cell biology* **17**:288-299.

Mostowy S and Cossart P (2012) Bacterial autophagy: restriction or promotion of bacterial replication? *Trends in cell biology* **22**:283-291.

Mózsik G (2014) Capsaicin as new orally applicable gastroprotective and therapeutic drug alone or in combination with nonsteroidal anti-inflammatory drugs in healthy human subjects and in patients. *Capsaicin as a Therapeutic Molecule*:209-258.

Munguia J and Nizet V (2017) Pharmacological targeting of the host–pathogen interaction: alternatives to classical antibiotics to combat drug-resistant superbugs. *Trends in pharmacological sciences* **38**:473-488.

Mvubu NE and Chiliza TE (2021) Exploring the use of medicinal plants and their bioactive derivatives as alveolar Nlrp3 inflammasome regulators during mycobacterium tuberculosis infection. *International Journal of Molecular Sciences* **22**:9497.

Nabar NR, Kehrl JH (2017) Focus: Infectious Diseases: The Transcription Factor EB Links Cellular Stress to the Immune Response. The Yale Journal of Biology and Medicine **90**(2):301.

Naga NG, El-Badan DE, Ghanem KM, Shaaban MI (2023) It is the time for quorum sensing inhibition as alternative strategy of antimicrobial therapy. Cell Communication and Signaling **1**:1-4.

Nakai T, Park SC (2002) Bacteriophage therapy of infectious diseases in aquaculture. Research in microbiology **153**(1):13-8.

Nandy S, Dutta S, Ghosh S, Ganai A, Rajahamsan J, Theodore RBJ and Sheikh NK (2011) Foodborne-associated *Shigella flexneri sonnei*, India, 2009 and 2010. *Emerging Infectious Diseases* **17**:2072.

Noad J, Von Der Malsburg A, Pathe C, Michel MA, Komander D and Randow F (2017) LUBAC-synthesized linear ubiquitin chains restrict cytosol-invading bacteria by activating autophagy and NF-κB. *Nature microbiology* **2**:1-10.

Ogawa M, Handa Y, Ashida H, Suzuki M and Sasakawa C (2008) The versatility of Shigella flexneri effectors. *Nature Reviews Microbiology* **6**:11-16.

Ogawa M, Yoshimori T, Suzuki T, Sagara H, Mizushima N and Sasakawa C (2005) Escape of intracellular Shigella flexneri from autophagy. *Science* **307**:727-731.

Oh S, Choi C-H and Jung Y-K (2010) Autophagy induction by Capsaicin in malignant human breast cells is modulated by p38 and ERK mitogen-activated protein kinases and retards cell death by suppressing endoplasmic reticulum stress-mediated apoptosis. *Molecular Pharmacology*.

Oh SH, Kim YS, Lim SC, Hou YF, Chang IY and You HJ (2008) DihydroCapsaicin (DHC), a saturated structural analog of Capsaicin, induces autophagy in human cancer cells in a catalase-regulated manner. *Autophagy* **4**:1009-1019.

Parsot C and Sansonetti P (1996) Invasion and the pathogenesis of *Shigella flexneri* infections. *Bacterial invasiveness*:25-42.

Pérez LAR, Basantes BHC, Cruz AER and Cruz LAR (2023) Colitis y absceso hepático amebiano sin antecedentes epidemiológicos. *Boletín de Malariología y Salud Ambiental* **63**:2-9.

Philpott DJ, Sorbara MT, Robertson SJ, Croitoru K and Girardin SE (2014) NOD proteins: regulators of inflammation in health and disease. *Nature Reviews Immunology* **14**:9-23.

Pinaud L, Sansonetti PJ and Phalipon A (2018) Host cell targeting by enteropathogenic bacteria T3SS effectors. *Trends in microbiology* **26**:266-283.

Prestinaci F, Pezzotti P, Pantosti A (2015) Antimicrobial resistance: a global multifaceted phenomenon. Pathogens and global health. Oct 3;109(7):309-18.

Puhar A and Sansonetti PJ (2014) Type III secretion system. *Current Biology* **24**:R784-R791.

Puzari M, Sharma M and Chetia P Journal of Infection and Public Health Emergence of antibiotic resistant *Shigella flexneri species*: A matter of concern.

Puzari M, Sharma M and Chetia P (2018) Emergence of antibiotic resistant *Shigella flexneri species*: A matter of concern. *Journal of infection and public health* **11**:451-454.

Ranganathan S, Doucet M, Grassel CL, Delaine-Elias B, Zachos NC and Barry EM (2019) Evaluating *Shigella flexneri* pathogenesis in the human enteroid model. *Infection and immunity* **87**:10.1128/iai. 00740-00718.

Reilly CA, Johansen ME, Lanza DL, Lee J, Lim JO, & Yost GS (2005). Calcium-dependent and independent mechanisms of Capsaicin receptor (TRPV1)-mediated cytokine production and cell death in human bronchial epithelial cells. Journal of biochemical and molecular toxicology, **19**(4), 266-275.

Rekha RS, Mily A, Sultana T, Haq A, Ahmed S, Mostafa Kamal S, van Schadewijk A, Hiemstra PS, Gudmundsson GH and Agerberth B (2018) Immune responses in the treatment of drug-sensitive pulmonary tuberculosis with phenylbutyrate and vitamin D3 as host directed therapy. *BMC Infectious Diseases* **18**:1-12.

Rekha RS, Rao Muvva SJ, Wan M, Raqib R, Bergman P, Brighenti S, Gudmundsson GH and Agerberth B (2015) Phenylbutyrate induces LL-37-dependent autophagy and intracellular killing of Mycobacterium tuberculosis in human macrophages. *Autophagy* **11**:1688-1699.

Rogawski McQuade ET, Shaheen F, Kabir F, Rizvi A, Platts-Mills JA, Aziz F, Kalam A, Qureshi S, Elwood S and Liu J (2020) Epidemiology of Shigella flexneri infections and diarrhea in the first two years of life using culture-independent diagnostics in 8 low-resource settings. *PLoS neglected tropical diseases* **14**:e0008536.

Rubinsztein DC, Codogno P and Levine B (2012) Autophagy modulation as a potential therapeutic target for diverse diseases. *Nature reviews Drug discovery* **11**:709-730.

Sardiello M, Palmieri M, Di Ronza A, Medina DL, Valenza M, Gennarino VA, Di Malta C, Donaudy F, Embrione V and Polishchuk RS (2009) A gene network regulating lysosomal biogenesis and function. *Science* **325**:473-477.

Sarpras M, Chhapekar SS, Ahmad I, Abraham SK, Ramchiary N. (2018) Analysis of bioactive components in Ghost chili (*Capsicum chinense*) for antioxidant, genotoxic, and apoptotic effects in mice. Drug and Chemical Toxicology **43**(2):182-91.

Schroeder GN and Hilbi H (2008) Molecular pathogenesis of *Shigella flexneri spp*.: controlling host cell signaling, invasion, and death by type III secretion. *Clinical microbiology reviews* **21**:134-156.

Sengupta A, Molkentin JD and Yutzey KE (2009) FoxO transcription factors promote autophagy in cardiomyocytes. *Journal of Biological Chemistry* **284**:28319-28331.

Settembre C, Di Malta C, Polito VA, Arencibia MG, Vetrini F, Erdin S, Erdin SU, Huynh T, Medina D and Colella P (2011) TFEB links autophagy to lysosomal biogenesis. *science* **332**:1429-1433.

Sturge CR and Yarovinsky F (2014) Complex immune cell interplay in the gamma interferon response during Toxoplasma gondii infection. *Infection and immunity* **82**:3090-3097.

Szallasi A and Blumberg P (1989) Resiniferatoxin, a phorbol-related diterpene, acts as an ultrapotent analog of Capsaicin, the irritant constituent in red pepper. *Neuroscience* **30**:515-520.

Szolcsányi J (2015) Effect of Capsaicin on thermoregulation: an update with new aspects. *Temperature* **2**:277-296.

Taneja N and Mewara A (2016) Shigellosis: epidemiology in India. *The Indian journal of medical research* **143**:565.

Taneja N, Tiewsoh JBA, Gupta S, Mohan B, Verma R, Shankar P, Narayan C, Yadav VK, Jayashree M and Singh S (2021) Antimicrobial resistance in *Shigella flexneri species*: Our five years (2015–2019) experience in a tertiary care center in north India. *Indian Journal of Medical Microbiology* **39**:489-494.

Tanner K (2016) Shigella flexneri Effector IpaH9. 8 Interacts with Autophagy Transcription Factor ZKSCAN3 and Increases Autophagy During Infection.

Tayseer I, Aburjai T, Abu-Qatouseh L, AL-Karabieh N, Ahmed W and Al-Samydai A (2020) *In vitro* anti-Helicobacter pylori activity of Capsaicin. *J Pure Appl Microbiol* **14**:279-286.

Theuretzbacher U (2017) Global antimicrobial resistance in Gram-negative pathogens and clinical need. *Current opinion in microbiology* **39**:106-112.

Thombre R, Jangid K, Shukla R, Dutta NK (2019) Alternative therapeutics against antimicrobial-resistant pathogens. Frontiers in microbiology. Sep 19;10:2173.

Tong Y and Song F (2015) Intracellular calcium signaling regulates autophagy via calcineurin-mediated TFEB dephosphorylation. *Autophagy* **11**:1192-1195.

Torraca V, Bielecka MK, Gomes MC, Brokatzky D, Busch-Nentwich EM and Mostowy S (2023) Zebrafish null mutants of Sept6 and Sept15 are viable but more susceptible to Shigella flexneri infection. *Cytoskeleton*.

Vakifahmetoglu-Norberg H, Xia H-g and Yuan J (2015) Pharmacologic agents targeting autophagy. *The Journal of clinical investigation* **125**:5-13.

Vashisht R and Brahmachari SK (2015) Metformin as a potential combination therapy with existing front-line antibiotics for tuberculosis. *Journal of translational medicine* **13**:1-3.

Visvikis O, Ihuegbu N, Labed SA, Luhachack LG, Alves A-MF, Wollenberg AC, Stuart LM, Stormo GD and Irazoqui JE (2014) Innate host defense requires TFEB-mediated transcription of cytoprotective and antimicrobial genes. *Immunity* **40**:896-909.

Wandel MP, Pathe C, Werner EI, Ellison CJ, Boyle KB, von der Malsburg A, Rohde J and Randow F (2017) GBPs inhibit motility of *Shigella flexneri* but are targeted for degradation by the bacterial ubiquitin ligase IpaH9. 8. *Cell host & microbe* **22**:507-518. e505.

Wassef JS, Keren DF and Mailloux JL (1989) Role of M cells in initial antigen uptake and in ulcer formation in the rabbit intestinal loop model of shigellosis. *Infection and immunity* **57**:858-863.

Welch MD and Way M (2013) Arp2/3-mediated actin-based motility: a tail of pathogen abuse. *Cell host & microbe* **14**:242-255.

Williams PC and Berkley JA (2018) Guidelines for the treatment of dysentery (shigellosis): a systematic review of the evidence. *Paediatrics and international child health* **38**:S50-S65.

Wu X, Ren Y, Wen Y, Lu S, Li H, Yu H, Li W and Zou F (2022) Deacetylation of ZKSCAN3 by SIRT1 induces autophagy and protects SN4741 cells against MPP+-induced oxidative stress. *Free Radical Biology and Medicine* **181**:82-97.

Yang J-Y, Lee S-N, Chang S-Y, Ko H-J, Ryu S and Kweon M-N (2014) A mouse model of shigellosis by intraperitoneal infection. *The Journal of infectious diseases* **209**:203-215.

Yang L, Hamilton SR, Sood A, Kuwai T, Ellis L, Sanguino A, Lopez-Berestein G and Boyd DD (2008) The previously undescribed ZKSCAN3 (ZNF306) is a novel "driver" of colorectal cancer progression. *Cancer research* **68**:4321-4330.

Yang Y, Guo W, Ma J, Xu P, Zhang W, Guo S, Liu L, Ma J, Shi Q and Jian Z (2018) Downregulated TRPV1 expression contributes to melanoma growth via the calcineurin-ATF3-p53 pathway. *Journal of Investigative Dermatology* **138**:2205-2215.

Young C, Walzl G and Du Plessis N (2020) Therapeutic host-directed strategies to improve outcome in tuberculosis. *Mucosal immunology* **13**:190-204.

Zhang C, Maruggi G, Shan H, Li J (2019) Advances in mRNA vaccines for infectious diseases. Frontiers in immunology **10**:594.

Zhang W, Li X, Wang S, Chen Y, Liu H (2020) Regulation of TFEB activity and its potential as a therapeutic target against kidney diseases. Cell death discovery **6**(1):32.

Zheng G, Zhan Y, Li X, Pan Z, Zheng F, Zhang Z, Zhou Y, Wu Y, Wang X and Gao W (2018) TFEB, a potential therapeutic target for osteoarthritis via autophagy regulation. *Cell Death & Disease* **9**:858.

SECTION 9

ABBREVIATIONS

- µg - Microgram
- µl – Microlitre
- Caps-Capsaicin
- 8-OHdG - 8-Hydroxy-2'-Deoxyguanosine
- ANOVA – One way analysis of variance
- Bax - Bcl-2-associated X protein
- BAPTA-AM - 1,2- bis(o-Aminophenoxy) ethane-N, N, N', N'-tetraacetic Acid Tetra(acetoxymethyl) Ester
- CAT – Catalase
- CFU – Colony forming Unit
- CLSI – Clinical and Laboratory Standards Institute
- DAPI – 4',6-diamidino-2'-phenylindole
- DCFDA - 2,7-Dichlorofluorescin diacetate
- DMSO – Dimethyl sulfoxide
- DNA – Deoxyribonucleic Acid
- DTNB - 5,5'-Dithiobis-2- nitrobenzoic acid
- ELISA- Enzyme linked immunosorbant assay
- FICI – Fractional Inhibitory Concentration Index
- GAPDH - Glyceraldehyde-3-Phosphate Dehydrogenase
- H_2O_2 - Hydrogen peroxide
- HRP - Horseradish peroxidase
- h - Hour
- HCl - Hydrochloric acid
- IHC - Immunohistochemistry
- IL-1β - Interleukin-1β
- IL-6 - Interleukin-6
- l – Litre
- LDH – Lactate Dehydrogenase
- MIC – Minimum Inhibitory Concentration

- min - Minutes

- ml – Milli litre
- mM – Millimolar
- MOI – Multiplicity of infection
- mRNA- Messenger Ribonucleic Acid
- $Na^+ K^+$ ATPase – Sodium Potassium ATPase
- NADPH- Nicotinamide adenine dinucleotide phosphate
- NaOH – Sodium hydroxide
- ng - Nanogram
- nm – Nano metre
- NO - Nitric oxide
- PAGE – Polyacrylamide gel electrophoresis
- PBS – Phosphate buffered saline
- PMSF – Phenyl methane sulfonyl fluoride
- RIPA – Radioimmune precipitation assay
- p53 – Tumour protein p53
- RNA- Ribonucleic Acid
- ROS – Reactive Oxygen Species
- RPM- Rotations Per Minute
- RT-PCR – Reverse transcriptase Polymerase chain reaction
- SDS – Sodium dodecyl sulfate
- S.E.M. – Standard error of mean
- TEM – Transmission electron microscopy
- TNF-α – Tumor necrosis factor alpha
- WHO- World Health Organization

SECTION 10

PUBLICATIONS AND CONFERENCES

JOURNAL ARTICLES PUBLISHED

- **Basak, P.,** Maitra, P., Khan, U., Saha, K., Bhattacharya, S. S., Dutta, M., & Bhattacharya, S. (2022). Capsaicin Inhibits *Shigella flexneri* Intracellular Growth by Inducing Autophagy. **Frontiers in pharmacology**, 13.

- Maitra, P., **Basak, P.,** Okamoto, K., Miyoshi, S. I., Dutta, S., & Bhattacharya, S. (2023). Asiatic acid inhibits intracellular *Shigella flexneri* growth by inducing antimicrobial peptide gene expression. ***Journal of Applied Microbiology***, *134*(2), lxac076

- Khan, U., Karmakar, B. C., **Basak, P.,** Paul, S., Gope, A., Sarkar, D., ... & Bhattacharya, S. (2023). Glycyrrhizin, an inhibitor of HMGB1 induces autolysosomal degradation function and inhibits *Helicobacter pylori* infection. **Molecular Medicine**, 29(1), 1-15.

- Das, S., Priyadarshani, N., **Basak, P.,** Maitra, P., Bhattacharya, S., & Bhattacharya, S. S. (2023). Capsaicin derived from endemic chili landraces combats Shigella flexneri pathogen: Insights on intracellular inhibition mechanism. **Microbial Pathogenesis**, 106210.

CONFERENCES ATTENDED

- Poster presented in Seminar on "Trends in Modern Biology: Techniques and Applications" 2019 at Visva-Bharati University, India. Title: Therapeutic intervention of *Shigella flexneri* host pathogen interaction by a small molecule compound". **Basak, P.,** Khan U., Bhattacharya SS., Bhattacharya S., 2019

frontiers | Frontiers in Pharmacology

ORIGINAL RESEARCH
published: 06 July 2022
doi: 10.3389/fphar.2022.903438

Capsaicin Inhibits *Shigella flexneri* Intracellular Growth by Inducing Autophagy

Priyanka Basak[1], *Priyanka Maitra*[1], *Uzma Khan*[1], *Kalyani Saha*[1], *Satya Sundar Bhattacharya*[2], *Moumita Dutta*[3] *and Sushmita Bhattacharya*[1]*

[1]Division of Biochemistry, National Institute of Cholera and Enteric Diseases, Kolkata, India, [2]Department of Environmental Science, Tezpur University, Tezpur, India, [3]Division of Electron Microscopy, National Institute of Cholera and Enteric Diseases, Kolkata, India

Antibiotic treatment plays an essential role in preventing *Shigella* infection. However, incidences of global rise in antibiotic resistance create a major challenge to treat bacterial infection. In this context, there is an urgent need for newer approaches to reduce *S. flexneri* burden. This study largely focuses on the role of the herbal compound capsaicin (Caps) in inhibiting *S. flexneri* growth and evaluating the molecular mechanism behind bacterial clearance. Here, we show for the first time that Caps inhibits intracellular *S. flexneri* growth by inducing autophagy. Activation of autophagy by Caps is mediated through transcription factor TFEB, a master regulator of autophagosome biogenesis. Caps induced the nuclear localization of TFEB. Activation of TFEB further induces the gene transcription of autophagosomal genes. Our findings revealed that the inhibition of autophagy by silencing TFEB and Atg5 induces bacterial growth. Hence, Caps-induced autophagy is one of the key factors responsible for bacterial clearance. Moreover, Caps restricted the intracellular proliferation of *S. flexneri*-resistant strain. The efficacy of Caps in reducing *S. flexneri* growth was confirmed by an animal model. This study showed for the first time that *S. flexneri* infection can be inhibited by inducing autophagy. Overall observations suggest that Caps activates TFEB to induce autophagy and thereby combat *S. flexneri* infection.

Keywords: *Shigella flexneri*, autophagy, TFEB, capsaicin, gene transcription

OPEN ACCESS

Edited by:
Dongsheng Zhou,
Beijing Institute of Microbiology and Epidemiology, China

Reviewed by:
Sue Twine,
National Research Council Canada (NRC-CNRC), Canada
Mingkai Li,
Fourth Military Medical University, China

***Correspondence:**
Sushmita Bhattacharya
durgasushmita@gmail.com

Specialty section:
This article was submitted to Pharmacology of Infectious Diseases, a section of the journal Frontiers in Pharmacology

Received: *24 March 2022*
Accepted: *16 May 2022*
Published: *06 July 2022*

Citation:
Basak P, Maitra P, Khan U, Saha K, Bhattacharya SS, Dutta M and Bhattacharya S (2022) Capsaicin Inhibits Shigella flexneri Intracellular Growth by Inducing Autophagy. Front. Pharmacol. 13:903438. doi: 10.3389/fphar.2022.903438

1 INTRODUCTION

Shigella flexneri, a common gastrointestinal pathogen, causes bacillary dysentery that affects millions every year worldwide (Nandy et al., 2011; Taneja and Mewara, 2016; Williams and Berkley, 2018; McQuade et al., 2020). According to the available information, *S. flexneri* infection is highly predominant in developing nations. Children below 5 years of age are affected with severe morbidity and mortality (Chang et al., 2016; Baker and The, 2018; Khalil et al., 2018; Chanin et al., 2019; Chen et al., 2020). The pathogen invades the intestinal epithelial and immune cells, causing ulcerative lesions in the gut under severe conditions (Killackey et al., 2016). To date, the only treatment option is antibiotics as no licensed vaccine has been developed (Hosangadi et al., 2019). Recently, the reverse vaccinology approach has been considered to improve vaccine research against *Shigella* (Hajialibeigi et al., 2021). Excessive use of antibiotics has led to a significant rise in antibiotic-resistant bacteria (Puzari et al., 2018; Ranjbar and Farahani, 2019). Hence, in the current scenario, there is an imperative need to search for alternative approaches in treating *S. flexneri* infection.

Presently, host-directed therapy is considered as an alternative therapeutic approach for the eradication of invasive pathogens (Rubinsztein et al., 2012; Kaufmann et al., 2018). Host-directed therapeutics can target the disease-causing signaling pathways and help eradicate microbes (Noad et al., 2017; Young et al., 2020). Autophagy plays a significant role among different host response mechanisms in combating infectious pathogens. Autophagy is a self-degradation mechanism used to eliminate unwanted materials like pathogens from the cell. Exploitation of autophagy has emerged as a new approach toward intracellular pathogens like *Mycobacterium tuberculosis* and *Salmonella typhimurium* (Kim et al., 2012; Ammanathan et al., 2020). In the context of infectious diseases, autophagy inducers such as vitamin D and antibiotics isoniazid and bedaquiline are reported to inhibit the proliferation of *Mycobacterium tuberculosis* and *H. pylori* (Yuk et al., 2009; Hu et al., 2019; Kim et al., 2019; Giraud-Gatineau et al., 2020). Similar strategies have also been used against viruses like HIV (Jo et al., 2013; Sharma et al., 2018). However, there are no such interventions reported against *S. flexneri*.

As autophagy is an important host defense mechanism occurring within the cell to clear pathogens, *S. flexneri* has evolved multiple ways to prevent autophagic recognition (Ogawa et al., 2005; Ra et al., 2016). *S. flexneri* circumvents autophagic degradation by releasing effector proteins (icsB and virA) and establishes itself in the intracellular niche of the colonic environment. Moreover, it has been reported earlier that Atg4b mutant cells inhibited *S. flexneri* associated maturation of autophagy (Ogawa et al., 2005; Weddle and Agaisse, 2018). Additionally, septin cages are known to promote autophagy; however, *Shigella* can polymerize actin and avoid septin caging (Krokowski et al., 2018; Lobato-Márquez et al., 2019). Hence, *S. flexneri* has developed an intricate machinery to avoid autophagy and establish infection within the host. As drug resistance is a major problem to tackle *S. flexneri,* thus boosting autophagy can curb intracellular *S. flexneri* infection.

Autophagy induction occurs by inducing several signaling molecules like mTOR, Akt, and AMPK (Floto et al., 2007; Rubinsztein et al., 2012; Young et al., 2020). Recent studies have shown the importance of a transcription factor known as TFEB (Ammanathan et al., 2020). TFEB activation leads to upregulation of autophagy genes. Boosting gene transcription induces host defense machinery and helps in the eradication of pathogens. Therefore, we searched for potent inducers of autophagy.

Capsaicin, a dietary compound from chilli plants, is reported to have anticancer properties (Lin S. R. et al., 2017). Emerging evidences have pointed out that capsaicin also possess antimicrobial activities against gastrointestinal pathogens (Füchtbauer et al., 2021). However, to date, there are no reports of its antibacterial action against *Shigella flexneri*.

Herein, we exploited the mechanism of autophagy induced by capsaicin to inhibit bacterial growth. This study showed for the first time that Caps induced an autophagy-dependent clearance of intracellular *S. flexneri*. Our findings indicate that Caps is a potential autophagy inducer that helps reduce *S. flexneri* infection.

2 MATERIALS AND METHODS

2.1 Bacterial Culture Conditions

Shigella flexneri (sf2457T) serotype 2a, plasmid-cured *Shigella flexneri* (sf2457T)2a, and *Shigella flexneri*-resistant strain (NA/CIP/NOR/OFX/TET/S/C/AM/E/ST) (BCH12702) were obtained from Dr Asish Mukherjee and Dr. Hemanta Koley (NICED, Kolkata, India). Bacteria were routinely cultured in Mueller Hinton Broth (Himedia) at 37°C incubator with a shaker.

2.2 Cell Culture Conditions

HT-29 (ATCC HTB-38) and murine macrophage RAW264.7 (ATCC TIB-71) cells were used during this study. HT-29 cells were cultured with a McCoy's 5A medium (Sigma-Aldrich) containing 10% heat inactivated FBS (Sigma-Aldrich, United States), 1% non-essential amino acids, and 1% penicillin–streptomycin (Himedia, India). Graphs represent CFU/ml of intracellular *S. flexneri*. RAW264.7 cells were grown in RPMI1640 with 10% FBS and 1% penstrep. Experiments were conducted in cells with maximum three to five passages. Cells were maintained in a 37 °C humidified incubator with 5% CO_2.

2.3 Plasmids

The eGFP-LC3 plasmid was a gift from Prof. Parimal Karmakar (Department of Biotechnology, Jadavpur University, India). pEGFP-N1-TFEB plasmid was a gift from Dr. Ravi Manjithaya, Autophagy lab, JNCASR, Bangalore. Control EGFP plasmid was a kind gift from Dr Santa Sabuj Das, ICMR, NICED, Kolkata. The plasmids were transformed in DH5α and purified by the mini-prep plasmid isolation kit (Promega). The plasmid DNA was suspended in nuclease free water and stored at −20°C.

2.4 MTT Assay

Cells were seeded in 96-well plates (1×10^4 cells/ml). At this seeding density, cells were treated with varying concentrations of Caps (16 μM, 32 μM) keeping an uninfected DMSO control and incubated for 24 h. Cell viability was checked using a Colorimetric Cell Viability Kit IV (MTT) (Promokine) followed by the addition of 20 μl of MTT reagent and incubated for 4 h at 37°C in a CO_2 incubator. Thereafter, 300 μl of DMSO was added to solubilize the purple crystal formazan, OD was measured at 570 nm, and % viability was calculated and graphically represented.

2.5 GFP-LC3B Fluorescence Assay and anti-*Shigella* Immunofluorescence

GFP-LC3 (2 ug/well) plasmid was transfected in HT 29 and Raw264.7 cells using lipofectamine 2000 reagent (Invitrogen. United States). At 85% confluency, cells were transfected with [plasmid (ug): lipofectamine (ul) = 1:3] following the manufacturer's protocol. After transfection for 48 h, cells were pre-treated with caps (16 μM) followed by *S. flexneri* infection. For *Shigella* immunofluorescence, GFP-LC3B-transfected cells were infected with *S. flexneri*. 400 μl of *S. flexneri* from an

overnight culture of O.D (0.5–0.6) was added in intestinal cells and macrophages. Cells were further subjected to immunofluorescence. Briefly, fixed cells were incubated with anti-Shigella antibody (1:250) (ab65282) dilution. Subsequently, TRITC-conjugated anti rabbit secondary antibody (1:2000) (Cat# AP132R) was used. Finally, coverslips were mounted on a ProLong™ Gold Antifade reagent containing DAPI (ThermoFisher) and observed under an inverted confocal microscope (Carl Zeiss LSM 710). GFP-positive cells per sample were selected for observation.

2.6 siRNA Transfection

The following siRNAs were purchased from IDT and used for the knockdown of those particular genes: ATG5 siRNA (Design ID hs. Ri. ATG5.13.1) and TFEB siRNA (Design ID hs. Ri. TFEB.13.1). HT-29 cells at 60%–70% confluency were transfected with 12 pmol of siRNA/Scrambled siRNA, and 2 ul of lipofectamine was added per well in a 6-well plate. Forty-eight hours after transfection, the infection assay was performed in cells infected with *S. flexneri* with and without Caps pre-treatment. Cells were lysed for CFU/ml counting.

2.7 Immunofluorescence Microscopy

For fluorescence microscopy, cells were grown on coverslips and Caps treatment was done for 2 h. After fixation with 4% formaldehyde, cells were further blocked in PBS containing 3% BSA and 0.1% Triton X100 for 1 h at room temperature. Overnight incubation was performed with anti-TFEB antibody (1:250 dilution). Following that, fixed cells were kept in a blocking buffer containing TRITC-conjugated anti-rabbit secondary antibody (1:2000) (Cat# AP132R). Finally, the coverslips mounting upon glass slides were done by adding a drop of ProLong™ Gold Antifade reagent containing DAPI (ThermoFisher). Images were scanned on a Zeiss LSM 710 confocal system (Carl Zeiss).

2.8 Infection Assay

Intestinal and macrophage cells ($1X10^5$) were cultured in 6-well plates for 24 h at 37 °C and 5% CO_2 prior to infection. Cells were further incubated overnight in antibiotic free media. *S. flexneri 2457t* colonies (red) were picked from Congo red plates as Congo red indicates the retention of virulence plasmid. *S. flexneri* was grown overnight in MHB at 37°C with shaking and sub-cultured to an OD_{600} of 0.5–0.6. Bacteria pellets were collected by centrifuging the culture at 12,000 g for 5 min at 4°C and further washed with PBS. Pellets were then re-suspended in incomplete tissue culture media. Intestinal cells were pre-treated with Caps (1.6, 3.2, 4.8, 6.4, 8, 16, 32 μM, or vehicle control (DMSO), for 2, 4, 6, 8, 12, and 24 h in incomplete media. Then, infection with *S. flexneri* was performed at an MOI of 200: 1. The infected plates were centrifuged for 15 min at 700 g for synchronization and incubated for 2 h to allow bacteria to enter the cells. Cells were thoroughly washed and treated with 50 μg/ml of gentamicin for 2 h, killing the extracellular bacteria. Further washing with PBS was done, and then cells were lysed using 0.1% triton X. The cell lysates were plated in MHA at 37°C for 18 h to count the number of colonies (CFU/ml). For post-treatment analysis, cells were infected with bacteria and then exposed to Caps for different time points. After incubation and infection, gentamicin was used to kill the extracellular bacteria, and further lysis was done and plated. This assay was also performed using *S. flexneri* highly resistant strain (BCH12702) with or without Caps 12 h post-treatment to compare invasion. Results were compared to 3-methyladenine (#SAE0107, sigma)-treated cells. For infection in macrophages, cells were preincubated with Caps for 2 h followed by 30 min of *S. flexneri* infection (MOI100). After infection, gentamicin was used for killing the extracellular bacteria and further lysis was done and plated. For post-infection analysis, cells were infected with *S flexneri* (MOI100) for 30 min followed by Caps treatment for 4 h. After that, gentamicin was used to kill the extracellular bacteria, and further lysis was performed and plated.

siATG5, siTFEB-transfected cells were pre-treated with Caps and infected for gentamicin survival assay to count CFU/ml compared to scrambled siRNA. TFEB overexpression was also performed by lipofectamine 2000 using pEGFP-N1-TFEB plasmid and empty vector (pcDNA3-EGFP).

2.9 Real-Time PCR

RNA isolation was performed using the RNA isolation kit (zymo research) from treated and untreated cells. TRIzol reagent was used for colon samples collected from mice. RNA samples were converted to c-DNAs using the Thermo Scientific c-DNAs synthesis kit. Real-Time PCR was done using SYBR green kit of Applied Biosystems. The expression patterns were analyzed using the $^{\Delta\Delta}$Ct method and normalized using the internal control GAPDH. $^{\Delta\Delta}$Ct were calculated by the following formula:

$$^{\Delta\Delta}\text{Ct} = \text{test} - \text{internal control} - \text{test control}$$

Human primer sequences used were listed as follows:

Gene	Forward primer	Reverse primer
GAPDH (human)	5′-GTCTTCACCACC ATGGAGAAGGC-3′	5′-CATGCCAGTGA GCTTCCCGTTCA-3′
MAP1LC3B (human)	5′-ACCATGCC GTCGGAGAAG-3′	5′-GGTTGGATGC TGCTCTCGAA-3′
ATG5 (human)	5′-GCAAGCCAGAC AGGAAAAAG-3′	5′-GACCTTCAGTG GTCCGGTAA-3′
GAPDH (mouse)	5′-GATCTTCGACAA GGGAGCTAAA-3′	5′- TCGCATTCTTCT ACACGATAACA-3′
MAP1LC3B (mouse)	5-GTCCTGGACAAG ACCAAGTTCC-3′	5′-CCATTCACCAGG AGGAAGAAGG-3′

Differential expression of genes involved in autophagy pathway was analyzed using a human autophagy PCR array. This array contained 84 key genes in a 96-well plate format. Fold change was plotted in a column graph to observe the differences among uninfected, infected, and infected with Caps. PCR array (#PAHS-084Z) (RT^2 Profiler™ PCR Array Human Autophagy) was performed to understand the complete autophagy profile of the control and treated samples following the manufacturer's instructions (Qiagen). RNA isolation was performed from two

groups of cells. cDNA was obtained using cDNA synthesis reagents and mixed with SYBR Green Mastermix (provided inside the kit). Quantitative real-time PCR was done in Applied biosystems StepOnePlus system. Obtained melt curves and $^{\Delta\Delta}$Ct values were analyzed in free web-based RT^2 Profiler™ PCR array data analysis software.

2.10 Western blot analysis

Untreated, treated, and infected cell lysates were prepared in RIPA (radioimmunoprecipitation assay buffer) lysis buffer (10 mM Tris–HCl, pH 8.0, 1 mM EDTA, 0.5 mM EGTA, 1% Triton X-100, 0.1% sodium deoxycholate, 0.1% SDS, 140 mM NaCl, 1 mM PMSF) (protease and phosphatase inhibitor added). Lysates were centrifuged at 7,000 rpm for 20 min at 4°C. Nuclear and cytosolic extracts were prepared by using NE-PER™ Nuclear and Cytoplasmic Extraction Reagents of Thermo Scientific (Cat#78833) following the manufacturer's instructions.

After protein estimation, lysates were boiled in SDS-PAGE sample buffer and run on 10% or 12.5% SDS- PAGE gel at 120 V. Gels were transferred to PVDF membrane. Blocking was performed with 5% skimmed milk dissolved in TBST (20 mM Tris–HCl, 150 mM NaCl, 0.1% Tween20) buffer for 1 h at room temperature, and the membranes were incubated overnight with primary antibodies at 4 °C. The primary antibodies utilized are rabbit monoclonal anti-GAPDH antibody (Cat#D16H11) (1:2,000), rabbit polyclonal Anti-SQSTM1/P62 antibody (Cat# ab91526) (1:1,000), rabbit monoclonal anti-ATG5 (Cat #ab228668) (1:1,000), rabbit monoclonal anti-beclin1 antibody (Cat #ab207612) (1: 1,000), rabbit polyclonal anti-LC3B antibody (Cat #ab51520) (1:1,000), and rabbit monoclonal anti-TFEB antibody (Cat #D2070). Following primary antibody treatment, membranes were kept in a shaker at room temperature for 2 h with horseradish peroxidase (HRP) conjugated goat anti-rabbit secondary antibody (dilution 1: 10,000) or goat anti-mouse secondary antibody (dilution 1: 10,000). Membranes were finally washed with TBST for 30 min. Bands were observed in the ChemiDoc MP Imaging System (Biorad) using Millipore immobilon western chemiluminescent HRP substrate (luminol and hydrogen peroxide) as a substrate.

2.11 Broth Dilution Assay

A broth dilution assay was performed in the presence of DMSO as a control, 16, 32, 64, and 80 μM Caps, and nalidixic acid (10 μg/ml) as a positive control in separate flasks containing MHB. A total of 10^5 *S. flexneri* from overnight culture was added to the flasks. $O.D._{600nm}$ was measured at regular intervals and graphically represented.

2.12 Determination of the Minimum Inhibitory Concentration

Shigella flexneri (BCH12702) was treated with antibiotics (NA/CIP/NOR/OFX/TET/S/C/AM/E/ST) at different concentrations. The minimum inhibitory concentrations of the antibiotics were determined by the CLSI broth microdilution method. The test was performed by serially diluting the antibiotics in LB media and incubating for 24 h in a 37°C incubator. The minimum inhibitory concentration (MIC) represents the lowest concentration of the antibiotics that resulted in a lack of visible bacterial growth. Tabular representation shows the MIC (μg/ml) and cutoff values for resistance according to CLSI guidelines.

2.13 Electron Microscopy

Uninfected and infected cells (HT-29 and RAW264.7) treated with or without Caps were fixed in 3% glutaraldehyde in 0.1 M sodium cacodylate buffer. Further fixation with 1% osmium tetroxide continued, and then dehydrated with increasing grades of acetone, eventually embedded in Agar 100 resin, and polymerized at 60 °C. Ultrathin sections (around 40–50 nm thickness) were made using a Leica Ultracut UCT ultramicrotome (Leica Microsystems, Germany), picked up on nickel grids, and dual-stained with 2% aqueous uranyl acetate and 0.2% lead citrate. We examined cell sections using an FEI Tecnai 12 Biotwin transmission electron microscope (FEI, Hillsboro, OR, United States) at an accelerating voltage of 100 kV. Percentage autophagosome formation was calculated: Cell number containing autophagosome/total cell number x 100% Autophagic bodies were outlined with the help of Adobe Photoshop.

2.14 Chromatin Immunoprecipitation Assay

HT-29 cells were treated with Caps for 4 h. After incubation, crosslinking was done in 1% formaldehyde and processed according to the protocol of the CHIP assay kit (#7-295; Merck Millipore). Briefly, cells were lysed in SDS lysis buffer and pelleted. After processing, chromatin was immunoprecipitated with anti-TFEB antibodies (5 μg/sample). The chromatin fraction, which lacks a primary antibody, was taken as "input." Real-time PCR was performed using the following chip primer assemblies. Primers were designed for amplifying CLEAR elements in the promoter region of TFEB using primer: MAP1LC3B-forward; 5′-GAAGGCTCGGGACAA AAGCAG-3′, reverse; 5′-GTGGGTGGCTTCCGGGGAG-3'. The PCR cycle was conducted in accordance with the manufacturer's instructions. The data were graphically represented as the % of input.

2.15 Transcription Factor Assay

The TFEB transcription factor assay was performed using the RayBio® Human TFEB TF-Activity Assay Kit Protocol. Nuclear extract collected from control and Caps-treated cells were used as samples. Samples were added to wells coated with oligonucleotides containing CLEAR sequence. After the addition of primary antibody, HRP-conjugated secondary antibody was added. This step was followed by the addition of the TMB substrate reagent, the reaction was stopped with stop solution, and O.D. was collected at 450 nm by a spectrophotometer. The fold change was calculated and graphically represented.

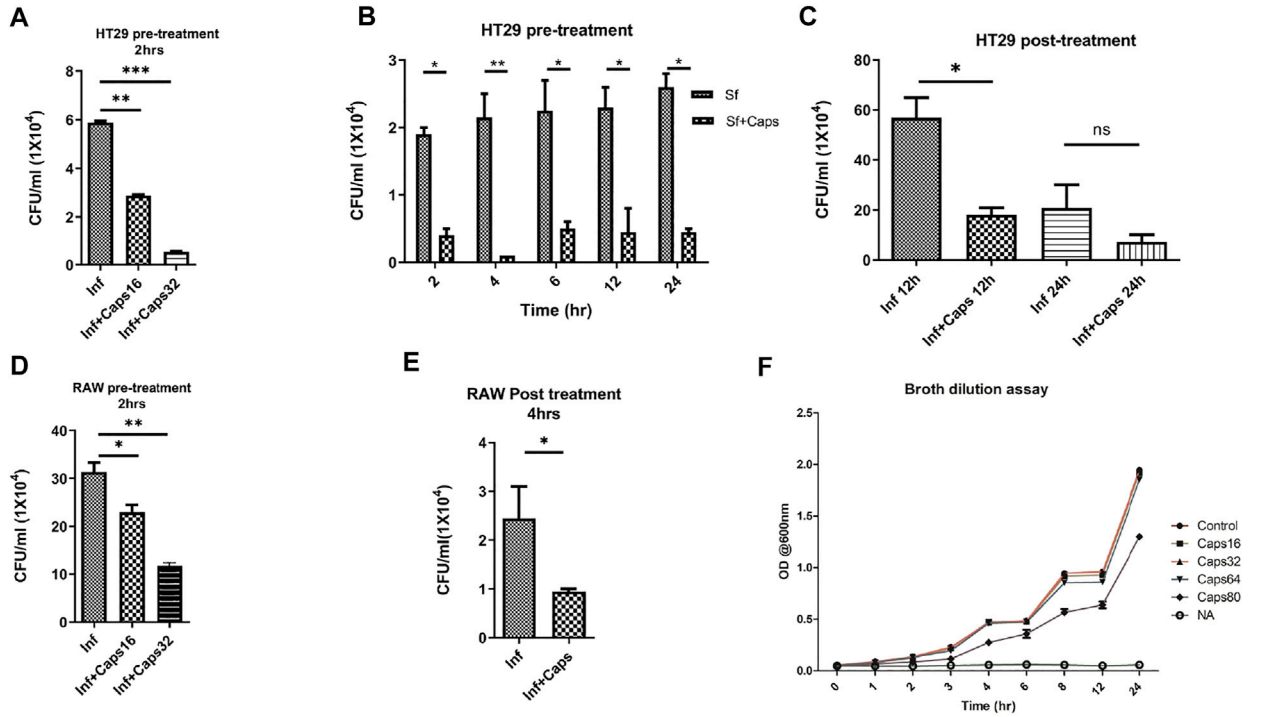

FIGURE 1 | Intracellular *S. flexneri* growth was inhibited by capsaicin (Caps) in both intestinal and macrophage cells. **(A)** Infection assay was performed in HT29 cells with different concentrations of capsaicin (Caps). Briefly, cells were pre-treated (16 μM, 32 μM) with Caps for 2 h followed by *S. flexneri* infection (MOI 200) for 2 h. Finally, gentamicin treatment was done to kill extracellular bacteria. Cells were lysed and plated overnight for counting the number of colonies (CFU/ml). Graphs represent CFU/ml of intracellular *S. flexneri*. One-way ANOVA was performed. **(B)** Caps pre-treatment (16 μM) for 2 h followed by *S. flexneri* (MOI 200) infection at different time points (2, 4, 6, 8, 12, 24 h) was done. Two-way ANOVA was performed. **(C)** HT29 cells were infected with MOI200 followed by post-treatment with Caps (16 μM) for 12 and 24 h. One-way ANOVA was performed. Cells were lysed and plated to count the number of colonies. **(D)** RAW 264.7 cells were infected with *S. flexneri* MOI 100 for 30 min after 2 h Caps pre-treatment. Cells were lysed and plated to count the number of colonies One-way ANOVA was performed. **(E)** RAW264.7 cells were infected with *S. flexneri* MOI 100, followed by post-treatment with Caps (16 μM) for 4 h. Graph represents CFU/ml of intracellular *S. flexneri*. One-way ANOVA was performed. **(F)** A broth dilution assay was performed in the presence of DMSO control, 16, 32, 64, and 80 μM Caps and nalidixic acid (10 μg/ml) (NA) followed by the addition of 10^5 *S. flexneri* overnight culture. The OD at 600 nm was measured at regular intervals. Graphs were represented using GraphPad Prism 5 as mean ± SEM (n = 3); Significance was calculated; $^*p < 0.05$, $^{**}p < 0.01$, $^{***}p < 0.001$.

2.16 *In Vivo* Experimental Design

2.16.1 Animals

Male BALB/c (8 weeks) mice weighing 20–22 g mice were used for *S. flexneri* infection. Animals were adjusted under standard laboratory conditions. Mice were provided with a standard diet and water ad libitum. IAEC (Institutional Animal Ethical Committee), NICED, Kolkata (PRO/157/-July 2022) guidelines were followed during all the experiments. Animals were maintained in the animal house with 75% humidity, and specific pathogen-free healthy individuals were selected.

After fasting for 6 h, mice were injected with pathogenic *Shigella flexneri* (sf2457T) intraperitoneally (Yang et al., 2014). After 2 h, Caps treatment was performed. In the experimental design, four groups (n = 4) were created accordingly: Group 1. Control: Only DMSO was used as the vehicle. Group 2. Infected: Received *S. flexneri* suspension (0.5×10^9 CFU/ml) in PBS. Group 3. Infected + Caps: Received *S. flexneri* suspension followed by Caps (20 mg kg−1 body weight) treatment for 2 h. Group 4. Caps: Received Caps (20 mg kg−1 body weight). Each group was kept in an individual cage. Experiments were repeated in triplicate (n = 3). The total number of mice in each group was 12.

2.16.2 Collection of Colon

After 2 h of Caps treatment, all the animals were sacrificed. Colon from drug-treated, untreated, infected, and control mice was aseptically removed. The crushed colon was plated for bacterial colony count. The tissues were kept at −80 °C until further experiments were performed.

2.16.3 Preparation of Colon Tissue Homogenate

Colon samples were collected following dissection, washed in PBS buffer, and further homogenized in an ice-cold RIPA lysis buffer for western blot and in TRIzol reagent (RNAiso Plus, TaKaRa) for RNA isolation. The homogenates were centrifuged at 12,000 rpm at 4 °C for 10 min. The supernatants collected were further utilized for experiments. RNA was isolated, and RNA to cDNA conversion was performed using a Verso cDNA Synthesis Kit (Thermo Scientific) followed by qRT PCR.

2.17 Statistical Analysis

Test information is presented as mean ± S.E.M. Statistical analyses were performed, and bar graphs were processed in GraphPad Prism 5 after the data processing in Microsoft Excel. For comparison

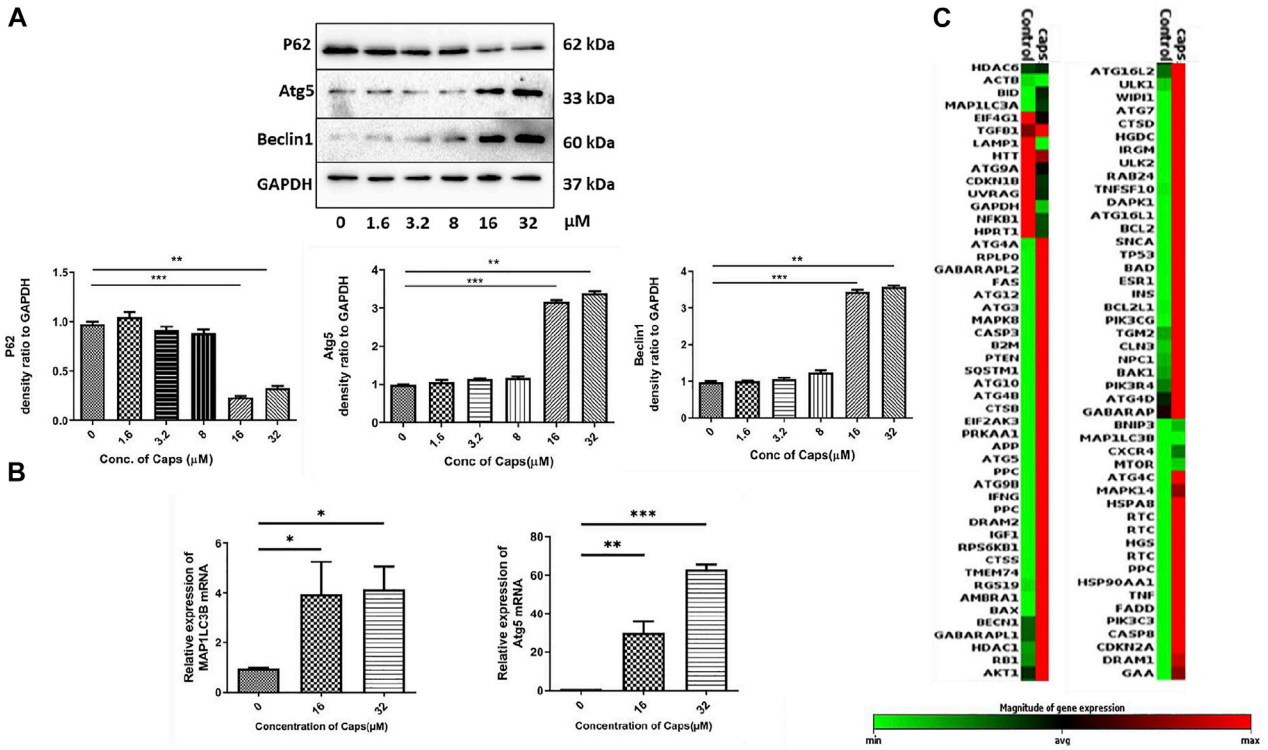

FIGURE 2 | Capsaicin (Caps) induces autophagy in intestinal cells. **(A)** HT29 cells were treated with Caps (1.6, 3.2, 8, 16, 32 μM) or DMSO for 2 h. Expression of major autophagy-associated marker proteins P62, Atg5, and Beclin1 was observed in western blot. GAPDH was used as a loading control. Densitometric analyses are graphically represented. **(B)** HT29 cells were treated with Caps (16, 32 μM) or DMSO for 2 h followed by qRT-PCR, Expression of the autophagy-associated marker genes (Map1LC3B, Atg5) was quantified using GAPDH as a housekeeping gene. One-way ANOVA was performed. **(C)** PCR array was performed with control and only Caps-treated samples. Caps treatment was done for 4 h. Heat map generated represents differential gene expression. All experiments were performed in triplicate. Graphs were generated using GraphPad Prism 5 were represented as mean ± SEM (n = 3); significance was calculated; $^{*}p < 0.05$, $^{**}p < 0.01$, $^{***}p < 0.001$.

between two groups, an unpaired *t*-test was performed, and for multiple comparison, one-way ANOVA is performed. For multiple variants, two-way ANOVA was performed. Significance level has been marked as * for $p < 0.05$, which implies significant, ** for $p < 0.01$, which implies very significant, and *** for $p < 0.001$, which implies highly significant.

3 RESULTS

3.1 Caps Inhibits Intracellular *S. flexneri* Growth

The antibacterial effects of capsaicin (Caps) are reported against *Vibrio cholerae*, *H. pylori* and other bacteria (Füchtbauer et al., 2021). However, there are no such reports of capsaicin-induced inhibition of intracellular *S. flexneri* growth. Here, we tested the effect of Caps on the intracellular clearance of *S. flexneri*. For this approach, we used an intracellular invasion assay in an *S. flexneri* infection model. Briefly, Caps was added in HT-29 cells for 2 h followed by *S. flexneri* infection to check intracellular bacterial clearance. Caps at different doses (16 and 32 μM) significantly reduced *S. flexneri* replication (**Figure 1A**). In addition, Caps significantly (16 μM) reduced *S. flexneri* multiplication after pre-treatment at different time points (2, 4, 6, 12, and 24 h) in HT-29 cells (**Figure 1B**). Moreover, we checked the effect of Caps by posttreatment analysis. *S. flexneri* growth was inhibited significantly at 12 h by Caps. However, at 24 h, cell death occurred in infected cells; hence, data are not significant (**Figure 1C**).

Similarly, we validated the results in macrophages, as macrophages are the immune cells and site of infection for *S. flexneri* during pathogenesis. Caps pre-treatment for 2 h significantly reduced bacterial growth in a dose-dependent manner (**Figure 1D**). Moreover, posttreatment analysis in macrophages showed that Caps is effective at 4 h in inhibiting *S. flexneri* growth (**Figure 1E**). Upon compound addition, bacterial growth was significantly reduced. However, the inhibition of bacterial burden could be due to a probable antibacterial property of Caps. Hence, we checked the effect of Caps on *S. flexneri* by the broth dilution method for extracellular bactericidal properties. There is no apparent change in bacterial growth for treated (Caps 16, 32, 64, and 80 μM) and untreated samples (**Figure 1F**). Collectively, the data revealed that exposure to Caps inhibits intracellular *S. flexneri* proliferation.

3.2 Capsaicin (Caps) Induces Autophagy in Intestinal Cells

As capsaicin has no direct antibacterial action against *S. flexneri,* we questioned the probable mechanism involved in reducing intracellular

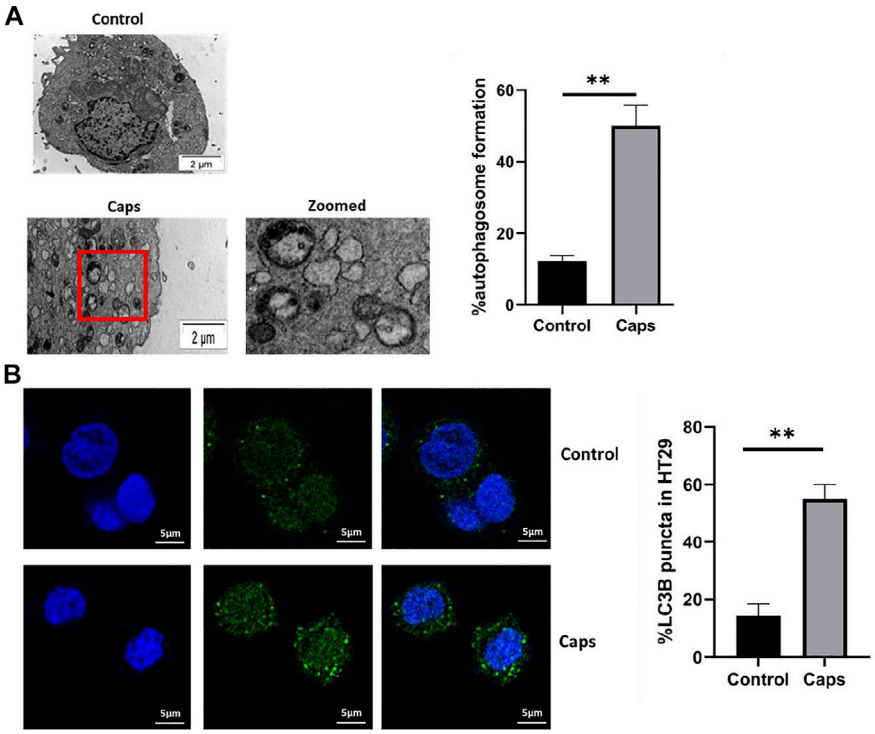

FIGURE 3 | Treatment with Caps enhances autophagosome formation. **(A)** Electron microscopic (TEM) pictures showed the presence of autophagosome formation in control and Caps-treated HT-29 cells for 4 h. Zoomed images of the marked area. Scale bar: 2 µm. Graphical representation of % autophagosome formation as observed in TEM. Unpaired *t*-test was performed. **(B)** Confocal microscopic images of GFP-LC3B transfected intestinal cells (HT-29) showed LC3B puncta (green) formation. Briefly, cells were transfected with GFP-LC3B plasmid, then treated with Caps for 4 h, and visualized under a confocal microscope. Graph representing the percentage of LC3B puncta formation. All experiments were performed in triplicate. Unpaired *t*-test was performed. Graphs generated using GraphPad Prism 5 were represented as mean ± SEM (n = 3); significance was calculated; $^{*}p < 0.05$, $^{**}p < 0.01$, $^{***}p < 0.001$.

bacterial growth. Previously, it was identified that Caps overexpressed autophagy proteins in nasopharyngeal cancer cells (Lin S. R. et al., 2017). However, there are no such reports on intestinal cells. Here, we examined the expression of autophagy proteins in intestinal epithelial cells by western blots. Caps overexpressed the autophagy proteins Atg5 and beclin1 in a dose-dependent manner in HT29 cells after treatment for 2 h (**Figure 2A**). Beclin1 is an autophagy regulator involved in autophagosome formation, while Atg5 helps in autophagosome maturation and LC3B lipidation (Brier et al., 2019). P62 degradation, another marker of autophagy initiation, takes place due to Caps treatment. Next, we examined the effect of Caps on autophagy genes at different concentrations. Caps significantly augmented the expression of MAP1LC3B and Atg5 genes in a dose-dependent manner (**Figure 2B**). To further assess the effect of Caps on autophagic gene expression, a PCR array was performed. Differential gene expression was observed due to Caps treatment in intestinal cells for 4 h. More than 78% of the genes are augmented by Caps alone at a dose of 16 µM (**Figure 2C**). As autophagy induction is often linked with cellular toxicity, we checked the toxicity of Caps in both intestinal and macrophage cells. Cytotoxicity assay of Caps in intestinal and macrophage cells showed insignificant effects due to Caps treatment for 24 h (**Supplementary Figure S1**). Together, these results indicate that Caps induces autophagic gene and protein expression in intestinal cells.

3.3 Treatment With Caps Enhances Autophagosome Formation

In addition to the stimulation of autophagic gene expression by Caps, we examined the potential effect of Caps on autophagosome formation by transmission electron microscopy (TEM) and confocal microscopy. The images showed autophagosome formation in cells treated with Caps (**Figure 3A**). Caps treatment alone showed 50% autophagosome formation in intestinal cells. Similar observations were validated by confocal microscopy. It is known that autophagosome formation is associated with membrane-bound LC3B. GFP-LC3B-transfected cells were exposed to Caps. Caps (16 µM) treatment for 2 h resulted in LC3B puncta formation in intestinal cells (**Figure 3B**). Together, these results confirm that Caps induces autophagosome formation in intestinal cells.

3.4 Caps-Induced Autophagy Targets *S. flexneri* to Autophagosome

Host-induced capture of pathogens by autophagosomes occurs during autophagy-mediated degradation. As *S. flexneri* is known to escape from autophagy, we checked the capture of bacteria by autophagosomes due to Caps treatment in infected cells. Caps treatment showed the

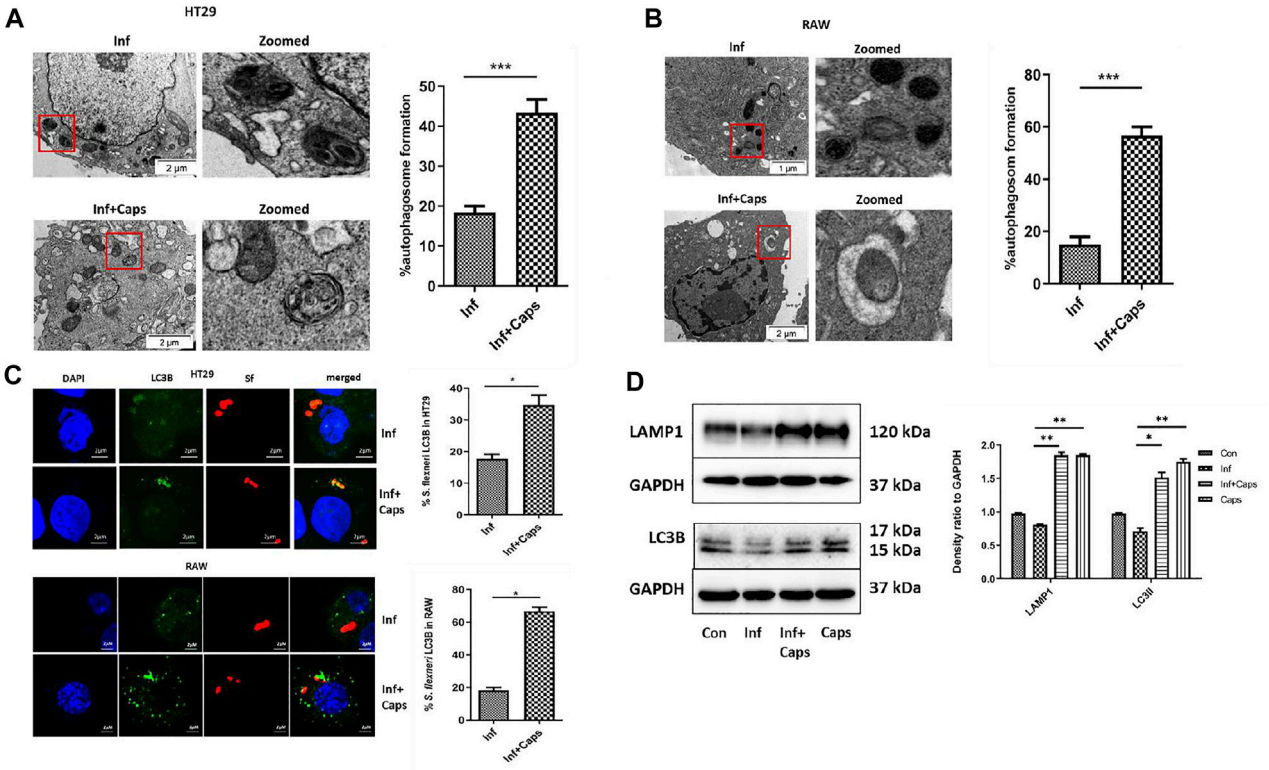

FIGURE 4 | Caps treatment results in the engulfment of bacteria by autophagosome. **(A)** Transmission electron microscopy (TEM) pictures showed the presence of autophagosome formation in infected intestinal cells with and without Caps treatment. Zoomed images of the marked area. Scale bar: 2 µm. Graphical representation of % autophagosome formation as observed in TEM. Unpaired *t*-test was performed. **(B)** Transmission electron microscopy (TEM) pictures of autophagosome formation in infected and infected + Caps RAW267.4 cells. Zoomed images of the marked area. Scale bar: 2 µm. **(C)** Microscopic images of GFP-LC3B transfected intestinal cells (HT-29) showed the recruitment of *S. flexneri* (red) to LC3B (green). Briefly, cells were transfected with GFP-LC3B plasmid, then treated with Caps for 2 h followed by *S. flexneri* infection for 2 h. Graph representing the percentage of bacteria localizing with LC3B. Microscopy images of GFP-LC3B transfected macrophages (RAW 267.4) infected with bacteria and treated with and without Caps. Graph representing the number of bacteria recruited to LC3B. Unpaired *t*-test was performed. Scale bar: 2 µM. **(D)** HT29 cells were pre-treated with Caps for 2 h followed by infection. After infection, cells were lysed. Cell lysates were subjected to immunoblotting. Increase in LC3B and LAMP1 expression was shown by western blotting, and densitometric analyses are graphically represented [Caps = Only Caps treatment at a dose of 16 µM]. Graphs were represented using GraphPad Prism 5 as mean ± SEM (n = 3); one-way ANOVA was performed. Significance was calculated; $^{*}p < 0.05$, $^{**}p < 0.01$, $^{***}p < 0.001$.

presence of autophagosome-like structures containing bacteria. We calculated the percentage of autophagosomes and observed that approximately 40% autophagosome formation takes place in *S. flexneri*-infected cells pre-treated with Caps (**Figure 4A**). Similar observations were observed in macrophage cells. Capture of bacteria by autophagosome was observed in drug-treated cells (**Figure 4B**). All these findings direct that Caps treatment induced autophagosome formation in *S. flexneri*-infected cells.

To confirm the capture of *S. flexneri* by autophagosomes, confocal microscopy was performed. Therefore, both macrophages and intestinal cells were transfected with GFP-LC3B, treated with Caps ($16\mu M$) for 2 h, and finally infected with bacteria. Caps treatment resulted in the increased recruitment of LC3B to bacteria. In intestinal cells, almost 34% of bacteria were localized with LC3B, whereas in macrophages, 60% of bacteria were bound with LC3B puncta, suggesting that autophagy is a tool for Caps-mediated bacterial clearance (**Figure 4C**). Moreover, the T3SS null strain (plasmid cured) was taken and the effect of Caps was observed. *Shigella flexneri* showed white colonies on Congo red plates instead of red as these colonies are defective in the activation of virulence factors (T3SS) (**Supplementary Figure S2**). Confocal microscopy revealed that the recruitment of bacteria to LC3B was absent in Caps-treated cells. Most of the bacteria were outside the cells. In addition, we verified Caps-induced activation of autophagy by western blot in infected and uninfected cells. Both LC3B and LAMP1 proteins, the end stage markers of autophagy, were induced in drug-treated (both infected and uninfected) cells (**Figure 4D**). Overall, these results suggest that Caps-induced autophagy is responsible for targeting bacteria to the autophagosomes.

3.5 Inhibition of Autophagy Increases *S. flexneri* Growth

Following our investigations, we tried to find out the impact of autophagy inhibition on *S. flexneri* growth. We used autophagy

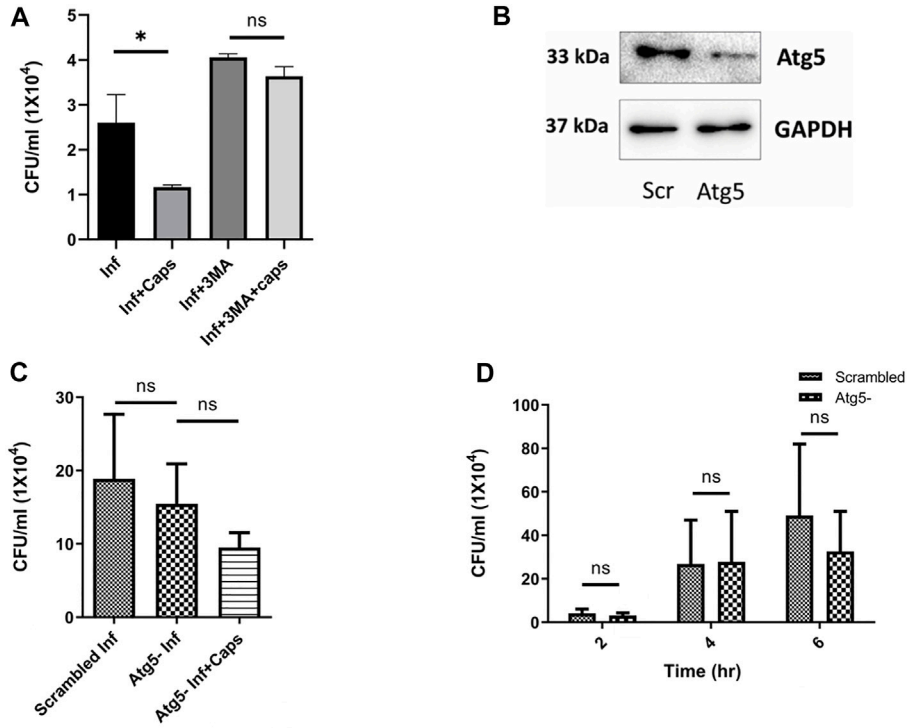

FIGURE 5 | Autophagy inhibition induced bacterial growth. **(A)** Intestinal cells were treated with 3MA (5 mM), Caps (16μM) for 2 h, further infected with *S. flexneri* for 2 h followed by gentamicin treatment. Infection assay was performed. Graph represents intracellular bacterial count. One-way ANOVA was performed. **(B)** Cells were transfected with scrambled and Atg5 siRNA. Western blot shows the Atg5 expression in scrambled and knockdown cells. GAPDH was kept as a housekeeping control. **(C)** Infection assay was performed in scrambled and Atg5 knockdown cells treated with Caps for 2 h followed by infection. CFU/ml was graphically represented. One-way ANOVA was performed. **(D)** Infection assay was performed in scrambled and Atg5 knockdown cells for different time points (2, 4, 6 h). Briefly, after transfection with scrambled and Atg5 siRNA, cells were infected for different time points. Cells were lysed and plated for CFU count. Graphs were represented using GraphPad Prism 5 as mean ± SEM (n = 3); significance was calculated by two-way ANOVA; $^{*}p < 0.05$, $^{**}p < 0.01$, $^{***}p < 0.001$.

inhibitors like 3-methyl adenine (3MA). As expected, 3MA increased intracellular *S. flexneri* proliferation. In the presence of 3MA, the anti-shigella activity of Caps was impaired, suggesting that the killing of bacteria is dependent on autophagy (**Figure 5A**). To rule out the nonspecific effect of inhibitors (3MA) a major autophagy player Atg5 was knocked down using siRNA to inhibit autophagy. Successful Atg5 knockdown was confirmed by western blot (**Figure 5B**). In Atg5 knockdown cells, Caps treatment failed to inhibit *S. flexneri* intracellular growth (**Figure 5C**).

Furthermore, to observe the effect of Atg5 knockdown in detail, we infected Atg5 knockdown cells for different time intervals (**Figure 5D**). Bacterial growth was unaffected due to the blockade of autophagy. These observations indicate that Caps-induced autophagy is responsible for *S. flexneri* death.

3.6 Capsaicin (Caps) Triggers Autophagy Gene Transcription by Nuclear Localization of TFEB

As Caps induced the transcription of autophagy genes, we searched for a potential transcription factor responsible for autophagosomal and lysosomal biogenesis. TFEB, a transcription factor, is reported to enhance autophagosome biogenesis. It binds to the promoter of CLEAR network (coordinated, lysosomal expression, and regulation) and induces autophagy genes (Polito et al., 2014; Sardiello, 2016; Vega-Rubin-de-Celis et al., 2017; Fan et al., 2018; Puertollano et al., 2018). HT29 cells were treated with Caps for 2 h followed by immunofluorescence. Herein, we observed an 80% increase in the nuclear expression of TFEB in Caps-treated cells as compared to that of untreated cells by the immunofluorescence assay (**Figure 6A**). To confirm TFEB nuclear localization and autophagic gene transcription, we performed promoter assays. Consistently, Caps augmented TFEB promoter activity significantly in treated cells as compared to that of untreated cells by binding to CLEAR sequence (**Figure 6B**). ChIP assay after chromatin immunoprecipitation also confirmed higher TFEB binding to MAP1LC3B promoter in cells treated with Caps (**Figure 6C**). Therefore, Caps triggered autophagic gene transcription via TFEB. Moreover, we examined the effect of Caps by immunoblotting. Caps treatment enhanced the nuclear expression of TFEB in both *S. flexneri*-infected and uninfected cells, whereas Caps reduced the cytosolic expression of TFEB (**Figure 6D**). These results suggest that Caps induced autophagic gene transcription by stimulating the nuclear translocation of TFEB.

To evaluate the relevance of TFEB activation in *S. flexneri* proliferation, we silenced TFEB by siRNA. TFEB knockdown

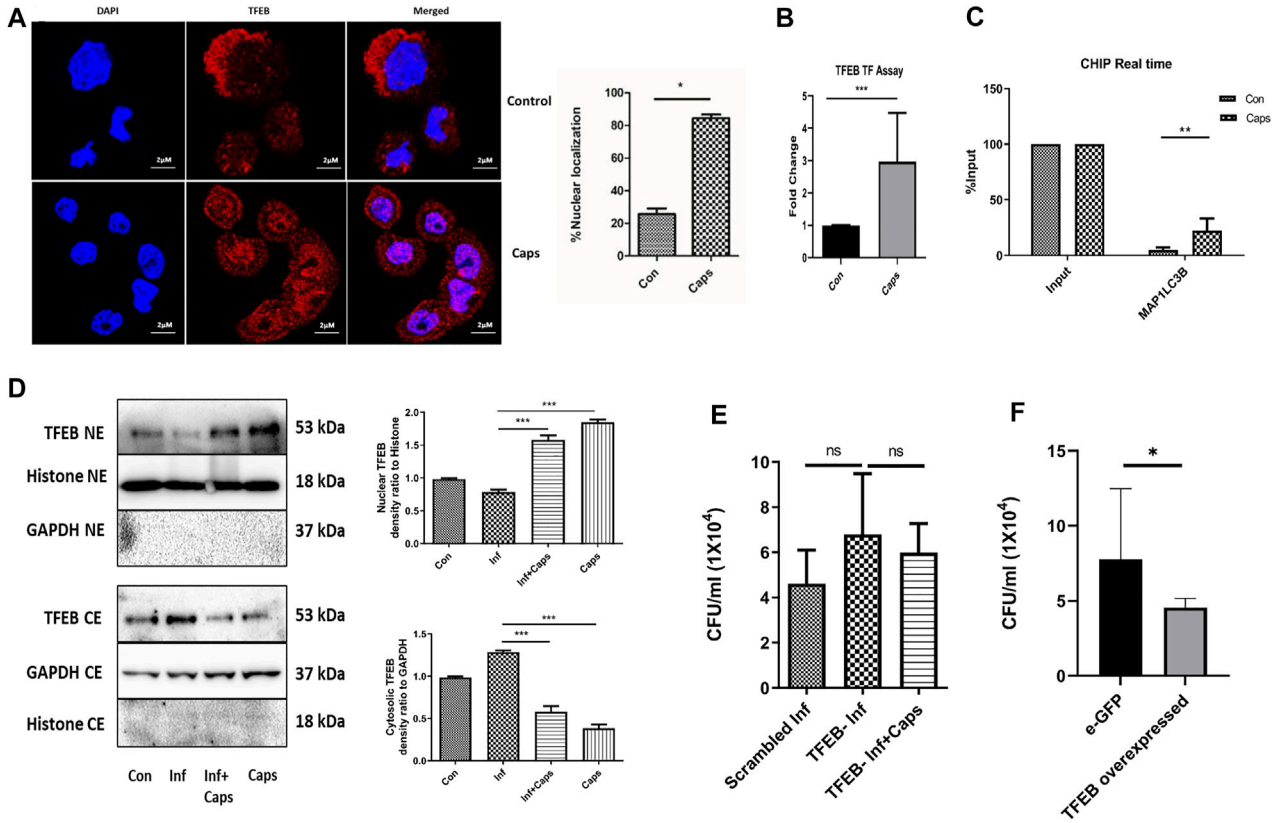

FIGURE 6 | Caps treatment induced TFEB nuclear localization. **(A)** Confocal microscopic data showing nuclear localization of TFEB upon Caps treatment. Briefly, HT29 cells were treated with Caps (16 μM) for 2 h followed by immunofluorescence microscopy. Scale bar: 2 μm. **(B)** Caps treated and untreated cells were subjected to TFEB transcription assay. Transcription factor assay was performed to show the activation of TFEB binding to CLEAR sequence by Caps. Unpaired *t*-test was performed. **(C)** CHIP assay was performed with or without anti-TFEB antibody (input). Expression of MAP1LC3B was checked and compared to input in real-time PCR assay for untreated and Caps-treated intestinal cells. The data were represented graphically and compared to input; two-way ANOVA was performed. **(D)** Western blot analysis was performed for determining the protein level of TFEB in both cytosolic (CE) and nuclear extracts (NE) after Caps treatment in *S. flexneri* infected and uninfected cells. GAPDH was kept as a housekeeping control for cytoplasmic cell extracts. Histone was used as a control for nuclear extracts. Densitometric analyses are shown and graphically represented. One-way ANOVA was performed. **(E)** Cells were transfected with scrambled siRNA or TFEB siRNA. After transfection, cells were treated with Caps for 2 h and infected with *S. flexneri* for 2 h followed by gentamicin treatment. Cell lysis was performed and plated. One-way ANOVA was performed. **(F)** Cells were transfected with an empty vector eGFP or eGFP-TFEB plasmid followed by *S. flexneri* infection. Cells were lysed and plated for colony count. Unpaired *t*-test was performed. Graphs were represented using GraphPad Prism 5 as mean ± SEM (n = 3); Significance was calculated; $^{*}p < 0.05$, $^{**}p < 0.01$, $^{***}p < 0.001$.

itself has no effect on *S. flexneri* growth; however, Caps treatment in TFEB-silenced cells fails to clear intracellular bacterial burden (**Figure 6E**). Similarly, the overexpression of eGFP-TFEB plasmid in HT 29 cells resulted in the reduction of *S. flexneri* growth significantly (**Figure 6F**). Silencing of TFEB by siRNA and overexpression in intestinal cells were confirmed by immunoblot analysis (**Supplementary Figure S3**). Taken together, these findings indicate that TFEB is a major player in reducing bacterial growth by Caps.

3.7 Capsaicin (Caps) Inhibits Intracellular Survival of *S. flexneri* in Both Cellular and Animal Models

To assess the efficacy of Caps in controlling *S. flexneri* infection, we checked the effect of Caps against a resistant strain of *S. flexneri*. We observed that Caps is effective in inhibiting the resistant *S. flexneri* strain growth significantly at a higher dose of 32 μM after 12 h post treatment. **Supplementary Table S1** shows the MIC values of the resistant strain against different antibiotics (**Figure 7A**). Finally, we validated the effect of Caps in mouse model. Mice were infected by intraperitoneal challenge with *S. flexneri* 2457T strain (**Figure 7B**). The dose of Caps was selected in the infection model based on the available data of capsaicin (Rollyson et al., 2014). After 2 h of infection, mice were treated with Caps (20 mg/kg body weight) for 2 h and then sacrificed for further studies. We took the colon from infected and Caps-treated mice samples. The bacterial count showed a decrease in *S. flexneri*-infected mice that received Caps (**Figure 7C**). Additionally, we examined the effect of Caps on MAP1LC3B gene expression in mice colon tissues. Caps significantly enhanced the MAP1LC3B gene expression in infected mice as compared to that in untreated mice. Caps alone also increased the MAP1LC3B gene expression significantly (**Figure 7D**). We

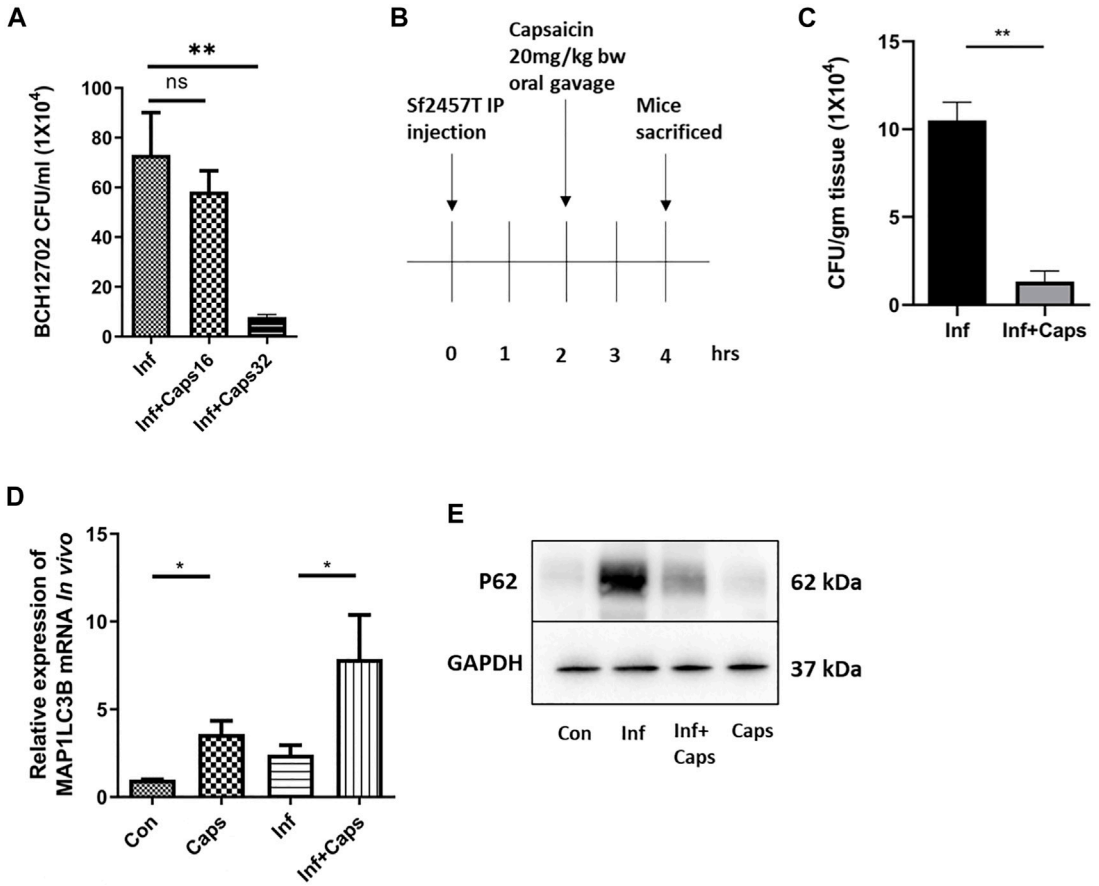

FIGURE 7 | Caps reduced bacterial growth in both cellular and *in vivo* conditions. **(A)** Cells were infected with resistant *S. flexneri 2a* (BCH12702) strain followed by 16 μM, 32 μM Caps post-treatment for 12 h and CFU/ml was graphically represented. One-way ANOVA was performed. **(B)** Caps treatment in *Shigella flexneri 2457T*-infected BALB/c mice. Briefly, mice were infected for 2 h followed by Caps (20 mg/kg b. w.) treatment for 2 h. Four groups (N = 4) were created accordingly: Group 1. Control: only DMSO was used as the vehicle. Group 2. Infected: Received *S. flexneri* suspension (0.5×10^9 CFU/ml) in PBS. Group 3. Infected + Caps: Received *S. flexneri* suspension followed by Caps (20 mg kg^{-1} body weight) treatment for 2 h. Group 4. Caps: Received Caps (20 mg kg−1 body weight). Each group was kept in an individual cage. Experiments were repeated in triplicate (n = 3). Total number of mice in each group were 12. **(C)** CFU was counted and plotted for *S. flexneri sf2457T* infected and infected + Caps-treated crushed colon samples. Unpaired *t*-test was performed. **(D)** qRT-PCR was performed for the expression of the autophagy-associated marker gene MAP1LC3B in control, infected, infected with caps treatment, and only Caps-treated mice tissues using GAPDH as a housekeeping gene control. One-way ANOVA was performed. **(E)** Expression of major autophagy-associated marker protein P62 was observed in western blot. GAPDH was used as a loading control. Graphs were represented using GraphPad Prism 5 as mean ± SEM (n = 3); significance was calculated: $^*p < 0.05$, $^{**}p < 0.01$, $^{***}p < 0.001$.

assessed the effect of Caps on p62 degradation, another marker of autophagy induction. Caps treatment induced p62 degradation in both infected and uninfected mice tissues (**Figure 7E**). These data confirm that Caps has the potential to be used as a therapeutic against *S. flexneri*.

4 DISCUSSION

There is a constant interplay between the host and pathogen to maintain cellular homeostasis. Both play diverse strategies to overcome each other. One of the powerful strategies to boost host defense is autophagy. However, intracellular pathogens evade autophagy to establish successful infection. In contrast, boosting autophagy results in the clearance of intracellular bacteria and thereby inhibits infection. Small-molecule enhancers of autophagy are reported to control bacterial infections like *Mycobacterium* and *Salmonella* (Kim et al., 2012; Noad et al., 2017; Ammanathan et al., 2020). Recent studies have also focused on major autophagy players, such as mTOR, akt, and TFEB, a transcription factor controlling autophagy to reduce bacterial burden (Floto et al., 2007; Lin Y.-T et al., 2017). Hence, in this era of antimicrobial resistance, there is an urgent need to identify new antimicrobial compounds to overcome the problem of resistance mechanisms by targeting host factors like autophagy.

This study is the first evidence to show that capsaicin (Caps) induces autophagy for the intracellular killing of *S. flexneri*. Caps, a known anticancer herbal compound, is able to stimulate autophagy in intestinal cells and macrophages. Autophagy, in turn, inhibited the intracellular infiltration of *S. flexneri*. This is a novel approach in inhibiting *S. flexneri* infection. Previous reports indicate that Caps induces autophagy in tumor cells by

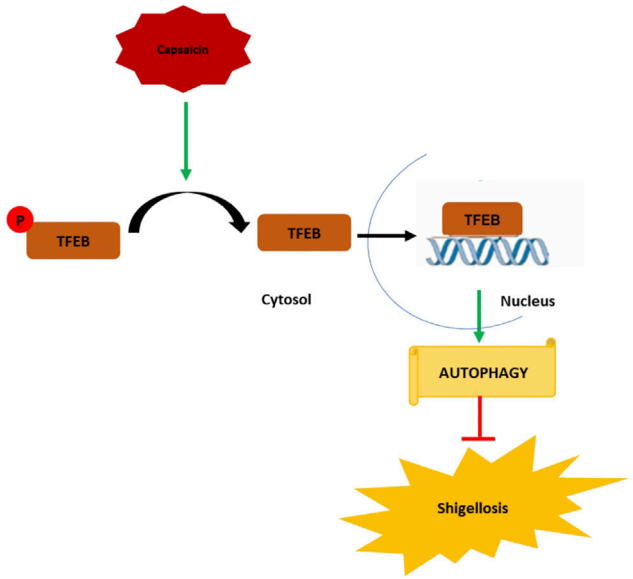

FIGURE 8 | Graphical representation of the mechanism of action of capsaicin (Caps). Caps inhibits TFEB phosphorylation. Dephosphorylated TFEB moves from cytosol to nucleus and binds to the promoter site of autophagy genes resulting in the upregulation of autophagy-associated marker genes. Induction of autophagy inhibits shigellosis by inhibiting *S. flexneri* growth in both *in vitro* and *in vivo* models.

overexpressing the autophagy proteins beclin1, Atg5, and LC3B (Jin et al., 2014). Consistent with these studies in cancer cells, we showed that Caps also augmented autophagy at a lower dose in intestinal epithelial cells at the protein level. This dose is nontoxic to cells, as reported earlier (Campbell-Valois et al., 2015). Further, we confirmed insignificant toxicity in HT29 cells and macrophages. Our findings showed for the first time that Caps treatment resulted in the overexpression of autophagy genes in intestinal cells. Unlike our knowledge of the overexpression of autophagy proteins by Caps, the transcriptional upregulation of autophagy by Caps has not been reported earlier. Furthermore, Caps induced autophagosome formation in intestinal and macrophage cells. Transcriptional activation of autophagy resulted in autophagosome formation.

In addition to autophagic stimulation, Caps attributed to the killing of *S. flexneri* in intestinal epithelial cells and macrophages. Along with bactericidal effects, our microscopic observations indicated autophagosome formation in Caps-treated cells. Electron and confocal microscopic studies revealed that bacteria are associated with autophagosomes in drug-treated cells. Consistently, we observed that Caps robustly increased LC3B puncta formation and targeted bacteria to autophagosome. In plasmid-cured avirulent strain of *S. flexneri* (lacking T3SS), Caps is unable to target bacteria, as most of the bacteria are outside the cells. Published reports have shown that the IcsB, VirA, and other proteins released by T3SS are required for the intracellular infiltration of *S. flexneri* (Ogawa et al., 2005; Vakifahmetoglu-Norberg et al., 2015). Hence, Caps targeted only intracellular bacteria. However, we checked whether Caps can directly kill the bacteria, but there is no direct effect of Caps on *S. flexneri*. Thus, it is confirmed that the anti-shigella effect of Caps is autophagy-dependent.

Previous reports of *S. flexneri* showed that Atg5, an essential autophagy protein, is needed for LC3 recruitment to *Shigella flexneri*. Here, we observed that the intracellular growth of *S. flexneri* remains unaffected due to the knockdown of Atg5 in intestinal cells. Caps treatment in Atg5 knockdown cells resulted in the loss of pathogen restriction, suggesting that autophagy plays an essential role in the inhibition of bacterial growth.

Having established that autophagy is the major player in Caps-mediated *S. flexneri* clearance, we explored the mechanistic details of autophagy induction by Caps. We observed that autophagic gene transcription is enhanced due to nuclear localization of TFEB (Sardiello, 2016). Drug treatment enhanced the nuclear translocation of TFEB in both infected and uninfected cells.

It has been reported that TFEB is a transcriptional regulator of autophagosomal biogenesis (Fan et al., 2018). It induces the transcription of several autophagosomal and lysosomal genes. Moreover, TFEB enhancers are currently reported for the development of therapeutics against intracellular pathogens (Ammanathan et al., 2020). Hence, it is a targeted transcription factor. Here, we observed for the first time that Caps induces TFEB binding to promoter elements to augment autophagic gene transcription.

Previous studies have shown that the depletion of TFEB induces the multiplication of pathogens by downregulating autophagy during infection (Gray et al., 2016). Similarly, in this study, TFEB knockdown in intestinal cells retained *S. flexneri* multiplication, and Caps treatment was unable to restrict bacterial growth, suggesting the importance of TFEB in controlling *S. flexneri* infection. In contrast, the overexpression of TFEB reduced bacterial growth. Therefore, TFEB is involved in Caps-mediated transcription of autophagy genes, resulting in the enhanced intracellular killing of *S. flexneri*. Moreover, capsaicin is known to selectively bind to the TRPV1 receptor and induce calcium influx (Liang et al., 2018; Allais et al., 2020). TRPV1 is expressed in intestinal cells and is known to induce autophagy (Chen et al., 2021; Wang et al., 2021). Hence, Caps-induced autophagy might be due to TRPV1 activation.

In the current study, we proved that the antimicrobial effect of Caps is mediated through autophagy. Moreover, we observed that Caps inhibited *S. flexneri* resistant strain growth at a higher dose. Thus, it is evident that probably Caps can address the problem of antimicrobial resistance in near future. Recent studies of *Salmonella* showed the effect of autophagy inducing compounds in mice (Ammanathan et al., 2020). Hence, we explored Caps's effectivity in an *in vivo* mouse model. We observed that Caps increased the clearance of *S. flexneri* in intestinal tissues of infected mice. Here, we also showed that Caps treatment in *in vivo* mouse model induced autophagy. Thus, Caps is effective in preclinical models to boost autophagy and simultaneously decrease *S. flexneri* burden.

In conclusion, the emergence of antibiotic resistance requires a constant effort for the development of new therapies, which can boost host mechanisms to enhance bactericidal activity. Our data

represent an important novel finding that drugs such as Caps manipulate host cellular defense mechanisms such as autophagy to achieve bactericidal effects against *S. flexneri*. The mechanistic details of Caps-activated autophagy uncovered a novel role of TFEB to be a potential target in treating *S. flexneri* infection. This is the first evidence of TFEB activation by Caps. Caps induced TFEB nuclear translocation by dephosphorylation of TFEB. TFEB in nucleus, in turn, binds to the promoter of autophagy genes to boost autophagy. Autophagy induction helps reduce *S. flexneri* growth and thereby inhibits shigellosis (**Figure 8**) Hence, a new alternative approach has been unraveled for the treatment of *S. flexneri* infection.

5 CONCLUSION

This study will open new avenues in treating shigellosis in the near future. More inducers of TFEB nuclear translocation, such as Caps, may be used to strengthen the host response against pathogens. However, Caps may not act as the only drug for the treatment of shigellosis, as most autophagy inducers are used in combination with other antibiotics for the treatment of bacterial pathogenesis. Host-directed therapy could be a new approach in adjunct to the use of antibiotics for infectious diseases. Moreover, Caps, as an autophagy inducer, might be effective against other intracellular pathogens.

DATA AVAILABILITY STATEMENT

The original contributions presented in the study are included in the article/**Supplementary Material**; further inquiries can be directed to the corresponding author.

ETHICS STATEMENT

The animal study was reviewed and approved by IAEC (Institutional Animal Ethical Committee), NICED, Kolkata (PRO/157/-July 2022).

AUTHOR CONTRIBUTIONS

PB: investigation and writing—review and editing. PM: investigation and data curation. UK: investigation and data curation. KS: methodology and validation. SB: writing—review and editing and data curation. MD: validation. SB: supervision and writing—review and editing, writing—original draft, funding acquisition, and investigation.

FUNDING

This work was funded by ICMR Extramural Project 59/01/2019/Online/BMS/TRM.

ACKNOWLEDGMENTS

The authors thank Dr. Shanta Dutta, Director, ICMR-National Institute of Cholera and Enteric Diseases (NICED), for her support in providing funding and infrastructure, Dr. Santasabuj Das, ICMR-NICED, for helping with confocal microscopy, real-time PCR, providing antibodies, EGFP plasmid, and RAW Cell line, Dr. Nabendu Sekhar Chatterjee ICMR-NICED for chemicals and reagents, Dr. Asish K Mukhopadhyay ICMR-NICED for bacterial strains, Dr. Mamta Chawla Sarkar ICMR-NICED for antibodies, Dr. Avinash Bajaj, Regional Centre for Biotechnology, Faridabad, for the kind gift of HT29 cell line, Prof. Parimal Karmakar, Jadavpur University, for eGFP-LC3 plasmid, and Dr. Ravi Manjithaya, JNCASR, Bangalore, for pEGFP-N1-TFEB plasmid. The authors also thank the Council for Scientific and Industrial Research (CSIR) and Department of Biotechnology (DBT) for providing fellowship to the authors.

SUPPLEMENTARY MATERIAL

The Supplementary Material for this article can be found online at: https://www.frontiersin.org/articles/10.3389/fphar.2022.903438/full#supplementary-material.

REFERENCES

Allais, L., Verschuere, S., Maes, T., De Smet, R., Devriese, S., Gonzales, G. B., et al. (2020). Translational Research into the Effects of Cigarette Smoke on Inflammatory Mediators and Epithelial TRPV1 in Crohn's Disease. *PloS one* 15 (8), e0236657. doi:10.1371/journal.pone.0236657

Ammanathan, V., Mishra, P., Chavalmane, A. K., Muthusamy, S., Jadhav, V., Siddamadappa, C., et al. (2020). Restriction of Intracellular Salmonella Replication by Restoring TFEB-Mediated Xenophagy. *Autophagy* 16 (9), 1584–1597. doi:10.1080/15548627.2019.1689770

Baker, S., and The, H. C. (2018). Recent Insights into Shigella: A Major Contributor to the Global Diarrhoeal Disease Burden. *Curr. Opin. Infect. Dis.* 31 (5), 449–454. doi:10.1097/QCO.0000000000000475

Brier, L. W., Ge, L., Stjepanovic, G., Thelen, A. M., Hurley, J. H., and Schekman, R. (2019). Regulation of LC3 Lipidation by the Autophagy-specific Class III Phosphatidylinositol-3 Kinase Complex. *Mol. Biol. Cell* 30 (9), 1098–1107. doi:10.1091/mbc.E18-11-0743

Campbell-Valois, F. X., Sachse, M., Sansonetti, P. J., and Parsot, C. (2015). Escape of Actively Secreting Shigella Flexneri from ATG8/LC3-Positive Vacuoles Formed during Cell-To-Cell Spread Is Facilitated by IcsB and VirA. *MBio* 6 (3), e02567–14. doi:10.1128/mBio.02567-14

Chang, Z., Zhang, J., Ran, L., Sun, J., Liu, F., Luo, L., et al. (2016). The Changing Epidemiology of Bacillary Dysentery and Characteristics of Antimicrobial Resistance of Shigella Isolated in China from 2004-2014. *BMC Infect. Dis.* 16 (1), 685. doi:10.1186/s12879-016-1977-1

Chanin, R. B., Nickerson, K. P., Llanos-Chea, A., Sistrunk, J. R., Rasko, D. A., Kumar, D. K. V., et al. (2019). Shigella Flexneri Adherence Factor Expression in In Vivo-like Conditions. *Msphere* 4 (6), e00751–19. doi:10.1128/mSphere.00751-19

Chen, Q., Rui, J., Hu, Q., Peng, Y., Zhang, H., Zhao, Z., et al. (2020). Epidemiological Characteristics and Transmissibility of Shigellosis in Hubei

Province, China, 2005 - 2017. *BMC Infect. Dis.* 20 (1), 272. doi:10.1186/s12879-020-04976-x

Chen, M., Dong, X., Deng, H., Ye, F., Zhao, Y., Cheng, J., et al. (2021). Targeting TRPV1-Mediated Autophagy Attenuates Nitrogen Mustard-Induced Dermal Toxicity. *Signal Transduct. Target. Ther.* 6 (1), 1–13. doi:10.1038/s41392-020-00389-z

Fan, Y., Lu, H., Liang, W., Garcia-Barrio, M. T., Guo, Y., Zhang, J., et al. (2018). Endothelial TFEB (Transcription Factor EB) Positively Regulates Postischemic Angiogenesis. *Circ. Res.* 122 (7), 945–957. doi:10.1161/CIRCRESAHA.118.312672

Floto, R. A., Sarkar, S., Perlstein, E. O., Kampmann, B., Schreiber, S. L., and Rubinsztein, D. C. (2007). Small Molecule Enhancers of Rapamycin-Induced TOR Inhibition Promote Autophagy, Reduce Toxicity in Huntington's Disease Models and Enhance Killing of Mycobacteria by Macrophages. *Autophagy* 3 (6), 620–622. doi:10.4161/auto.4898

Füchtbauer, S., Mousavi, S., Bereswill, S., and Heimesaat, M. M. (2021). Antibacterial Properties of Capsaicin and its Derivatives and Their Potential to Fight Antibiotic Resistance - A Literature Survey. *Eur. J. Microbiol. Immunol. (Bp)* 11 (1), 10–17. doi:10.1556/1886.2021.00003

Giraud-Gatineau, A., Coya, J. M., Maure, A., Biton, A., Thomson, M., Bernard, E. M., et al. (2020). The Antibiotic Bedaquiline Activates Host Macrophage Innate Immune Resistance to Bacterial Infection. *Elife* 9, e55692. doi:10.7554/eLife.55692

Gray, M. A., Choy, C. H., Dayam, R. M., Ospina-Escobar, E., Somerville, A., Xiao, X., et al. (2016). Phagocytosis Enhances Lysosomal and Bactericidal Properties by Activating the Transcription Factor TFEB. *Curr. Biol.* 26 (15), 1955–1964. doi:10.1016/j.cub.2016.05.070

Hajialibeigi, A., Amani, J., and Gargari, S. L. M. (2021). Identification and Evaluation of Novel Vaccine Candidates against Shigella Flexneri through Reverse Vaccinology Approach. *Appl. Microbiol. Biotechnol.* 105 (3), 1159–1173. doi:10.1007/s00253-020-11054-4

Hosangadi, D., Smith, P. G., and Giersing, B. K. (2019). Considerations for Using ETEC and Shigella Disease Burden Estimates to Guide Vaccine Development Strategy. *Vaccine* 37 (50), 7372–7380. doi:10.1016/j.vaccine.2017.09.083

Hu, W., Zhang, L., Li, M. X., Shen, J., Liu, X. D., Xiao, Z. G., et al. (2019). Vitamin D3 Activates the Autolysosomal Degradation Function against Helicobacter pylori through the PDIA3 Receptor in Gastric Epithelial Cells. *Autophagy* 15 (4), 707–725. doi:10.1080/15548627.2018.1557835

Jin, J., Lin, G., Huang, H., Xu, D., Yu, H., Ma, X., et al. (2014). Capsaicin Mediates Cell Cycle Arrest and Apoptosis in Human Colon Cancer Cells via Stabilizing and Activating P53. *Int. J. Biol. Sci.* 10 (3), 285–295. doi:10.7150/ijbs.7730

Jo, E. K., Yuk, J. M., Shin, D. M., and Sasakawa, C. (2013). Roles of Autophagy in Elimination of Intracellular Bacterial Pathogens. *Front. Immunol.* 4, 97. doi:10.3389/fimmu.2013.00097

Kaufmann, S. H. E., Dorhoi, A., Hotchkiss, R. S., and Bartenschlager, R. (2018). Host-directed Therapies for Bacterial and Viral Infections. *Nat. Rev. Drug Discov.* 17 (1), 35–56. doi:10.1038/nrd.2017.162

Khalil, I. A., Troeger, C., Blacker, B. F., Rao, P. C., Brown, A., Atherly, D. E., et al. (2018). Morbidity and Mortality Due to shigella and Enterotoxigenic Escherichia coli Diarrhoea: The Global Burden of Disease Study 1990-2016. *Lancet Infect. Dis.* 18 (11), 1229–1240. doi:10.1016/S1473-3099(18)30475-4

Killackey, S. A., Sorbara, M. T., and Girardin, S. E. (2016). Cellular Aspects of Shigella Pathogenesis: Focus on the Manipulation of Host Cell Processes. *Front. Cell Infect. Microbiol.* 6, 38. doi:10.3389/fcimb.2016.00038

Kim, J. J., Lee, H. M., Shin, D. M., Kim, W., Yuk, J. M., Jin, H. S., et al. (2012). Host Cell Autophagy Activated by Antibiotics Is Required for Their Effective Antimycobacterial Drug Action. *Cell Host Microbe* 11 (5), 457–468. doi:10.1016/j.chom.2012.03.008

Kim, Y. S., Silwal, P., Kim, S. Y., Yoshimori, T., and Jo, E. K. (2019). Autophagy-activating Strategies to Promote Innate Defense against Mycobacteria. *Exp. Mol. Med.* 51 (12), 1–10. doi:10.1038/s12276-019-0290-7

Krokowski, S., Lobato-Márquez, D., Chastanet, A., Pereira, P. M., Angelis, D., Galea, D., et al. (2018). Septins Recognize and Entrap Dividing Bacterial Cells for Delivery to Lysosomes. *Cell Host Microbe* 24 (6), 866–e4. doi:10.1016/j.chom.2018.11.005

Liang, Q., Lv, X., Cai, Q., Cai, Y., Zhao, B., and Li, G. (2018). Novobiocin, a Newly Found TRPV1 Inhibitor, Attenuates the Expression of TRPV1 in Rat Intestine and Intestinal Epithelial Cell Line IEC-6. *Front. Pharmacol.* 9, 1171. doi:10.3389/fphar.2018.01171

Lin, S. R., Fu, Y. S., Tsai, M. J., Cheng, H., and Weng, C. F. (2017). Natural Compounds from Herbs that Can Potentially Execute as Autophagy Inducers for Cancer Therapy. *Int. J. Mol. Sci.* 18 (7), 1412. doi:10.3390/ijms18071412

Lin, Y.-T., Wang, H.-C., Hsu, Y.-C., Cho, C.-L., Yang, M.-Y., and Chien, C.-Y. (2017). Capsaicin Induces Autophagy and Apoptosis in Human Nasopharyngeal Carcinoma Cells by Downregulating the PI3K/AKT/mTOR Pathway. *Ijms* 18 (7), 1343. doi:10.3390/ijms18071343

Lobato-Márquez, D., Krokowski, S., Sirianni, A., Larrouy-Maumus, G., and Mostowy, S. (2019). A Requirement for Septins and the Autophagy Receptor P62 in the Proliferation of Intracellular Shigella. *Cytoskeleton* 76 (1), 163–172. doi:10.1002/cm.21453

McQuade, E. T. R., Shaheen, F., Kabir, F., Rizvi, A., Platts-Mills, J. A., Aziz, F., et al. (2020). Epidemiology of Shigella Infections and Diarrhea in the First Two Years of Life Using Culture-independent Diagnostics in 8 Low-Resource Settings. *PLoS Negl. Trop. Dis.* 14 (8), e0008536. doi:10.1371/journal.pntd.0008536

Nandy, S., Dutta, S., Ghosh, S., Ganai, A., Rajahamsan, J., Theodore, R. B., et al. (2011). Foodborne-associated Shigella Sonnei, India, 2009 and 2010. *Emerg. Infect. Dis.* 17 (11), 2072–2074. doi:10.3201/eid1711.110403

Noad, J., Von Der Malsburg, A., Pathe, C., Michel, M. A., Komander, D., and Randow, F. (2017). LUBAC-synthesized Linear Ubiquitin Chains Restrict Cytosol-Invading Bacteria by Activating Autophagy and NF-Kb. *Nat. Microbiol.* 2 (7), 17063. doi:10.1038/nmicrobiol.2017.63

Ogawa, M., Yoshimori, T., Suzuki, T., Sagara, H., Mizushima, N., and Sasakawa, C. (2005). Escape of Intracellular Shigella from Autophagy. *Science* 307 (5710), 727–731. doi:10.1126/science.1106036

Polito, V. A., Li, H., Martini-Stoica, H., Wang, B., Yang, L., Xu, Y., et al. (2014). Selective Clearance of Aberrant Tau Proteins and Rescue of Neurotoxicity by Transcription Factor EB. *EMBO Mol. Med.* 6 (9), 1142–1160. doi:10.15252/emmm.201303671

Puertollano, R., Ferguson, S. M., Brugarolas, J., and Ballabio, A. (2018). The Complex Relationship between TFEB Transcription Factor Phosphorylation and Subcellular Localization. *EMBO J.* 37 (11), e98804. doi:10.15252/embj.201798804

Puzari, M., Sharma, M., and Chetia, P. (2018). Emergence of Antibiotic Resistant Shigella Species: A Matter of Concern. *J. Infect. Public Health* 11 (4), 451–454. doi:10.1016/j.jiph.2017.09.025

Ra, E. A., Lee, T. A., Won Kim, S., Park, A., Choi, H. J., Jang, I., et al. (2016). TRIM31 Promotes Atg5/Atg7-independent Autophagy in Intestinal Cells. *Nat. Commun.* 7 (1), 11726. doi:10.1038/ncomms11726

Ranjbar, R., and Farahani, A. (2019). Shigella: Antibiotic-Resistance Mechanisms and New Horizons for Treatment. *Infect. Drug Resist* 12, 3137–3167. doi:10.2147/IDR.S219755

Rollyson, W. D., Stover, C. A., Brown, K. C., Perry, H. E., Stevenson, C. D., McNees, C. A., et al. (2014). Bioavailability of Capsaicin and its Implications for Drug Delivery. *J. Control Release* 196, 96–105. doi:10.1016/j.jconrel.2014.09.027

Rubinsztein, D. C., Codogno, P., and Levine, B. (2012). Autophagy Modulation as a Potential Therapeutic Target for Diverse Diseases. *Nat. Rev. Drug Discov.* 11 (9), 709–730. doi:10.1038/nrd3802

Sardiello, M. (2016). Transcription Factor EB: From Master Coordinator of Lysosomal Pathways to Candidate Therapeutic Target in Degenerative Storage Diseases. *Ann. N. Y. Acad. Sci.* 1371 (1), 3–14. doi:10.1111/nyas.13131

Sharma, V., Verma, S., Seranova, E., Sarkar, S., and Kumar, D. (2018). Selective Autophagy and Xenophagy in Infection and Disease. *Front. Cell Dev. Biol.* 6, 147. doi:10.3389/fcell.2018.00147

Taneja, N., and Mewara, A. (2016). Shigellosis: Epidemiology in India. *Indian J. Med. Res.* 143 (5), 565–576. doi:10.4103/0971-5916.187104

Vakifahmetoglu-Norberg, H., Xia, H. G., and Yuan, J. (2015). Pharmacologic Agents Targeting Autophagy. *J. Clin. Invest.* 125 (1), 5–13. doi:10.1172/JCI73937

Vega-Rubin-de-Celis, S., Peña-Llopis, S., Konda, M., and Brugarolas, J. (2017). Multistep Regulation of TFEB by MTORC1. *Autophagy* 13 (3), 464–472. doi:10.1080/15548627.2016.1271514

Wang, C., Huang, W., Lu, J., Chen, H., and Yu, Z. (2021). TRPV1-Mediated Microglial Autophagy Attenuates Alzheimer's Disease-Associated Pathology and Cognitive Decline. *Front. Pharmacol.* 12, 763866. doi:10.3389/fphar.2021.763866

Weddle, E., and Agaisse, H. (2018). Spatial, Temporal, and Functional Assessment of LC3-dependent Autophagy in Shigella Flexneri Dissemination. *Infect. Immun.* 86 (8), e00134–18. doi:10.1128/IAI.00134-18

Williams, P. C. M., and Berkley, J. A. (2018). Guidelines for the Treatment of Dysentery (Shigellosis): A Systematic Review of the Evidence. *Paediatr. Int. Child. Health* 38 (Suppl. 1), S50–S65. doi:10.1080/20469047.2017.1409454

Yang, J. Y., Lee, S. N., Chang, S. Y., Ko, H. J., Ryu, S., and Kweon, M. N. (2014). A Mouse Model of Shigellosis by Intraperitoneal Infection. *J. Infect. Dis.* 209 (2), 203–215. doi:10.1093/infdis/jit399

Young, C., Walzl, G., and Du Plessis, N. (2020). Therapeutic Host-Directed Strategies to Improve Outcome in Tuberculosis. *Mucosal Immunol.* 13 (2), 190–204. doi:10.1038/s41385-019-0226-5

Yuk, J. M., Shin, D. M., Lee, H. M., Yang, C. S., Jin, H. S., Kim, K. K., et al. (2009). Vitamin D3 Induces Autophagy in Human Monocytes/macrophages via Cathelicidin. *Cell Host Microbe* 6 (3), 231–243. doi:10.1016/j.chom.2009.08.004

Conflict of Interest: The authors declare that the research was conducted in the absence of any commercial or financial relationships that could be construed as a potential conflict of interest.

Publisher's Note: All claims expressed in this article are solely those of the authors and do not necessarily represent those of their affiliated organizations, or those of the publisher, the editors, and the reviewers. Any product that may be evaluated in this article, or claim that may be made by its manufacturer, is not guaranteed or endorsed by the publisher.

Molecular Medicine

RESEARCH ARTICLE

Open Access

Glycyrrhizin, an inhibitor of HMGB1 induces autolysosomal degradation function and inhibits *Helicobacter pylori* infection

Uzma Khan[1], Bipul Chandra Karmakar[2], Priyanka Basak[1], Sangita Paul[2], Animesh Gope[3], Deotima Sarkar[1], Asish Kumar Mukhopadhyay[2], Shanta Dutta[2] and Sushmita Bhattacharya[1*]

Abstract

Background *Helicobacter pylori* is a key agent for causing gastric complications linked with gastric disorders. In response to infection, host cells stimulate autophagy to maintain cellular homeostasis. However, *H. pylori* have evolved the ability to usurp the host's autophagic machinery. High mobility group box1 (HMGB1), an alarmin molecule is a regulator of autophagy and its expression is augmented during infection and gastric cancer. Therefore, this study aims to explore the role of glycyrrhizin (a known inhibitor of HMGB1) in autophagy during *H. pylori* infection.

Main methods Human gastric cancer (AGS) cells were infected with the *H. pylori* SS1 strain and further treatment was done with glycyrrhizin. Western blot was used to examine the expression of autophagy proteins. Autophagy and lysosomal activity were monitored by fluorescence assays. A knockdown of HMGB1 was performed to verify the effect of glycyrrhizin. *H. pylori* infection in in vivo mice model was established and the effect of glycyrrhizin treatment was studied.

Results The autophagy-lysosomal pathway was impaired due to an increase in lysosomal membrane permeabilization during *H. pylori* infection in AGS cells. Subsequently, glycyrrhizin treatment restored the lysosomal membrane integrity. The recovered lysosomal function enhanced autolysosome formation and concomitantly attenuated the intracellular *H. pylori* growth by eliminating the pathogenic niche. Additionally, glycyrrhizin treatment inhibited inflammation and improved gastric tissue damage in mice.

Conclusion This study showed that inhibiting HMGB1 restored lysosomal activity to ameliorate *H. pylori* infection. It also demonstrated the potential of glycyrrhizin as an antibacterial agent to address the problem of antimicrobial resistance.

Keywords *Helicobacter pylori*, Autophagy, Glycyrrhizin, HMGB1, LMP

Background

Infection with *Helicobacter pylori* is one of the key factors responsible for causing gastric disorders and a major risk factor for progression to gastritis and gastric cancer. It is a gram-negative bacterium that has evolved with the ability to colonize and take refuge in epithelial cells of the stomach (Khatoon et al. 2016; Li et al. 2017; Jung et al. 2017; González et al. 2021). This is considered as one of the possible reasons owing to the rise of antibiotic resistance

*Correspondence:
Sushmita Bhattacharya
durgasushmita@gmail.com
[1] Division of Biochemistry ICMR-NICED, ICMR-National Institute of Cholera and Enteric Diseases (ICMR-NICED), Kolkata 700010, India
[2] Division of Bacteriology ICMR-NICED, ICMR-National Institute of Cholera and Enteric Diseases (ICMR-NICED), Kolkata 700010, India
[3] Division of Clinical Medicine, ICMR-NICED, ICMR- National Institute of Cholera and Enteric Diseases (ICMR-NICED), Kolkata, India

of *H. pylori* (Tshibangu-Kabamba et al. 2021; Thung et al. 2016). On account of this, WHO has considered *H. pylori* in the high-priority pathogens list (Shrivastava et al. 2018). Mounting evidence suggests that reprogramming host cellular pathways are an obligatory facet of *H. pylori* infection (Chmiela et al. 2017; Libânio et al. 2015Sierra et al. 2020). On the other end of the spectrum, to eliminate an incoming pathogen, the host often deploys several cellular defense strategies. Autophagy is one of the important pathways involved in recognizing and capturing intracellular bacteria for their degradation (Yang et al. 2016, 2018; Raju et al. 2012). *H. pylori* infection in epithelial cells often induces the host autophagic machinery during early infection while survival and colonization of *H. pylori* are favoured by inhibition of autophagy at later stages (Yang et al. 2018, 2022; Tang et al. 2012; Kim et al. 2018). *H. pylori* secreted effector proteins like CagA and VacA have an impact on autophagy during infection. CagA inhibits autophagy and helps in the survival of bacteria within the host (Terebiznik et al. 2009 and Tsugawa et al. 2019). Moreover, autophagy is dynamically altered in response to infection (Levine et al. 2011).

Prior studies have shown that High mobility group box 1 (HMGB1) is augmented during *H. pylori* infection (Lin et al. 2016). Research over the past has also established that HMGB1 induces pro-autophagic activities (Yin et al. 2017; Tang et al. 2010). However, the role of HMGB1-mediated autophagy in *H. pylori* infection is unknown. Keeping in mind this scenario of *H. pylori* infection and autophagy impairment; drug designing is inevitable as antibiotic resistance is well known. In this study, we have used an inhibitor of HMGB1, glycyrrhizin (Mollica et al. 2007) to explore the role of the autophagy-lysosomal pathway during *H. pylori* infection in both in vitro and in vivo conditions. Here, we observed that pharmacological inhibition of HMGB1 reduces *H. pylori* infection by inducing autophagosomal lysosomal maturation.

Methods

Helicobacter pylori culture

Helicobacter pylori, Sydney Strain SS1 (*cagA* +, *vacA* s2m2) were grown on brain heart infusion (BHI) agar (Difco, USA) containing 7% heat-inactivated horse serum (Invitrogen), antibiotics, and IsoVitaleX as mentioned previously (Saha et al. 2022). Plates were kept in a microaerophilic atmosphere at 37 °C for five to six days. Stock cultures were stored at − 70 °C for further usage. Isolates were re-streaked on fresh BHI agar and incubated for 24 h which was used for experimental studies. *H. pylori* resistant strain [OT-14(3)] (*cagA-*, *vacA* s2m2), (clarithromycin, metronidazole resistant) isolated from a gastric cancer patient at IPGMER and SSKM hospital, Kolkata was cultured with the same protocol.

Cell culture

The human gastric cancer cell line AGS was gifted by Dr. Asish Kumar Mukhopadhyay (ICMR-NICED, Kolkata). AGS cells were grown in F12 media (Sigma-Aldrich) supplemented with 10% heat-inactivated FBS (Sigma, USA), 1% penicillin–streptomycin (Sigma, USA), and maintained in an incubator at 37 °C and 5% CO_2.

In vitro infection assay

A cell density of 0.5×10^6 per 60 mm cell culture dish was plated. *H. pylori* SS1 culture was dissolved in sterile phosphate-buffered saline (PBS) and adjusted to an OD of 1 at 600 nm followed by centrifugation at 10,000 g for 10 min. The cells were starved overnight in 2 mL antibiotic and FBS- free incomplete F12 media. Cells were further infected with or without *H. pylori* with a multiplicity of infection (MOI) 1:100 for 4 h followed by gentamicin (100 μg/ml) treatment for 1 h, to kill the extracellular bacteria. Cells were then washed with PBS and incubated in fresh medium and treatment was done with glycyrrhizin GLZ (200 μM) for another 4 h. Cell lysis was performed by adding 0.1% saponin for 15 min at room temperature and serial dilution was prepared and then 100μL of diluted suspension were plated on BHIA plates to determine the number of invaded bacteria into the AGS cells. Colonies were then counted after 5–7 days of incubation. The CFU was determined by plating various serial dilutions of these bacterial suspensions on BHI agar plates (Hu et al. 2019). A similar assay was also performed for the *H. pylori*-resistant strain [OT-14(3)] with or without glycyrrhizin for 4 h. In the case of chloroquine and bafilomycin treatment, cells were infected with or without *H. pylori* with an (MOI) 1:100 for 4 h followed by gentamicin treatment for 1 h and further treatment was done with glycyrrhizin (200 μM) and/or chloroquine (50 μM) and/or bafilomycin (50 nM) for 4 h and/or 18 h.

Real-time PCR

Further, cDNA was prepared from RNA utilizing a Thermo Scientific cDNA synthesis kit. SYBR green kit of Applied Biosystems was used for Quantitative PCR. ΔΔCt method was used to calculate and normalization was performed with the housekeeping gene control GAPDH. ΔΔCt = test − internal control-test control. The relative density of *H. pylori* was quantified by performing semi-quantitative PCR, detecting *H. pylori*- specific 16S-ribosomal DNA (rDNA) primer, FP (5′-AGAGAA GCAATACTGTGAA- 3′) & RP (5′-CGATTACTAGCG ATTCCA- 3′). GAPDH was measured for normalization, FP (5′-GTCTTCACCACCATGGAGAAGGC-3′), and RP

(5′-CATGCCAGTGAGCTTCCCGTTCA-3′). The PCR efficiency for both the test gene (93%) and GAPDH (96%) are within the desired efficiency range which is 90–105% (Kralik et al. 2017).

Immunofluorescence

For immunofluorescence staining, cells were fixed in 4% paraformaldehyde at room temperature for 1 h and blocked in PBS containing 3% BSA and 0.01% Triton X100 for 1 h. Next, coverslips were incubated with anti-LAMP1 and anti-Galectin-3 at 4 °C overnight. Subsequently, secondary antibody incubation was done using TRITC-conjugated anti-rabbit secondary antibody (1:1000) (Cat# AP132R) and FITC- conjugated anti-mouse secondary antibody (1:1000). Lastly, the coverslips were mounted on glass slides by adding ProLong™ Gold Antifade reagent with DAPI (Thermo Fisher) and examined using an inverted confocal microscope (Carl Zeiss LSM 710). For LAMP1 and LC3B immunofluorescence staining, the same protocol was followed.

Transfection of plasmid and siRNA

The tandem fluorescent LC3B (tfLC3B) plasmid was a gift from Dr. Dhiraj Kumar ICGEB, New Delhi, India. To examine autophagosomes and autolysosomes, AGS cells were transiently transfected with tf-LC3B plasmid using Lipofectamine 2000 (Invitrogen). 48 h after transfection, cells were incubated with or without *H. pylori* and treated with glycyrrhizin. In the end, coverslips were mounted on ProLong™ Gold Antifade reagent with DAPI (Thermo Fisher) and imaged using an inverted confocal microscope. The following siRNAs were purchased from IDT: ATG5siRNA (ID hs.Ri. ATG5.13.1) and HMGB1 siRNA (ID hs.Ri.HMGB1.13.1) and used for transfection at 70% confluence with siRNA/ Non-specific siRNA using lipofectamine 2000 in a 35 mm dish. 48 h after transfection, cells were infected with or without *H. pylori* as described.

Live-cell confocal microscopy

AGS cells (2×10^5) were seeded on coverslips. After 24 h, cells were incubated with *H. pylori* (MOI 100) for 4 h followed by drug treatment for 4 h.

GFP-LAMP1

To monitor the lysosomes expressing LAMP1, *H. pylori*-infected and drug-treated AGS cells were subjected to live-cell imaging by adding 5 µl of baculovirus expressing Lamp1-GFP construct (Cell Light™ Lysosomes-GFP, BacMam 2.0, #C10507) for 16 h. Finally, cells were observed in the confocal microscope.

LysoTracker staining

To investigate the acidification of lysosomes, cells were incubated with LysoTracker Red DND-99 (Invitrogen, L7528) for 30 min. Cells were then observed under an inverted confocal microscope.

Dextran staining

Lysosomal destabilization was examined using Dextran, Alexa Fluor™ 488, and 10,000 MW (D22910, Invitrogen). Cells were incubated with 200 µg/ml dextran for 2 h at 37 °C after infection and drug treatment was then observed under an inverted confocal microscope.

MTT assay

Cellular toxicity was examined using a Colorimetric Cell Viability Kit (MTT) (Promokine) in 96-well plates. MTT reagent (3-(4,5-dimethylthiazol-2-yl)-2,5-diphenyltetrazolium bromide) was added and kept for 4 h. Purple crystal formazan formed was solubilized with DMSO. The amount of formazan salt was measured in a microplate reader (Bio-Rad Serial no. 19901) at an OD of 590 nm.

Measurement of reactive oxygen species (ROS) levels

Intracellular ROS levels were monitored by using 2,7-dichlorodihydrofluorescein diacetate (DCFH-DA). 10 µM of DCFH-DA was added to control, infected, and drug-treated cells for 30 min and kept at 37 °C. Excess DCFH-DA was washed with PBS three times. Finally, fluorescence was monitored (Ex-485 nm and Em-520 nm) using a multimode reader, Molecular devices Spectramax M2.

Immunoblotting

Control, drug-treated and infected cells were lysed in RIPA (Radio immunoprecipitation assay buffer) lysis buffer containing protease and phosphatase inhibitors. After cell lysis, centrifugation was done at 7000 rpm for 20 min at 4 °C. Further, protein level was determined and run on 10% or 12.5% SDS- PAGE gel at 120 V. Gels were further transferred to the PVDF membrane. 5% skimmed milk dissolved in TBST (20 mM Tris–HCl, 150 mM NaCl, 0.1% Tween20) buffer was used for blocking and incubated for 1 h at room temperature. In the next step, the membranes were kept overnight with primary antibodies at 4 °C. Eventually, after secondary antibody incubation, membranes were developed and scanned in a ChemiDoc. The primary antibodies used are rabbit polyclonal Anti-SQSTM1/P62 antibody (Cat# ab91526), rabbit monoclonal anti- ATG5 (Cat #ab228668), mouse monoclonal anti- LAMP1 (Cat# 15665S), rabbit monoclonal anti-beclin1 antibody (Cat

#ab207612), rabbit polyclonal anti-LC3B antibody (Cat#ab51520), mouse polyclonal anti-β-actin (Cat #sc-47778), mouse monoclonal anti-Galectin-3 (Cat #sc-53127), rabbit polyclonal anti-α-Tubulin (Cat #BB-AB0118), anti-rabbit secondary HRP-conjugate (Cat #12-348), anti-mouse secondary HRP-conjugate (Cat #12-349).

Enzyme-linked immunosorbent assay (ELISA)

Pro-inflammatory cytokine (IL-8, IL-6) levels from media and serum were estimated using the Krishgen Biosystems kit as per the manufacturer's instructions. All experiments were done in triplicate.

H. pylori infection in C57BL/6 mice and treatment with glycyrrhizin

Mice were maintained in the animal house under 12-h dark–light cycles. Experiments were conducted under the guidelines of the Institutional Animal Ethical Committee, NICED, Kolkata (PRO/157/- 260 July 2022). 8 weeks of male C57BL/6 mice bred in-house were used for the experiments. Three different experimental sets of mice were grouped: Control group (CON), n = 5, *H. pylori* SS1 infected group (HP), n = 5, infected group treated with GLZ (HP + GLZ), n = 5. All groups of mice were treated every day for seven days with an antibiotic cocktail (Ciprofloxacin, Metronidazole, Erythromycin, Albendazole) to avoid any other bacterial/ parasite infections. A Group of mice (HP & HP + GLZ) were inoculated with 10^8 CFU/mouse/inoculation of *H. pylori* SS1 on three alternative days or PBS (CON). After two weeks of inoculation, a group of mice (HP + GLZ) was orally injected with glycyrrhizin (10 mg/kg) for 4 weeks, while a group of mice (CON) received sterile water. At the end of week 4, all mice were sacrificed. Gastric tissues were isolated and blood was collected for experimental purposes as described previously (Saha et al. 2022). Experiments were repeated three times. The total number of mice in each set of experiments was 15.

Statistical analysis

All data were represented as mean ± S.E.M. Two groups were compared using an Unpaired t-test, and multiple comparisons were done by one-way ANOVA. The significance level has been marked as, * for $p < 0.05$, which implies significance, ** for $p < 0.01$, which implies very significance, and *** for $p < 0.001$, which implies highly significant.

Results

Glycyrrhizin induces autophagy in gastric epithelial cells

Previous reports indicated that glycyrrhizin induces autophagy in myoblast cells but there are no such reports in gastric cells till date (Lv et al. 2020). Here, we checked the expression levels of different autophagy proteins upon glycyrrhizin treatment in AGS gastric cancer cells. Glycyrrhizin treatment for 4 h elevated the expression of autophagy proteins LC3B-II and LAMP1 in a dose-dependent manner (100 μM, 200 μM). At 50 μM dose of glycyrrhizin, expression of LC3B-II and also LAMP1 was found to be almost the same. At 100 μM dose of glycyrrhizin treatment, although LC3B-II and LAMP1 increased but it was not statistically significant (p value for LC3B-II is 0.2334 and for LAMP1 is 0.3152). Interestingly, further increase in glycyrrhizin concentration e.g., at 200 μM dose, expression of LC3B-II increased significantly by 1.5 fold change (p value: 0.0136) and LAMP1 increased by 1.65 fold change (p value: 0.0419). On the other hand, glycyrrhizin reduced HMGB1 expression with an increase in concentration such as at 50 μM by 1.3 fold change (p value: 0.0332), at 100 μM by 1.4 fold change (p value: 0.0175) and at 200 μM by 2.4 fold change (p value: 0.0011) respectively (Fig. 1A). The most effective dose was 200 μM. To examine the possibility of toxicity of glycyrrhizin on AGS cells, we checked the effect of glycyrrhizin on the viability of AGS cells (Additional file 1: Fig. S1A). Glycyrrhizin treatment for 24 h at different concentrations (50, 100, 200 μM) did not show significant toxicity. Further, we confirmed glycyrrhizin-induced autophagy by immunofluorescence of LC3B. Drug treatment for 4 h showed a significant enhancement of LC3B puncta formation by 3.2 fold change (unpaired t-test and p value: 0.0071) (Fig. 1B). Subsequently, we assessed the effect of glycyrrhizin-induced autophagosomal maturation in gastric cancer cells. LAMP1 is known to be a marker for lysosomal activity, therefore, we labeled lysosomes with LAMP1-GFP construct after exposure to glycyrrhizin treatment. Subsequently, glycyrrhizin induced LAMP1 expression significantly by a factor of 1.587 (p value: 0.0191) in live cells as compared to control (Fig. 1C). Together, these results suggest that glycyrrhizin induces an autophagic response in gastric cells.

Glycyrrhizin-induced autophagy inhibits intracellular *H. pylori* growth

Since *H. pylori* is known to invade gastric epithelial cells, we examined the effect of drug treatment on the expression of autophagy proteins by immunoblotting in *H. pylori*-infected gastric cancer cells. *H. pylori* Sydney Strain SS1 was used for infection in gastric cells for 4 h and post-treatment was done with 200 μM glycyrrhizin (4 h). We observed upregulation of LC3B-II by 1.38 fold (p value: 0.0254) and LAMP1 by 1.74 (p value: 0.0028) in glycyrrhizin-treated *H. pylori*-infected cells as compared to the only *H. pylori*-infected cells (Fig. 2A). Moreover, LC3B-II by 1.63 fold (p value: 0.0123) and LAMP1 by

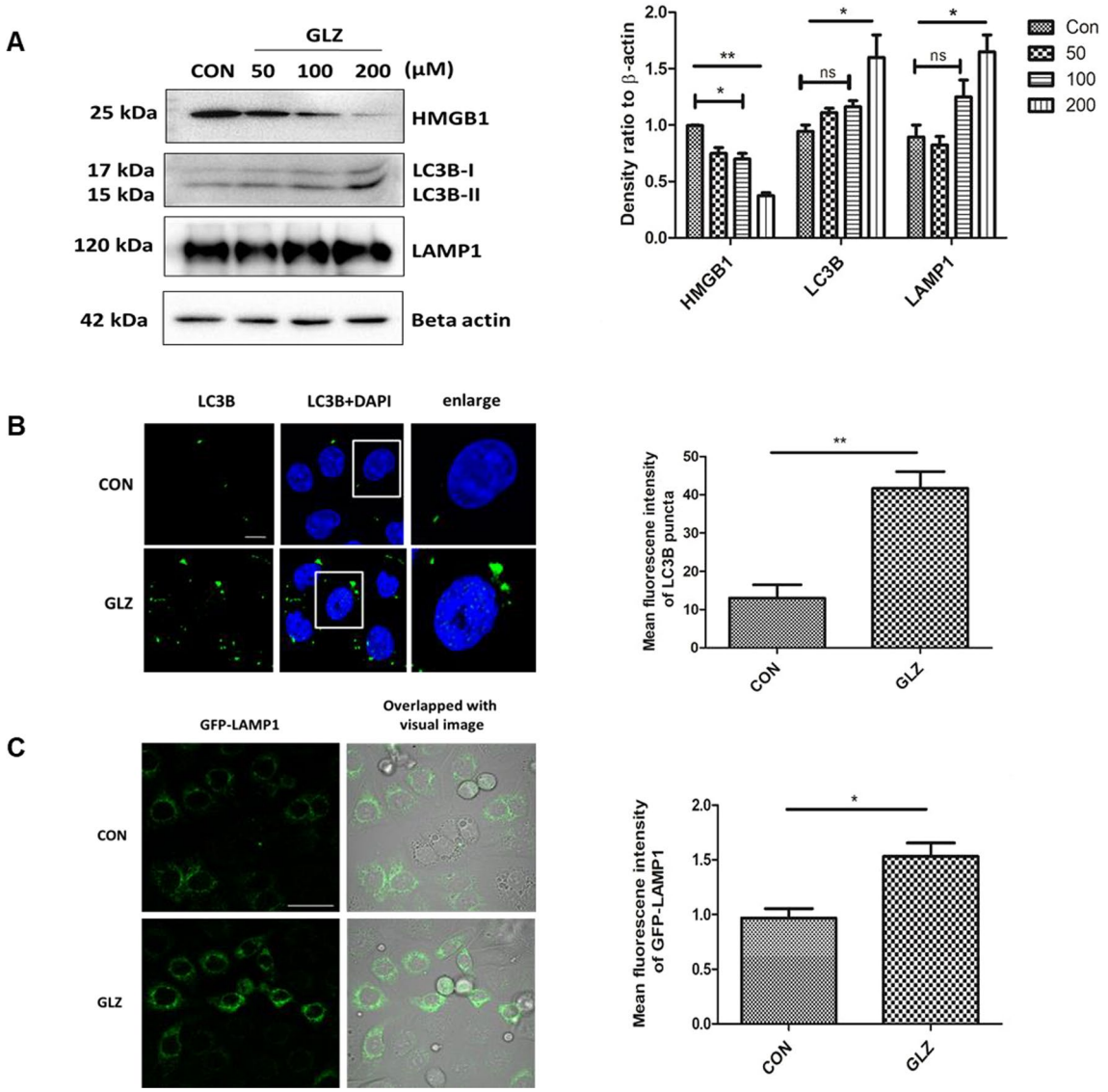

Fig. 1 Glycyrrhizin treatment overexpresses autophagy proteins. AGS cells were treated with glycyrrhizin GLZ (200 μM) or DMSO for 4 h **a** Cell lysates were prepared and expression level of HMGB1 and autophagy marker proteins LC3B-II and LAMP1 was observed by western blot analysis. Beta-actin was used as a protein loading control. Densitometry analyses are represented graphically. **b** Control and drug-treated cells were subjected to immunofluorescence and changes in the mean fluorescence intensity were measured. Scale bar: 5 μm. Confocal microscopy showed LC3B puncta (green) formation. LC3B puncta formation was quantified and graphically plotted. **c** Live cell imaging was performed using a construct, LAMP1-GFP for labeling lysosomes under confocal microscopy. Fold change in the mean fluorescence intensity of GFP-LAMP1 was calculated. Scale bar: 10 μm. Graphs were represented as mean ± SEM (n = 3); Unpaired t-test was done and significance was calculated; *p < 0.05 and **p < 0.01

1.5 fold (p value: 0.0002) were also upregulated in glycyrrhizin-treated control cells as previously explained in (Fig. 1A, B). To verify the findings of LC3B and LAMP1 expression, we additionally performed an immunofluorescence assay and live-cell analysis of drug-treated and *H. pylori*-infected cells. Consistently, in comparison to untreated infected cells, glycyrrhizin treatment resulted in 2.5 fold (p value: 0.0252) increased LC3B puncta formation and 2.3 fold (p value: 0.0347) higher LAMP1 expression (Fig. 2B, C). The results showed that autophagosomal and lysosomal activities are increased by glycyrrhizin.

Next, we sought to examine the effect of autophagy induction on intracellular bacterial growth. We performed real-time PCR (RT-PCR) and checked *H. pylori*-specific 16SrDNA. Intracellular *H. pylori* level was significantly reduced by glycyrrhizin treatment for 4 h by 2.08 fold (p value: 0.0381) and 18 h by 2.7 fold (p value: 0.0037)

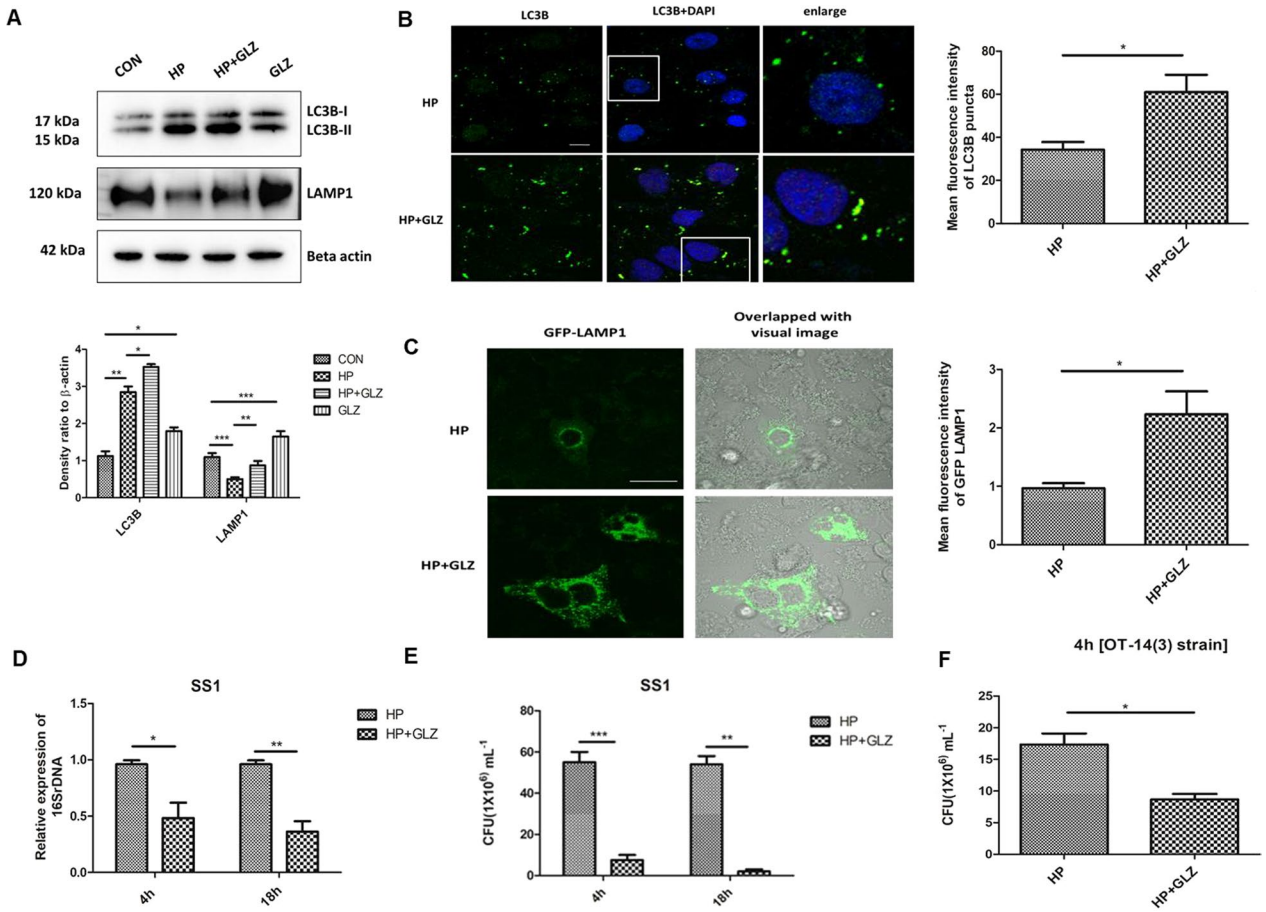

Fig. 2 Exposure to Glycyrrhizin reduces intracellular *H. pylori* growth in AGS cells. **a–c** Infection with *H. pylori* SS1 strain (MOI 100) was performed in cells for 4 h and further exposed to glycyrrhizin (GLZ) (200 µM) for 4 h. **a** Immunoblotting was performed for quantification of autophagy-associated marker proteins (LC3B-II and LAMP1). Beta-actin was used as a loading control. Densitometry analyses are represented graphically. One-way ANOVA was performed. **b** Confocal microscopy showed LC3B puncta (green) in *H. pylori* (HP) infected & *H. pylori* + glycyrrhizin (HP + GLZ) treated cells, LC3B puncta formation was quantified and change in the mean fluorescence intensity was measured and graphically plotted. Scale bar: 5 µm. **c** Live cell imaging of LAMP1 under confocal microscopy showed GFP-LAMP1 puncta formation. Fold change in the mean fluorescence intensity of GFP-LAMP1 was calculated, unpaired t-test was performed and graphically represented Scale bar: 10 µm. **d, e** Cells were incubated with *H. pylori* SS1 strain (MOI 100) for 4 h followed by gentamicin treatment to kill extracellular bacteria. Finally, cells were treated with glycyrrhizin GLZ (200 µM) at two different time points for 4 h and 18 h **d** Intracellular *H. pylori* DNA (16SrDNA) was determined by real-time PCR. GAPDH was used as the internal control. **e** Cells were lysed and plated on BHIA plates with serial dilutions, for 4–5 days for counting colonies and CFU/ml was graphically represented. **f** Infection with *H. pylori* resistant strain [OT-14(3)] (MOI 100) for 4 h was performed in gastric cells followed by glycyrrhizin GLZ (200 µM) treatment for 4 h and CFU/ml was graphically represented. Graph were represented as mean ± SEM (n = 3); Unpaired t-test was done and significance was calculated; *p < 0.05, **p < 0.01 and ***p < 0.001

(Fig. 2D). Of interest, we additionally examined the bacterial proliferation by bacterial adhesion assay. In line, intracellular *H. pylori* burden decreased significantly due to drug exposure for 4 h by tenfold (p value: 0.0005) and 18 h by 14.7 (p value: 0.0011) (Fig. 2E). Since antimicrobial resistance is a problem to curb *H. pylori* infection, we treated a resistant strain of *H. pylori* with glycyrrhizin for 4 h in AGS cells. Glycyrrhizin significantly reduced the growth of *H. pylori*-resistant strain [OT-14 (3)] by a factor of 2.0 (p value: 0.0117) (Fig. 2F). However, glycyrrhizin failed to reduce *H. pylori* growth in BHIA media which indicates glycyrrhizin has no direct bactericidal effect on *H. pylori* at 200 µM concentration (Additional file 1: Fig. S2A). Taken together, these data indicate that glycyrrhizin induces autophagy in gastric cancer cells and inhibits intracellular *H. pylori* growth.

Enhancement of autophagic flux by glycyrrhizin contributed to anti-*H. pylori* activity

As *H. pylori* infection is involved in defective autophagosomal lysosomal maturation and degradation, we determined the effect of glycyrrhizin on autophagic flux. To assess the activation of autophagic flux by glycyrrhizin, we performed a double-immunofluorescence assay for both LC3B and LAMP1 protein. Results demonstrated that both LC3B and LAMP1 colocalized in *H. pylori*-infected and glycyrrhizin-treated infected cells (Fig. 3A). The data indicated that glycyrrhizin-induced autophagosomal lysosomal maturation by 1.8 fold (p value: 0.0125). Next, we examined the stage of glycyrrhizin-mediated autophagic degradation in both autophagosomes and lysosomes by transfecting the AGS cells with tandem fluorescent LC3B (tfLC3B) plasmid. In the case of *H. pylori*-infected gastric cells, autophagosomes appeared as yellow dots due to the colocalization of both GFP and RFP (fold change: 3.8 and p value: 0.0004). On the other hand, we observed more free red dots as GFP and RFP did not colocalize in infected cells followed by glycyrrhizin treatment (fold change: 1.5 and p value: 0.0238). Autolysosomes appear red due to the acidic pH of lysosomes which quench GFP (Fig. 3B). All together, these

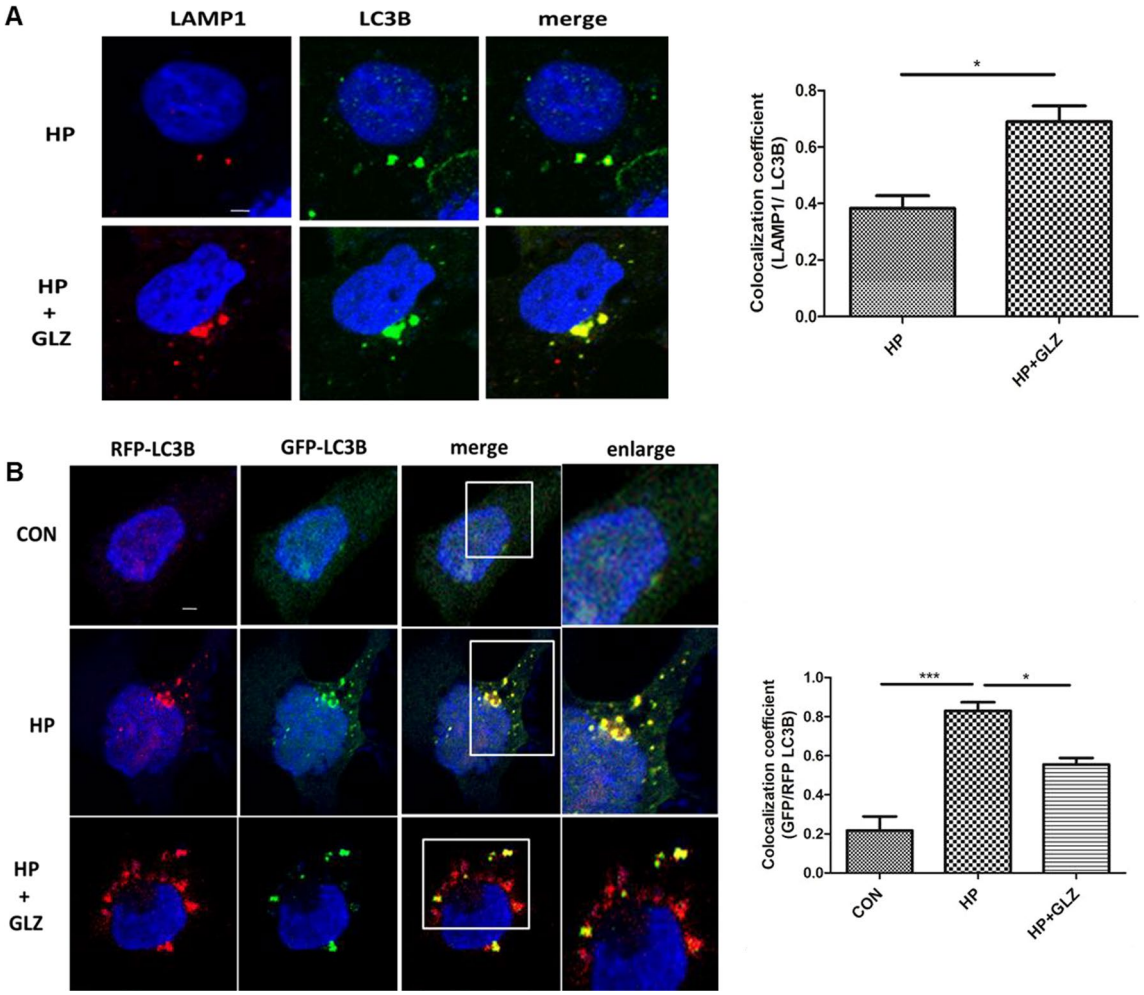

Fig. 3 Activation of autophagic flux by glycyrrhizin treatment **(a, b)** Cells were incubated with *H. pylori* SS1 strain (4 h) followed by glycyrrhizin GLZ (200 μM) exposure for 4 h. **a** Glycyrrhizin (GLZ) exposure to *H. pylori*-infected cells for 4 h was subjected to LAMP1 and LC3B double immunofluorescence. Confocal microscopy showed yellow puncta with co-localization of LC3B puncta (green) & LAMP1 (red). Change in the co-localization coefficient of each group was calculated. Scale bar: 2 μm. **b** AGS cells were transfected with a tandem mRFP-GFP tag (tfLC3B) plasmid & further infected with *H. pylori* SS1 strain (MOI 100) for 4 h and finally, glycyrrhizin (GLZ) (200 μM) treatment was done for 4 h. Confocal microscopy showed LC3B puncta formation in control (CON), *H. pylori* (HP) infected & *H. pylori* + glycyrrhizin (HP + GLZ) treated cells. The yellow puncta showed autophagosomes. The free red puncta are autolysosomes. Change in the co-localization coefficient of each group was calculated. Scale bar: 2 μm. Graph represented as mean ± SEM (n = 3); Significance was determined by Unpaired t-test; *p < 0.05, ***p < 0.001

results revealed that glycyrrhizin prevents *H. pylori*-mediated inhibition of autolysosome formation in the infected cells by promoting lysosomal maturation.

Anti-*H. pylori* effect and autophagic degradation by glycyrrhizin is mediated through HMGB1 inhibition

To confirm or rule out the possible involvement of HMGB1 in *H. pylori* infection, AGS cells were transiently transfected with non-specific siRNA and HMGB1- specific siRNA followed by infection with *H. pylori* for 4 h and subjected to immunoblotting. Western blot revealed that HMGB1 is silenced in AGS cells after 48 h transfection (Additional file 1: Fig. S3A). HMGB1 knockdown elevated the level of LC3B-II by 2.2 fold change (p value: 0.0073)and LAMP1 by 1.3 fold (unpaired t-test and p value: 0.0018) significantly (Fig. 4A, B). In addition, we examined the level of intracellular *H. pylori* by RT-PCR. HMGB1 silencing attenuated intracellular *H. pylori* burden significantly by 5.9 fold (p value: 0.0001) (Fig. 4C).

Further, we confirmed the effect of glycyrrhizin on autophagic flux. One of the best targets of autophagic flux is p62. Hence, we checked the level of SQSTM1/p62, a key protein involved in autophagy. Western blotting showed that p62 is increased due to *H. pylori* infection at both 4 h (Fig. 4D) and 18 h (Fig. 4E) time points. Long-term exposure to *H. pylori*, resulted in p62 accumulation.

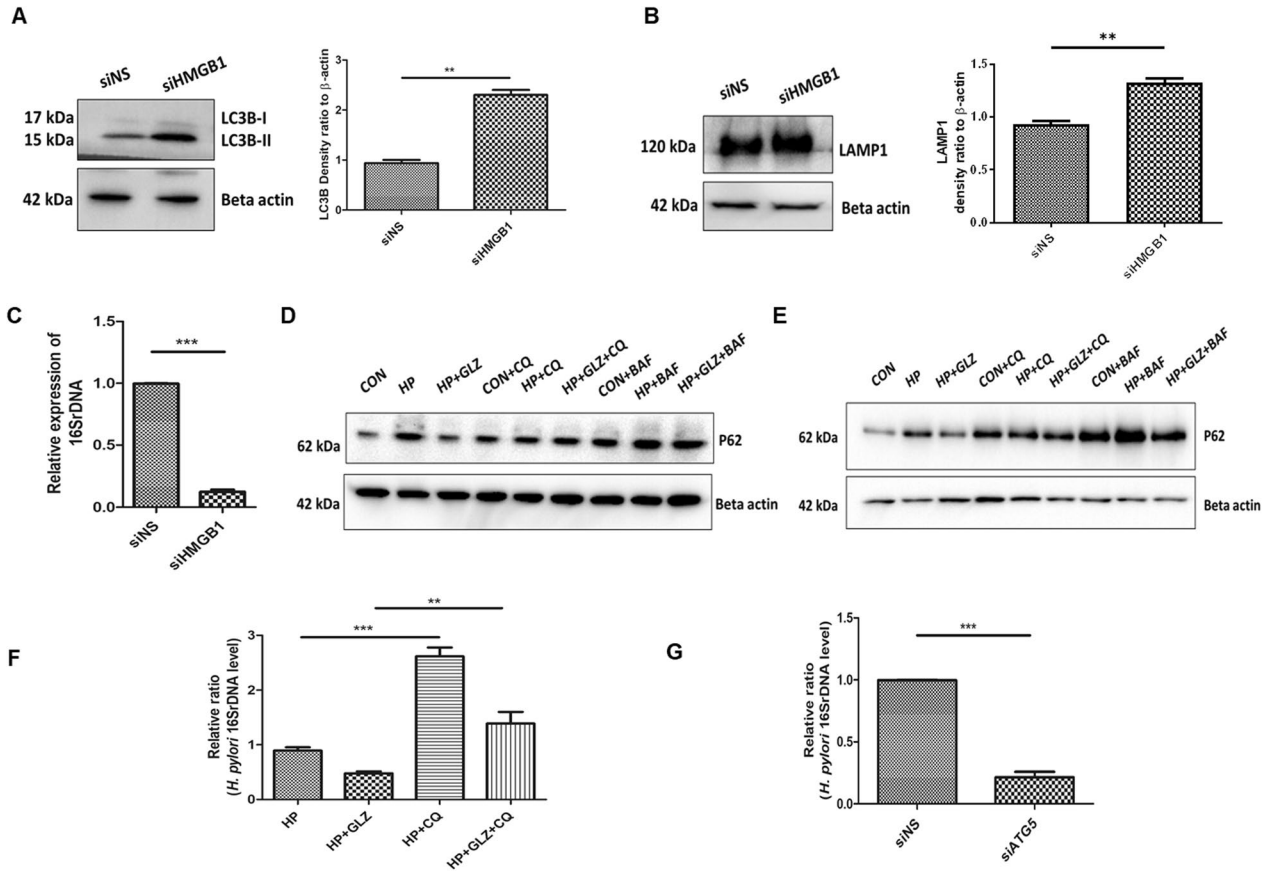

Fig. 4 HMGB1 inhibition reduces bacterial growth while impairment of lysosomal activity induces bacterial survivability. **a–c** After transfection for 48 h, nonspecific siRNA (siNS) and HMGB1 siRNA (siHMGB1) transfected cells were further infected with *H. pylori* SS1 strain (MOI of 100) for 4 h. **a, b** Immunoblotting was performed in infected cell lysates for expression of LC3B-II and LAMP1. Beta-actin was used as a protein loading control. Densitometry analyses are represented graphically. **c** Intracellular *H. pylori* DNA (16SrDNA) was determined by RT- PCR. GAPDH was used as the internal control. Unpaired t-test was performed **(d, e)** AGS cells incubated with the *H. pylori* SS1 strain for 4 h and 18 h followed by exposure to glycyrrhizin GLZ (200 μM) and/or chloroquine CQ (50 μM) and/or bafilomycin BAF (50 nM) for 4 h and 18 h treatment respectively. Cell lysates were subjected to a western blot to determine P62 protein levels for 4 h **(d)** and 18 h **(e)**. Beta-actin was used as a protein loading control. **f** AGS cells were incubated with the *H. pylori* SS1 strain for 4 h followed by exposure to glycyrrhizin GLZ (200 μM) and/or chloroquine CQ (50 μM) for 4 h. Intracellular *H. pylori* DNA (16SrDNA) was measured by RT- PCR. GAPDH was used as the internal control. **g** Cells were transfected with non-specific siRNA (siNS) and ATG5 siRNA (siATG5) & then incubated with *H. pylori* SS1 strain for 4 h, and intracellular *H. pylori* DNA was measured by RT- PCR. GAPDH was kept as an internal control. Graphs were represented as mean ± SEM (n = 3); One-way ANOVA was performed and significance was calculated; $^{**}p < 0.01$, $^{***}p < 0.001$

This is evident due to the impairment of autolysosomal degradation. On the other hand, glycyrrhizin treatment induces p62 degradation at 4 h and 18 h.

To validate the effect of glycyrrhizin on autophagic flux, we treated the AGS cells with chloroquine (CQ), a potent lysosomal inhibitor, and bafilomycin (BAF), specific for inhibition of autophagosomal lysosomal fusion and acidification. P62 accumulates in both *H. pylori*-infected and uninfected cells treated with glycyrrhizin after exposure to CQ and BAF. Additionally, we analyzed the effect of CQ on glycyrrhizin-mediated *H. pylori* clearance. Due to the blocking of autophagic flux, CQ promptly elevated *H. pylori* infection by 2.9 fold and counteracted the antimicrobial action of glycyrrhizin (p value: 0.0074) (Fig. 4F).

According to previous reports, *H. pylori* can survive within non-digestive autophagosomes (Raju et al. 2012). We analyzed the effect of Atg5 knockdown (Atg5 is an autophagy marker protein required for autophagosome formation) on intracellular *H. pylori* survival. Western blot showed that Atg5 is silenced in AGS cells after 48 h transfection (Additional file 1: Fig. S3B). Consistently, bacterial clearance occurred significantly by 4.6 fold due to the silencing of Atg5 (p value: 0.0001) (Fig. 4G). Cumulatively, these data demonstrated that *H. pylori* proliferate within autophagosomes inside the host while glycyrrhizin, an inhibitor of HMGB1 promotes autophagosomal lysosomal degradation which in turn reduces intracellular *H. pylori* growth.

Lysosomal acidification was recovered by glycyrrhizin

Further, we investigated in detail the restored lysosomal degradation capacity of glycyrrhizin. We performed Acridine Orange staining to monitor the acidic compartment of lysosomes in AGS cells. A lower red signal in *H. pylori*-infected cells was observed as compared to control because lysosomal acidification was compromised

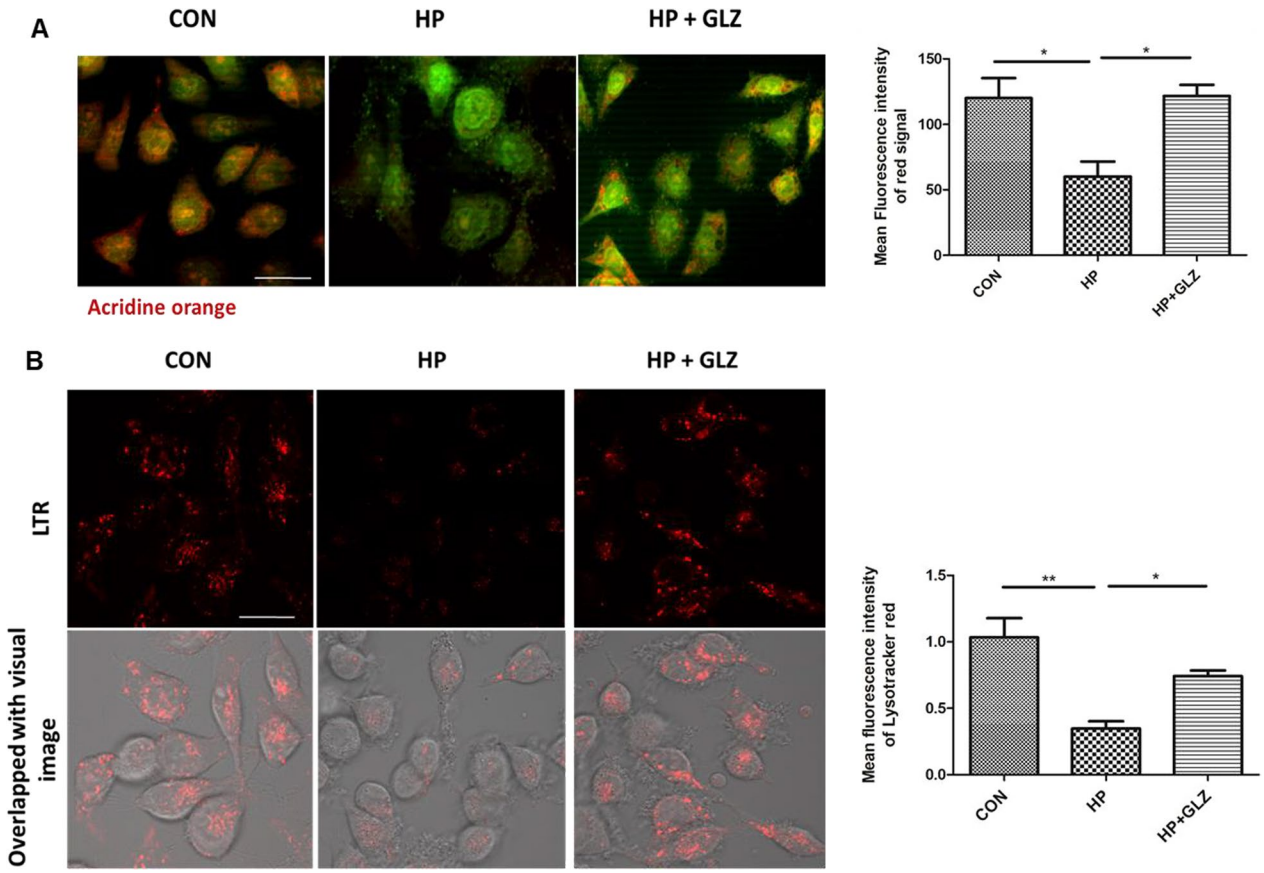

Fig. 5 Lysosomal function is restored by glycyrrhizin. **a–b** Infection with *H. pylori* SS1 strain (MOI 100) was performed for 4 h followed by glycyrrhizin (GLZ) (200 μM) exposure for 4 h. **a** Lysosomal membrane integrity was monitored by Acridine Orange (AO) staining in a fluorescence microscope. Briefly, cells were incubated with 10 μg/ml of acridine orange (15 min) and examined. The mean fluorescence intensity of the red signal was determined and graphically represented. Scale bar: 10 μm. **b** Live cell imaging of drug-treated, infected and control cells was done with LysoTracker Red incubation (100 nM, 30 min) to label lysosomes and mean fluorescence intensity was assessed under the confocal microscope. Scale bar: 10 μm. Fold change was quantified and graphs were generated using GraphPad Prism 5 and represented as mean ± SEM (n = 3); Significance was calculated by one-way ANOVA; *p < 0.05, **p < 0.01

whereas glycyrrhizin treatment increased red intensity by restoring lysosomal acidification by a factor of 2.0 (p value: 0.0263) (Fig. 5A). Additionally, to evaluate lysosomal acidification, we exposed the cells to Lysotracker Red which selectively binds to vesicles that have low pH. Here, *H. pylori* infection affected lysosomal pH and reduced the fluorescent signals as compared to the control. Glycyrrhizin exposure restored the acidic pH and showed red signals in infected cells as compared to only infected cells (fold change: 2.139 and p value: 0.0495) (Fig. 5B). The data indicates that glycyrrhizin restored the disrupted lysosomal function during *H. pylori*-infection.

Glycyrrhizin enhanced lysosomal degradation by inhibiting lysosomal membrane permeabilization (LMP)

According to previous reports, *H. pylori* reduced lysosomal degradation capacity due to lysosomal membrane permeabilization (LMP) (Bravo et al. 2019). Moreover, HMGB1 is also involved in LMP (Feng et al. 2022). Therefore, we determined whether the effect of glycyrrhizin in restoring lysosomal function is mediated by LMP. We performed double immuno-fluorescence of galectin3 and LAMP1. Colocalization of galectin3 with LAMP1 remarkably increased in *H. pylori* infection than control as galectin3 binds to lysosomal membrane glycoproteins which are exposed after LMP. But, glycyrrhizin treatment in infected cells reduced co-localization of galectin3 and LAMP1 probably due to inhibition of LMP (fold change: 2.07 and p value: 0.0074) (Fig. 6A). Additionally, we validated LMP by loading control, *H. pylori*-infected and drug-treated cells with Alexa Fluor conjugated dextran molecules. The redistribution of dextran was observed in infected cells (diffuse staining) indicating lysosomal efflux but not in the case of glycyrrhizin-treated infected

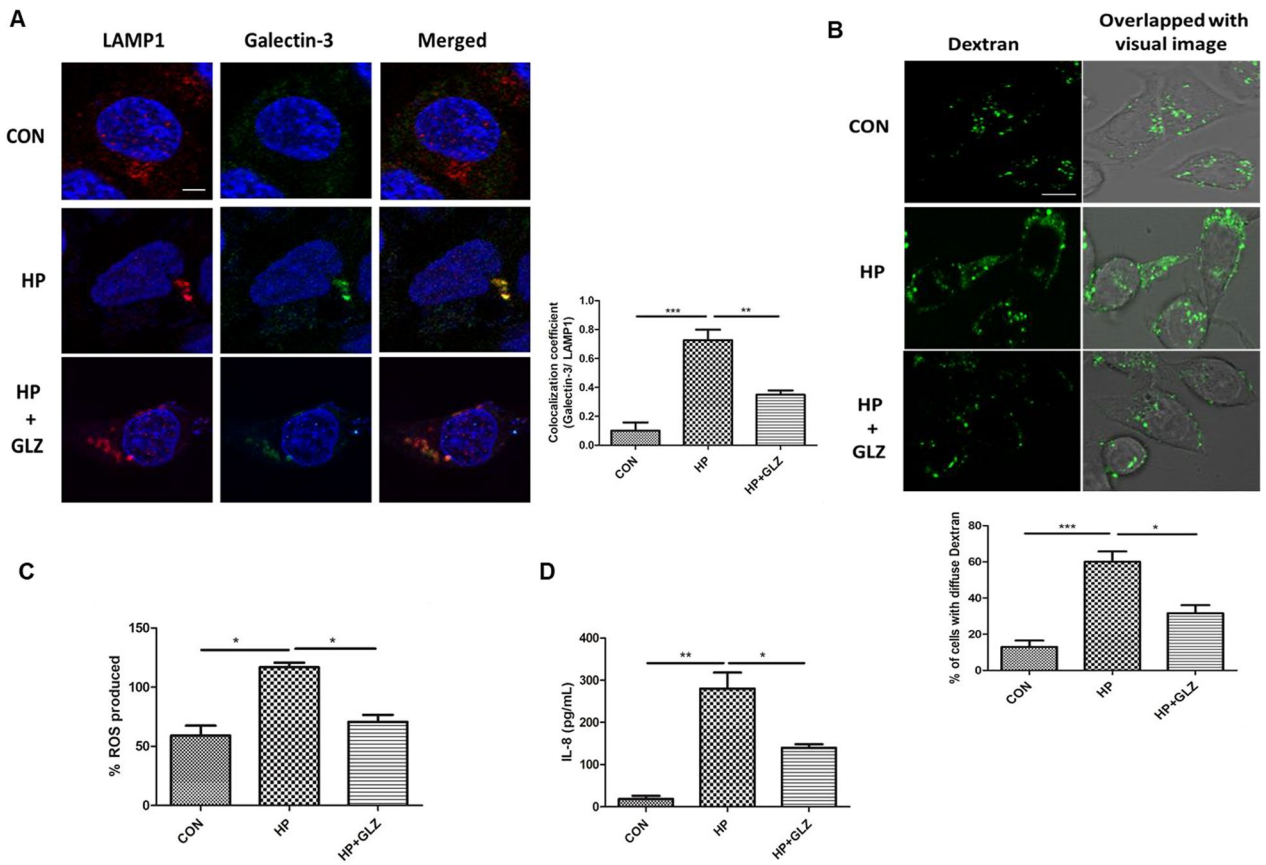

Fig. 6 Lysosomal membrane integrity is restored by glycyrrhizin. **a–d** Infection with *H. pylori* SS1 strain (MOI 100) was performed for 4 h followed by glycyrrhizin (GLZ) (200 μM) treatment (4 h). **a** Double immunofluorescence was done with LAMP1 & Galectin-3 antibodies to confirm LMP. Cells were observed under the confocal microscope and the difference in the co-localization coefficient of each group was calculated. Scale bar: 2 μm. **b** Lysosomal destabilization was estimated using live cell imaging after staining with dextran (0.5 mg/ml) for 2 h under the confocal microscope and the number of cells with diffused dextran was counted Scale bar: 5 μm. **c** Expression of reactive oxygen species (ROS) in infected and drug-treated cells was determined by DCFDA methods for 30 min in a fluorimeter. **d** The expression of IL-8 from media collected after treatment was analyzed by ELISA in a microplate reader. Graphs were generated using GraphPad Prism 5 and represented as mean ± SEM (n = 3); Significance was calculated by one-way ANOVA; *p < 0.05, **p < 0.01, ***p < 0.001

cells. Confined punctate structures of dextran indicated exclusive lysosomal localization in drug-treated cells (Fig. 6B). Subsequently, we examined the effect of the inhibition of LMP by glycyrrhizin on ROS and inflammatory cytokines as LMP is linked to inflammation and oxidative stress. In line, glycyrrhizin-exposed cells dramatically reduced both ROS levels (fold change: 1.65 and p value: 0.0289) and IL-8 secretion (fold change: 2 and p value: 0.0456) significantly as compared to only infected cells (Fig. 6C, D). Taken together, these data indicate that glycyrrhizin improved lysosomal degradation activity and induced protective effects by inhibiting LMP.

In in vivo mice model, glycyrrhizin induces autophagy and reduces gastric damages

Eventually, we validated the activity of glycyrrhizin in in vivo mice model. We have infected mice with the *H. pylori* SSI strain. After infection, mice were treated with glycyrrhizin for 30 days at a 10 mg/kg body weight dose (Additional file 1: Fig. S4A). The effective dose of glycyrrhizin was determined for *H. pylori*-infected mice from previous data on glycyrrhizin (Lv et al. 2020; Fu et al. 2014). We performed western blots with control, infected, and glycyrrhizin-treated-infected gastric tissues. Glycyrrhizin reduced the level of HMGB1 significantly by 1.64 fold (p value: 0.0262) and induced p62 degradation by 1.73 fold (p value: 0.0010) which is a marker of autophagosomal lysosomal degradation. It also strongly augmented LAMP1 expression by 7.55 fold (p value: 0.003) (Fig. 7A). Furthermore, we checked the effect of glycyrrhizin on IL-6 levels in the serum collected from treated mice. Glycyrrhizin significantly reduced IL-6 expression by a factor of 1.6 (p value: 0.0086) (Fig. 7B). To further assess the anti-*H. pylori* effect of glycyrrhizin, we examined gastric tissues for changes in morphology. There were changes in the gastric histopathology when

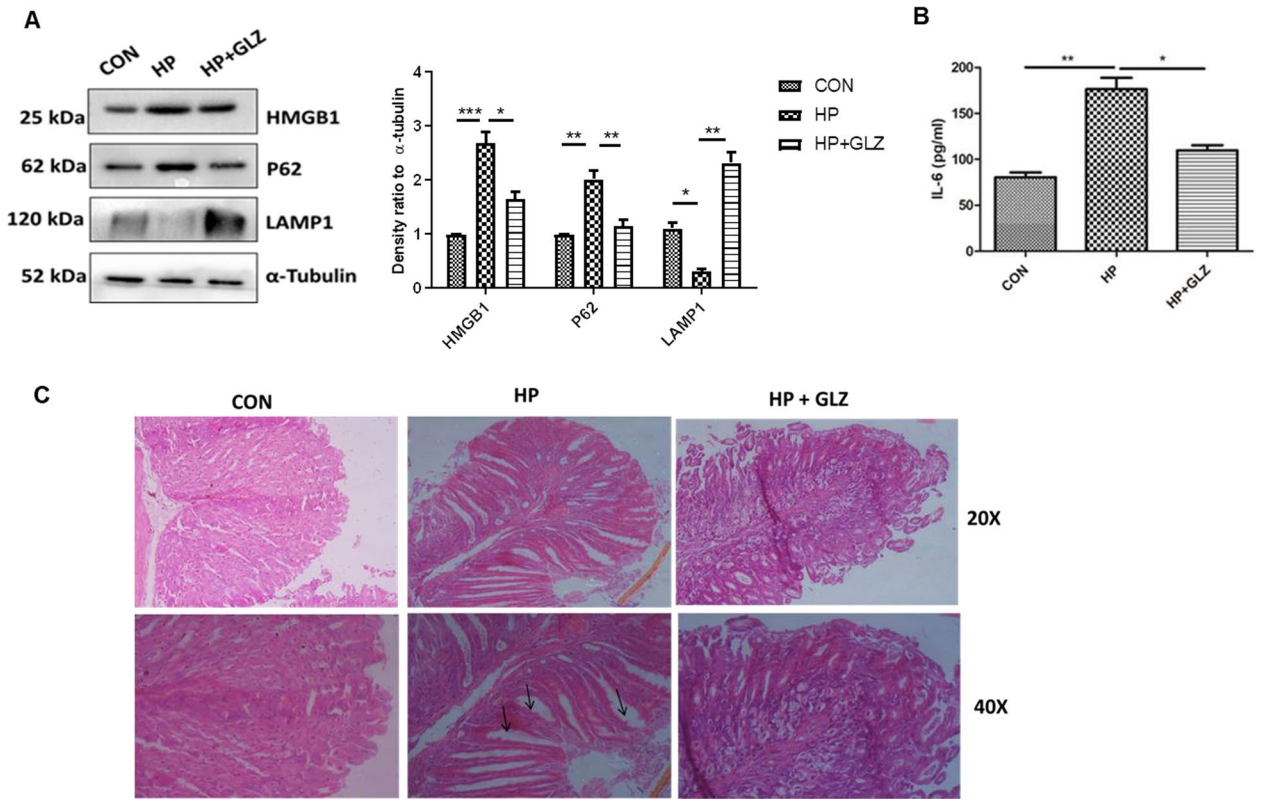

Fig. 7 Glycyrrhizin treatment induces autophagy in *H. pylori*-infected mice and ameliorates gastric tissue damage **(a–c)** C57BL/6 mice (n = 5 per group) were treated with antibiotics every 7 days. Then after 7 days incubation period, mice were infected with the *H. pylori* SS1 strain thrice a week on alternate days. Mice were incubated for 14 days and then administered with or without glycyrrhizin GLZ (10 mg /kg body weight), every day for 4 weeks. After treatment mice were sacrificed, and gastric tissues and serum were collected. **a** Immunoblot showing the expression of HMGB1 and autophagy proteins (HMGB1, P62, LAMP1) of mouse gastric tissues. α-tubulin was used as a protein loading control. Densitometry analyses are represented graphically. **b** The expression of IL-6 was determined by ELISA in a microplate reader. **c** Histology images of Control (CON), *H. pylori* (HP) infected, and *H. pylori*-infected plus glycyrrhizin treated (HP + GLZ) gastric tissues at 20X and 40X respectively representing the inflammatory changes. Black arrows (↑) indicate gastric tissue damages. Graphs were represented as mean ± SEM (n = 3); Significance was determined by one-way ANOVA; *p < 0.05, **p < 0.01, ***p < 0.001

compared with a control group for *H. pylori*-infected gastric tissues (Fig. 7C). *H. pylori*-induced inflammation and inflammatory cell infiltration in gastric tissues caused epithelial cell damage whereas glycyrrhizin reduced inflammation and repaired tissue damage. Hence, collectively these data revealed that glycyrrhizin induced autophagy and consequently decreased inflammation and gastric tissue damage in in vivo mice model.

Discussion

Current evidence suggests that autophagy plays a major role to protect the host from bacterial pathogens (Giraud-Gatineau et al. 2020; Kim et al. 2012). But the pathogens have their mechanisms to subvert autophagy and persistently invade the host and promote intracellular survival. *Salmonella*, *Shigella,* and *Mycobacterium* are known to avoid autophagy (Xie et al. 2020; Ogawa et al. 2005; Basak et al. 2022; Padhi et al. 2019). However, there are reports which showed that *H. pylori* induce autophagy at the beginning but gradually it inhibits autophagy (Yang et al. 2018; Tang et al. 2012). The mechanisms behind initial activation and subsequent impairment involve a complex interplay between host and bacterial factors. *H. pylori* secretes virulent factors like CagA and VacA (Raju et al. 2012). Both these factors contribute to pathogenesis. Although previous literature suggests that VacA induces autophagy but later it has been reported by Raju et al. that prolonged exposure to VacA inhibits autophagy (Raju et al. 2012; Terebiznik et al. 2009). Recent studies have also revealed that autophagy is down-regulated in *cagA* + strains as compared to *cagA* mutant strains. This inhibition of autophagy is accompanied by the accumulation of p62 and decreased LAMP1 expression (Li et al. 2017). Henceforth, in the current study, we have used the *H. pylori* SS1 strain which is *cagA* positive but expresses non-functional *vacA* and this strain is also capable of mice infection.

Here, we investigated the effect of HMGB1 inhibition during *H. pylori* infection. HMGB1 is reported to be overexpressed in *H. pylori*-infected gastric cells (Lin et al. 2016). Recent reports suggested that HMGB1 causes impairment of autophagy by inducing lysosomal membrane permeabilization (LMP) in diabetic retinopathy (Feng et al. 2022). Hence, we have targeted HMGB1 for treating *H. pylori* infection. Here, glycyrrhizin, an inhibitor of HMGB1 decreased the intracellular *H. pylori* burden in gastric cancer cells. To find out the details behind bacterial clearance, we observed that glycyrrhizin induces autophagy in gastric cells. This is consistent with previous studies of glycyrrhizin in myoblast cells (Lv et al. 2020). Glycyrrhizin treatment attenuated *H. pylori* infection and also induced the expression of autophagy marker proteins. Moreover, glycyrrhizin showed co-localization of both LC3B and LAMP1 in *H. pylori*-infected gastric cancer cells. We also observed that LAMP1 expression has increased due to glycyrrhizin treatment. This indicates autolysosome formation as LAMP1 expression is necessary for autophagosomal maturation (Tsugawa et al. 2019). Keeping in mind that antibiotic resistance of *H. pylori* is a major problem (Gene et al. 2003; Huang et al. 2017), glycyrrhizin was tested for its ability to eradicate the growth of resistant *H. pylori* strain in in vitro conditions. Glycyrrhizin successfully showed clearance of antibiotic-resistant *H. pylori.* In addition, transient knock-down of HMGB1 resulted in parallel to glycyrrhizin treatment, hence the probable mechanism behind the induction of autophagy by glycyrrhizin is due to its inherent anti- HMGB1 property. Bacterial clearance by autophagy induction is a general mechanism as recent reports revealed that autophagy inducers like vitamin D and statin controlled *H. pylori* infection (Hu et al. 2019; Liao et al. 2017). Further, we determined the effect of glycyrrhizin in the later stages of autophagy. Consistent with the results of initial autophagy induction, our results demonstrated that glycyrrhizin treatment augments lysosomal degradation resulting in reduced bacterial burden. It is reported that *H. pylori* induce p62 accumulation which is a characteristic feature of inhibition of autophagic flux. In contrast, glycyrrhizin treatment augmented p62 degradation to improve the autophagic flux. Subsequently, p62 accumulation was observed due to the inhibition of autophagosomal maturation and flux by chloroquine and bafilomycin**.** Glycyrrhizin further is unable to inhibit *H. pylori* growth due to CQ treatment indicating the involvement of autophagic flux during infection (Hu et al. 2019). To gain a deeper insight into autophagic activity by glycyrrhizin we searched for the probable mechanisms. Previous studies suggested that *H. pylori* survived in undigested autophagosomes (Raju et al. 2012). Consistently, we proved that Atg5 knockdown inhibited *H. pylori* growth as Atg5 is responsible for autophagosome formation. Furthermore, the accumulation of undigested autophagosomes results in lysosomal membrane permeabilization (LMP) (Feng et al. 2022). HMGB1 is associated with LMP causing defective lysosomal activity and *H. pylori* is also reported to have impairment of lysosomal acidification by inducing LMP (Bravo et al. 2019; Feng et al. 2022). In this study, inhibition of HMGB1 by glycyrrhizin rescued LMP in *H. pylori*-infected cells and further restored the degradative capacity of autophagy proving that LMP is responsible for the inhibition of autophagosome degradation. Moreover, we observed that lysosomal pH has been restored by glycyrrhizin using Lysotracker Red staining as acidic pH is extremely important for the proper digestive action of lysosomes. Further, we examined Alexa Fluor conjugated

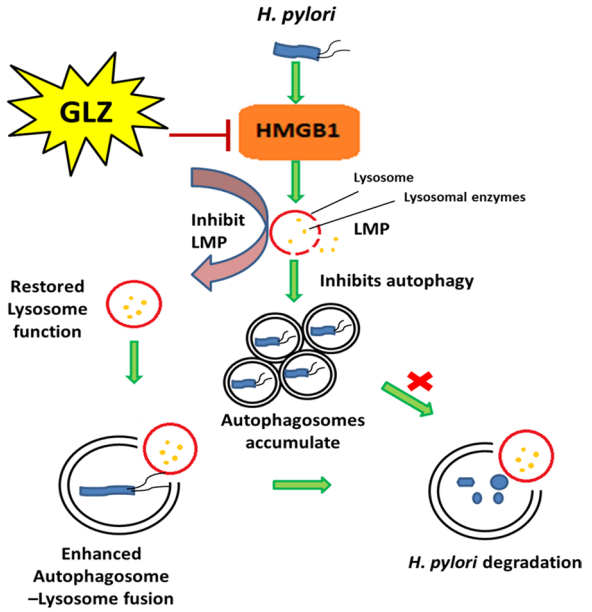

Fig. 8 Schematic diagram represents the mechanism that inhibiting HMGB1 induces autophagy through lysosomal membrane permeabilization(LMP). Glycyrrhizin inhibiting the HMGB1 expression induces autophagy by restoration of lysosomal membrane integrity. Recovered lysosomal membrane reduces LMP along with enhanced autolysosome formation which ultimately degrades the intracellular *H. pylori* from its gastric niche

dextran activity to inhibition of LMP by glycyrrhizin. Here, also we found that glycyrrhizin exposure reduced LMP by inducing consistent puncta formation of dextran granules indicating intact lysosomes whereas in infected cells diffuse staining is observed due to lysosomal efflux. Additionally, both HMGB1 and *H. pylori* infection are responsible for LMP (Bravo et al. 2019; Feng et al. 2022). Thus it has been proved that glycyrrhizin induces autophagy and lysosomal degradation by reducing LMP. Moreover, LMP is linked to the activation of ROS and inflammation (Kavčič et al. 2017). We evaluated the effect on ROS generation and cytokine expression. ROS level and inflammatory cytokine expression are commonly enhanced during infection (Hardbower et al. 2013). Consistently, the results showed that glycyrrhizin inhibited ROS production and inflammatory cytokine level in AGS cells. Therefore, our findings confirmed that inhibiting HMGB1 by glycyrrhizin induced autophagosomal maturation and lysosomal degradation in *H. pylori*-infected gastric cells by rescuing them from LMP.

Further, we verified our findings in in vivo mice model. In line, our results showed inhibition of HMGB1 expression and induction of autophagy by glycyrrhizin in gastric tissues. Inflammation is a major problem during *H. pylori* infection. Inflammation induces gastric damage and causes further complications. Here, glycyrrhizin induces autophagy accompanied by a reduction in inflammation. Furthermore, glycyrrhizin is able to repair gastric tissue damages.

Conclusion

Our results demonstrated for the first time that induction of autophagy by inhibiting HMGB1 can reduce *H. pylori* infection in both in vitro and in vivo conditions. In addition, our data revealed that restoring the degradative capacity of autophagy by inhibiting HMGB1- induced LMP resulted in the inhibition of *H. pylori* pathogenesis (Fig. 8). As both the host and pathogen play critical roles in disease progression, induction of autophagy and lysosomal degradation further affects downstream responses like inflammation and ROS generation. Hence, in the future glycyrrhizin might be used as a potent inducer of autophagy that reduces *H. pylori* infection to inhibit the progression of gastric disorders. The mechanism of antibacterial action of glycyrrhizin would provide novel strategies and targets to address the problem of antimicrobial resistance. Glycyrrhizin could also be used in synergistic composition with other drugs for *H. pylori* infection as standard *H. pylori* treatment requires triple therapy.

Supplementary Information

The online version contains supplementary material available at https://doi.org/10.1186/s10020-023-00641-6.

Additional file 1: Figure S1. MTT assay of glycyrrhizin for different doses. (a) AGS cells were treated with glycyrrhizin (50-200μM) or DMSO for 24 h. MTT assay was performed to measure the % viability level. Densitometric analyses are graphically represented. Graphs generated using GraphPad Prism 5 were represented as mean±SEM (n=3); One-way ANOVA was performed and significance was calculated. ns=nonsignificant. **Figure S2.** Standard agar dilution method for determination of *Helicobacter pylori* viability. Briefly, serially diluted bacterial suspension of OD at 600nm 0.1 were spotted on BHIA medium containing glycyrrhizin of 200μM concentration along with control where no glycyrrhizin was added and incubated them in the microaerophilic condition for 3-4 days. *H. pylori* viability was determined by counting the number of bacterial colonies (CFU/mL) in the BHIA medium. Graphs generated using GraphPad Prism 5 were represented as mean±SEM (n=3); One-way ANOVA was performed and significance was calculated. ns=nonsignificant. **Figure S3.** Transfection of siHMGB1, siATG5 and nonspecific siRNA in AGS cells. (a) Cells were transfected with non-specific siRNA (siNS) and HMGB1 siRNA for 48h. Immunoblotting was performed for quantification of HMGB1 inhibition. (b) Cells were transfected with non-specific siRNA (siNS) and ATG5 siRNA (siATG5) for 48h. Immunoblotting was performed for quantification of ATG5 inhibition. Beta-actin was used as a loading control. **Figure S4.** Glycyrrhizin treatment in *H. pylori*-infected mice. C57BL/6 mice (n = 5 per group) were treated with antibiotics every 7 days. Then after 7 days incubation period, mice were infected with the *H. pylori* SS1 strain thrice a week on alternate days. Mice were incubated for 14 days and then administered with or without GLZ (10 mg /kg body weight), every day for 4 weeks. At the end of treatment, mice were sacrificed and gastric tissues and serum were collected. (b) Immunoblot showing the expression of autophagy proteins LC3B-II of mouse gastric tissues. α-tubulin was used as a protein loading control.

Acknowledgements
The authors thank the Indian Council of Medical Research (ICMR), Council for Scientific and Industrial Research (CSIR), Department of Biotechnology (DBT), and University Grants Commission (UGC) for fellowship assistance.

Author contributions
Conceptualization and design: SB and UK. Analysis and interpretation: SB, AKM, SD, UK, BCK and PB. Data collection: SB, UK, BCK, DS, SP, PB, AG. Writing the article: SB and UK. Final approval of the article: UK, BCK, SP, PB, DS, AG, SB, AKM and SD. All authors read and approved the final manuscript.

Funding
This research was funded by a grant from the Department of Biotechnology (DBT), Government of India, and Project (BT/PR3093/BIC/101/1076/2018).

Availability of data and materials
All required data included in text and supplementary. Any further any formation required is available with the corresponding author.

Declarations

Ethics approval and consent to participate
Experiments were conducted under the guidelines of the Institutional Animal Ethical Committee, NICED, Kolkata (PRO/157/- 260 July 2022).

Consent for publication
Not applicable.

Competing interests
Authors declare no Competing interests.

Received: 30 December 2022 Accepted: 21 March 2023
Published online: 10 April 2023

References

Basak P, Maitra P, Khan U, Saha K, Bhattacharya SS, Dutta M, Bhattacharya S. Capsaicin inhibits Shigella flexneri intracellular growth by inducing autophagy. Front Pharmacol 2022;13.

Bravo J, Díaz P, Corvalán AH, Quest AF. A novel role for *Helicobacter pylori* gamma-glutamyltranspeptidase in regulating autophagy and bacterial internalization in human gastric cells. Cancers. 2019;11:801.

Chmiela M, Karwowska Z, Gonciarz W, Allushi B, Stączek P. Host pathogen interactions in *Helicobacter pylori* related gastric cancer. World J Gastroenterol. 2017;23:1521.

Feng L, Liang L, Zhang S, Yang J, Yue Y, Zhang X. HMGB1 downregulation in retinal pigment epithelial cells protects against diabetic retinopathy through the autophagy-lysosome pathway. Autophagy. 2022;18:320–39.

Fu Y, Zhou E, Wei Z, Liang D, Wang W, Wang T, Guo M, Zhang N, Yang Z. Glycyrrhizin inhibits the inflammatory response in mouse mammary epithelial cells and a mouse mastitis model. FEBS J. 2014;281:2543–57.

Gene E, Calvet X, Azagra R, Gisbert J. Triple vs. quadruple therapy for treating *Helicobacter pylori* infection: a meta-analysis. Aliment Pharmacol Ther. 2003;17:1137–43.

Giraud-Gatineau A, Coya JM, Maure A, Biton A, Thomson M, Bernard EM, Marrec J, Gutierrez MG, Larrouy-Maumus G, Brosch R. The antibiotic bedaquiline activates host macrophage innate immune resistance to bacterial infection. Elife. 2020;9: e55692.

González MF, Díaz P, Sandoval-Bórquez A, Herrera D, Quest AF. *Helicobacter pylori* outer membrane vesicles and extracellular vesicles from *Helicobacter pylori*-infected cells in gastric disease development. Int J Mol. 2021;22:4823.

Hardbower DM, de Sablet T, Chaturvedi R, Wilson KT. Chronic inflammation and oxidative stress: the smoking gun for *Helicobacter pylori*-induced gastric cancer? Gut Microbes. 2013;4:475–81.

Hu W, Zhang L, Li MX, Shen J, Liu XD, Xiao ZG, Wu DL, Ho IH, Wu JC, Cheung CK. Vitamin D3 activates the autolysosomal degradation function against *Helicobacter pylori* through the PDIA3 receptor in gastric epithelial cells. Autophagy. 2019;15:707–25.

Huang C-C, Tsai K-W, Tsai T-J, Hsu P-I. Update on the first-line treatment for *Helicobacter pylori* infection-a continuing challenge from an old enemy. Biomarker Res. 2017;5:1–6.

Jung DE, Yu SS, Lee YS, Choi BK, Lee YC. Regulation of SIRT3 signal related metabolic reprogramming in gastric cancer by *Helicobacter pylori* oncoprotein CagA. Oncotarget. 2017;8:78365.

Kavčič N, Pegan K, Turk B. Lysosomes in programmed cell death pathways: from initiators to amplifiers. Bio Chem. 2017;398:289–301.

Khatoon J, Rai RP, Prasad KN. Role of *Helicobacter pylori* in gastric cancer: updates. World J Gastrointest Oncol. 2016;8:147.

Kim J-J, Lee H-M, Shin D-M, Kim W, Yuk J-M, Jin HS, Lee S-H, Cha G-H, Kim J-M, Lee Z-W. Host cell autophagy activated by antibiotics is required for their effective antimycobacterial drug action. Cell Host Microbe. 2012;11:457–68.

Kim I-J, Lee J, Oh SJ, Yoon M-S, Jang S-S, Holland RL, Reno ML, Hamad MN, Maeda T, Chung HJ. *Helicobacter pylori* infection modulates host cell metabolism through VacA-dependent inhibition of mTORC1. Cell Host Microbe. 2018;23(583–593): e588.

Kralik P, Ricchi M. A basic guide to real time PCR in microbial diagnostics: definitions, parameters and everything. Front Microbiol. 2017;8:108.

Levine B, Mizushima N, Virgin HW. Autophagy in immunity and inflammation. Nature. 2011;469(7330):323–35.

Li N, Tang B, Jia Y-P, Zhu P, Zhuang Y, Fang Y, Li Q, Wang K, Zhang W-J, Guo G. *Helicobacter pylori* CagA protein negatively regulates autophagy and promotes inflammatory response via c-Met-PI3K/Akt-mTOR signaling pathway. Front Cell Infect Microbio. 2017;7:417.

Liao W-C, Huang M-Z, Wang ML, Lin C-J, Lu T-L, Lo H-R, Pan Y-J, Sun Y-C, Kao M-C, Lim H-J. Statin decreases *Helicobacter pylori* burden in macrophages by promoting autophagy. Front Cell Infect Microbio. 2017;6:203.

Libânio D, Dinis-Ribeiro M, Pimentel-Nunes P. *Helicobacter pylori* and microRNAs: Relation with innate immunity and progression of preneoplastic conditions. World J Clin Oncol. 2015;6:111.

Lin H-J, Hsu F-Y, Chen W-W, Lee C-H, Lin Y-J, Chen Y-YM, Chen C-J, Huang M-Z, Kao M-C, Chen Y-A. *Helicobacter pylori* activates HMGB1 expression and recruits RAGE into lipid rafts to promote inflammation in gastric epithelial cells. Front Immunol. 2016;7:341.

Lv X, Zhu Y, Deng Y, Zhang S, Zhang Q, Zhao B, Li G. Glycyrrhizin improved autophagy flux via HMGB1-dependent Akt/mTOR signaling pathway to prevent Doxorubicin-induced cardiotoxicity. Toxicology. 2020;441: 152508.

Mollica L, De Marchis F, Spitaleri A, Dallacosta C, Pennacchini D, Zamai M, Agresti A, Trisciuoglio L, Musco G, Bianchi ME. Glycyrrhizin binds to high-mobility group box 1 protein and inhibits its cytokine activities. Chem Bio. 2007;14:431–41.

Ogawa M, Yoshimori T, Suzuki T, Sagara H, Mizushima N, Sasakawa C. Escape of intracellular Shigella from autophagy. Science. 2005;307:727–31.

Padhi A, Pattnaik K, Biswas M, Jagadeb M, Behera A, Sonawane A. Mycobacterium tuberculosis LprE suppresses TLR2-dependent cathelicidin and autophagy expression to enhance bacterial survival in macrophages. J Immunol. 2019;203:2665–78.

Raju D, Hussey S, Ang M, Terebiznik MR, Sibony M, Galindo-Mata E, Gupta V, Blanke SR, Delgado A, Romero-Gallo J. Vacuolating cytotoxin and variants in Atg16L1 that disrupt autophagy promote *Helicobacter pylori* infection in humans. Gastroenterol. 2012;142:1160–71.

Saha K, Sarkar D, Khan U, Karmakar BC, Paul S, Mukhopadhyay AK, Dutta S, Bhattacharya S. Capsaicin inhibits inflammation and gastric damage during *H pylori* infection by targeting NF-kB–miRNA axis. Pathogens. 2022;11:641.

Shrivastava SR, Shrivastava PS, Ramasamy J. World health organization releases global priority list of antibiotic-resistant bacteria to guide research, discovery, and development of new antibiotics. J Med Soc. 2018;32:76.

Sierra JC, Piazuelo MB, Luis PB, Barry DP, Allaman MM, Asim M, Sebrell TA, Finley JL, Rose KL, Hill S. Spermine oxidase mediates *Helicobacter pylori*-induced gastric inflammation, DNA damage, and carcinogenic signaling. Oncogene. 2020;39:4465–74.

Tang D, Kang R, Livesey KM, Cheh C-W, Farkas A, Loughran P, Hoppe G, Bianchi ME, Tracey KJ, Zeh HJ III. Endogenous HMGB1 regulates autophagy. J Cell Bio. 2010;190:881–92.

Tang B, Li N, Gu J, Zhuang Y, Li Q, Wang H-G, Fang Y, Yu B, Zhang J-Y, Xie Q-H. Compromised autophagy by MIR30B benefits the intracellular survival of *Helicobacter pylori*. Autophagy. 2012;8:1045–57.
Terebiznik MR, Raju D, Vázquez CL, Torbricki K, Kulkarni R, Blanke SR, Yoshimori T, Colombo MI, Jones NL. Effect of *Helicobacter pylori's* vacuolating cytotoxin on the autophagy pathway in gastric epithelial cells. Autophagy. 2009;5:370–9.
Thung I, Aramin H, Vavinskaya V, Gupta S, Park J, Crowe S, Valasek M. the global emergence of *Helicobacter pylori* antibiotic resistance. Aliment Pharmacol Ther. 2016;43:514–33.
Tshibangu-Kabamba E, Yamaoka Y. *Helicobacter pylori* infection and antibiotic resistance—from biology to clinical implications. Nat Rev Gastroenterol & Hepatol. 2021;18:613–29.
Tsugawa H, Mori H, Matsuzaki J, Sato A, Saito Y, Imoto M, Suematsu M, Suzuki H. CAPZA1 determines the risk of gastric carcinogenesis by inhibiting *Helicobacter pylori* CagA-degraded autophagy. Autophagy. 2019;15(2):242–58.
Xie Z, Zhang Y, Huang X. Evidence and speculation: the response of Salmonella confronted by autophagy in macrophages. Future MicrobioL. 2020;15:1277–86.
Yang X-J, Si R-H, Liang Y-H, Ma B-Q, Jiang Z-B, Wang B, Gao P. Mir-30d increases intracellular survival of *Helicobacter pylori* through inhibition of autophagy pathway. World J Gastroenterol. 2016;22:3978.
Yang L, Li C, Jia Y. MicroRNA-99b promotes *Helicobacter pylori*-induced autophagy and suppresses carcinogenesis by targeting mTOR. Oncol Lett. 2018;16:5355–60.
Yang Y, Shu X, Xie C. An overview of autophagy in *Helicobacter pylori* infection and related gastric cancer. Front Cell Infect Mi. 2022;12:410.
Yin H, Yang X, Gu W, Liu Y, Li X, Huang X, Zhu X, Tao Y, Gou X, He W. HMGB1-mediated autophagy attenuates gemcitabine-induced apoptosis in bladder cancer cells involving JNK and ERK activation. Oncotarget. 2017;8:71642.

Publisher's Note

Journal of Applied Microbiology, 2022, 0, 1–12
https://doi.org/10.1093/jambio/lxac076
Advance access publication date: 15 December 2022
Research Article

JOURNAL OF APPLIED MICROBIOLOGY
OXFORD UNIVERSITY PRESS

Asiatic acid inhibits intracellular *Shigella flexneri* growth by inducing antimicrobial peptide gene expression

Priyanka Maitra[1], Priyanka Basak[1], Keinosuke Okamoto[2], Shin-ichi Miyoshi[3], Shanta Dutta[4], Sushmita Bhattacharya[1,*]

[1]Division of Biochemistry, National Institute of Cholera and Enteric Diseases, Kolkata 700010, India
[2]Collaborative Research Center of Okayama University for Infectious Diseases in India, National Institute of Cholera and Enteric Diseases, Kolkata 700010, India
[3]Division of Pharmaceutical Sciences, Graduate School of Medicine, Dentistry and Pharmaceutical Sciences, Okayama University, Okayama, Japan
[4]Department of Bacteriology, National Institute of Cholera and Enteric Diseases, Kolkata 700010, India

*Corresponding author. Division of Biochemistry, ICMR-National Institute of Cholera and Enteric Diseases, P-33, C.I.T. Road, Scheme XM, Beliaghata, Kolkata 700010, India. E-mail: durgasushmita@gmail.com

Abstract

Aims: A rapid rise in resistance to conventional antibiotics for *Shigella spp.* has created a problem in treating shigellosis. Hence, there is an urgent need for new and non-conventional anti-bacterial agents. The aim of this study is to show how Asiatic acid, a plant-derived compound, inhibits the intracellular growth of *Shigella flexneri*.

Methods and results: *Shigella flexneri* sensitive and resistant strains were used for checking antimicrobial activity of Asiatic acid by gentamicin protection assay. Asiatic acid inhibited the intracellular growth of all strains. Gene expression analysis showed antimicrobial peptide (AMP) up-regulation by Asiatic acid in intestinal cells. Further western blot analysis showed that ERK, p38, and JNK are activated by Asiatic acid. ELISA was performed to check IL-8, IL-6, and cathelicidin secretion. The antibacterial effect of Asiatic acid was further verified in an *in vivo* mouse model.

Conclusions: The reason behind the antibacterial activities of Asiatic acid is probably over-expression of antimicrobial peptide genes. Besides, direct antimicrobial activities, antimicrobial peptides also carry immunomodulatory activities. Here, Asiatic acid increased IL-6 and IL-8 secretion to induce inflammation. Overall, Asiatic acid up-regulates antimicrobial peptide gene expression and inhibits intracellular *S. flexneri* growth. Moreover, Asiatic acid reduced bacterial growth and recovered intestinal tissue damages in *in vivo* mice model.

Significance and impact of the study

This study shows that Asiatic acid can be used as a novel anti-infective in the near future for the treatment of *Shigella flexneri* infection.

Keywords: *Shigella flexneri*, Asiatic acid (Aa), antimicrobial peptides (AMPs), cathelicidin (CAMP), myeloperoxidase (MPO)

Materials and methods

Bacteria and growth conditions

Shigella flexneri (sf2457T) *serotype 2a* and multidrug-resistant (NOR/OFX/NA/CIP//TET/S/AM/E/ST) *S. flexneri serotype 2a* (BCH12654 and BCH12702), were used for experimentation. All strains were regularly grown in MHB media (Mueller Hinton broth, Himedia, India) at 37°C with aeration.

Cell culture

Human intestinal cells HT-29 (ATCC HTB-38) and murine macrophage cells RAW 264.7 (ATCC TIB-71) were used for experimentation. HT29 cells were maintained in McCoy's 5A medium (Sigma-Aldrich, USA). RAW 264.7 cells were cultured in RPMI-1640 medium (Sigma-Aldrich, USA). The media were further supplemented with 10% heat-inactive FBS (Sigma, USA) containing 1% non-essential amino acids and pen-strep (Himedia, India). Cells were maintained in a humidified 5% CO_2 incubator at 37°C.

Broth dilution assay

The inhibition of *S. flexneri* growth was monitored in Mueller Hinton Broth (MHB). Briefly, an overnight culture of bacteria at 1:1000 dilution was inoculated in fresh broth supplemented with 25, 50, and 100 μg ml^{-1} of Asiatic acid (#546712, Sigma), keeping DMSO as the vehicle control. Cultures were kept at 37°C with shaking. The bacterial O.D. at 600 nm was checked at regular time intervals, and serial dilutions were plated and kept overnight at 37°C for calculating the percentage viability ($\frac{CFU\ of\ test}{CFU\ of\ control} \times 100\%$) (Nickerson et al. 2017, Sur et al. 2020).

Cell viability assay

HT29 cells were grown in 96 well culture plates at a density of 1×10^4 cells. At confluency, cells were treated with varying concentrations of Asiatic acid (5–20 μg ml^{-1}), keeping DMSO as a negative control and 0.1% Triton X-100 as a positive control. Cells were kept in a 5% CO_2 incubator for 24 h at 37°C. Cellular viability was calculated using the Cell Counting Kit-8 (Sigma) reagent. A total of 10 μl of reagent was added and incubated for 4 h at 37°C. Color intensity was determined at

Received: August 12, 2022. **Revised:** November 17, 2022. **Accepted:** December 13, 2022

450 nm, and percentage viability was calculated and graphically represented.

Gentamicin protection assay

Intestinal and macrophage cells (1×10^5) were grown in six well plates and incubated at 37°C in a 5% CO_2 incubator. Cells were kept in serum-free and antibiotic-free incomplete media overnight before experimentation. For infection, Congo red-positive *S. flexneri* sf2457T, BCH12654, and BCH12702 were sub-cultured to an $O.D._{600nm}$ of 0.5. Bacterial cultures were pelleted by centrifugation, washed with PBS (pH 7.4), and re-suspended in incomplete tissue culture media.

For pre-treatment experiments, cells were treated with 5, 10, and 15 μg ml^{-1} of Asiatic acid, keeping DMSO as a control for 24 h. Treatments were also performed for different time points (2, 4, 6, and 12 h). After treatment, cells were infected with an MOI of 100:1 unless otherwise mentioned. The infected plates were spun at 700 g for 15 min and incubated for 2 h. After successful bacterial infection, cells were further washed and incubated with 50 μg ml^{-1} gentamicin solution in incomplete media. Following antibiotic treatment, cells were washed, and lysis was done in 0.1% Triton X-100 for 5 min at 37°C. Serial dilutions of the lysed cell suspension were plated and incubated overnight at 37°C for counting CFU ml^{-1} (Ra et al. 2016, Lapaquette et al. 2017). Experiments were also performed at different MOIs (50:1 and 200:1) following the above protocol.

For post-treatment, overnight serum-starved cells were infected with *S. flexneri* (MOI 100:1), centrifuged for 15 min at 700 g, and incubated for a period of 2 h. After infection, cells were washed and incubated with 50 μg ml^{-1} gentamicin solution for 2 h. Thereafter, cells were washed and treated with 5 and 10 μg ml^{-1} of Asiatic acid, keeping DMSO as a control for 24 h in a 10 μg ml^{-1} gentamicin solution. Following treatment, cells were washed, lysed, and plated as described previously for counting CFU ml^{-1}.

For inhibitor studies, cells were treated with MAPK inhibitors, i.e. 10 μM ERK (U0126) (#9903S, CST), 10 μM p38 (SB201290) (#S7067, Sigma), or 10 μM JNK (SP600125) (#S5567, Sigma) for 4 h, followed by treatment with 10 μg ml^{-1} of Asiatic acid or DMSO control for 24 h. Cells were then infected with an MOI of 100:1 and proceeded as described above for counting CFU ml^{-1}.

Quantitative PCR

TRIzol reagent was used for the isolation of RNA. Isolated RNA was converted to cDNA (cDNA synthesis kit; Thermo Scientific). We used SYBR green real-time reagent from Applied Biosystems for real-time PCR. The fold change was calculated using the ΔΔCt method. The expression of all genes was normalized using GAPDH as an internal control. ΔΔCt was calculated using the formula

$$\Delta\Delta Ct = \text{test} - \text{internal control} - \text{test control}.$$

Human primer sequences used in this study are as follows:

GAPDH 5′-GTCTTCACCACCATGGAGAAGGC-3′ and 5′-CATGCCAGTGAGCTTCCCGTTCA-3′

CAMP 5′-TGATAAGGATAACAAGAG-3′ and 5′-TCTCATAGTTTATTTCTCA-3′

MPO 5′-CTTGTATCCTCTGGTTCTTC-3′ and 5′-TGCCTCTATATGCTTCTCA-3′

A differential gene expression study of the antibacterial response pathway in response to Asiatic acid treatment was performed using the Human Antibacterial Response PCR Array (#PHAS-148ZA) ($RT^2Profiler^{TM}$ PCR Array Human Antimicrobial Response), following the manufacturer's instructions (Qiagen). Briefly, RNA was isolated from control and Asiatic acid treated (24 h) samples using the RNeasy Plus Kit (Qiagen). cDNA was synthesized and further added to the SYBR Green mastermix (Qiagen). qRT-PCR was performed on the Applied Biosystems StepOnePlus system. Data were analyzed in Qiagen's web-based Gene Globe $RT^2Profiler^{TM}$ software for PCR array analysis.

Immunoblotting

Control, infected, treated, and treated plus infected cells were lysed in RIPA lysis buffer containing PMSF, protease, and phosphatase inhibitors. Clear supernatants were collected after centrifugation at 7000 g for 20 min at 4°C. Estimated proteins were boiled in protein loading buffer and run on SDS-PAGE gel. Next, gels were transferred to PVDF membranes, blocked with 5% non-fat dry milk or BSA, and further kept overnight at 4°C with primary antibodies. The primary antibodies used are as mentioned: rabbit monoclonal anti-GAPDH antibody (Cat#D16H11) (1:2000), anti-Phospho-p44/42 MAPK (Erk1/2) (Cat#9101) (1:1000), anti-p44/42 MAPK (Erk1/2) (Cat#4696) (1:1000), anti-Phospho-p38 MAPK (Thr180/Tyr182) (Cat#9211) (1:1000), anti-p38 MAPK Antibody (Cat#9212) (1:1000), anti-Phospho-JNK (Thr 183/Tyr 185) (Cat#9255) (1:1000), anti-JNK (Cat#SC-7345) (1:1000), and anti-CAP-18 (Cat#Sc-130552) (1:1000). Membranes were further incubated in horseradish peroxidase (HRP) conjugated goat anti-mouse secondary antibody (1:10000) or goat anti-rabbit secondary antibody (1:10000) for 2 h, washed and bands were visualized using Chemi-DocMP Imaging System (Biorad, USA) using chemiluminescent HRP substrate (Millipore).

ELISA assay

Enzyme-linked immunosorbent assay was used to determine the concentration of Cathelicidin antimicrobial peptide, IL-6 and IL-8 secreted into the cultured media of infected and treated HT29 cells using Cathelicidin ELISA KIT (MyBioSource) (#MBS720523), GENLISA ELISA kit for human IL-6 (Krishgen) (#catKB1068) and IL-8 (Krishgen) (#catKB1070). The $O.D._{450nm}$ was determined using an ELISA microplate reader (Biorad). Values were expressed as the average of three independent experiments.

Immunofluorescence microscopy

Intestinal cells were seeded on coverslips and treated with 10 μg ml^{-1} of Asiatic acid (24 h). Cells were further infected for 2 h, followed by 2 h of gentamicin (50 μg ml^{-1}) treatment. After washing, fixation was done with 4% formaldehyde and then blocked with PBS (3% BSA and 0.1% Triton X-100) for 1 h. Further antibody treatment was performed with anti-CAP-18 antibody (Cat#sc-130552) (1:100) and anti-*Shigella* antibody (Cat#ab65282) (1:200) for overnight at 4°C. Following that, cells were incubated with TRITC-conjugated anti-rabbit secondary antibody (1:2000) (Cat#T6778) and FITC-conjugated anti-mouse secondary antibody (1:2000) (Cat#F0257). Coverslips were mounted using $ProLong^{TM}$ Gold Antifade reagent, which contains DAPI (ThermoFisher).

Finally, images were captured using the Zeiss LSM 710 confocal system (Carl Zeiss).

In vivo experimental design

Adult BALB/c mice, weighing ~20–24 g, were used for *in vivo* experiments. All animals were accustomed to standard laboratory conditions in the animal house with 75% humidity. Animals were fed with standard pellet diet (Agro Corporation Private Ltd., Bangalore, India) and water ad libitum. Experiments were performed following the IAEC (Institutional Animal Ethical Committee), NICED, Kolkata -approved guidelines.

Fasted mice were injected intra-peritoneally with *S. flexneri* (sf2457T) for 4 h. After infection, treatments were performed for 24 h among four experimental groups created as follows: Group 1: Control—received only DMSO. Group 2: Infected—received *S. flexneri* (0.5×10^9 CFU ml^{-1}) + DMSO. Group 3: Infected + Asiatic acid—received *S. flexneri* (0.5×10^9 CFU ml^{-1}) + Asiatic acid (50 mg kg^{-1}). Group 4: Asiatic acid—received only Asiatic acid (50 mg kg^{-1}). Experiments were repeated thrice.

In vivo bacterial count

After successful treatment, all animals were sacrificed, and colons were aseptically removed. Equal quantity of colon and stool samples were homogenized in PBS, diluted and plated for determining bacterial load. All tissues were stored at −80°C until further experimentation.

Tissue homogenate

Dissected colons were thoroughly washed in chilled PBS buffer and homogenized in chilled RIPA buffer. Homogenates were further subjected to centrifugation for 10 min at 14 000 g, and the collected supernatants were subjected to a western blot.

Histopathological study

Colonic tissues were fixed with 10% buffered formalin. Gradient dehydration with ethanol (50–100%) was performed, followed by xylene treatment. Tissues were then embedded in paraffin (56–58°C) at 58 ± 1°C for 4 h. After deparaffinization with xylene, the staining was done with hematoxylin-eosin (H and E) and mounted in DPX under a clean cover slip. Histological variations were visualized using a bright field microscope (Motic, Germany), and images were captured at different magnifications.

Statistical analysis

All data were represented as mean ± S.E.M. and analyzed with GraphPad Prism 5.0 software. The difference in statistical level was performed using one-way ANOVA (Tukey's multiple comparison tests), two-way ANOVA, or an unpaired t-test. P values <0.05 were taken as statistically significant. Significant levels are denoted as ∗for $P < 0.05$, ∗∗for $P < 0.01$, and ∗∗∗for $P < 0.001$.

Introduction

Shigella spp. are gram-negative gastrointestinal bacteria that cause bloody diarrhea and affect millions of people globally (Nandy et al. 2011, Taneja and Mewara 2016, Baker and The 2018, Chen et al. 2020). Specifically, children <5 years of age are affected (Williams and Berkley 2018, Rogawski McQuade et al. 2020). It enters the host through the colonic epithelium and exploits the host defense mechanism for intracellular survival. Currently, treatment of *S. flexneri* infection is limited to antibiotics, as there is no licensed vaccine on the market. As per WHO recommendations, antibiotics like ciprofloxacin are considered first-line therapy for the treatment of shigellosis. Oral rehydration therapy and zinc supplementation are also recommended (Williams and Berkley 2018, WHO 2021). However, antibiotic resistance of *Shigella spp.*, especially *S. flexneri*, is a major concern nowadays. The development of drug resistance as well as treatment failure has led to the search for new antimicrobial agents (Puzari et al. 2018, Ranjbar and Farahani 2019). Among new antimicrobial approaches, phage therapy is considered a promising approach, but there are also limitations (Tang et al. 2019). Therefore, novel therapeutic approaches need to be explored to control host pathogenesis during *S. flexneri* infection.

Different host-protective therapeutic approaches provide an opportunity for exploration against infectious diseases (Mahlapuu et al. 2016, Kaufmann et al. 2018, Sechet et al. 2018, Young et al. 2020). Among different host defense mechanisms, production of antimicrobial peptides (AMP) is important (Mahlapuu et al. 2016, Sechet et al. 2018). They are short-cationic peptides present in a wide variety of organisms. Most AMPs can directly kill the pathogen, whereas they can act indirectly by activating the host defense machinery (Le et al. 2017, Jiang et al. 2019). As there is a rapid increase in antimicrobial resistance to conventional antibiotics, efforts are being made to bring AMPs into clinical use. Several AMPs like cathelicidin (CAMP) are in clinical trials (Dijksteel et al. 2021). The importance of antimicrobial peptides has been reported previously, showing infection susceptibility in mice lacking the gene cathelicidin related antimicrobial peptide (CRAMP) (Pfalzgraff et al. 2018). AMPs can attack both gram-positive and gram-negative bacteria. AMP-induced bacterial death is caused by multi-factorial mechanisms. They can either directly kill the bacteria or activate the immune response for bacterial clearance (Chi and Raffetto 2015, Le et al. 2017, Blyth et al. 2020). The rapid killing of bacteria by AMPs makes them promising therapeutic anti-infective. In mammals, AMPs are mainly secreted by epithelial cells and neutrophil granules (Chi and Raffetto 2015, Le et al. 2017). Specifically, intestinal epithelial cells, which interact with microbes at first are known to produce an array of genes encoding antimicrobial peptides, pro-inflammatory cytokines, and chemokines. Antimicrobial peptide genes such as cathelicidin further secrete antimicrobial peptides (AMPs) to induce antimicrobial activity (Zheng et al. 2007). These AMPs are recently under clinical trial not only as antimicrobials but also as agents to activate the immune response (Pfalzgraff et al. 2018, Blyth et al. 2020, Dijksteel et al. 2021). Hence, boosting host endogenous AMPs by activating gene transcription can be an alternative option for treating bacterial infections like shigellosis. Stimulating gene transcription would provide antimicrobial protection and immunomodulation.

Natural products are a rich source of various antimicrobial agents. A wide range of medicinal plants are used to extract phytochemicals as they possess varied antibacterial properties (Savoia 2012, Gyawali and Ibrahim 2014, Stan et al. 2021). Clinical microbiologists have a great interest in the use of medicinal plants for developing alternative drugs

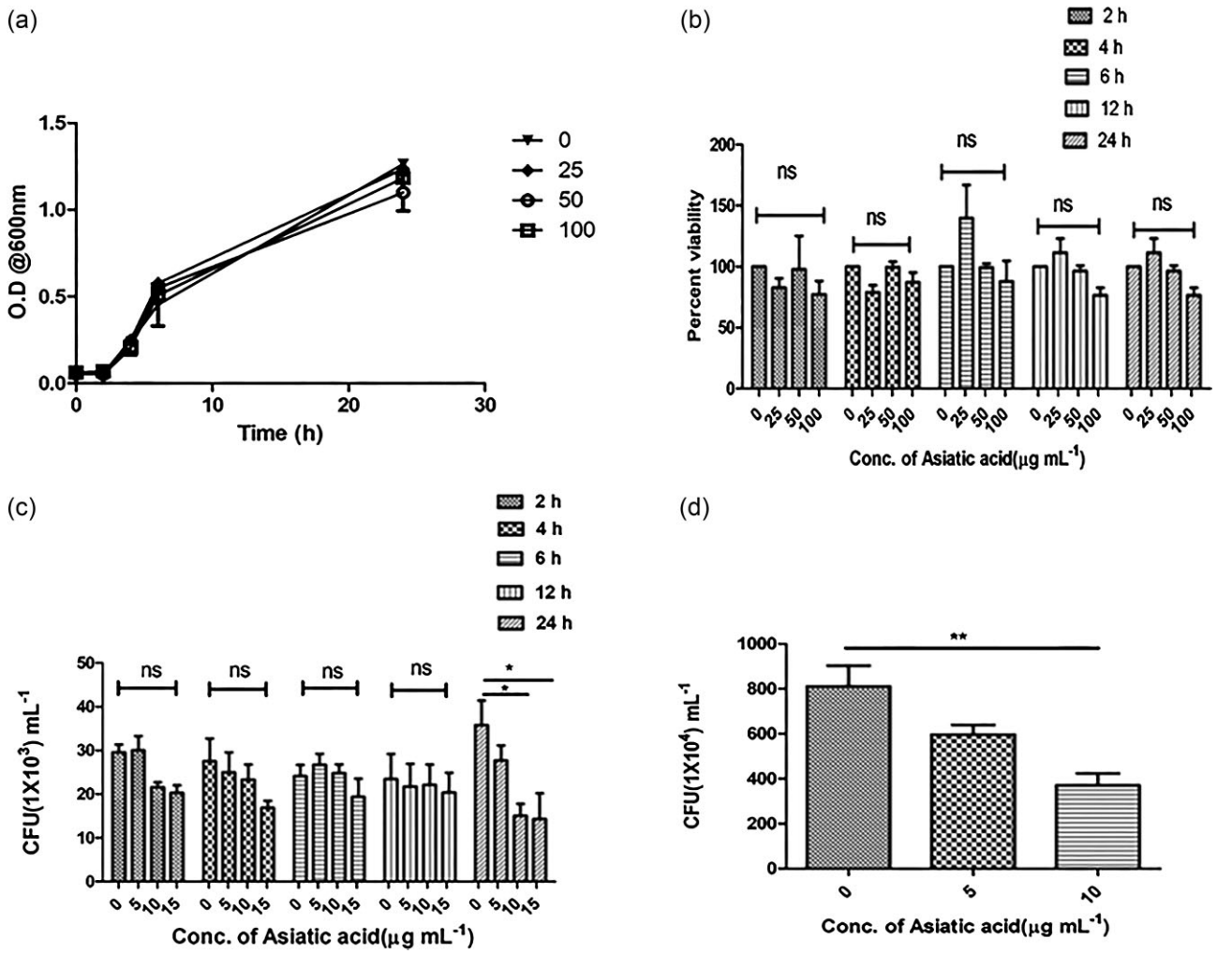

Figure 1. Effect of Asiatic acid on *S. flexneri* (sf2457T) growth. A broth dilution assay was performed in the presence of DMSO control, 25, 50, and 100 μg ml^{-1} of Asiatic acid, followed by the addition of *S. flexneri* overnight culture. (a) O.D.$_{600}$ nm was measured, and (b) % viability was calculated from CFU after plating overnight and graphically represented. Invasion assay was performed in Asiatic acid pre/post-treated HT29 cells. (c) Cells were treated with Asiatic acid (5, 10, and 15 μg ml^{-1}) for the indicated time periods (2, 4, 6, 12, and 24 h), followed by a 2 h of *S. flexneri* (sf2457T) infection at MOI 100. Gentamicin treatment was followed to kill extracellular bacteria. The change in intracellular bacterial burden was expressed as CFU ml^{-1} and graphically represented. (d) Infection with sf2457T at MOI 100 was followed by Asiatic acid post-treatment (5 and 10 μg ml^{-1}) for 24 h. The change in intracellular bacterial burden was graphically represented as CFU ml^{-1}. One-way ANOVA was performed. All data are represented as mean ± S.E.M. ($n = 3$); significance levels were denoted as ∗for $P < 0.05$, ∗∗for $P < 0.01$, and ∗∗∗for $P < 0.001$.

(Khameneh et al. 2019). The anti-bacterial activities of plant products may reside in a variety of different components, including alkaloids, flavonoids, and other phenolic compounds (Savoia 2012). Moreover, plant-based compounds boost various host protective mechanisms to induce antibacterial activities. There are several plant-derived compounds known to activate the antimicrobial response by boosting the transcription of antimicrobial peptide genes (Meneguetti et al. 2017).

Centella asiatica is a common medicinal plant present in many traditional formulations. It is rich in secondary metabolites like saponins, brahminoside, and centelloside (Nagoor Meeran et al. 2018). Leaves of this plant are used for its antibacterial activities but the mechanism behind antimicrobial activities is not well explored. Therefore, in this current scenario, an extensive biological and chemical investigation is necessary to characterize active antibacterial principles from plants like *Centella asiatica*, which will help us to determine the underlying mechanism behind bacterial clearance and develop novel therapeutics. One of the bioactive compounds of *Centella asiatica* is Asiatic acid. Previously, it has been reported that Asiatic acid from *Syzygium guineense* showed antimicrobial activities against *Shigella sonnie*, but there are no reports against *S. flexneri (*Djoukeng et al. 2005*)*.

In this study, we have screened a few compounds from *Centella asiatica* and observed that Asiatic acid (Aa), one of the bioactive compounds, possesses an anti-bacterial effect against both antibiotic sensitive and resistant strains of *S. flexneri*. Overall, the study highlights an alternative mechanism for combating antibiotic resistance by using a herbal compound that can boost antimicrobial peptide (AMP) gene expression. This work shows an innovative way of treating *S. flexneri* infection by inducing AMP gene expression.

Results

Asiatic acid inhibits intracellular *Shigella flexneri* growth

To find out the antibacterial activity against *S. flexneri*, we searched for a few natural bioactive compounds. One of the bioactive compounds of *Centella asiatica* is Asiatic acid (Nagoor Meeran et al. 2018). It has various antimicrobial activities. First, we have checked the effect of Asiatic acid on direct antibacterial action (Fig. 1a and b). Treatment with Asiatic acid for 24 h at a relatively higher dose (100 μg ml^{-1}) did not affect bacterial growth measured by bacterial O.D. and viability count (CFU). We further checked cellular viability, where Asiatic acid showed insignificant toxicity at different doses in HT-29 cells (Supplementary Fig. S1). Next treatments were performed in HT29 intestinal cells, as the major site of *S. flexneri* infection is the intestinal epithelial cells. Cells were pre-treated with Asiatic acid at varying doses (5, 10, and 15 μg ml^{-1}) and different time points (2, 4, 6, 12, and 24 h). After drug treatment, cells were infected with the *S. flexneri* 2457T strain at MOI 100 for 2 h, followed by gentamicin treatment. Asiatic acid inhibited the growth of *S. flexneri* at 10 and 15 μg ml^{-1} after 24 h of pre-treatment significantly (Fig. 1c). At earlier time points, Asiatic acid did not affect the growth of *S. flexneri*. Similarly, cells post-treated with different doses (5 and 10 μg ml^{-1}) of Asiatic acid showed a significant reduction in intracellular bacterial load at 10 μg ml^{-1} (Fig. 1d). Collectively, these results showed that 24 h of Asiatic acid treatment inhibits intracellular bacterial growth in intestinal cells.

Treatment with Asiatic acid reduces the growth of antibiotic resistant strains

Antibiotic resistance is highly predominant in *S. flexneri*; hence, we examined the effect of Asiatic acid on resistant strains of *S. flexneri*. To assess the efficacy of Asiatic acid against resistant strains of *S. flexneri*, two clinical isolates were selected for the current study. Both strains were identified as being resistant to 9 antibiotics. Intestinal cells were pre/post-treated with Asiatic acid for 24 h with different concentrations of Asiatic acid and then examined for antibacterial activity. Asiatic acid pre-treatment at 15 μg ml^{-1} concentration inhibited the growth of resistant strain BCH12702 significantly (Fig. 2a), but not for BCH12654 (Fig. 2b). Similarly, Asiatic acid post-treatment reduced intracellular bacterial burden significantly at 5 and10 μg ml^{-1} for both strains (Fig. 2c and d). In addition, to assess the resistance of *S. flexneri* to drugs, we cultured the residual bacterial colonies left over after Asiatic acid treatment and further performed an intracellular growth assay. Notably, there was no change in intracellular *S. flexneri* growth when cells were infected with fresh or residual cultures. However, Asiatic acid treatment at the same dose reduced bacterial proliferation compared to infected cells with residual bacteria (Supplementary Fig. S2). This data indicates that drug treatment is effective against antibiotic resistant strains and residual bacteria after Asiatic acid treatment is not more virulent in causing infection.

As drug treatment showed a reduction in the replication of intracellular *S. flexneri* in a dose-dependent manner, we further validated our results in macrophage cells. Both intestinal and macrophage cells are attacked by *S. flexneri* during intracellular infiltration (Killackey et al. 2016, Brunner et al. 2019). To examine the antimicrobial activity of Asiatic acid, we pre-treated HT-29 and RAW264.7 cells with Asiatic acid for different doses. After drug treatment, HT-29 cells were infected with the *S. flexneri* 2457T strain for different MOI (50 and 200) (Supplementary Fig. S3) as well as RAW264.7 for MOIs (50, 100, and 200) (Supplementary Fig. S4). Finally, intracellular replication was quantified by CFU count. Asiatic acid showed a dose-dependent reduction in bacterial growth significantly at MOI 50 for HT-29 cells and at MOI 50, 100, and 200 for RAW macrophage cells. Together, these results indicate that Asiatic acid inhibits intracellular bacterial growth in both intestinal and macrophage cells.

Asiatic acid induces antimicrobial peptide gene expression

As Asiatic acid is reported to have different immunomodulatory functions (Park et al. 2017), we searched for a potential host-induced mechanism. To investigate whether any antimicrobial response genes are responsible for the inhibition of *S. flexneri* growth, we performed gene expression analysis by using a RT-PCR array, which included several antibacterial response genes. Human intestinal HT-29 cells were left untreated (Con) or treated with different doses of Asiatic acid (5AA-5 and 10AA-10 μg ml^{-1}) for 24 h and analyzed. Among the different antibacterial genes screened, we observed up-regulation of the CAMP (cathelicidin) and MPO (myeloperoxidase) genes. Several MAPK and TLR genes were also up-regulated due to the Asiatic acid treatment. Both of these antimicrobial peptide genes are important as they can directly kill the bacteria and also modulate host defense machinery to inhibit infection (Fig. 3a). Further to validate the expression of these antimicrobial peptides, we pre-treated the cells with Asiatic acid and then infected them with *S. flexneri* at MOI 100 for 2 h, followed by gentamicin treatment. Consistent with PCR array data, Asiatic acid treatment up-regulated the expression of genes (MPO and CAMP) in Asiatic acid treated and infected cells (Fig. 3b and c). Collectively, these results indicate that Asiatic acid over-expresses cathelicidin and myeloperoxidase gene expression in *S. flexneri* infected cells.

Asiatic acid induces MAPK activation and inflammation

MAPKs activation is known to be involved in antimicrobial peptide gene expression (Kida et al. 2006, Li et al. 2009). Therefore, we examined the activation of ERK, p38, and JNK by Asiatic acid in intestinal cells. We treated the cells with Asiatic acid for 24 h, and then a western blot was performed to check MAPKs' activation. We observed increased phosphorylation of ERK, p38, and JNK at different doses (Fig. 4a). Moreover, we checked the effect of Asiatic acid on MAPK activation in infected cells. Consistently, we observed enhanced expression of P-ERK and P-p38 as compared to infected cells. But Asiatic acid failed to substantially increase JNK phosphorylation as compared to infected cells (Fig. 4b). To further confirm the effect of MAPK activation on *S. flexneri* intracellular growth, we used ERK, p38, and JNK inhibitors. After pre-treatment with specific inhibitors, cells were treated with Asiatic acid for 24 h and eventually infected with *S. flexneri*. Both ERK (U0126) and p38 (SB201290) inhibition led to a significant increase in bacterial proliferation compared to infected cells (Fig. 4c). In addition, Asiatic acid in combination with the inhibitors failed to inhibit intracellular *S. flexneri* growth as compared to infected cells. However, the JNK in-

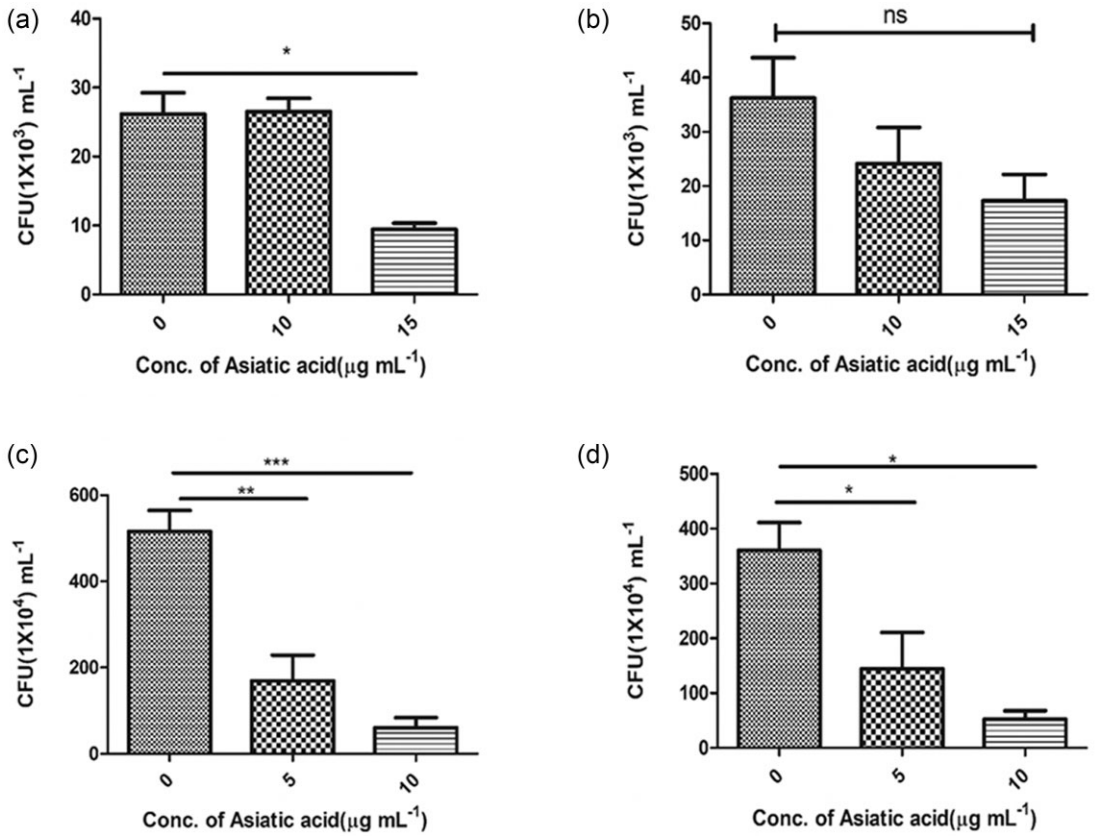

Figure 2. Asiatic acid treatment inhibits the growth of antibiotic resistant bacteria in HT29 cells. Asiatic acid pre-treated (10 and 15 μg ml^{-1}) cells were infected for 2 h with multidrug resistant *S. flexneri* (a) BCH12702 and (b) BCH12654 at MOI 100. The change in intracellular bacterial burden was graphically represented as CFU ml^{-1}. Infection with (c) BCH12702 and (d) BCH12654 at MOI 100 was followed by Asiatic acid post-treatment (5 and 10 μg ml^{-1}) for 24 h. The change in intracellular bacterial burden was graphically represented as CFU ml^{-1}. All data are represented as mean ± S.E.M. ($n = 3$); one-way ANOVA was performed. Significance levels were denoted as ∗for $P < 0.05$, ∗∗for $P < 0.01$, and ∗∗∗for $P < 0.001$.

hibitor (SP600125) reduced bacterial growth significantly as compared to infected cells. Furthermore, we assessed IL-6 and IL-8 levels by ELISA (Fig. 4d and e), as MAPKs and cathelicidin are known to activate inflammation and the secretion of IL-6 and IL-8 (Khine et al. 2006, Zheng et al. 2007, Bucki et al. 2010). Asiatic acid stimulated both IL-6 and IL-8 production in both infected and uninfected cells significantly as compared to untreated cells. Altogether, these results suggest that Asiatic acid stimulated antimicrobial peptide gene expression and cytokine secretion by activating MAPK signaling cascades.

Asiatic acid induced cathelicidin over-expression targets *S. flexneri*

To further investigate the expression of cathelicidin by Asiatic acid, drug exposed intestinal cells were infected with *S. flexneri*, and ELISA was performed on culture supernatants. Cathelicidin was detected at a significant level in Asiatic acid treated uninfected and infected cells, respectively (Fig. 5a). Hence, Asiatic acid specifically induces the release of cathelicidin.

We then investigated the effect of Asiatic acid on cathelicidin expression in *S. flexneri* infected cells by immunofluorescence microscopy. Briefly, HT-29 cells were pre-treated with Asiatic acid and further infected with *S. flexneri*. Immunofluorescence microscopy showed that Asiatic acid exposure recruited cathelicidin to *S. flexneri* as compared to only infected cells (Fig. 5b). Thus, these experiments revealed that Asiatic acid induces cathelicidin expression, which in turn targets *S. flexneri*.

Asiatic acid inhibits *S. flexneri* infection in *in vivo* mice model and rescues intestinal tissue damage

To examine the effectivity of Asiatic acid as an antimicrobial agent, we investigated the effect of Asiatic acid in *in vivo*

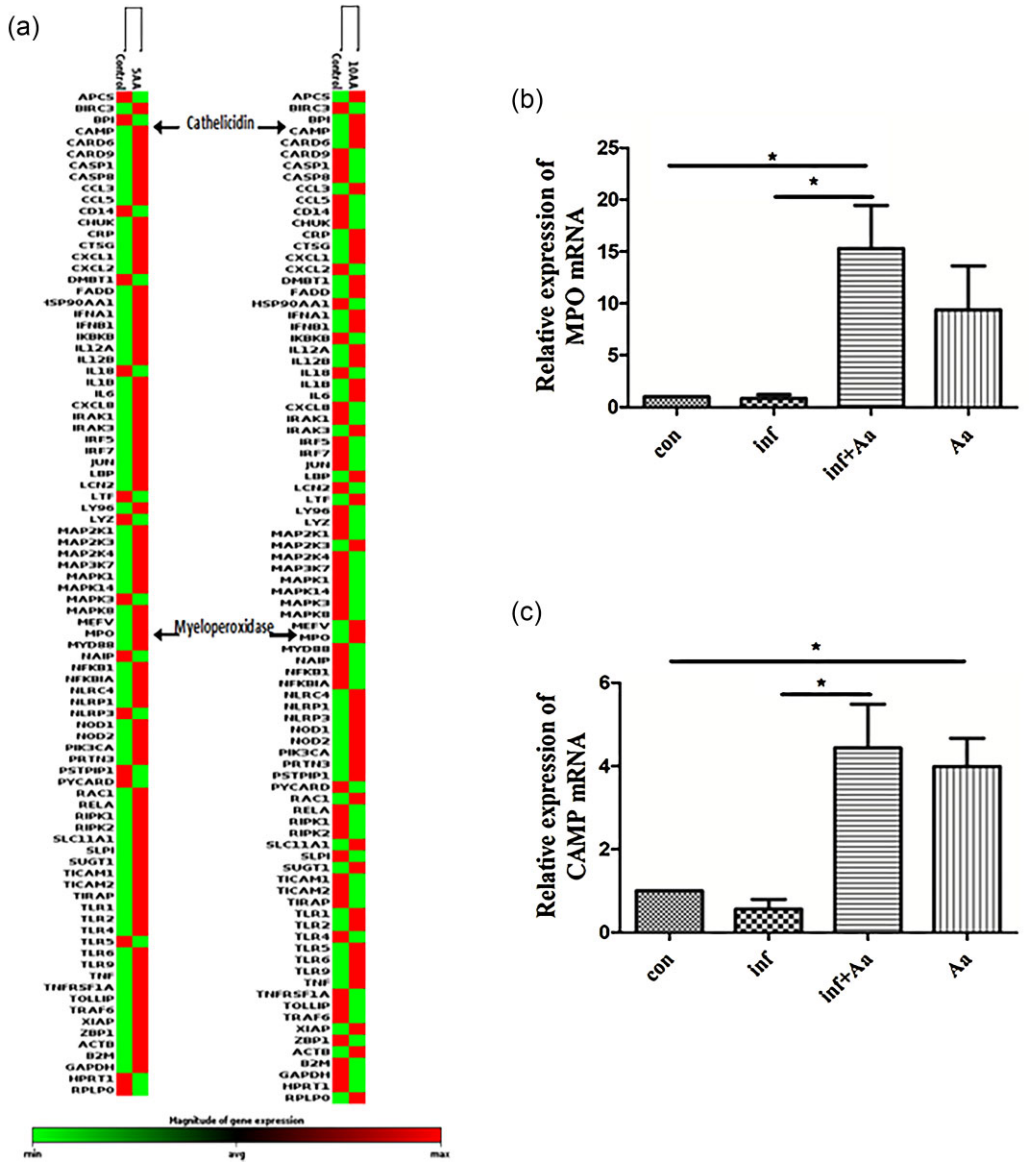

Figure 3. Asiatic acid activates antimicrobial response gene expression in HT29 cells. (a) PCR array of human antimicrobial response genes was performed in control and 24 h Asiatic acid (5–10 μg ml^{-1}) treated samples. Multiplot diagram generated represents differential gene expression. Quantitative real-time PCR was performed following Asiatic acid treatment (10 μg ml^{-1}) and bacterial infection (MOI 100) to evaluate the expression of antimicrobial peptides (b) myeloperoxidase (MPO) and (c) cathelicidin (CAMP) in control, infected, infected plus Aa, and Aa treated cells. GAPDH was kept as an internal control. Relative expression was graphically represented as mean ± S.E.M. ($n = 3$); one-way ANOVA was performed. Significance levels were denoted as ∗for $P < 0.05$, ∗∗for $P < 0.01$, and ∗∗∗for $P < 0.001$.

mice model. Mice were intra-peritoneally infected with the *S. flexneri* 2457T strain. The dose of Asiatic acid for the *in vivo* model was selected based on available data (Lee et al. 2012, Lu et al. 2021). After 4 h of infection, mice were treated with Asiatic acid for 24 h and further sacrificed. We collected the stool samples and dissected the colon from infected and infected Asiatic acid challenged mice samples. The bacterial load (CFU) decreased in infected mice receiving Asiatic acid in both stool (Fig. 6a) and colon (Fig. 6b) samples. We further performed histological studies to check the effect of the drug on intestinal tissue damage caused by infection. We detected intestinal tissue damage due to *S. flexneri* infection. On the other hand, Asiatic acid treatment recovered intestinal tissue damage in infected mice (Fig. 6c). Hence, Asiatic acid reduced *S. flexneri* infection and recovered intestinal tissue damage in the mouse model. Asiatic acid also induced the expression of cathelicidin in *S. flexneri* infected mice colon tissues significantly compared to only infected mice (Fig. 6d). In correlation with *in vitro* data, immunoblots showed CRAMP (cathelicidin related antimicrobial peptide) up-regulation in Asiatic acid treated colon samples. All these data suggest that Asiatic acid inhibited *S. flexneri* infection in an *in vivo* mouse model and repaired intestinal tissue damage.

Discussion

Shigella spp. are invasive enteric pathogens that cause morbidity and mortality worldwide, with the estimated number of cases exceeding 165 million per year (Nandy et al. 2011, Taneja and Mewara 2016, Baker and The 2018, Chen et al.

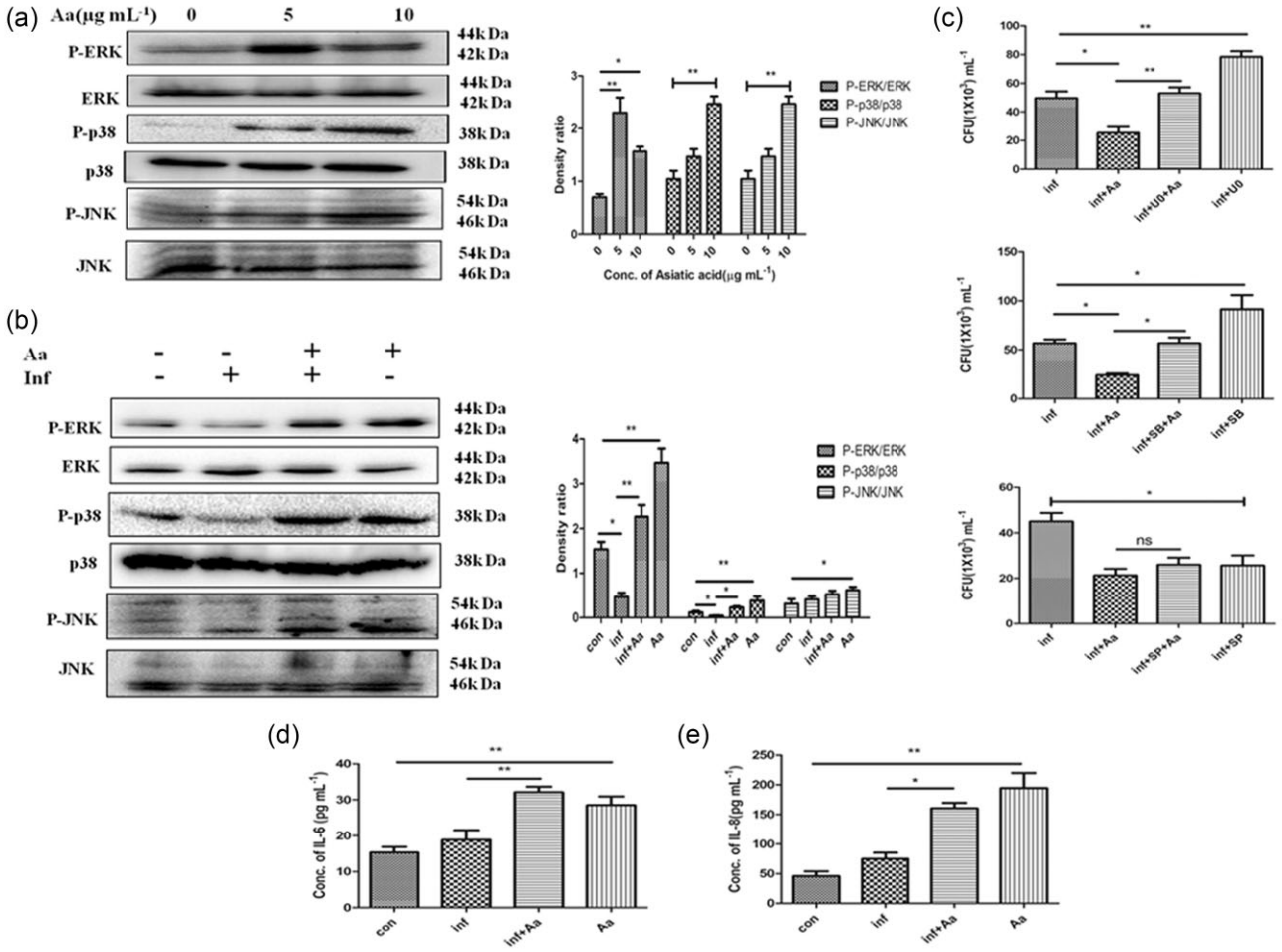

Figure 4. Asiatic acid activates the MAPK pathway and inflammation in HT29 cells. (a) HT29 cells were treated with Asiatic acid (5 and 10 μg ml^{-1}) for 24 h. Expression of major MAPKs (ERK, p38, and JNK) was observed in a western blot. Densitometric analysis was performed and graphically represented. (b) Expression of MAPKs (ERK, p38, and JNK) was also observed following Asiatic acid treatment (10 μg ml^{-1}) and bacterial infection (MOI 100), in control, infected, infected plus Aa, and Aa treated cells. Densitometric analysis was performed and graphically represented. (c) Cells were treated with MAPK inhibitors, i.e. U0 (ERK), SB (p38), or SP (JNK) for 4 h, followed by treatment with or without Asiatic acid (10 μg ml^{-1}) for 24 h and infection at MOI 100. The change in intracellular bacterial burden was graphically represented as CFU ml^{-1}. ELISA was performed to examine the release of (d) IL-6 and (e) IL-8 in media of control, infected, infected plus Aa, and Aa treated cells. Cytokine release was graphically represented. One-way ANOVA was performed. All data are represented as mean ± S.E.M. ($n = 3$). Significance levels were denoted as ∗for $P < 0.05$, ∗∗for $P < 0.01$, and ∗∗∗for $P < 0.001$.

2020). They are highly adapted to the host cellular environment. Among different *Shigella spp.*, *S. flexneri* is highly infectious and can be transmitted through personal contact or contaminated food products or water (Williams and Berkley 2018, Rogawski McQuade et al. 2020). Existing antimicrobial treatments are compromised due to growing evidence of antibiotic resistance. In the developing world, the cost of antibiotics is also a major concern, so there is a need for an efficient vaccine (Kaufmann et al. 2018, Puzari et al. 2018, Ranjbar and Farahani 2019). Currently, there is no available licensed vaccine for the treatment of shigellosis (Hosangadi et al. 2019, Hajialibeigi et al. 2021). Therefore, designing effective alternative therapeutic approaches is required for the treatment of shigellosis.

Natural products with their bioactive compounds are known to have antimicrobial activities (Savoia 2012, Gyawali and Ibrahim 2014, Stan et al. 2021). Herbal compounds are mostly reported to have *in vitro* bactericidal activities against multi drug resistant *S. flexneri strains*. But till date, there are few reports showing inhibition of intracellular growth of *S. flexneri* by natural compounds. Here, we have studied a bioactive compound named Asiatic acid, which is known to have anti-cancer, anti-inflammatory, antimicrobial, and wound healing properties. Asiatic acid is commonly found in the leaves of the plant *Centella asiatica* (Nagoor Meeran et al. 2018).

Pre-treatment and post-treatment analyses showed a dose-dependent inhibition of bacterial growth in intestinal cells by Asiatic acid. Hence, Asiatic acid has the property of killing *S. flexneri* during the intracellular phase of growth. Further, we checked the activity of Asiatic acid on direct bacterial killing. Asiatic acid at relatively higher concentrations was unable to kill *S. flexneri*. Therefore, the intracellular killing of bacteria was not due to the direct antibacterial effect of Asiatic acid but to some other mechanisms. As antibiotic resistance is a major problem with *S. flexneri*, we checked the effect of Asiatic acid on two clinical isolates of *S. flexneri* that are resistant to multiple antibiotics. Asiatic acid was able to inhibit the intracel-

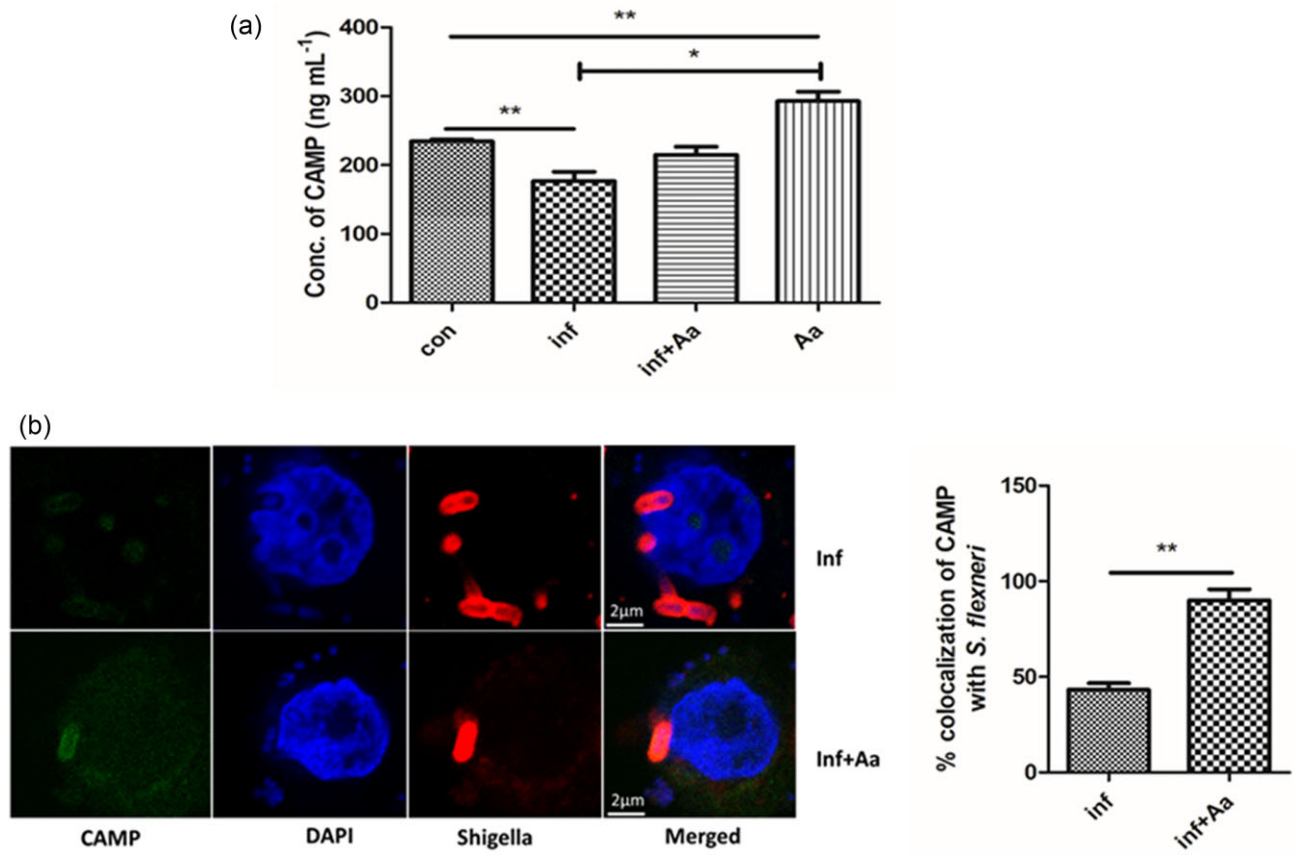

Figure 5. Asiatic acid treatment increases cathelicidin expression. The expression of cathelicidin in HT29 cells upon Asiatic acid (10 μg ml^{-1}) treatment was measured. (a) ELISA was performed to examine the release of cathelicidin in the media of control, infected, infected plus Aa, and Aa treated cells. The cathelicidin release was graphically represented. One-way ANOVA was performed. (b) Confocal microscopic images of HT29 cells showed an increase in the co-localization of *S. flexneri* (red) with cathelicidin (green). Briefly, after Asiatic acid treatment for 24 h, *S. flexneri* infected cells were fixed, and double immunofluorescence microscopy was performed. Scale bar: 2 μm. Percentage colocalization was calculated and graphically represented. Unpaired t-test was performed. All data are represented as mean ± S.E.M. ($n = 3$). Significance levels were denoted as ∗for $P < 0.05$, ∗∗for $P < 0.01$, and ∗∗ for $P < 0.001$.

lular growth of one of the resistant strains by pre-treatment. Post-treatment analysis showed inhibition of bacterial growth of both the resistant strains by Asiatic acid. In order to assess the efficacy of Asiatic acid as a sensitive drug for *S. flexneri*, we cultured the reminiscence bacteria after drug treatment and infected the intestinal cells. Similar intracellular bacterial growth with reminiscent or freshly cultured bacteria indicated that residual bacteria are not more virulent after drug treatment. We have also investigated the effect of Asiatic acid on intracellular bacterial growth after infection with reminiscent bacteria. Asiatic acid at the same dose showed antimicrobial activity; hence, there is no bacterial resistance to Asiatic acid. Therefore, Asiatic acid is able to target the antibiotic-resistant strains of *S. flexneri*. As macrophage cells are also the site of infection for *S. flexneri*, we further examined the effect of Asiatic acid on macrophage cells. In parallel to intestinal cells, Asiatic acid showed antibacterial activity in macrophage cells too.

Further, we searched for the probable reason behind the reduction of intracellular infection. Intestinal epithelial and immune cells like macrophages are endowed with innate immune defense machinery (Günther and Seyfert 2018). Epithelial cells are considered the first line of defense against microbes. These cells have the property of inducing the expression of antimicrobial peptides (Bals 2000, Bedran et al. 2014, Dupont et al. 2014). Antimicrobial peptide (AMP) genes are one of the important components of host defense machinery (Dupont et al. 2014). Thus, to delineate the mechanism behind Asiatic acid's antibacterial action, a PCR array was performed. Here, we identified for the first time that Asiatic acid over-expresses several antimicrobial peptide genes by PCR array. Other than antimicrobial peptides, MAPK and TLR genes were also over-expressed due to Asiatic acid treatment. The two most important antimicrobial peptide genes are cathelicidin (CAMP) and myeloperoxidase (MPO). Both the peptides possess direct bactericidal activities. Cathelicidin has the property of killing both gram-negative and gram-positive bacteria. Cathelicidin mediated membrane perforation leads to the killing of gram-negative bacteria. Besides direct microbial killing, cathelicidin and other AMPs carry immunomodulatory properties. Moreover, cathelicidin down-regulation is reported during *S. flexneri 2a* infection (Islam et al. 2001). Here, we observed that Asiatic acid boosts transcription of host endogenous AMPs for greater protection from *S. flexneri*. Another important gene up-regulated by Asiatic acid treatment in infected cells is myeloperoxidase. Myeloperoxidase is reported to directly kill bacteria by generating hypochlorous and hypohalous acids, which possess bactericidal properties (Denys et al. 2019). Hence, Asiatic acid probably can inhibit intracellular growth of *S. flexneri* by inducing the transcription of AMP genes.

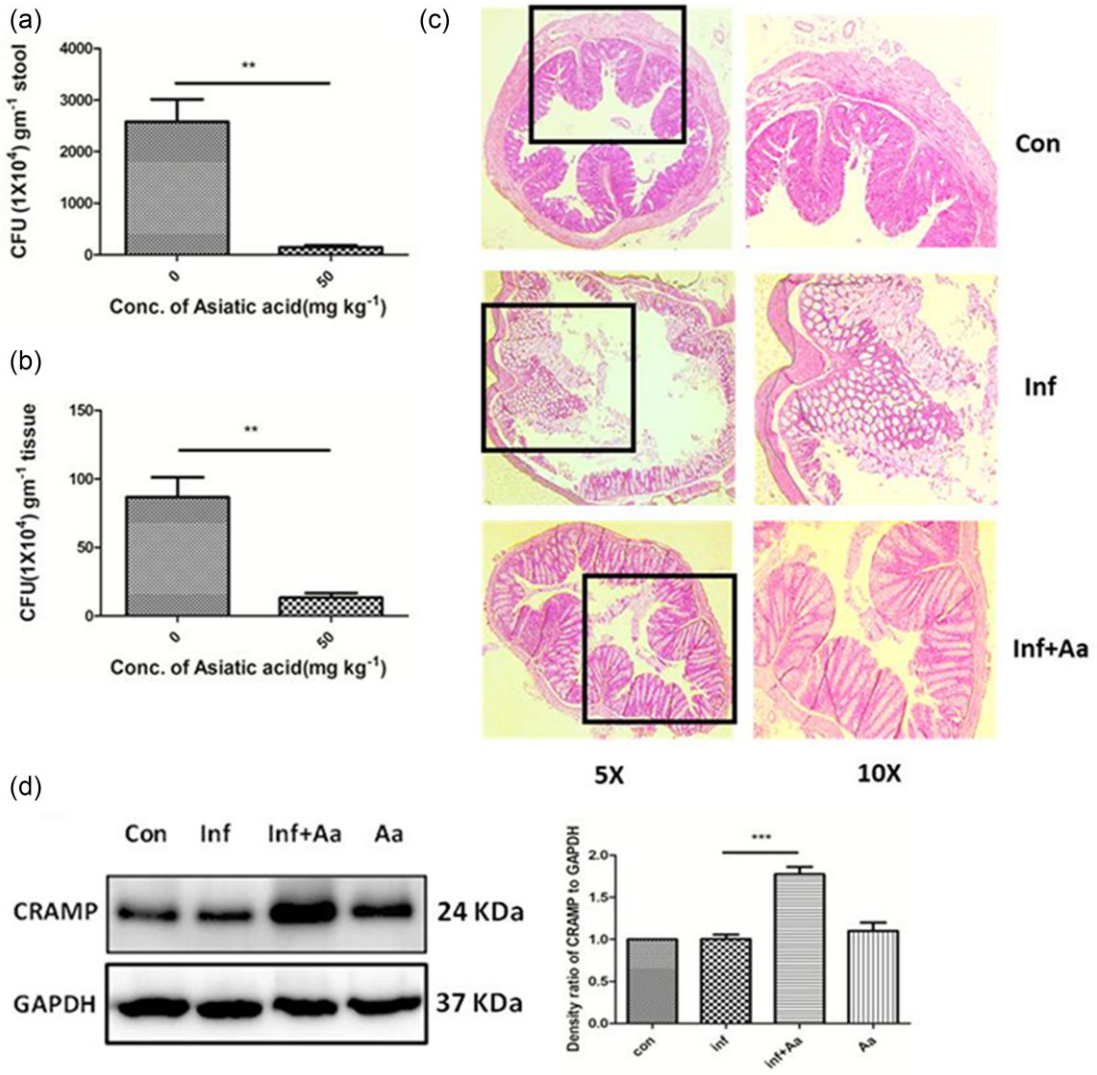

Figure 6. Asiatic acid ameliorated *S. flexneri* infection *in vivo*. Infected mice were treated with Asiatic acid for 24 h. Collected (a) stool and (b) colon were crushed and plated on Congo red plates. CFU gm^{-1} was calculated and graphically represented as mean ± S.E.M. ($n = 3$); unpaired t-test was performed. (c) Histopathological images of colonic tissue (H and E) from control, infected, and infected plus Aa treated mice at 5X and 10X magnification. *Shigella flexneri* infection causes overall distortion of colonic tissue. Asiatic acid (Aa) treatment ameliorates the effects of *S. flexneri* infection significantly. (d) Expression of mouse cathelicidin related antimicrobial peptide (CRAMP) was observed in control, infected, infected plus Aa, and Aa treated mice in immunoblot. Densitometric analysis was performed and graphically represented. One-way ANOVA was performed. All data are represented as mean ± S.E.M. ($n = 3$). Significance levels were denoted as ∗for $P < 0.05$, ∗∗for $P < 0.01$, and ∗∗∗for $P < 0.001$.

Moreover, we identified the probable signaling pathway to be involved in this up-regulation of AMP genes. It has been previously reported that MAPK pathways are involved in inducing antimicrobial peptide gene expression (Sechet et al. 2018). This study showed that the antibacterial activity of Asiatic acid is probably through activation of ERK, p38, and JNK. This was consistent with a previous report which showed that Asiatic acid induces ERK and AKT phosphorylation (Qi et al. 2017). Further, we used specific MAPK inhibitors to confirm that the antimicrobial activity of Asiatic acid is dependent on MAPK activation. Intracellular bacterial growth analysis indicated that antimicrobial activity is dependent on p38 and ERK activation but independent of JNK. These results are not unexpected, as it has been previously reported that the *S. flexneri* type III secretion system releases OspF, which selectively dephosphorylates p38 and ERK to dampen inflammation, whereas it potentiates the activation of JNK (Reiterer et al. 2011). Moreover, we checked the inflammatory response induced by Asiatic acid. Asiatic acid enhanced IL-8 and IL-6 secretion in infected and uninfected cells. These results are consistent with previous reports of cathelicidin induced antibacterial activity. Cathelicidin and MAPK are reported to mediate IL-8 and IL-6 release (Khine et al. 2006, Zheng et al. 2007, Bucki et al. 2010). Moreover, butyrate-induced cathelicidin expression is known to have a therapeutic effect on shigellosis by activating the immune response (Sarker et al. 2011). Hence, Asiatic acid probably can inhibit infection by inducing AMP like cathelicidin gene expression. The overall mechanism suggests that MAPKs are involved in antimicrobial peptide gene up-regulation. This up-regulation of genes is responsible for bacterial killing along with pro-inflammatory cytokine production, which also helps in bactericidal activities. Moreover, we observed that cathelicidin is specifically released by Asiatic acid in the culture su-

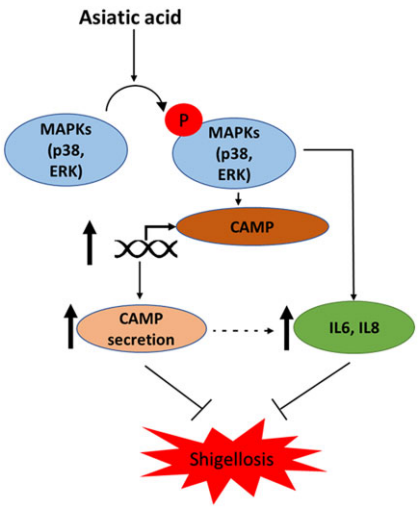

Figure 7. Graphical representation of the mechanism of action of Asiatic acid. Asiatic acid activates MAPKs (ERK and p38) via phosphorylation. Activated MAPKs induce the transcription of various antimicrobial peptides (AMPs), mainly cathelicidin (CAMP). Activated MAPKs and CAMP induce pro-inflammatory cytokine release. Asiatic acid mediates CAMP and cytokine secretion, which inhibits *S. flexneri* growth.

pernatant of infected and uninfected cells. Immunofluorescence microscopy further indicated that Asiatic acid induced cathelicidin expression targets *S. flexneri* in intestinal cells. Therefore, Asiatic acid specifically induces antimicrobial peptide cathelicidin expression to cause bacterial killing. To clarify the effectivity of Asiatic acid as an anti-shigella agent, we further performed *in vivo* experiments. In line with *in vitro* data, Asiatic acid reduced *S. flexneri* infection and repaired intestinal tissue damages. Henceforth, in conclusion, Asiatic acid induced MAPK (P-p38 and P-ERK) mediated cathelicidin expression and inflammatory cytokine release, thereby reducing *S. flexneri* burden (Fig. 7).

Thus, in view of the rapid emergence of multidrug resistant *Shigella* strains, there is an urgent need for anti-infective drug therapy. This has induced interest in host-driven antimicrobial defense mechanisms. Antimicrobial peptide activation is an important host-mediated response that not only induces bactericidal properties but also activates an immunomodulatory response. Here, we have demonstrated that Asiatic acid stimulates antimicrobial peptide gene expression and inhibition of intracellular *S. flexneri* growth. Asiatic acid may be used in the future to enhance the potency of antimicrobials to attack intracellular bacterial pathogens like *Shigella spp*.

Acknowledgements

We thank Hemanta Koley for providing *Shigella flexneri (*sf2457T*) serotype 2a*, Asish Kumar Mukhopadhyay for providing multidrug-resistant strains (BCH12654 and BCH12702), and Mamta Chawla Sarkar for editing the manuscript. PM thanks the Council for Scientific and Industrial Research (CSIR) and PB thanks Department of Biotechnology (DBT) for supporting with fellowship.

Supplementary data

Supplementary data are available at *JAMBIO* Online.

Conflict of interest statement

All authors declare that they have no conflict of interest.

Funding

This work was supported by the NICED Okayama Collaborative Project OUP 3–9.

Authors contribution statement

PM and SB conceptualized the study. PM, PB, and SB performed the experiments. PM, PB, SB, and SD prepared the original draft of the manuscript. SD, KO, and SM collaborated on this study. All authors did data analysis, draft review, editing, and approval.

Data availability statement

The original data is available upon request from the corresponding author.

References

Baker S, The HC. Recent insights into *Shigella*: a major contributor to the global diarrhoeal disease burden. *Curr Opin Infect Dis* 2018; **31**: 449.

Bals R. Epithelial antimicrobial peptides in host defense against infection. *Respir Res* 2000; **1**: 1–10.

Bedran TBL, Mayer MPA, Spolidorio DP *et al*.. Synergistic anti-inflammatory activity of the antimicrobial peptides human beta-defensin-3 (hBD-3) and cathelicidin (LL-37) in a three-dimensional co-culture model of gingival epithelial cells and fibroblasts. *PLoS One* 2014; **9**: e106766.

Blyth GA, Connors L, Fodor C *et al*.. The network of colonic host defense peptides as an innate immune defense against enteropathogenic bacteria. *Front Immunol* 2020; **11**: 965.

Brunner K, Samassa F, Sansonetti PJ *et al*.. Shigella-mediated immunosuppression in the human gut: subversion extends from innate to adaptive immune responses. *HumVaccines Immunother* 2019; **15**: 1317–25.

Bucki R, Leszczyńska K, Namiot A *et al*.. Cathelicidin LL-37: a multitask antimicrobial peptide. *Arch Immunol Ther Exp (Warsz)* 2010; **58**: 15–25.

Chen Q, Rui J, Hu Q *et al*.. Epidemiological characteristics and transmissibility of shigellosis in Hubei Province, China, 2005–2017. *BMC Infect Dis* 2020; **20**: 1–13.

Chi Y-W, Raffetto JD. Venous leg ulceration pathophysiology and evidence based treatment. *Vasc Med* 2015; **20**: 168–81.

Denys GA, Devoe NC, Gudis P *et al*.. Mechanism of microbicidal action of E-101 solution, a myeloperoxidase-mediated antimicrobial, and its oxidative products. *Infect Immun* 2019; **87**: e00261–00219.

Dijksteel GS, Ulrich MM, Middelkoop E *et al*.. Lessons learned from clinical trials using antimicrobial peptides (AMPs). *Front Microbiol* 2021; **12**: 287.

Djoukeng JD, Abou-Mansour E, Tabacchi R *et al*.. Antibacterial triterpenes from *Syzygium guineense* (Myrtaceae). *J Ethnopharmacol* 2005; **101**: 283–6.

Dupont A, Heinbockel L, Brandenburg K *et al*.. Antimicrobial peptides and the enteric mucus layer act in concert to protect the intestinal mucosa. *Gut Microbes* 2014; **5**: 761–5.

Günther J, Seyfert H-M. The first line of defence: insights into mechanisms and relevance of phagocytosis in epithelial cells. *Semin Immunopathol* 2018;**40**:555–565

Gyawali R, Ibrahim SA. "Natural products as antimicrobial agents". *Food Control* 2014; **46**: 412–29.

Hajialibeigi A, Amani J, Gargari SLM. Identification and evaluation

of novel vaccine candidates against *Shigella flexneri* through reverse vaccinology approach. *Appl Microbiol Biotechnol* 2021; **105**: 1159–73.

Hosangadi D, Smith PG, Giersing BK. Considerations for using ETEC and *Shigella* disease burden estimates to guide vaccine development strategy. *Vaccine* 2019; **37**: 7372–80.

Islam D, Bandholtz L, Nilsson J *et al*.. Downregulation of bactericidal peptides in enteric infections: a novel immune escape mechanism with bacterial DNA as a potential regulator. *Nat Med* 2001; **7**: 180–5.

Jiang S, Deslouches B, Chen C *et al*.. Antibacterial properties and efficacy of a novel SPLUNC1-derived antimicrobial peptide, α4-short, in a murine model of respiratory infection. *MBio* 2019; **10**: e00226–00219.

Kaufmann SH, Dorhoi A, Hotchkiss RS *et al*.. Host-directed therapies for bacterial and viral infections. *Nat Rev Drug Discovery* 2018; **17**: 35–56.

Khameneh B, Iranshahy M, Soheili V *et al*.. Review on plant antimicrobials: a mechanistic viewpoint. *Antimicrob Resist Infect Control* 2019; **8**: 1–28.

Khine AA, Del Sorbo L, Vaschetto R *et al*.. Human neutrophil peptides induce interleukin-8 production through the P2Y6 signaling pathway. *Blood* 2006; **107**: 2936–42.

Kida Y, Shimizu T, Kuwano K. Sodium butyrate up-regulates cathelicidin gene expression via activator protein-1 and histone acetylation at the promoter region in a human lung epithelial cell line, EBC-1. *Mol Immunol* 2006; **43**: 1972–81.

Killackey SA, Sorbara MT, Girardin SE. Cellular aspects of *Shigella* pathogenesis: focus on the manipulation of host cell processes. *Front Cell Infect Microbiol* 2016; **6**: 38.

Lapaquette P, Fritah S, Lhocine N *et al*.. *Shigella* entry unveils a calcium/calpain-dependent mechanism for inhibiting sumoylation. *Elife* 2017; **6**: e27444.

Le C-F, Fang C-M, Sekaran SD. Intracellular targeting mechanisms by antimicrobial peptides. *Antimicrob Agents Chemother* 2017; **61**: e02340–02316.

Lee KY, Bae ON, Serfozo K *et al*.. Asiatic acid attenuates infarct volume, mitochondrial dysfunction, and matrix metalloproteinase-9 induction after focal cerebral ischemia. *Stroke* 2012; **43**: 1632–8.

Li G, Domenico J, Jia Y *et al*.. NF-κB-dependent induction of cathelicidin-related antimicrobial peptide in murine mast cells by lipopolysaccharide. *Int Arch Allergy Immunol* 2009; **150**: 122–32.

Lu CW, Lin TY, Pan TL *et al*.. Asiatic acid prevents cognitive deficits by inhibiting calpain activation and preserving synaptic and mitochondrial function in rats with kainic acid-induced seizure. *Biomedicines* 2021; **9**: 284.

Mahlapuu M, Håkansson J, Ringstad L *et al*.. Antimicrobial peptides: an emerging category of therapeutic agents. *Front Cell Infect Microbiol* 2016; **6**: 194.

Meneguetti BT, Machado LS, Oshiro KG *et al*.. Antimicrobial peptides from fruits and their potential use as biotechnological tools—a review and outlook. *Front Microbiol* 2017; **7**: 2136.

Nagoor Meeran MF, Goyal SN, Suchal K *et al*.. Pharmacological properties, molecular mechanisms, and pharmaceutical development of asiatic acid: a pentacyclic triterpenoid of therapeutic promise. *Front Pharmacol* 2018; **9**: 892.

Nandy S, Dutta S, Ghosh S *et al*.. Foodborne-associated *Shigella sonnei*, India, 2009 and 2010. *Emerg Infect Dis* 2011; **17**: 2072.

Nickerson KP, Chanin RB, Sistrunk JR *et al*.. Analysis of *Shigella flexneri* resistance, biofilm formation, and transcriptional profile in response to bile salts. *Infect Immun* 2017; **85**: e01067–16.

Park J-H, Seo YH, Jang J-H *et al*.. Asiatic acid attenuates methamphetamine-induced neuroinflammation and neurotoxicity through blocking of NF-kB/STAT3/ERK and mitochondria-mediated apoptosis pathway. *J Neuroinflammation* 2017; **14**: 1–15.

Pfalzgraff A, Brandenburg K, Weindl G. Antimicrobial peptides and their therapeutic potential for bacterial skin infections and wounds. *Front Pharmacol* 2018; **9**: 281.

Puzari M, Sharma M, Chetia P. Emergence of antibiotic resistant *Shigella* species: a matter of concern. *J Infect Public Health* 2018; **11**: 451–4.

Qi Z, Ci X, Huang J *et al*.. Asiatic acid enhances Nrf2 signaling to protect HepG2 cells from oxidative damage through Akt and ERK activation. *Biomed Pharmacother* 2017; **88**: 252–9.

Ra EA, Lee TA, Won Kim S *et al*.. TRIM31 promotes Atg5/Atg7-independent autophagy in intestinal cells. *Nat Commun* 2016; **7**: 1–15.

Ranjbar R, Farahani A. *Shigella*: antibiotic-resistance mechanisms and new horizons for treatment. *Infect Drug Resist* 2019; **12**: 3137.

Reiterer V, Grossniklaus L, Tschon T *et al*.. *Shigella flexneri* type III secreted effector OspF reveals new crosstalks of proinflammatory signaling pathways during bacterial infection. *Cell Signalling* 2011; **23**: 1188–96.

Rogawski McQuade ET, Shaheen F, Kabir F *et al*.. Epidemiology of *Shigella* infections and diarrhea in the first two years of life using culture-independent diagnostics in 8 low-resource settings. *PLoS NeglTrop Dis* 2020; **14**: e0008536.

Sarker P, Ahmed S, Tiash S *et al*.. Phenylbutyrate counteracts *Shigella* mediated downregulation of cathelicidin in rabbit lung and intestinal epithelia: a potential therapeutic strategy. *PLoS One* 2011; **6**: e20637.

Savoia D. Plant-derived antimicrobial compounds: alternatives to antibiotics. *Future Microbiol* 2012; **7**: 979–90.

Sechet E, Telford E, Bonamy C *et al*.. Natural molecules induce and synergize to boost expression of the human antimicrobial peptide β-defensin-3. *Proc Natl Acad Sci* 2018; **115**: E9869–78.

Stan D, Enciu A-M, Mateescu AL *et al*.. Natural compounds with antimicrobial and antiviral effect and nanocarriers used for their transportation. *Front Pharmacol* 2021; **12**: 2405.

Sur VP, Mazumdar A, Kopel P *et al*.. A novel ruthenium based coordination compound against pathogenic bacteria. *Int J Mol Sci* 2020; **21**: 2656.

Taneja N, Mewara A. Shigellosis: epidemiology in India. *Indian J Med Res* 2016; **143**: 565.

Tang SS, Biswas SK, Tan WS *et al*.. Efficacy and potential of phage therapy against multidrug resistant *Shigella* spp. *PeerJ* 2019; **7**: e6225.

Williams PC, Berkley JA. Guidelines for the treatment of dysentery (shigellosis): a systematic review of the evidence. *Paediatr Int Child Health* 2018; **38**: S50–65.

World Health Organization; Geneva.Global antimicrobial resistance and use surveillance system (GLASS) report 2021.Licence: CC BY-NC-SA 3.0 IGO.

Young C, Walzl G, Du Plessis N. Therapeutic host-directed strategies to improve outcome in tuberculosis. *Mucosal Immunol* 2020; **13**: 190–204.

Zheng Y, Niyonsaba F, Ushio H *et al*.. Cathelicidin LL-37 induces the generation of reactive oxygen species and release of human alpha-defensins from neutrophils. *Br J Dermatol* 2007; **157**: 1124–31.

Microbial Pathogenesis 181 (2023) 106210

Contents lists available at ScienceDirect

Microbial Pathogenesis

journal homepage: www.elsevier.com/locate/micpath

Capsaicin derived from endemic chili landraces combats *Shigella* pathogen: Insights on intracellular inhibition mechanism

Subhasish Das [a,**], Nayana Priyadarshani [b], Priyanka Basak [c], Priyanka Maitra [c], Sushmita Bhattacharya [c], Satya Sundar Bhattacharya [b,*]

[a] Department of Environmental Science, Pachhunga University College, Mizoram University (A Central University), Aizawl, 796001, Mizoram, India
[b] Soil Agro Bio-engineering Laboratory, Department of Environmental Science, Tezpur University, Sonitpur, 784028, Assam, India
[c] Department of Biochemistry, ICMR-National Institute of Cholera and Enteric Diseases, Beleghata, Kolkata, 700010, India

ARTICLE INFO

Keywords:
Capsicum
Capsaicin
Pungency
Shigella flexneri
Inflammation

ABSTRACT

Ethnic tribals in northeast India have been growing and maintaining local chili landraces for ages. These chilies are known for their characteristic pungency and immense therapeutic properties. Capsaicin, a significant chili metabolite, is recognized as a natural drug for pain relief, diabetic neuropathy, psoriasis, arthritis, etc. In this study, we tried to observe the influence of locality factors on the pungency and bioactive features of *Capsicum annuum* L. landraces. We also checked the gastro-protective ability of these chilies, especially in the cure of shigellosis. Phytometabolite characterization and estimation were done through spectrophotometric methods. Preparative and analytical HPLC techniques were employed for extracting and purifying capsaicin-enriched fractions. *Shigella flexneri* growth retardation was determined through the broth dilution method. Gentamicin protection assay and ELISA were done to assess the intracellular invasion and IL-1β inflammasome production by *S.flexneri.* The correlation analyses postulated that phenols, flavonoids, chlorophylls, β-carotene, and capsaicin synthase upregulation strongly influenced capsaicin biosynthesis in chili cultivars. Correspondingly, the inhibitory efficacy of the HPLC-purified Balijuri-derived capsaicin was more effective than the Raja-derived capsaicin in inhibiting intracellular *Shigella* growth. Reduced levels of pro-inflammatory cytokine (IL1β) in capsaicin-treated *Shigella*-infected cells probably reduced inflammation-mediated intestinal damage, limiting bacterial spread. This investigation advocates the unique potential of local chilies in curing deadly 'shigellosis' with mechanistic evidence. Our observation justifies the traditional healing practices of the ethnic people of NE India.

1. Introduction

Shigella flexneri, a gram-negative bacterium, is the primary pathogen causing bacillary dysentery (shigellosis) in humans, which leads to 1.1 million deaths annually all over the world [1]. It is a highly infectious organism exhibiting about 19 seral types characterized based on the cell envelope liposaccharide-based O-antigen [2,3]. According to World Health Organization, beta-lactams, quinolone, and macrolide-based antibiotics are recommended to treat shigellosis—however [4], revealed that multi-drug resistant (MDR) strains of *Shigella* sp. have become immune to fluoroquinolone, cephalosporins, and azithromycin. Moreover, these synthetic drugs carry several side effects that significantly compromise the musculoskeletal and nervous systems in humans [5,6]. On the other hand, no licensed vaccine is available in the market. The most common therapeutics/antibiotics for shigellosis entail high production cost, limited efficiency, and severe side effects [7]. Thus, there is an utmost need for herbal drugs containing bioactive compounds that can act as anti-microbial agents. Interestingly, plant-sourced drugs have significantly overcome multidrug resistance to pathogens [8,9]. [10] reported the anti-shigellosis activity of *Picralima nitida* (Stapf) T. Durand & H. Durand. Extract of *Punica granatum* L. is traditionally used in Iran for curing diarrhea [11]. The essential oil of *Thymus schimperi* Ronniger also has good inhibitory activity against *Shigella* [12]. These studies, however, could not reveal the mechanism of the anti-*Shigella* action of the plant extracts and the biomolecules involved in the pathway.

Northeastern India boasts different types of endemic local landraces of *Capsicum* with distinct genotypes and phenotypic features [13]. These

* Corresponding author. Department of Environmental Science, Tezpur University, Assam, 784028, India.
** Corresponding author. Department of Environmental Science, Mizoram University (PUC), Aizawl, 796001, Mizoram, India.
E-mail addresses: dassubhasish@pucollege.edu.in (S. Das), satya72@tezu.ernet.in (S.S. Bhattacharya).

https://doi.org/10.1016/j.micpath.2023.106210
Received 26 April 2023; Received in revised form 16 June 2023; Accepted 18 June 2023
Available online 19 June 2023

landraces are adapted to the organic-matter-rich dark soils of this region that impart high pungency and taste [14]. *C. annuum* traditionally documented in Indian medicinal literature *viz.* "*Ayurveda*" (as Rakta-maricha, Lanka, Katuvira), "*Unani*" (as Filfil-e-Ahmar and Filfil-e-Surkh), and "*Siddha*" (as Maligay) bears gastro-protective, pain-relief (muscle pain and toothache), and anti-septic properties [15]. The "*Mishing*" community of Assam claims that oral consumption of *C. annuum* (locally named "*Surging Mirsi*") instantly relieves stomach [16]. In the valleys of the Alaknanda region (Western Himalayas of India), traditional animal healers (locally called "*Pashu Vaidya*") use *C. annuum* milled with the bark of *Zanthoxylum armatum* DC to cure thyroid hard-knot disease in milch cattle [17]. The medicinal importance of *C. annum* in pain relief can be traced back to pre-Hispanic times in the book of the Aztecs and Mayans named "*Libellus de Medicinabilus Indorum Herbtis*" [18]. Healers practicing traditional African medicine (TAM) refer to *C. annuum* as an antidote for muscle spasms, tussis, irritation, etc. (Elujoba et al., 2004). In the Tibetan pharmacopeia, "Blue Beryll" *C. annuum* is associated with better digestion and reduced hemorrhoids in humans [19]. In an in vitro model [20], *C. annuum* extract possesses significantly higher bioavailability of carotenoids in the intestinal cells rendering higher anti-oxidative capability. Similarly, dry powder of *C. annuum* tested *in vivo* has harmful sterols in Winstar rats [21]. [22] reviewed the importance of *C. annuum* extract (enriched with capsaicin) as an analgesic in internal medicine and dentistry. However, the studies related to the scientific validity of ethno-pharmacological information are often inconclusive due to the incoherent molecular pharmacological data [23].

Capsaicin (N-vanillyl-8-methyl-6-nonenamide; $C_{18}H_{27}NO_3$; mol. weight: 305.41), the major chili capsaicinoids, is responsible for the hotness and pungency of *Capsicum* fruits. Capsaicin is formed via the phenylpropanoid pathway where an enzyme capsaicin synthase (encoded by the *Csy1* gene) catalyzes the reaction between vanilylamine and 8-methyl-6-nonenoic acid CoA [24]. Capsaicin plays an essential role in suppressing gastric ulcers by selective stimulation of the afferent nerves in the gastric mucosa, thereby inhibiting the acid secretion, enhancing the mucous secretion, and mainly hastens the gastric mucosal blood flow, which aids in the prevention and healing of ulcers [25]. The inhibitory potential of capsaicin has also been found for several microbial pathogens. For example, Pure capsaicin can retard chlamydial (*Chlamydia trachomatis, C. pneumoniae*) growth by influencing TRPV1, PPARγ, and LXRα receptors in the host cell [26]. Capsaicin extract (100 $ngmL^{-1}$) could inhibit *Salmonella typhimurium* growth [27]. Capsaicin extract shuffled the abundance of *Faecalibacterium, Akkermansia, Roseburia, Helicobacter,* and *Bacteroides* in the intestines of rats [28]. Evidence of capsaicin induced-autophagy in *Shigella flexneri*-infected cells has recently been observed by Ref. [29]. However, the direct inhibitory effect of plant-derived capsaicin on the *Shigella* pathogen has not been explored.

According to Ref. [13]; the capsaicin biosynthetic pathway in chili is influenced by soil organic C, stable C-compounds (humic and fulvic acids), microbial biomass C, soil N content, and pH evident from the upregulation and downregulation of capsaicin biosynthetic loci *viz., Csy1*, *Pun1,* and *Pun1*^{2}. [30] also observed wide heterogeneity in *C. annuum* landraces of northeast India, which can serve as a reservoir for chili breeders. RAPD-based genetic studies have shown that *C. annuum* has the maximum genotypic plasticity compared to *Capsicum chinense* Jacq. and *Capsicum frutescens* L. [11,31]. As such, seven endemic landraces of the *C. annuum* of northeast India differed from the accessions grown in other parts of India [31]. Therefore, the therapeutic potential of *C. annuum* landraces needs more attention.

Although capsaicin is widely found in different chilies, its production and availability differ [32]. reported 36.7% higher capsaicin production in *Capsicum chinense* when grown in their native location than in other sites. Capsaicin content and pungency also varied significantly among two different landraces even when cultivated in their endemic location [13]. Capsaicin bioavailability also varies among the chili species, a general order being *Capsicum chinense* > *C. annum* ≥ *C. frutescens* > *C. pubescens* Ruiz & Pav. >*C. baccatum* L. [33]. Additionally [34], observed varying concentrations of capsaicin within different parts of the chili fruit. In this context, the opinion of [23] on the concentration-effect paradigm for natural products provides the basis for the authenticity of experimental approaches toward improved scientific quality. Nevertheless, the appropriate evidence of the pharmacological action of capsaicin-enriched *C. annuum* extract is poor in the literature. Based on the dark areas identified above, novel research questions for the present endeavor were: (i) How capsaicin content varies in two dominant local *C. annuum* landraces, and which metabolites are the significant indicators of capsaicin levels?; (ii) Does the chili-derived capsaicin arrest/diminish *Shigella* growth?; and (iii) What is the mode of action of chili-derived capsaicin? Accordingly, two local landraces were cultivated with their traditional method and assessed for capsaicin content, pungency, and other metabolites. The capsaicin was purified and tested for anti-shigellosis activity in *Shigella flexneri* model.

2. Materials and methods

2.1. Germplasm collection and cultivation of the landraces

One-month-old seedlings of two *C. annuum* landraces (*i.e.,* Balijuri and Raja) were procured from the home gardens of traditional farmers in Assam. We collected the Balijuri seedlings from Thelamara village (26.6943° N, 92.5569° E), while the Raja seedlings were brought from Hahchara village (26.7348° N, 91.8391° E). The seedlings were surface sterilized with 5% sodium hypochlorite solution to avoid fungal infections and kept inside a net house at the Tezpur University campus for acclimatization for seven days. Then, ten actively growing seedlings (5 each for Balijuri and Raja) were transplanted in earthen pots filled with a 5 kg mixture (1:10) of soil and cow dung manure (CDM). The soil was brought from the nearby agricultural fields. The proportion of CDM in the mixture was determined per the chili farmers' conventional practice. Chemical fertilizers were not used in the present study. A 50-ppm dose of the gibberellic acid formulation was uniformly applied using a sprayer machine during the flowering stage to stabilize the fruit set. Intercultural operations like weeding and irrigation were uniformly conducted on a need basis. The fruits were harvested thrice from 90 days after transplanting (DAT) and 120 DAT.

2.2. Determination of capsaicin content and pungency in different portions of the fruits

We followed the protocol [35] developed for determining capsaicin content in chili fruits. The fruits (500 mg), obtained from the final harvest (i.e., at 120 DAT), were macerated in a mortar pestle with acetone (10 mL) followed by 3 h mechanical shaking (Remi, India). The supernatant was decanted in tubes and centrifuged for 10 min at 10000 g (REMIR–8C, India). The clear supernatant was then carefully poured into 25 mL glass beakers and kept for evaporation in a water bath till dry residue occurred. Finally, 0.4% NaOH (5 mL) and 3% phosphomolybdic acid solution (3 mL) were added to the residue and appropriately dissolved. The solution was then filtered and processed for spectrophotometric assessment at 650 nm in a UV–vis spectrophotometer (Agilent Cary 60, USA). We used authentic capsaicin standard (Sigma Aldrich, USA) for determining the standard curve. Capsaicin concentration was then calculated using the standard curve, and the results were expressed in mg capsaicin per 100 g fruit. Correspondingly, pungency in the fruits was determined by following equation (1) as reported by Ref. [36]:

$$Pungency\ (SHU) = Capsaicin\ content\ \left(mg\ 100g^{-1}\ FW\ chili\right) \times 1.6 \times 10^7 \quad (1)$$

2.3. Assessment of capsaicin synthase activity

Capsaicin synthase activity was determined in the chilies, as suggested by Ref. [24]. Briefly, 1 g fruit tissue was homogenized in 10 ml of 0.1 M potassium phosphate buffer (pH 6.8) in the presence of 100 mg ascorbic acid and 5 μM 2-mercaptoethanol. The contents were centrifuged for 30 min at 4000×*g* in a refrigerated centrifuge (4 °C) (Eppendorf, Germany). Correspondingly, 1 ml of the extract was paired with 0.5 M potassium phosphate buffer, 1 μMMgCl_2, 1 μM ATP, 5 μM vanillylamine, and 5 μM 8-methylnonenoic acid CoA and incubated at 37 °C for 2 h; a few drops of 0.5 M HCl were added to stop the reaction and then the extract was re-suspended in 100 μL methanol. This suspension was processed through an HPLC unit (Waters, USA) to enumerate the capsaicin synthase activity. The HPLC-mediated separation was conducted on a C-18 column (pore size = 10 μm; l × b = 3.9 mm × 150 mm; Waters, USA). The mobile phase consisted of methanol and ultrapure water (70:30, v/v). The injection volume was 10 μL with a flow rate of 1 mL per min. The detection was made at 280 nm, and the total run time was 30 min.

2.4. Extraction and purification of capsaicin from the chilies

Fresh pepper (10.0 g) samples (Balijuri and Raja) were weighed, finely chopped, and ground for 10 min using a mortar and pestle. Then, 30 mL of acetonitrile was added as an extraction solvent and the pepper samples were ground for 20 min. Insoluble plant materials were removed by vacuum filtration. The obtained solvent extract (25 mL) was then re-suspended in 25 mL acetonitrile. The final volume (50 mL) was evaporated in a rotary evaporator (Eyela, Japan) for 15 min and reduced to 30 mL. The extract was then diluted by 1 mL in 10 mL acetonitrile bringing the total volume to 300 mL [37]. Subsequently, 10 mL of the capsaicin extract was injected into a preparative HPLC system comprised of a μ-Bondapak C18 column (10 μm, 3.9 mm × 150 mm, Waters) coupled with a guard column (μ-Bondapak Guard-Pak, Waters). The eluent was a mixture of MeOH/H_2O (70:30 v/v) at a flow rate of 1.0 mL min^{-1}. We executed total 30 injections for 25 min run time and recorded the optical absorbance at 280 nm. The corresponding peak (retention time 2.1 min–3.8 min) was collected for each injection (approximate volume 2 mL). In the end, all eluted samples were re-constituted and a final volume of 180 mL was acquired. We ascertained the authenticity of the isolated capsaicin-enriched eluent with a 10 min quick-run in an analytical HPLC system fitted with Waters Symmetry™ C18 (IS) column (3.5 μm, 3.9 mm × 20 mm). At the same time, the other operational attributes were the same. Consequently, the eluent volume was subjected to a rotary evaporator until dry. The dried material (pure capsaicin) was collected and weighed.

2.5. Determination of different metabolites in the two landraces (total phenol, total flavonoids, total carotenoids, β-carotene, lycopene, chlorophyll-a, and chlorophyll-b)

The samples were washed and further processed to identify plant metabolites. The fruit tissue was pulverized in methanol (MeOH) and double distilled water (DDW) (1/4, W/V) to prepare the extract. Phenolic content of *C. annuum* was spectrophotometrically determined with the help of the Folin-Ciocalteu reagent assay as described by Ref. [38]. Around 100 μL of the extract was mixed with (850 μL) DDW, 0.5 ml of Folin-Ciocalteu reagent, and 2 mL of Na_2CO_3; they were mixed well and read at 760 nm. Total flavonoid content was analyzed as described in Ref. [39]. About 1 mL of the extract was mixed with 3 mL methanol, 0.2 mL of 10% $AlCl_3$ solution, and 5%sodium potassium tartrate solution. Readings were taken spectrophotometrically at 415 nm and expressed as mg per kg. Chlorophyll (a and b) and carotenoid contents were calculated using standard protocols [40].

For estimating lycopene and β-carotene, 1 g of the fruit sample was pulverized in 16 mL of acetone and n-hexane (4:6, v/v). The mixture was set to stand for 30 min till the two phases of the mixture separated. The aliquot from the upper layer was read at 663, 645, 505, and 453 nm [41]. Equations (2) and (3) were followed for enumerating lycopene and β-carotene concentrations, respectively:

$$Lycopene\ \left(mg\ g^{-1}\right) = -0.0458 \times A_{663} + 0.204 \times A_{645} + 0.372 \times A_{505} - 0.806 \times A_{453} \quad (2)$$

$$\beta - carotene\ \left(mg\ g^{-1}\right) = 0.216 \times A_{663} - 1.22 \times A_{645} - 0.304 \times A_{505} + 0.452 \times A_{453} \quad (3)$$

2.6. Growth inhibition studies

2.6.1. Bacterial culture conditions

Shigella flexneri (sf2457T) serotype 2a was obtained from Dr Hemanta Koley, NICED, Kolkata, India. Bacteria were routinely cultured in Mueller Hinton Broth (HiMedia, India) at 37 °C in an incubator-shaker.

2.6.2. Cell culture conditions

HT-29 (ATCC HTB-38) cells were cultured with McCoy's 5A Medium (Sigma-Aldrich, USA) containing 10% heat-inactivated fetal bovine serum (FBS) (Sigma, USA),1% non-essential amino acids, and 1% penicillin-streptomycin (HiMedia, India). Cells were maintained in a 37 °C humidified incubator with 5% CO_2.

2.6.3. Broth dilution and Gentamicin protection assays – identifying the minimum inhibitory concentration (MIC)

Considering the importance of these assays for determining the impact and mode of action of chili-derived capsaicin, the established guidelines for ethnopharmacological studies were meticulously followed after [42].

Broth dilution assay: Initially, a standard stock solution (20 mg mL^{-1}) of the capsaicin-enriched extracts of Balijuri and Raja chilies was prepared in 100% di-methyl sulfoxide (DMSO), and different gradient concentrations (0–150 μg mL^{-1}) of the extracts were eventually developed. All the containers (Erlenmeyer flask) were properly sealed to ensure the stability of the solvent (i.e., DMSO). Here, the 0 level, i.e., only DMSO was considered as control. Correspondingly, the broth dilution assay was performed in separate flasks containing Muller-Hinton (MH) broth by adding the overnight culture of *S. flexneri* (10^5) at 37 °C in an incubator-shaker for 2 h. Then, the bacterial culture was withdrawn at 1-h intervals, diluted, and plated overnight for counting CFU mL^{-1}), and the MIC was determined.

Gentamicin protection assay: The Gentamicin protection assay was performed to appreciate the impacts of Balijuri and Raja chili-derived capsaicin-enriched extracts on the invasiveness of the *Shigella flexneri* pathogenicity. The intestinal cells (1×10^5) were cultured in 6 well plates for 24h at 37 °C and 5% CO_2 before infection. Cells were further incubated overnight in antibiotic-free media. The *S. flexneri* was grown overnight in MHB at 37 °C with shaking and sub-cultured to an optical density of 0.5–0.6 at 600 nm [29]. Bacteria pellets were collected by centrifuging the culture at 12000g for 5 min at 4 °C and washed with PBS. The pellets were then re-suspended in incomplete tissue culture media. Afterward, the intestinal cells were pre-treated with a few sub-lethal concentrations of capsaicin-enriched extracts from 0 (only DMSO) to 60 μg mL^{-1} for 1h and 2 h, respectively, in incomplete media. The sub-lethal doses were determined on the basis of the MIC values obtained from the broth dilution assay. Similar to that of the broth dilution assay, Ciprofloxacin (2.5 μg mL^{-1}) was taken as the positive control. Correspondingly, the infection with *S. flexneri* was performed at a multiplicity of infection (MOI) of 200:1. The infected plates were centrifuged for 15 min at 700 g for synchronization and incubated for 2

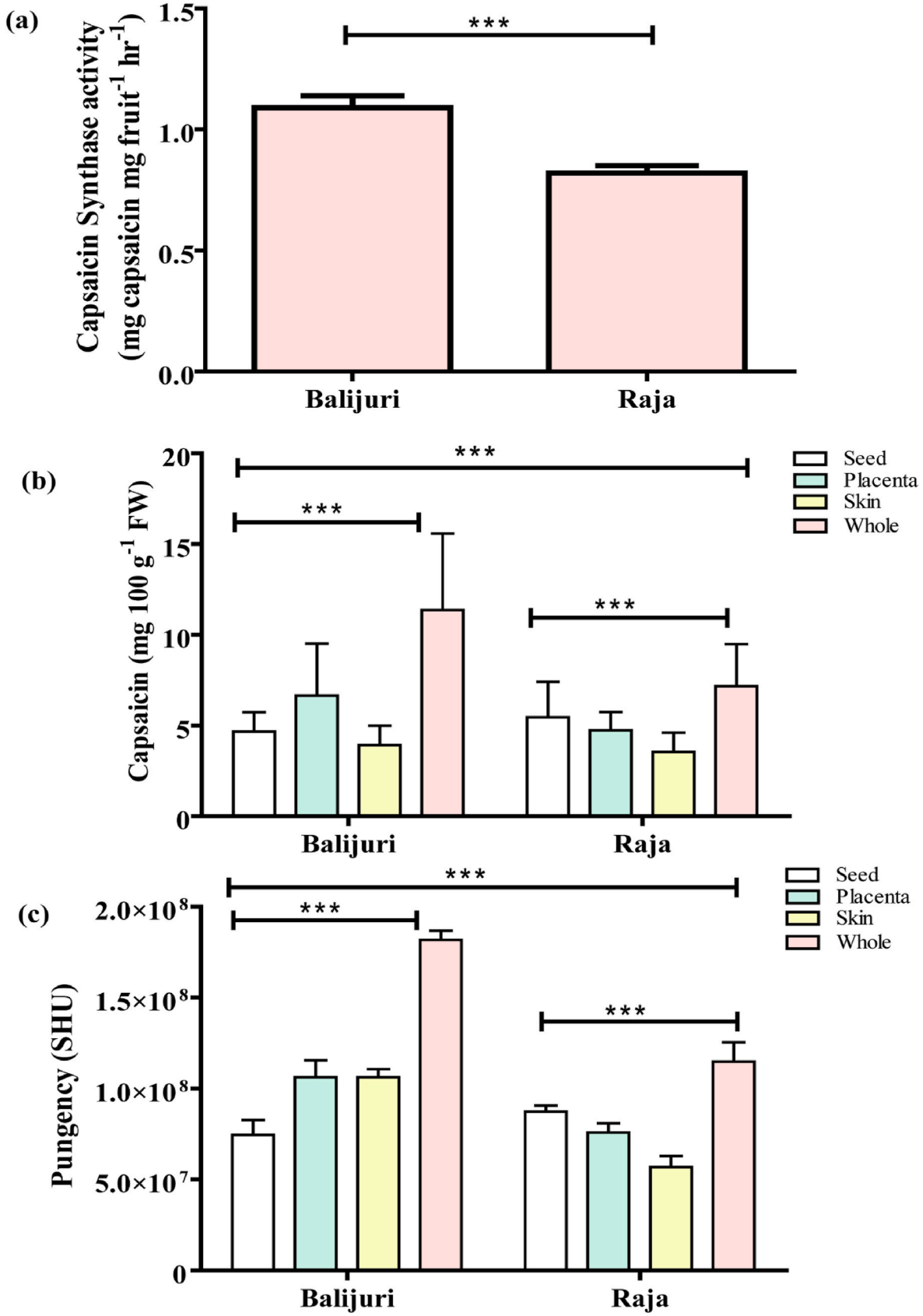

Fig. 1. (a) Capsaicin synthase activity in the whole fruits of Balijuri and Raja chilies; (b) capsaicin content and (c ~~b~~) pungency observed in the whole and different parts of the Balijuri and Raja fruits. Student's t-test was conducted for capsaicin synthase activity using chili variety as the source of variation. Capsaicin concentration and pungency data were analyzed through two-way ANOVA, where the sources of variation were chili varieties and body parts of the chili fruits. Values are represented as mean ± standard deviation. Significance was calculated; ***$p < 0.001$.

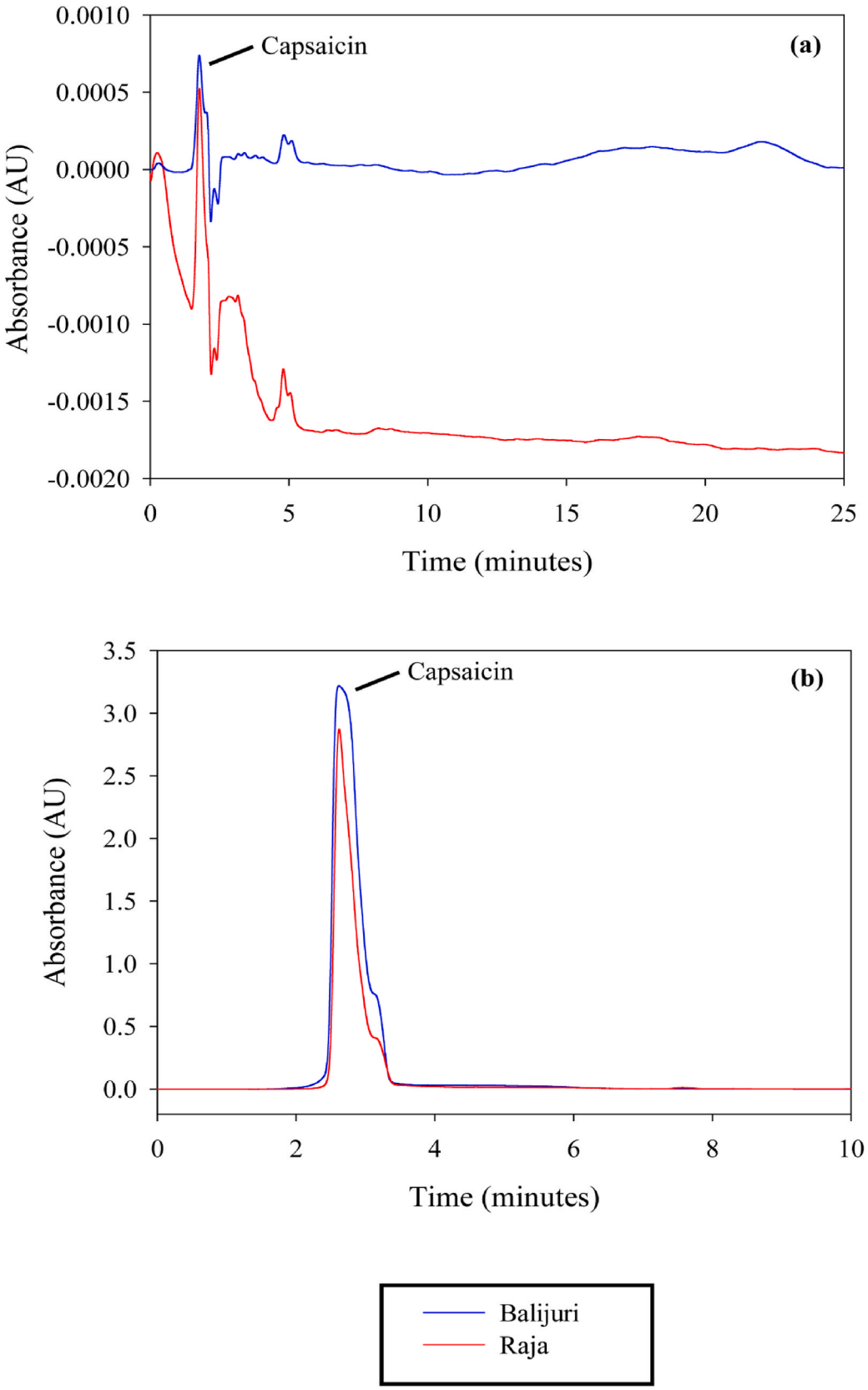

Fig. 2. HPLC chromatograms of the fruit extracts of Balijuri and Raja varieties. (a) Preparative HPLC chromatogram showing the presence of capsaicin and other secondary metabolites (attributed to the different peaks) in the fruit extracts of Balijuri and Raja varieties. The portions eluted in the 2–3.7 min were collected and purified for further assessments; (b) chromatograms representing capsaicin detected in the purified fractions of both varieties through the analytical HPLC method.

Table 1
Concentration of different metabolites measured in the fruits and leaves of Balijuri and Raja chilies. Values are represented as mean ± standard deviation.

Order		Total phenol (mg kg^{-1} DWf)	Total flavonoid (mg kg^{-1} DWf)	Lycopene (mg g^{-1} FWf)	β-carotene (mg g^{-1} FWf)
1	Balijuri	326.1 ± 39.2	724.9 ± 80.2	1.98 ± 0.2	0.565 ± 0.1
2	Raja	155.1 ± 17.2	58.4 ± 12.2	0.99 ± 0.16	0.32 ± 0.09
	df	4	4	4	4
	t	3.94	235.8	34.1	23.8
	F	12.1	2.37	0.031	0.093
	p	0.017	0.000	0.000	0.000

Order		Total carotenoid (mg g^{-1} FWf)	Chlorophyll A (mg g^{-1} FWl)	Chlorophyll B (mg g^{-1} FWl)
1	Balijuri	2.02 ± 0.96	19.2 ± 1.66	13.6 ± 2.13
2	Raja	2.13 ± 0.36	15.1 ± 2.02	9.88 ± 1.18
	df	4	4	4
	t	23.8	2.267	5.502
	F	0.093	2.355	0.991
	p	0.000	0.086	0.005

FWf- Fresh weight of fruit; DWf-Dry weight of fruit; FWl-Fresh weight of leaf; DWl-Dry weight of leaf.

h to allow bacteria to enter the cells. Cells were thoroughly washed and treated with 50 μg mL^{-1} of gentamicin for 2 h, killing the extracellular bacteria. Further washing with PBS was done, and then cells were lysed using 0.1% triton X. The cell lysates were plated in MHA at 37 °C for 18 h to count the number of colonies (CFU mL^{-1}). Eventually, the MICs for both extracts were computed.

We have repeated both the broth dilution assay with the industrially suitable doses of the capsaicin-enriched extracts derived from the two chili cultivars in comparison with Ciprofloxacin (2.5 μg mL^{-1}) as the positive control to appreciate the prospects of the extracts towards drug development. Concurrently, the Gentamicin protection assay was performed with Ciprofloxacin (2.5 μg mL^{-1}) as the positive control.

2.6.4. Enzyme-linked immunosorbent assay (ELISA) and real time PCR

HT 29 cells were pre-incubated with capsaicin-enriched extracts of the two cultivars (Balijuri and Raja) for 2h, followed by infection with *S. flexneri* for 2 h. Media was collected to carry out ELISA. ELISA was performed using a human interleukin-1β (IL1β) ELISA assay kit (BD Biosciences). The optical density (at 450 nm) was measured from the media collected after infection and capsaicin treatment, and the concentration of IL1β released (pg mL^{-1}) was calculated and graphically represented.

Prior the PCR analysis, the HT29 cells were pre-treated with pure capsaicin (Caps) (5 μg ml^{-1}) for 2 h and subsequently infected with *Shigella flexneri* (MOI200) as detailed above. The RNA from cells (Control, infected, and infected + Caps-treated) was isolated using RNA isolation kit (Qiagen). Isolated RNA was converted to c-DNAs using the Thermo Scientific c-DNAs synthesis kit. The real Time PCR was performed using SYBR green (Thermo) using the human IL-1β gene with the following primer sequence:

FP: 5′-GGCCAATAAGATGGGTCTGA-3′ and RP: 5′-CACTGCCTCCAGTGTCTTCA-3′

The expression patterns were analyzed using $^{\Delta\Delta}$Ct method and normalized using the internal control GAPDH. $^{\Delta\Delta}$Ct was calculated by the following formula: $^{\Delta\Delta}$Ct = test - internal control-test control. Fold change compared to control was calculated and graphically represented.

2.7. Statistical analysis

We assessed the normality and homoscedasticity of the accrued date using the normality test in SPSS v. 16 (SPSS Inc, Chicago, IL, USA). The normality of the data was assured after achieving a value of ±1 for both skewness and kurtosis. We used an independent sample *t*-test, one-way analysis of variance (ANOVA), and two-way ANOVA for the different data sets. The data on capsaicin concentration and pungency of the two chilies were subjected to one-way ANOVA, assuming the different chili parts/portions as the primary factor. Significant variations in capsaicin synthase activity and the data of other chili metabolites (*i.e.,* total phenol, total flavonoid, carotenoid, chlorophyll *a-b*, lycopene, and β-carotene) were enumerated through independent sample *t*-test. Pearson's correlation was used to check any significant interaction of capsaicin with other metabolites (total phenol, total flavonoid, carotenoid, chlorophyll *a-b*, lycopene, and β-carotene). The statistical significance of capsaicin-mediated *S. flexneri* anti-inflammation was determined by one-way ANOVA, whereas two-way ANOVA was conducted for the growth-inhibition study of *S. flexneri*. All statistical analysis and graphical representation were done using SPSS v. 16 (SPSS Inc, Chicago, IL, USA) and GraphPad Prism v. 7.0 (San Diego, CA, USA) if not specified separately.

3. Results and discussion

3.1. The influence of genotypic variation on capsaicin content, pungency, and capsaicin synthase activity

Capsaicin synthase (CS) is the last and the most vital enzyme in the capsaicinoid biosynthesis pathway because it catalyzes the condensation of vanilylamine and 8-methyl-6-nonenoic acid CoA to form capsaicin molecules [24,43]. The activity of the CS was significantly higher in the Balijuri chilies than in the Raja variety (Fig. 1a). According to Ref. [44]; CS activity triggers capsaicin production and further localization in the vesicles and vacuoles of the placental epidermis in chili fruits. Hence, we presumed that capsaicin concentrations and the pungency should also vary according to the CS activity. Correspondingly, capsaicin concentration and the pungency of the Balijuri cultivar were significantly higher than the Raja cultivar (Fig. 1b & c). We also determined the capsaicin and pungency contents in different parts of the chilies apart from the entire fruits. Interestingly, in Balijuri fruits, capsaicin variation was found to be in the order: Whole fruit > Placenta > Seed > Skin; while in Raja variety, the trend was: Whole fruit > Seed ≥ Placenta > Skin (Fig. 1). We observed a similar pattern in the pungency variation in both the studied chilies, wherein apart from the whole fruit, the seeds accorded for the highest pungency followed by the placenta and skin (Fig. 1). Capsaicinoid biosynthesis and accumulation is a genetically determined trait in chili pepper fruits as differences in pungency. Pungency results from the accumulation of capsaicinoid alkaloids in the fruit's placenta and is unique to the Capsicum genus [45]. It has also been found that capsaicinoid localization varies from chili to chili [46]. observed considerable variation in capsaicin concentration among the ovary, upper-lower epidermis, and five C. chinense cultivars seeds. Our findings also agree with a previous report [47] that some *C. annuum* cultivars contain higher concentrations of capsaicinoid (mainly dihydrocapsaicin) than those found in the Habanero variety of *C. chinense*.

Fig. 2 presents the HPLC chromatograms of the chili extracts. The capsaicin content and pungency data provided a solid basis for deriving capsaicin-enriched extracts through HPLC-mediated step-wise purification. The whole fruits obtained from the plants of two chili cultivars were extracted. The specific peak for capsaicin was identified using a standard marker in HPLC (Fig. 2). Eventually, a total capsaicin yield of approximately 69% and 43% from Balijuri and Raja chilies could be retrieved. After drying, we could derive 12.4 mg g^{-1} and 7.74 mg g^{-1} capsaicin-enriched dry extracts from Balijuri and Raja fruits, respectively. This result implied that capsaicin content in endemic chilies

Table 2
Co-linearity of capsaicin with other metabolites ascertained through (a) Pearson's correlation and (b) stepwise regression method [capsaicin (Cap) with Capsaicin synthase (Cap Syn), total phenol (Tot Phen), total flavonoid (Tot Flav), chlorophyll A and B (ChlA and ChlB), total carotenoids (Tot Car), lycopene (Lyc), and β-carotene (Beta C)].

(a)				Cap Syn	Tot Phen	Tot Flav	ChlA	ChlB	Tot Car	Lyc	Beta C
Cap	Pearson Correlation			0.984[a]	0.927[b]	0.999[a]	0.776	0.952[b]	−0.793	0.999[b]	0.995[a]
	Sig. (2-tailed)			<0.001	<0.01	<0.001	NS	<0.01	NS	<0.001	<0.001
	N			6	6	6	6	6	6	6	6
	Bootstrap[d]	Bias		−0.017	−0.029	−0.027	−0.016	−0.026	0.049	−.006[e]	−.037[e]
		Std. Error		0.155	0.261	0.189	0.221	0.239	0.306	.069[e]	.258[e]
		95% Confidence Interval	Lower	0.804	0.410	0.655	0.272	0.874	−0.996	.926[e]	.830[e]
			Upper	0.999	1.000	1.000	0.998	0.999	0.587	1.000[e]	1.000[e]

(b)

Order	Regression equation	F	R^2	p
1	Cap = 2.913159 + 0.368906 CapSyn - 2.160844 Tot Phen + 4.408793 Tot Flav - 0.713125 ChlA - 0.00211214 ChlB + 7.983942 Tot Car + 0.267538 Beta C	3.37	0.731	<0.05
2	Cap = −11.758189 + 0.723042 Tot Phen - 1.112471 Tot Flav - 4.648139 ChlA + 5.132499 ChlB - 0.847732 Tot Car + 8.781722 Lyc - 3.936635 Beta C	1.28	0.532	<0.05
3	Cap = −2.917175 - 0.375133 Tot Flav - 0.179471 ChlA + 1.257351 ChlB - 0.83726 Tot Car - 0.360089 Lyc - 1.433126 Beta C	0.16	0.382	NS
4	Cap = 0.018187–0.179714 ChlA + 0.871288 ChlB - 1.126488 Tot Car + 1.161819 Lyc - 1.127781 BetaC	0	NaN	NaN
5	Cap = 0.516624–0.7781 Cap Syn +0.1018 Tot Phen + 0.3107 Flv +0.7576 Lyc	38.1	0.954	<0.01
6	Cap = 1.3903 + 1.8107 Cap Syn - 0.1646 Tot Phen	53.1	0.967	<0.01
7	Cap = 0.9979 + 1.4577 Cap Syn	120.5	0.999	<0.001

NaN = Not a number.
*Correlation is significant at the 0.05 level (2-tailed).
NS = Not significant.
[a] Correlation is significant at the 0.001 level (2-tailed).
[b] Correlation is significant at the 0.01 level (2-tailed).
[d] Unless otherwise noted, bootstrap results are based on 1000 bootstrap samples.
[e] Based on 998 samples.

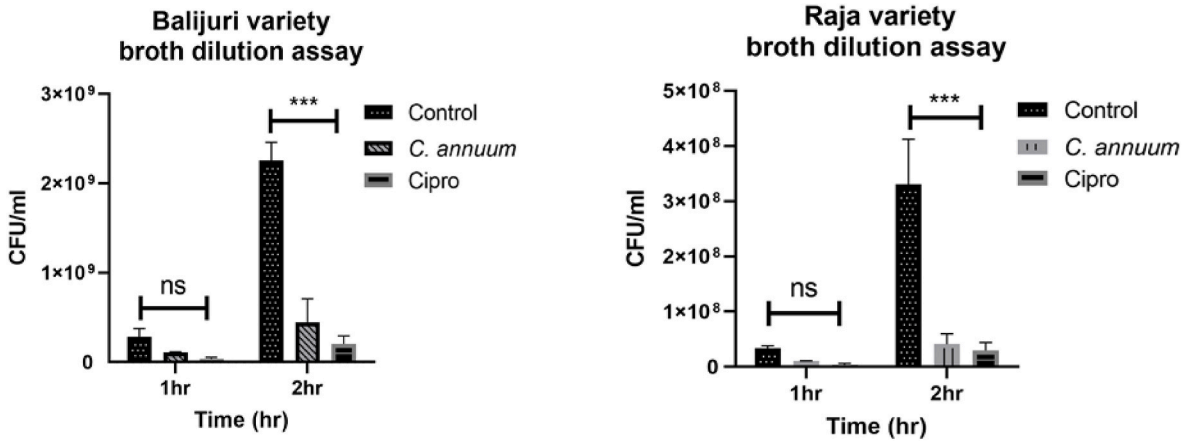

Fig. 3. *S. flexneri* growth was inhibited by *C annuum* varieties in broth culture. Broth dilution assay was performed in the presence of DMSO or acetone control, 65 μg ml^{-1} (Balijuri), and 120 μg ml^{-1} (Raja) of *C annuum,* followed by the addition of 10^9 *S. flexneri* overnight culture. Ciprofloxacin (Cipro), 10 μg/ml, was used as a positive control. The table shows % inhibition of *S flexneri* growth. Bacterial dilutions were plated and incubated overnight for counting viable no. of bacteria (CFU/ml). Two-way ANOVA was performed. Graphs were represented using GraphPad Prism 5 as mean ± SEM (n = 3); Significance was calculated; *p < 0.05, **p < 0.01, ***p < 0.001.

would likely differ depending upon the cultivar, even under identical growing conditions. Our previous research showed that the expression of secondary metabolites in endemic plants (e.g., *Ocimum sanctum* L., *Ocimum basilicum* L., and *Capsicum chinense*) substantially fluctuates among genotypes and cultivars [13,48].

3.2. The concentration of different plant metabolites influenced by the genotype

Table 1 presents the measured concentration of total phenol, flavonoids, chlorophyll *a* and *b*, carotenoids, lycopene, and β-carotene in the two chili varieties. The total phenol concentration in Balijuri was 326.1 ± 39.2, while Raja chili recorded 155.1 ± 17.2 in mg kg^{-1} of the fruits. Our results agree with [49] reported a significant variation of phenolic compounds in Iran's five high-yielding *C. annuum* varieties (Arian, Marona, Zorro, Y-43-07, and Y-43-09). Similarly, total flavonoid concentration was also 12.4 folds more elevated in the Balijuri chilies than in Raja chilies (t = 235.8; p < 0.001; Table 1). Flavonoids are one of the largest classes of plant secondary metabolites. A comprehensive analysis of flavonoids in 14 plant species showed that, of the different modified types of flavonoids, mainly methylated and glycosylated forms have specific accumulation patterns among various species [50]. Capsaicin is a product of the phenylpropanoid and fatty acid synthesis pathways, which presents total phenolics as a good indicator of capsaicin enrichment in chilies. Our assumptions corroborate a previous study [51].

The chlorophyll measurements were conducted on the leaf samples

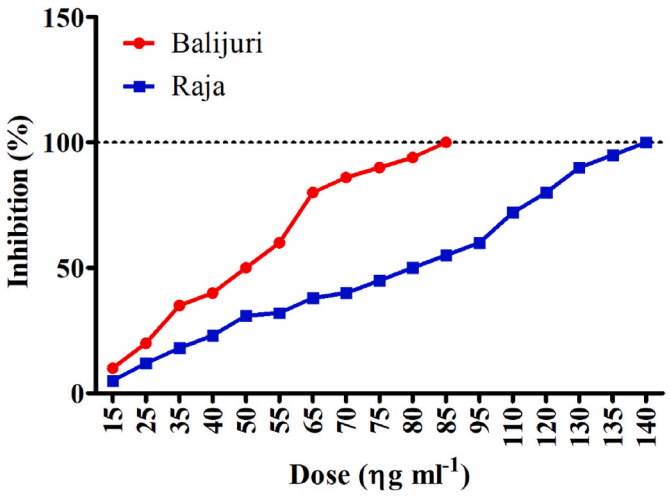

Fig. 4. The percentage of inhibition of the *S. flexneri* cells derived from the CFU mL^{-1} counts under broth dilution assay (100% inhibition levels are considered as minimum inhibitory concentrations (MIC) doses.

of both the chilies, and the values are presented in Table 1. Overall, the trend of chlorophyll variation among the two landraces was in the order: of Balijuri > Raja. Although chlorophyll *a* and *b* were higher in Balijuri, chlorophyll *b* concentration was significantly higher in the leaves of Balijuri over Raja ($t = 5.502$; $p < 0.01$). Chlorophyll is a crucial metabolite that aids plants to adjust and adapt to different environments (Li et al., 2018). Our findings are in agreement with [52]. According to Ref. [30]; chlorophyll production is a genetic trait that can be inherited among the plant community over generations. Conversely, the total carotenoid concentration was higher in the Raja fruits than in the Balijuri fruits. However, lycopene and β-carotene were noticeably more elevated in the Balijuri chilies (Table 1). Genetic variability greatly influences carotenoid production in pepper cultivars [43]. Our findings are justified by the correlation output wherein significant *r* values for β-carotene (0.995) and lycopene (0.999) were noticed with capsaicin (Table 2). Moreover, lycopene, β-carotene, capsanthin, capsorubin, tocopherol, violaxanthin, and several other carotenoids have been reported to vary significantly within the same chili genotype depending on the developmental stage, climate, and growth conditions [53,54].

3.3. *Insights on the impact of other metabolites on capsaicin generation in chilies: Correlation and regression-based assessment*

The biosynthesis of metabolites (total phenols, flavonoids, chlorophylls, carotenoids, β-carotene, and lycopene) and capsaicin synthase activity in chilies may influence the capsaicin generation to a great extent [32]. However, the specific roles of these compounds have not been comprehensively ascertained so far. Therefore, the overall relations of these compounds with capsaicin production in the selected endemic chili cultivars were assessed by performing correlation statistics (Table 2a). Their specific roles were appreciated by step-wise regression analysis (Table 2b). Pearson's correlation analysis revealed a significant correlation between capsaicin content and capsaicin synthase activity ($r = 0.984$; $p < 0.01$; Table 2). Additionally, we recorded significant positive correlations of capsaicin content with total phenol ($r = 0.927$; $p < 0.01$) and total flavonoid ($r = 0.999$; $p < 0.001$). Capsaicin content in the chili cultivars was also positively correlated with chlorophyll-B ($r = 0.952$; $p < 0.01$), lycopene ($r = 0.999$; $p < 0.001$), and β-carotene ($r = 0.995$; $p < 0.001$). In contrast, a weak but negative correlation between capsaicin and total carotenoid contents.

Performing a comprehensive regression model incorporating all the studied secondary metabolites revealed non-significant results (Table 2b). Stepwise multiple regression models provide a much clearer idea about the collinearity of variables by highlighting the most influential contributors toward the significant change in the dependent variable [55]. We observed capsaicin synthase, total phenol, flavonoid, and lycopene as the predictors for capsaicin variability in the studied chilies ($R^2 = 0.954$; $p < 0.01$; Table 2b). A stepwise removal of lycopene enhanced the R^2 to 0.967 ($p < 0.01$). Phenolic compounds are an integral part of the phenylpropanoid pathway, a synthetic route for capsaicin production in the chilies [56].

Additionally, the mevalonate pathway that produces lycopene is also responsible for acetyl CoA, which is quintessential for capsaicin production [57]. Interestingly, the R^2 sharply and most significantly increased when capsaicin was regressed with capsaicin synthase and total phenol content. As such, capsaicin synthase is the primary catalyst

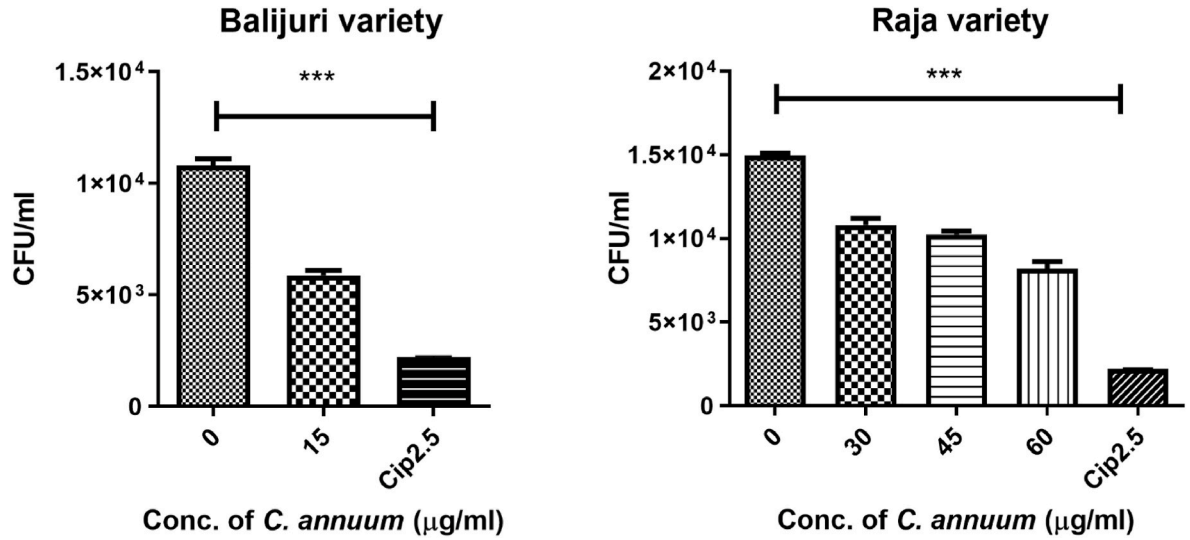

Fig. 5. Intracellular *S. flexneri* growth was inhibited by *C annuum* varieties in intestinal cells. Gentamicin protection assay was performed in HT29 cells with different concentrations of Capsaicin extracts. Cells were pre-treated (15 μg ml^{-1} for Balijuri and 30, 45, and 60 μg ml^{-1} for Raja variety) with Caps for 2h, followed by *S. flexneri* infection (MOI 200) for 2 h. Ciprofloxacin (CIP), 2.5 μg/ml, was used as a positive control. Finally, gentamicin treatment was done to kill extracellular bacteria. Cells were lysed and plated overnight to count the number of colonies (CFU/ml). Graphs represent CFU/ml of intracellular *S. flexneri*. Table shows % inhibition of *S flexneri* intracellular growth. Two-way ANOVA was performed. Graphs were represented using GraphPad Prism 5 as mean ± SEM (n = 3); Significance was calculated: *p < 0.05, **p < 0.01, ***p < 0.001.

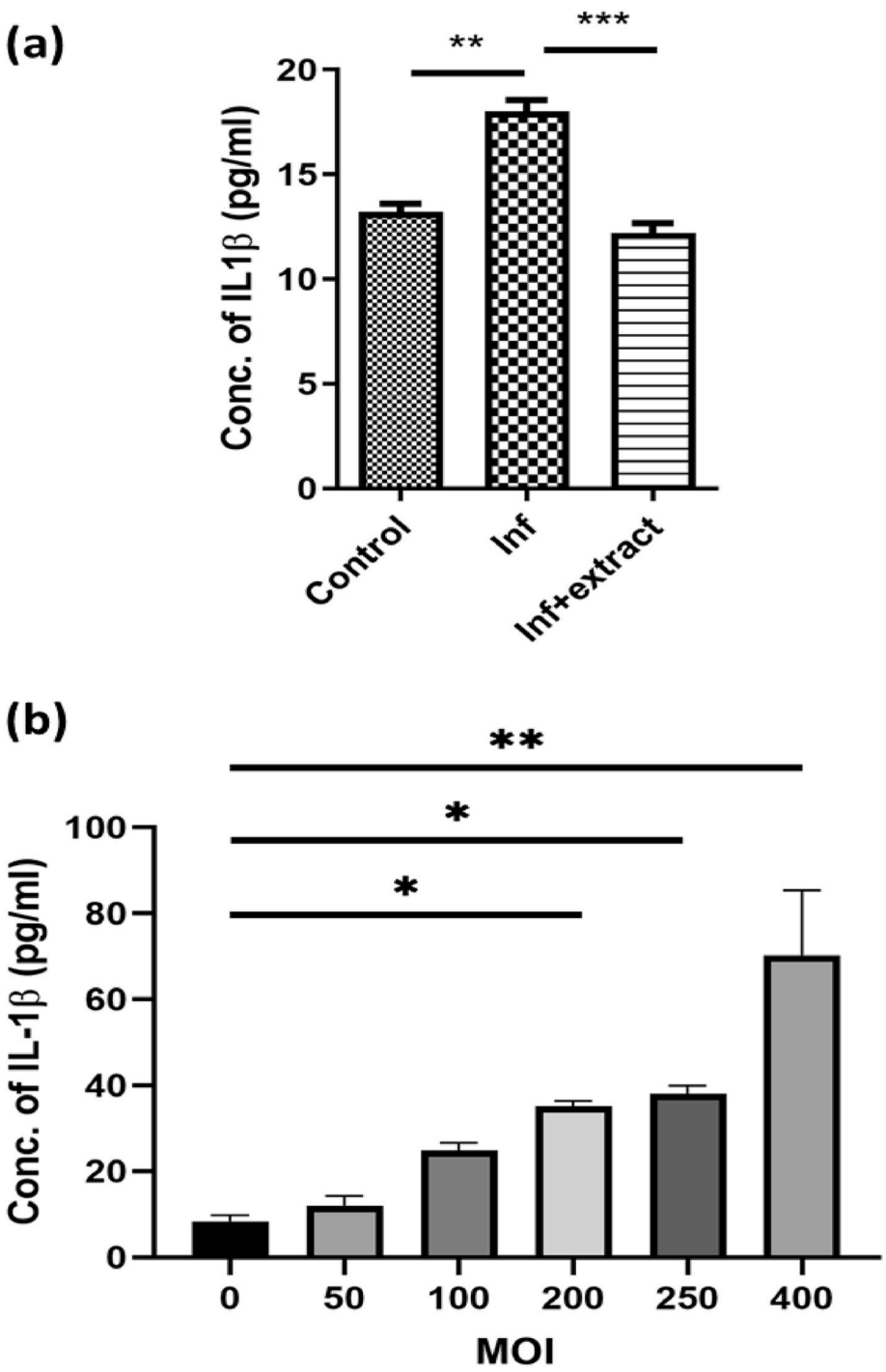

Fig. 6. Capsaicin-enriched Balijuri variety reduces inflammation in *S. flexneri* infected intestinal cells. (a) ELISA performance of the supernatants collected from infected and capsaicin Balijuri (15 μg ml^{-1}) treated cells. OD 450 nm was measured and concentration of IL1β was calculated and graphically represented. (b) detailed profile of the IL-1β concentrations in relation to the multiplicity of infection (MOI) of *S. flexneri*. One-way ANOVA was performed. Significance was calculated: *$p < 0.05$, **$p < 0.01$, ***$p < 0.001$.

responsible for condensing vanilylamine and 8-methyl-6-nonenoic acid CoA into capsaicin molecules [24]. This justifies the primary dependency of capsaicin on capsaicin-synthase activity, while the total phenol and lycopene remain as secondary effectors in capsaicin biosynthesis.

3.4. Role of capsaicin on Shigella flexneri growth

The inhibitory role of the Balijuri and Raja-derived capsaicin was ascertained through the broth dilution assay (Fig. 3). Generally, the dilution method is a dependable tool to determine the MIC values for any compound or extract [42]. The detailed impact of all the concentrations of the capsaicin-enriched extracts from both cultivars is presented in Fig. 4. In addition, a comparative study with Ciprofloxacin is shown in Fig. 3. Ciprofloxacin is one of the highest prescribed medicines for controlling *Shigella*-induced diarrhea. At the same time, its resistance to the *Shigella* pathogen is also well-known [58]. *Shigella* growth was significantly inhibited with xs. Overall, the inhibitory potential of the Balijuri extract was more pronounced than the Raja extract, as observed from the MIC values for both extracts (85 μg mL^{-1} – Balijuri; 140 μg mL^{-1} - Raja) (Fig. 4). This may be due to the higher capsaicin yield from the Balijuri chilies than the Raja chilies. However, a significant extent of inhibition (i.e., 80%) was considered to appreciate Balijuri and Raja-derived capsaicin's suitability for future drug development. Thus a comparative study with a positive control was necessary at this juncture [23]. Interestingly, the inhibitory impact of the desired

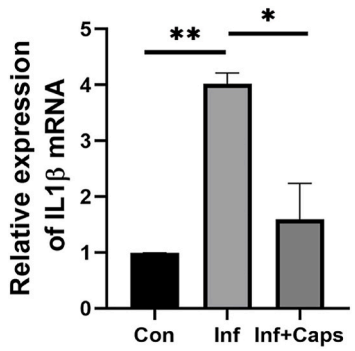

Fig. 7. Capsaicin (Caps) downregulates the IL1β gene. Caps-pre-treated HT29 cells were infected with *S flexneri* (MOI 200) for 2 h followed by qRT-PCR. The expression of human IL1β gene was quantified using GAPDH as the housekeeping gene. One-way ANOVA was performed. Significance was calculated: *p < 0.05, **p < 0.01, ***p < 0.001.

levels (65 μg mL^{-1} of Balijuri and 120 μg mL^{-1} of Raja) of both the extracts was quite similar to that of the positive control (i.e., Ciprofloxacin) after 2 h of incubation ($p < 0.001$). Hence, we were assured that the antibacterial potential of the chili-derived capsaicin-enriched extracts was noteworthy.

3.5. Role of capsaicin on Shigella flexneri intracellular growth

Apart from the direct antibacterial activity of capsaicin extracts from two varieties of chili, we examined the effect on intracellular invasion of *Shigella flexneri* by performing the Gentamicin assay. This assay provides factual information about the extent of invasiveness of the *Shigella* pathogen [59]. As detailed in the method section, various gradient concentrations of the Balijuri and Raja-derived extracts were used. Their corresponding effects are presented in Fig. 4. Fig. 5 shows that the extracts of both chilies induced an inhibitory effect on the *S. flexneri* invasiveness at lower doses (5–10 μg mL^{-1}). However, the impact of Balijuri-derived capsaicin was more robust than the Raja-derived capsaicin. Interestingly, the Balijuri-derived *C annum* extract dramatically reduced *S. flexneri* counts (50% inhibition) in the invaded cells at only 15 μg mL^{-1} (Fig. 5). Therefore, the 15 μg mL^{-1} may also be considered as the IC_{50} value for Balijuri-derived capsaicin as this concentration could induce 50% growth inhibition of the pathogen [42]. On the other hand, the inhibitory effect of Raja-derived *C annum* extract was mild at lower concentrations. Still, interestingly, the increasing doses of Raja-derived *C annum* extract (e.g., 30, 45, and 60 μg/mL) inhibited the pathogen load in the infected cells (Fig. 5). Overall, it was also interesting to note that the performance of low doses (15 and 60 μg/mL) Balijuri and Raja-derived capsaicin was comparable to a high dose of one of the most effective antibiotic, Ciprofloxacin (i.e., 2.5 μg mL^{-1}). The colony forming units (CFU) generally reveal the metabolically active cell counts of microorganisms and thus strongly indicate microbial growth [60]. Interestingly, the chili-derived capsaicin could efficiently arrest the *Shigella flexneri* cell growth in the present study (Fig. 4). Specifically, the Balijuri-derived capsaicin was significantly more effective than the Raja-derived capsaicin in inhibiting intracellular *S. flexneri* growth. Our data are consistent with a study showing in vitro effectiveness of capsaicin extract isolated from C. chinense, preventing adhesion and internalization of S. typhimurium cells [27]. Therefore, intracellular *S. flexneri* growth was susceptible to the bactericidal effect of capsaicin extract.

3.6. Role of Capsaicin on Shigella flexneri-mediated inflammation

It is well known that *Shigella flexneri* infection activates the NLRP3 inflammasome pathway to secrete pro-inflammatory cytokines like IL1β [61]. Prolonged inflammation aggravates host cellular damage, which further facilitates bacterial spreading. In this context, capsaicin-enriched *C. annum* extract was highly effective in arresting bacterial growth. This could be due to the inherent anti-inflammatory property of the extract. Hence, we were interested in studying the mechanism of capsaicin extract-induced inflammatory changes in *S. flexneri*-infected human intestinal cells.

Interestingly, the ELISA assay revealed that Balijuri-derived capsaicin-enriched extract readily downregulates the IL1β production significantly in *S. flexneri*-infected intestinal cells, thereby resulting in recovery from inflammation (Fig. 6A). Although no report is available on chili-derived capsaicin, a few plant-derived compounds (e.g., Parthenolide and Betaine) potently inhibit the protease activity of caspase-1, thereby facilitating pro-IL-1β cleavage [62,63]. We have also evaluated the detailed profile of the IL-1β concentrations concerning the multiplicity of infection (MOI) of the pathogen (Fig. 6B) and observed a steady increase in IL-1 β with increasing MOI and the increment in IL-1β was dramatically sharp between 300 and 450 MOI (Fig. 6B). Previously, we have reported that a sharp rise in bacterial population readily causes *S. flexneri* autophagy [29]. Therefore, the cell count corresponding to an intermediate MOI (i.e., MOI 200) was utilized for the study. In general, we could postulate that the capsaicin-enriched extract-mediated reduction of inflammatory IL 1β in infected cells may limit the intracellular spread of *S flexneri* to adjacent cells by maintaining cellular integrity. To appreciate this hypothesis, the expression of IL-1β gene was assessed in infected cells. Although the IL-1β gene was significantly upregulated during *Shigella flexneri* infection as compared to uninfected cells, the capsaicin treatment dramatically down-regulated the IL-1β expression in infected cells (Fig. 7). The significant difference of IL-1β expression between infected and caps pre-treated infected cells representing indicates efficient anti-inflammatory activity of capsaicin against *S flexneri* infection.

4. Conclusion

The present investigation emphasized understanding the significant differences in the phytochemistry and bioactivity of two *C. annuum* landraces. We observed higher capsaicin content and pungency in the Balijuri chilies compared to Raja. The activity of capsaicin synthase enzyme was also 1.57 folds higher in the Balijuri fruits. Additionally, concentrations of phenolic (total phenol and flavonoids) and carotenoids revealed a significant variation among the studied chilies suggesting the rich phytochemistry of the Balijuri landrace. The potent role of purified capsaicin from Balijuri fruits against *Shigella flexneri* was evident from the growth inhibition and reduced inflammatory cytokine levels. Balijuri extract has potential antibacterial activity against *S flexneri* among the two varieties of *C annum*. Balijuri extract has a direct bactericidal action and blocks the intestinal invasion of *S flexneri*. Overall, this study concludes that genotypic variation significantly regulates chilies' metabolite production and corresponding bioactivity. This investigation could be a preliminary endeavor toward shigellosis drug development and warrants in-depth research in the future. In particular, the mode action of the chili-derived capsaicin for *S flexneri*-induced inflammasome regulation via inhibition of pro-inflammatory cytokines like IL1β would be interesting to study in days to come.

CRediT authorship contribution statement

Subhasish Das: Writing – original draft, Visualization, Methodology, Investigation. **Nayana Priyadarshani:** Methodology, Investigation. **Priyanka Basak:** Writing – original draft, Methodology, Investigation, Data curation. **Priyanka Maitra:** Writing – original draft, Methodology, Investigation, Data curation. **Sushmita Bhattacharya:** Writing – review & editing, Visualization, Validation, Supervision, Methodology, Data curation. **Satya Sundar Bhattacharya:** Writing – review & editing, Visualization, Validation, Supervision, Methodology, Data curation, Conceptualization.

Declaration of competing interest

The authors declare the following financial interests/personal relationships which may be considered as potential competing interests: None.

References

[1] P. Bardhan, A.S.G. Faruque, A. Naheed, D.A. Sack, Decreasing shigellosis-related deaths without Shigella spp.–specific interventions, Asia, Emerg. Infect. Dis. J. 16 (2010) 1718, https://doi.org/10.3201/eid1611.090934.

[2] S.-R. Han, D.W. Kim, B. Kim, Y.M. Chi, S. Kang, H. Park, S.-H. Jung, J.H. Lee, T.-J. Oh, Complete genome sequencing of Shigella sp. PAMC 28760: identification of CAZyme genes and analysis of their potential role in glycogen metabolism for cold survival adaptation, Microb. Pathog. 137 (2019), 103759, https://doi.org/10.1016/j.micpath.2019.103759.

[3] M.U. Hossain, M.A. Khan, A. Hashem, M.M. Islam, M.N. Morshed, C.A. Keya, M. Salimullah, Finding potential therapeutic targets against Shigella flexneri through proteome exploration, Front. Microbiol. 7 (2016) 1–13.

[4] M. Puzari, M. Sharma, P. Chetia, Emergence of antibiotic resistant Shigella species: a matter of concern, J. Infect. Public Health 11 (2018) 451–454, https://doi.org/10.1016/j.jiph.2017.09.025.

[5] C.C. Butler, J. Dorward, L.-M. Yu, O. Gbinigie, G. Hayward, B.R. Saville, O. Van Hecke, N. Berry, M. Detry, C. Saunders, M. Fitzgerald, V. Harris, M.G. Patel, S. de Lusignan, E. Ogburn, P.H. Evans, N.P.B. Thomas, F.D.R. Hobbs, Azithromycin for community treatment of suspected COVID-19 in people at increased risk of an adverse clinical course in the UK (PRINCIPLE): a randomised, controlled, open-label, adaptive platform trial, Lancet 397 (2021) 1063–1074, https://doi.org/10.1016/S0140-6736(21)00461-X.

[6] B. Mathews, A.A. Thalody, S.S. Miraj, V. Kunhikatta, M. Rao, K. Saravu, Adverse effects of fluoroquinolones: a retrospective cohort study in a south Indian tertiary healthcare facility, Antibiot. (Basel, Switzerland) 8 (2019) 104, https://doi.org/10.3390/antibiotics8030104.

[7] Farhat Ullah, M. Ayaz, A. Sadiq, Farman Ullah, I. Hussain, M. Shahid, Z. Yessimbekov, A. Adhikari-Devkota, H.P. Devkota, Potential role of plant extracts and phytochemicals against foodborne pathogens, Appl. Sci. (2020), https://doi.org/10.3390/app10134597.

[8] K.M. Parmar, S.K. Sinha, R.S. Prasad, M.S. Jogi, D. Laloo, M. Dhobi, S.S. Gurav, S. K. Prasad, Identifying the mechanism of eriosematin E from Eriosema chinense Vogel. for its antidiarrhoeal potential against Shigella flexneri-induced diarrhoea using in vitro, in vivo and in silico models, Microb. Pathog. 149 (2020), 104582, https://doi.org/10.1016/j.micpath.2020.104582.

[9] M.Z.M. Salem, S.I. Behiry, A.Z.M. Salem, Effectiveness of root-bark extract from Salvadora persica against the growth of certain molecularly identified pathogenic bacteria, Microb. Pathog. 117 (2018) 320–326, https://doi.org/10.1016/j.micpath.2018.02.044.

[10] L.B.M. Kouitcheu, J.L. Tamesse, J. Kouam, The anti-shigellosis activity of the methanol extract of Picralima nitida on Shigella dysenteriae type I induced diarrhoea in rats, BMC Compl. Alternative Med. 13 (2013) 211, https://doi.org/10.1186/1472-6882-13-211.

[11] A. Mahboubi, J. Asgarpanah, P.N. Sadaghiyani, M. Faizi, Total phenolic and flavonoid content and antibacterial activity of Punica granatum L. var. pleniflora flowers (Golnar) against bacterial strains causing foodborne diseases, BMC Compl. Alternative Med. 15 (2015) 366, https://doi.org/10.1186/s12906-015-0887-x.

[12] M. Nasir, K. Tafess, D. Abate, Antimicrobial potential of the Ethiopian Thymus schimperi essential oil in comparison with others against certain fungal and bacterial species, BMC Compl. Alternative Med. 15 (2015) 260, https://doi.org/10.1186/s12906-015-0784-3.

[13] S. Das, S. Sarkar, M. Das, P. Banik, S.S. Bhattacharya, Influence of soil quality factors on capsaicin biosynthesis, pungency, yield, and produce quality of chili: an insight on Csy1, Pun1, and Pun12 signaling responses, Plant Physiol. Biochem. 166 (2021) 427–436, https://doi.org/10.1016/j.plaphy.2021.06.012.

[14] T. Yatung, R.K. Dubey, V. Singh, G. Upadhyay, Genetic diversity of chilli (Capsicum annuum L.) genotypes of India based on morpho-chemical traits, Aust. J. Crop. Sci. 8 (2014) 97–102.

[15] C.P. Khare, in: C.P. Khare (Ed.), Capsicum Annuum Linn. BT - Indian Medicinal Plants: an Illustrated Dictionary, Springer New York, New York, NY, 2007, p. 1, https://doi.org/10.1007/978-0-387-70638-2_286.

[16] D. Borah, P. Mipun, J. Sarma, C. Mili, D. Narah, Quantitative documentation of traditionally used medicinal plants and their significance to healthcare among the Mishing community of Northeast India, Ecol. Quest. 32 (2021) 61–94, https://doi.org/10.12775/EQ.2021.034.

[17] P.C. Phondani, R.K. Maikhuri, C.P. Kala, Ethnoveterinary uses of medicinal plants among traditional herbal healers in Alaknanda catchment of Uttarakhand, India, African J. Tradit. Complement. Altern. Med. AJTCAM 7 (2010) 195–206, https://doi.org/10.4314/ajtcam.v7i3.54775.

[18] F. Domínguez, A. Alonso-Castro, M. Anaya, M. González-Trujano, H. Salgado-Ceballos, S. Orozco-Suárez, Mexican traditional medicine: traditions of yesterday and phytomedicines for tomorrow, in: M. Duarte, M. Rai (Eds.), Therapeutic Medicinal Plants: from Lab to the Market, CRC Press, Boca Raton, Florida, 2015, pp. 10–46.

[19] S. Basu, A.K. De, A. De, Capsicum: historical and botanical perspectives, in: A.K. De (Ed.), Capsicum: the Genus Capsicum, Taylor & Francis, New York, NY, 2003, pp. 1–15.

[20] D. Hervert-Hernández, S.G. Sáyago-Ayerdi, I. Goñi, Bioactive compounds of four hot pepper varieties (Capsicum annuum L.), antioxidant capacity, and intestinal bioaccessibility, J. Agric. Food Chem. 58 (2010) 3399–3406, https://doi.org/10.1021/jf904220w.

[21] K. Aizawa, T. Inakuma, Dietary capsanthin, the main carotenoid in paprika (*Capsicum annuum*), alters plasma high-density lipoprotein-cholesterol levels and hepatic gene expression in rats, Br. J. Nutr. 102 (2009) 1760–1766, https://doi.org/10.1017/S0007114509991309.

[22] L.M. Catalfamo, G. Marrone, M. Basilicata, I. Vivarini, V. Paolino, D. Della-Morte, F.S. De Ponte, F. Di Daniele, D. Quattrone, D. De Rinaldis, P. Bollero, N. Di Daniele, A. Noce, The utility of capsicum annuum L. in internal medicine and in dentistry: a comprehensive review, Int. J. Environ. Res. Publ. Health 19 (2022), https://doi.org/10.3390/ijerph191811187.

[23] J. Gertsch, How scientific is the science in ethnopharmacology? Historical perspectives and epistemological problems, J. Ethnopharmacol. 122 (2009) 177–183, https://doi.org/10.1016/j.jep.2009.01.010.

[24] B.C.N. Prasad, V. Kumar, H.B. Gururaj, R. Parimalan, P. Giridhar, G. A. Ravishankar, Characterization of capsaicin synthase and identification of its gene (csy1) for pungency factor capsaicin in pepper (Capsicum sp.), Proc. Natl. Acad. Sci. USA 103 (2006) 13315–13320, https://doi.org/10.1073/pnas.0605805103.

[25] J.Y. Kang, C.H. Teng, F.C. Chen, Effect of capsaicin and cimetidine on the healing of acetic acid induced gastric ulceration in the rat, Gut 38 (1996) 832–836.

[26] K. Yamakawa, J. Matsuo, T. Okubo, S. Nakamura, H. Yamaguchi, Impact of capsaicin, an active component of chili pepper, on pathogenic chlamydial growth (Chlamydia trachomatis and Chlamydia pneumoniae) in immortal human epithelial HeLa cells, J. Infect. Chemother. Off. J. Japan Soc. Chemother. 24 (2018) 130–137, https://doi.org/10.1016/j.jiac.2017.10.007.

[27] J.A. Ayariga, D.A. Abugri, B. Amrutha, R. Villafane, Capsaicin potently blocks Salmonella typhimurium invasion of vero cells, Antibiot (2022), https://doi.org/10.3390/antibiotics11050666.

[28] F. Wang, X. Huang, Y. Chen, D. Zhang, D. Chen, L. Chen, J. Lin, Study on the effect of capsaicin on the intestinal flora through high-throughput sequencing, ACS Omega 5 (2020) 1246–1253, https://doi.org/10.1021/acsomega.9b03798.

[29] P. Basak, P. Maitra, U. Khan, K. Saha, S.S. Bhattacharya, M. Dutta, S. Bhattacharya, Capsaicin inhibits Shigella flexneri intracellular growth by inducing autophagy, Front. Pharmacol. 13 (2022) 1–15.

[30] M. Khodadadi, H. Dehghani, M.H. Fotokian, B. Rain, Genetic diversity and heritability of chlorophyll content and photosynthetic indexes among some Iranian wheat genotypes, J. Biodivers. Environ. Sci. (JBES) 4 (2014) 12–23.

[31] K. Sanatombi, S. Sen-Mandi, G.J. Sharma, DNA profiling of Capsicum landraces of Manipur, Sci. Hortic. 124 (2010) 405–408, https://doi.org/10.1016/j.scienta.2010.01.006.

[32] S. Das, K.C. Teja, B. Duary, P.K. Agrawal, S.S. Bhattacharya, Impact of nutrient management, soil type and location on the accumulation of capsaicin in Capsicum chinense (Jacq.): one of the hottest chili in the world, Sci. Hortic. 213 (2016) 354–366, https://doi.org/10.1016/j.scienta.2016.10.041.

[33] T.L. Olatunji, A.J. Afolayan, Comparison of nutritional, antioxidant vitamins and capsaicin contents in Capsicum annuum and C. frutescens, Int. J. Veg. Sci. 26 (2020) 190–207, https://doi.org/10.1080/19315260.2019.1629519.

[34] R.F. Yenny, N. Rostini, Anas Hersanti, Correlation between fruit characters with capsaicin content in F_2 population of chili, IOP Conf. Ser. Earth Environ. Sci. 334 (2019), 12017, https://doi.org/10.1088/1755-1315/334/1/012017.

[35] M.W. Siddiqui, C. Momin, P. Acharya, J. Kabir, M. Debnath, R.S. Dhua, Dynamics of changes in bioactive molecules and antioxidant potential of Capsicum chinense Jacq. cv. Habanero at nine maturity stages, Acta Physiol. Plant. 35 (2013) 1141–1148, https://doi.org/10.1007/s11738-012-1152-2.

[36] P.H. Todd, M.G. Bensinger, T. Biftu, Determination of pungency due to capsicum by gas-liquid chromatography, J. Food Sci. 42 (1977) 660–665, https://doi.org/10.1111/j.1365-2621.1977.tb12573.x.

[37] J. Huang, S.A. Mabury, J.C. Sagebiel, Hot chili peppers: extraction, cleanup, and measurement of capsaicin, J. Chem. Educ. 77 (2000) 1630, https://doi.org/10.1021/ed077p1630.

[38] N.A. Siddique, M. Mujeeb, A.K. Najmi, M. Akram, Evaluation of antioxidant activity, quantitative estimation of phenols and flavonoids in different parts of Aegle marmelos, Afr. J. Plant Sci. 4 (2010) 1–5.

[39] A. Özkök, B. D'arcy, K. Sorkun, Total phenolic acid and total flavonoid content of Turkish pine honeydew honey, J. ApiProduct ApiMed. Sci. 2 (2010) 65–71, https://doi.org/10.3896/IBRA.4.02.2.01.

[40] T. Ignat, Z. Schmilovitch, J. Feföldi, N. Bernstein, B. Steiner, H. Egozi, A. Hoffman, Nonlinear methods for estimation of maturity stage, total chlorophyll, and carotenoid content in intact bell peppers, Biosyst. Eng. 114 (2013) 414–425, https://doi.org/10.1016/j.biosystemseng.2012.10.001.

[41] M. Nagata, I. Yamashita, Simple method for simultaneous determination of chlorophyll and carotenoids in tomato fruit, Journal-Japanese Soc. Food Sci. Technol. 39 (1992) 925.

[42] P. Cos, A.J. Vlietinck, D. Vanden Berghe, L. Maes, Anti-infective potential of natural products: How to develop a stronger in vitro 'proof-of-concept, J. Ethnopharmacol. 106 (2006) 290–302, https://doi.org/10.1016/j.jep.2006.04.003.

[43] J.H. Kim, Y.D. Jo, C.H. Jin, Isolation of soluble epoxide hydrolase inhibitor of capsaicin analogs from Capsicum chinense Jacq. cv, Habanero. Int. J. Biol. Macromol. 135 (2019) 1202–1207, https://doi.org/10.1016/j.ijbiomac.2019.06.028.

[44] Z.-X. Zhang, S.-N. Zhao, G.-F. Liu, Z.-M. Huang, Z.-M. Cao, S.-H. Cheng, S.-S. Lin, Discovery of putative capsaicin biosynthetic genes by RNA-Seq and digital gene

expression analysis of pepper, Sci. Rep. 6 (2016), 34121, https://doi.org/10.1038/srep34121.
[45] A. González-Zamora, E. Sierra-Campos, J.G. Luna-Ortega, R. Pérez-Morales, J. C. Rodríguez Ortiz, J.L. García-Hernández, Characterization of different Capsicum varieties by evaluation of their capsaicinoids content by high performance liquid chromatography, determination of pungency and effect of high temperature, Molecules 18 (2013) 13471–13486, https://doi.org/10.3390/molecules181113471.
[46] V. Supálková, H. Stavělíková, S. Krizkova, V. Adam, A. Horna, L. Havel, P. Ryant, P. Babula, R. Kizek, Study of capsaicin content in various parts of pepper fruit by liquid chromatography with electrochemical detection, Acta Chim. Slov. 54 (2007) 55–59.
[47] A. Garcés-Claver, M.S. Arnedo-Andrés, J. Abadía, R. Gil-Ortega, A. Álvarez-Fernández, Determination of capsaicin and dihydrocapsaicin in capsicum fruits by liquid Chromatography−Electrospray/time-of-flight mass spectrometry, J. Agric. Food Chem. 54 (2006) 9303–9311, https://doi.org/10.1021/jf0620261.
[48] S. Das, S. Barman, R. Teron, S.S. Bhattacharya, K.-H. Kim, Secondary metabolites and anti-microbial/anti-oxidant profiles in Ocimum spp.: role of soil physico-chemical characteristics as eliciting factors, Environ. Res. 188 (2020), 109749, https://doi.org/10.1016/j.envres.2020.109749.
[49] M. Ghasemnezhad, M. Sherafati, G.A. Payvast, Variation in phenolic compounds, ascorbic acid and antioxidant activity of five coloured bell pepper (Capsicum annum) fruits at two different harvest times, J. Funct.Foods 3 (2011) 44–49, https://doi.org/10.1016/j.jff.2011.02.002.
[50] M. Peng, R. Shahzad, A. Gul, H. Subthain, S. Shen, L. Lei, Z. Zheng, J. Zhou, D. Lu, S. Wang, E. Nishawy, X. Liu, T. Tohge, A.R. Fernie, J. Luo, Differentially evolved glucosyltransferases determine natural variation of rice flavone accumulation and UV-tolerance, Nat. Commun. 8 (2017) 1975, https://doi.org/10.1038/s41467-017-02168-x.
[51] G.T.S. Sora, C.W.I. Haminiuk, M.V. da Silva, A.A.F. Zielinski, G.A. Gonçalves, A. Bracht, R.M. Peralta, A comparative study of the capsaicinoid and phenolic contents and in vitro antioxidant activities of the peppers of the genus Capsicum: an application of chemometrics, J. Food Sci. Technol. 52 (2015) 8086–8094, https://doi.org/10.1007/s13197-015-1935-8.
[52] E.L. Arumingtyas, J. Kusnadi, R. Mastuti, N.S. Faradise, The effect of ethyl methane sulfonate on the antioxidant content of chili pepper (Capsicum frutescens L.), AIP Conf. Proc. 2019 (2018) 20010, https://doi.org/10.1063/1.5061846.
[53] H.M. Berry, D.V. Rickett, C.J. Baxter, E.M.A. Enfissi, P.D. Fraser, Carotenoid biosynthesis and sequestration in red chilli pepper fruit and its impact on colour intensity traits, J. Exp. Bot. 70 (2019) 2637–2650, https://doi.org/10.1093/jxb/erz086.
[54] C.S. Lekala, K.S.H. Madani, A.D.T. Phan, M.M. Maboko, H. Fotouo, P. Soundy, Y. Sultanbawa, D. Sivakumar, Cultivar-specific responses in red sweet peppers grown under shade nets and controlled-temperature plastic tunnel environment on antioxidant constituents at harvest, Food Chem. 275 (2019) 85–94, https://doi.org/10.1016/j.foodchem.2018.09.097.
[55] M.Z.I. Chowdhury, T.C. Turin, Variable selection strategies and its importance in clinical prediction modelling, Fam. Med. Community Heal. 8 (2020), e000262, https://doi.org/10.1136/fmch-2019-000262.
[56] M. Hamed, D. Kalita, M.E. Bartolo, S.S. Jayanty, Capsaicinoids, Polyphenols and Antioxidant Activities of Capsicum Annuum: Comparative Study of the Effect of Ripening Stage and Cooking Methods, vol. 8, Antioxidants, Basel, Switzerland, 2019, https://doi.org/10.3390/antiox8090364.
[57] C. Schwartz, K. Frogue, J. Misa, I. Wheeldon, Host and pathway engineering for enhanced lycopene biosynthesis in yarrowia lipolytica, Front. Microbiol. 8 (2017) 2233, https://doi.org/10.3389/fmicb.2017.02233.
[58] C. Gaudreau, R. Ratnayake, P.A. Pilon, S. Gagnon, M. Roger, S. Lévesque, Ciprofloxacin-resistant Shigella sonnei among men who have sex with men, Canada, 2010, Emerg. Infect. Dis. 17 (2011) 1747–1750, https://doi.org/10.3201/eid1709.102034.
[59] S. Paetzold, S. Lourido, B. Raupach, A. Zychlinsky, Shigella flexneri phagosomal escape is independent of invasion, Infect. Immun. 75 (2007) 4826–4830, https://doi.org/10.1128/IAI.00454-07.
[60] S.K. Nandy, K. Venkatesh, Study of CFU for individual microorganisms in mixed cultures with a known ratio using MBRT, Amb. Express 4 (2014) 38, https://doi.org/10.1186/s13568-014-0038-7.
[61] L.-H. Li, T.-L. Chen, H.-W. Chiu, C.-H. Hsu, C.-C. Wang, T.-T. Tai, T.-C. Ju, F.-H. Chen, O.V. Chernikov, W.-C. Tsai, K.-F. Hua, Critical role for the NLRP3 inflammasome in mediating IL-1β production in Shigella sonnei-infected macrophages, Front. Immunol. 11 (2020) 1–14.
[62] C. Juliana, T. Fernandes-Alnemri, J. Wu, P. Datta, L. Solorzano, J.-W. Yu, R. Meng, A.A. Quong, E. Latz, C.P. Scott, E.S. Alnemri, Anti-inflammatory compounds parthenolide and Bay 11-7082 are direct inhibitors of the inflammasome, J. Biol. Chem. 285 (2010) 9792–9802, https://doi.org/10.1074/jbc.M109.082305.
[63] Y. Xia, S. Chen, G. Zhu, R. Huang, Y. Yin, W. Ren, Betaine inhibits interleukin-1β production and release: potential mechanisms, Front. Immunol. 9 (2018) 1–12.